Graduate Theses and Dissertations   Graduate School

November 2017

The Role of Sgs1 and Exo1 in the Maintenance of Genome Stability.

Lillian Campos-Doerfler
University of South Florida, lilliand@mail.usf.edu

The Role of Sgs1 and Exo1 in the Maintenance of Genome Stability

By

Lillian Campos-Doerfler

A dissertation submitted in partial fulfillment
of the requirements for the degree of
Doctor of Philosophy
With a concentration in Cell and Molecular Biology
Department of Cell Biology, Microbiology and Molecular Biology
College of Arts and Sciences
University of South Florida

Major Professor: Kristina Schmidt, Ph.D.
Meera Nanjundan, Ph.D.
Stanley Stevens, Ph.D.
Sandy Westerheide, Ph.D.

Date of Approval:
November 17, 2017

Keywords: Genome Instability, DNA repair, RecQ Helicases, Sgs1, Exo1

Dedication

I would like to dedicate this dissertation to my amazing and supportive family. To my husband Eric for his constant encouragement and patience, my sister Connie for her motivational phone calls and guidance, and my parents Wanda and Jaime for everything they have done that allowed for me to pursue my dream.

Acknowledgements

I would first like to acknowledge my advisor Dr. Kristina Schmidt for the

opportunity and privilege to study under her expertise. I thank my committee members

for their time and input that helped guide my studies. To current and former graduate

students that shared in my triumphs and failures, always helping me take both in stride.

I would like to thank our former post-doctoral fellow Lorena for encouraging me when I

was just a technician to believe in myself enough to take the leap and apply to graduate

school. I appreciate the help and guidance of all those mentioned that contributed to

my success.

Table of Contents

iv

List of Tables

List of Figures

Abstract

Genome instability is a hallmark of human cancers. Patients with Bloom's syndrome, a rare chromosome breakage syndrome caused by inactivation of the RecQ helicase BLM, result in phenotypes associated with accelerated aging and develop cancer at a very young age. Patients with Bloom's syndrome exhibit hyper-recombination, but the role of BLM and increased genomic instability is not fully characterized. Sgs1, the only member of the RecQ family of DNA helicases in *Saccharomyces cerevisiae*, is known to act both in early and late stages of homology-dependent repair of DNA damage. Exo1, a 5′–3′ exonuclease, first discovered to play a role in mismatch repair has been shown to participate in parallel to Sgs1 in processing the ends of DNA double-strand breaks, an early step of homology-mediated repair. Here we have characterized the genetic interaction of *SGS1* and *EXO1* with other repair factors in homology-mediated repair as well as DNA damage checkpoints, and characterize the role of post-translational modifications, and protein-protein interactions in regulating their function in response to DNA damage. In *S. cerevisiae* cells lacking Sgs1, spontaneous translocations arise by homologous recombination in small regions of homology between three non-allelic, but related sequences in the genes *CAN1, LYP1,* and *ALP1.* We have found that these translocation events are inhibited if cells lack Mec1/ATR kinase while Tel1/ATM acts as a suppressor, and that they are dependent on Rad59, a protein known to function as one of two sub-pathways of Rad52 homology-directed repair.

Through a candidate screen of other DNA metabolic factors, we identified Exo1 as a strong suppressor of chromosomal rearrangements in the *sgs1Δ* mutant. The Exo1 enzymatic domain is located in the N-terminus while the C-terminus harbors mismatch repair protein binding sites as well as phosphorylation sites known to modulate its enzymatic function at uncapped telomeres. We have determined that the C-terminus is dispensable for Exo1's roles in resistance to DNA-damaging agents and suppressing mutations and chromosomal rearrangements. Exo1 has been identified as a component of the error-free DNA damage tolerance pathway of template switching. Exo1 promotes template switching by extending the single strand gap behind stalled replication forks. Here, we show that the dysregulation of the phosphorylation of the C-terminus of Exo1 is detrimental in cells under replication stress whereas loss of Exo1 suppresses under the same conditions, suggesting that Exo1 function is tightly regulated by both phosphorylation and dephosphorylation and is important in properly modulating the DNA damage response at stalled forks.

It has previously been shown that the strand exchange factor Rad51 binds to the C-terminus of Sgs1 although the significance of this physical interaction has yet to be determined. To elucidate the function of the physical interaction of Sgs1 and Rad51, we have generated a separation of function allele of *SGS1* with a single amino acid change (*sgs1-FD)* that ablates the physical interaction with Rad51. Alone, the loss of the interaction of Sgs1 and Rad51 in our *sgs1-FD* mutant did not cause any of the defects in response to DNA damaging agents or genome rearrangements that are observed in the *sgs1Δ* mutant. However, when we assessed the *sgs1-FD* mutant in combination with the loss of Sae2, Mre11, Exo1, Srs2, Rrm3, and Pol32 we observed genetic

interactions that distinguish the *sgs1-FD* mutant from the *sgs1Δ* mutant. Negative and positive genetic interactions with *SAE2, MRE11, EXO1, SRS2, RRM3,* and *POL32* suggest the role of the physical interaction of Sgs1 and Rad51 is in promoting homology-mediated repair possibly by competing with single-strand binding protein RPA for single-stranded DNA to promote Rad51 filament formation.

Together, these studies characterize additional roles for domains of Sgs1 and Exo1 that are not entirely understood as well as their roles in combination with DNA damage checkpoints, and repair pathways that are necessary for maintaining genome stability.

Chapter One:

Introduction

Proper repair of DNA damage is essential for maintaining genome integrity and cellular function. Cells can encounter genomic insults via endogenous and exogenous damage caused by replication error, DNA damaging agents, reactive oxygen species, DNA base damage (such as deamination, alkylation), ionizing radiation, and ultraviolet rays [1]. Defects in genes that are involved in preventing genomic instability can lead to cancer, cell death, and premature aging; genomic instability is also a hallmark of cancer. A variety of enzymes contribute to the prevention of disease resulting from genes involved in the prevention of chromosome breakage (see Table 1). Defects in genes that prevent chromosome breakage results in severe phenotypes and an increased predisposition to cancer. In humans, defects in three helicases BLM, WRN, RECQ4 (listed in bold in Table 1) result in genetic disorders that lead to premature aging and early development of cancer. The helicases BLM, WRN, RECQL4, are three of the five helicases in humans that belong to the RecQ family of helicases so named after the first discovered in *E. coli*. The RecQ family of helicases has been implicated in DNA recombination and repair, highlighting their importance in maintaining genomic stability and prevention of disease.

Table 1.1 Chromosome breakage syndromes

Syndrome/Disease	Gene in Humans	Cancer Predisposition/ Most common cancer	Defect	Reference
Ataxia telangiectasia	*ATM*	Lymphomas, Leukemias	DNA damage checkpoint	[2-4]
Nijmegen breakage syndrome	*NBS1*	Lymphomas	Double strand break repair	[5-7]
Fanconi anemia	*FANC* genes (A,B,C,D1,D2, E,F,G,J,L,M,N,O,P,Q)	Leukemia, squamous cell carcinoma	Genome Monitoring	[8]
Werner's	***WRN***	Sarcomas	Recombination	[9-11]
Bloom's	***BLM***	Lymphomas, Leukemias		
Rothmund Thomson/ Rapadilino/ Baller-Gerold	***RECQL4***	Osteosarcoma/Lymphoma	DNA replication	

Table adapted from a review by Duker (2002).

Human Disease Linked to Defects in the RecQ helicases

Bloom's Syndrome

Bloom's syndrome (BS) is a rare autosomal recessive disorder as a result of the loss of function of *BLM.* BS was initially described in 1954 by Dr. David Bloom in a case study of a two-year-old patient presenting telangiectatic erythema resembling lupus erythematosus from hypersensitivity to sun exposure, low birth weight, high-pitched voice, and short stature [12]. By 1965, nineteen individuals with the described syndrome were known. Of these patients, most were of Jewish ancestry, and some patients were siblings or had parents that shared common lineage; this led to the idea that this

2

syndrome was inherited. It was also observed that chromosomes in Bloom's patients had increased genomic instability in the form of chromosome breakage, rearrangements, and an observed increase of sister-chromatid exchanges (SCE) something that is still used for diagnosis today [13-15]. Currently, the clinical features of BS are short stature, immune deficiency, insulin resistance, an increased risk for diabetes, low fertility, and an increased risk to develop cancer early in life [11, 16].

Figure1.1 Clinical presentations of Bloom syndrome in individuals. Patient on the right has facial telangiectasias. The patients in the center are siblings with the person to the left positive for Bloom syndrome. Images are from the Bloom syndrome registry, Weill Cornell Medical College.
[17]

BS as a monogenic disorder and only requires the inactivation of the BLM protein as a result of a mutation. The mutation that inactivates BLM in patients varies and is not as a result of a single unique mutation in *BLM.* Instead, some mutations have been found in BS patients that lead to a premature stop codon, truncated protein, or inactivation of the catalytic function of BLM [17]. BS has been found to be prevalent in the Ashkenazi Jewish population with the *blm^Ash* (6-bp deletion and 7-bp insertion at nucleotide position 2281) mutation being the most common BS causing mutation [18, 19].

In *C. elegans*, the loss of function of the BLM ortholog, Him-6 has adverse effects on lifespan, increased germline apoptosis, mortal germ-line phenotype, IR sensitivity, and low brood size, all linked to genomic instability [20, 21]. In mouse, the BLM^{-/-} mutation is embryonic lethal and has been shown to increase apoptosis during embryogenesis [22]. Mice containing a loss of function mutation in BLM that was not lethal were created and found to have an increased predisposition to cancer. In this study, the mice heterozygous for a loss-of-function mutation in BLM developed more metastatic T-cell lymphomas after injection with murine leukemia virus. The *BLM^{-/+}* mice were crossed to mice that were heterozygous for the *Apc[Min/+]* mutation, a mutation known to mediate intestinal tumorigenesis, and more intestinal tumors were observed in the *B[LM-/+]* than the *Blm^{+/+}* mice. Moreover, the non-mutant allele of BLM allele was found to be functional in these tumors suggesting *BLM* haploinsufficiency [23]. Interestingly, *BLM* haploinsuffinciency in the formation of colorectal cancer has also been implicated in humans heterozygous for *blm[Ash]* [24].

Functionally, BLM is a helicase with 3′-5′ polarity, and it is expressed highly in S/G2 phase of the cell cycle [25-27]. BLM is expressed in the thymus, testis, and spleen and localizes at promyelocytic leukemia (PML) bodies and telomeres [28-30]. BLM is known to function in resection of DNA double-strand breaks (DSB) and has a role in dissolving recombination intermediates and functions in a complex with Top3α, Rmi1, and Rmi2 to dissolve double Holliday junctions (dHJ), as well as the reversal of D-loops coated with Rad51 *in vitro* [31-34]. BLM is a target for the checkpoints ATM and ATR and is phosphorylated at residues T99 and T122 [35-38]. Cells treated with hydroxyurea (HU) have stalled replication. Cells that have a BLM mutant unable to be

phosphorylated fail to recover from HU treatment and stall at the G2/M checkpoint. It was also shown that this BLM mutant had no effect on sister chromatid exchange frequency, leading to the idea that BLM is necessary for replication to restart [35, 37]. Besides, it has been shown *in vitro* that BLM can catalyze replication fork reversal, a mechanism suggested to promote lesion bypass [39, 40].

Werner Syndrome

Werner syndrome (WS) is a rare autosomal recessive disorder linked to defects of the RecQ helicase WRN. Werner syndrome is considered adult progeria disorder [41]. Otto Werner first described WS in his doctoral dissertation on the presentation of cataracts with scleroderma observed in four out of five siblings in a single family. The parents of the patients appeared normal, and one sibling (and her three children) did not display the characteristics of premature aging that the other siblings exhibited. Otto Werner compared this case with those described previously by Rothmund in 1868. Between 1934 and 1941 Oppenheimer and Kugel, both internists had assigned Werner syndrome to the described disease, and in 1996 Epstein *et al.* distinguished WS from what was later designated Rothmund-Thompson Syndrome (RTS), another syndrome that results from the dysfunction of another RecQ helicase, RecQL4 [41-44].

WS does not typically present symptoms until after the patient is ten years old and diagnosis must meet the criteria either of all cardinal symptoms or just three of the cardinal symptoms and genetic confirmation. Suspected cases are those that present at least two of the cardinal symptoms and at least two additional symptoms that are not as common in all WS patients.

Cardinal symptoms were categorized in a survey of WS patients as those that appear early and are likely found in >75% of WS patients. Cardinal symptoms include progeroid changes of hair, cataracts, skin ulcers, soft tissue calcification, bird-like face, and abnormal voice (hoarse, high-pitched, squeaky). The list of symptoms that are not as prevalent across all WS patients but are used for diagnosis is abnormal glucose or lipid metabolism, bone deformation or abnormalities, cancer, parental consanguinity, premature atherosclerosis, hypogonadism, and short stature [41, 45]. Genetic testing is now included as part of diagnostic criteria to help distinguish WS from other syndromes caused by defects in other RecQ helicases due to the common symptoms they share. Genetic testing can help distinguish the syndromes based on the defects in BLM (BS), RECQL4 (RTS) [41, 45] as well Hutchinson-Gilford progeria syndrome, which is caused by the mutation of *LMNA,* a gene that codes for a component of the nuclear envelope, not a RecQ-helicase [46].

Figure 1.2 Accelerated aging of an individual with Werner syndrome.   Individual with Werner syndrome at ages thirteen, twenty-one, forty-eight, and fifty-six (from left to right) exhibits signs of accelerated aging. Image from the University of Washington.

Similar to its RecQ family member, BLM, defects in WRN lead to an increased predisposition to cancer, in particular sarcomas, and increased cellular defects associated with genomic instability. WRN structurally shares all the domains in BLM except the strand exchange domain, and instead, the N-terminus contains a 3′-5′ exonuclease domain only found in its homolog in *X. laevis*, *FFA-1* (Figure 1.4) [47]. Over seventy mutations in WRN have been identified in WS patients, a majority resulting in a premature stop codon, insertions/deletions, genomic rearrangements, missense mutations, or splicing defect resulting in a functionally null WRN protein [48].

In mice, the knockout of *WRN* did not appear to age prematurely, although Lebel et al. reported that two male mice had extensive myocardial fibrosis at ten months and a female developed T cell lymphoma at 13.5 months not observed in the control mice [49-51]. When *WRN$^{-/-}$* mice were crossed to have a defect of the RNA in telomerase, age-related defects were observed such as graying hair, alopecia, osteoporosis, type II diabetes, cataracts, and premature death [52, 53].

Functionally, WRN function has been implicated in different DNA repair pathways. WRN physically interacts with the tumor suppressor P53. It is believed in cells under replication stress, the physical interaction of WRN and P53 is vital in regulating WRN exonuclease activity and helicase activity at Holliday junctions [54-57]. WRN deficient cells are sensitive to DNA damaging agents camptothecin (CPT), 4-nitroquinoline 1-oxide (4-NQO), and MMS [58, 59].

In yeast, while human BLM can complement the *sgs1Δ* defect of the slow growth in cells lacking Top3, WRN was not capable of complementation [60]. In other organisms, WRN homologs have many functional differences. In *Xenopus* egg extracts,

the WRN homolog FFA-1 accumulates on the chromatin following replication arrest and the induction DNA double-strand breaks while the BLM homolog, xBLM only slightly increased under these conditions [61]. WRN in *Xenopus* also plays a more dominant role than human WRN in DNA break end resection [62, 63]. In humans, WRN appears to play a role in resection with BLM. In mouse, WRN is found only in the nucleoplasm and does not have the NLS found in human WRN that is necessary for nucleolar localization [64], and as *WRN*$^{-/-}$ mice appear to develop normally, it is unsurprising that this would not show any defects. In mice, the localization does not seem to play a role in its function whereas in humans mutations that truncate the NLS in WRN are known to cause WS [64, 65]. Together this highlights an important role for WRN in humans and the differences in function in other organisms.

Rothmund-Thomson Syndrome

Rothmund-Thomson Syndrome (RTS) is a rare autosomal recessive genetic disorder caused by defects in the RecQ helicase RECQL4. Patients with RTS exhibit a characteristic face rash, Poikiloderma, as well as a combination of features including short stature, alopecia including eyelashes and eyebrows, juvenile cataracts, skeletal abnormalities, a predisposition to osteosarcoma and malignant tumor originating in bone, as well as premature aging (figure 1.3) [66-68]. RTS was first reported by in 1868 by German ophthalmologist Rothmund. In 1936, the English dermatologist Thomson had three similar patients that displayed Poikiloderma, short stature and had skeletal defects, including bilateral thumb aplasia and hypoplastic radii and ulnae, and unlike the previously reported case, these patients did not have cataracts [66]. In 1957, the name 'Rothmund-Thomson syndrome' was adopted after three other patients with the

described clinical features were reported by Taylor [69]. RAPADILINO and Baller-Gerald syndrome (BGS) are also associated with recessive mutations in the RECQL4 gene. Baller-Gerold syndrome is characterized by radial hypoplasia and craniosynostosis. RAPADILINO is mainly observed in Finland, and the name of the syndrome is derived from the clinical features of *RA*dial hypoplasia, *P*atella hypoplasia and cleft or *A*rched palate, *DI*arrhoea and dislocated joints, *LI*ttle size and limb malformation, slender *N*ose and n*O*rmal intelligence [70-73].

The molecular basis of the defects in RECQL4 that lead to RTS is yet to be elucidated. Over 50 mutations of *RECQL4* are known to be associated with the development of RTS, and four are either RTS and RAPADALINO, or RTS and BGS associated [74-77]. These changes result in missense mutations, resulting in premature stop codons, frameshift from insertion/deletion mutations, and mutations that cause mis-splicing alterations.

Knockout mice that disrupted exons 5–8 were embryonic lethal between 3-6 days. When knockout mice were generated by deleting exon 13, a coding exon of the helicase domain, the mice were viable, but only 5% survived two weeks. The survivors exhibited severe growth defects, abnormalities in several tissues including skin and bone defects, as well as impeded cell division [78]. The knock-out mice exhibit RTS phenotypes in seen humans, making them an excellent model to study the molecular defects. In another study, a viable Recql4 mutant mouse was created by replacing a 1075 bp fragment spanning from within exon 9 through exon 13, a mutation located in the helicase domain, with a PGKHprt mini-gene. Fibroblast from this knockout mouse displayed an increase in genomic instability in the form of aneuploidy, premature

chromosome separation, and an increase of spontaneous micronuclei. It was also suggested that a cohesion defect contributes to the chromosomal instability [79]. These mouse studies indicate that function of RECQL4 resulting from specific defects in DNA repair mechanisms and can be explored in mice as they mimic the defects observed in humans.

Figure 1.3 Clinical features of patients with Rothmund-Thomson Syndrome. The individual on the left shows the characteristic facial rash Poikiloderma. The individual in the center panel is 21 years old and has Poikiloderma with alopecia. The right panel illustrates the hand of an individual with RTS that has thumb aplasia. Images are from Larizza 2010 [66].

RecQ family of helicases

RecQ helicases unwind DNA from 3'-5' and belong to the SF2 family of helicases. In *S. cerevisiae, S. pombe,* only have a single known RecQ-like helicase Sgs1, and Rcq1, respectively. The number of RecQ-like helicases varies in single and multicellular organisms as is illustrated by the number of different homologs found in humans (BLM, WRN, Recql1, Recql4, Recql5) and *C. elegans* (HIM-6, WRN-1, RECQ1, and RECQ5) [80, 81]. RecQ helicases are defined by a conserved helicase domain consisting of seven helicase motifs [82, 83]. Outside of the helicase domain both the length and domains of the N and C-terminus vary between species. In the founding member RecQ in *E. coli*, there are two additional domains the RecQ-carboxy-terminal

(RQC), unique to RecQ family members, and the Helicase and RNase D C-terminal (HRDC). The RQC and HRDC domains are not found in all members of the RecQ helicases in other organisms, and conversely, RecQ helicases have domains not found in the founding member, *E. coli* RecQ for example in humans, WRN also has an exonuclease domain and nuclear localization signal (see Figure 1.1).

610	*E. coli*	RecQ
1432	*H. sapiens*	WRN
1417	*H. sapiens*	BLM
1208	*H. sapiens*	RECQL4
649	*H. sapiens*	RecQL1
991	*H. sapiens*	RecQL5β
1447	*S. cerevisiae*	Sgs1
1328	*S. pombe*	Rqh1
1436	*X. laevis*	FFA-1
1367	*X. laevis*	xBLM
1056	*C. elegans*	WRN-1
998	*C. elegans*	HIM6/BLM1
801	*C. elegans*	RCQ-5

Strand exchange domain | Helicase domain | HRDC domain
Exonuclease domain | Acidic domain | RQC domain
Nuclear localization signal

Figure 1.4 RecQ helicase conservation in unicellular and multicellular organisms. The helicase core is the most conserved domain containing motifs for ATP binding and hydrolysis. Many RecQ family members contain the RecQ C-terminal (RQC) domain, the conserved helicase and RNase D C-terminal (HRDC). WRN, BLM, and RECQL1 contain a nuclear localization sequence. WRN has an exonuclease domain.

Initially discovered in a search for mutants that resist thymine starvation, *E. coli* RecQ was found to be involved in the RecF pathway. The *recq* mutant was described to be defective in recombination and sensitive to UV-induced damage [84]. The crystal structure of *E. coli* RecQ and human BLM and WRN have revealed the structure of the helicase, RQC, and HRDC domains. This revealed two regions that form a cleft containing an ATP-binding site in the helicase core and opposite that, on the cleft, is a ssDNA binding site. After the seven helicase motifs is a zinc-binding domain that contains four conserved cysteine residues, and a winged-helix for DNA binding, helix-hairpin-helix, β motif that forms the RQC domain that together is required for catalytic function [85]. All mutations in BS patients have been described to inactivate in the catalytic function of BLM or lead to premature protein-translation termination [17].

The HRDC domain is found in some members of the RecQ helicases. It is not required for enzymatic function, and exact function of the HRDC has yet to be elucidated. In *S. cerevisiae* (Sgs1) and *E. coli* (RecQ), the HRDC domain was capable of binding ssDNA, but human BLM and WRN were not found to have this capability *in vitro* [86-90]. The function of the HRDC domain may be different in various organisms, as is implicated by the reduced conservation. In human BLM, the HRDC domain has been found to be required for dissolution of Holliday Junctions, recruitment of BLM and WRN to DSBs, and induced DNA damage by methyl methanesulfonate (MMS) and mitomycin C [91, 92].

Sgs1 in *S. cerevisiae* and BLM in humans have a domain in the unstructured N-terminus that has been shown to interact with single strand DNA, has strand exchange

capability *in vitro,* and the function of which will be discussed with the role of complex

formed by Sgs1 with Top3-Rmi1 [93].

RecQ-like helicase Sgs1 in *Saccharomyces cerevisiae.*

Yeast has been utilized as a model organism to study RecQ helicase function in

its role to protect the genome [80]. Sgs1, the only RecQ helicase in *S. cerevisiae,* was

discovered as a suppressor of the slow growth phenotype observed in *top3Δ* mutants

and subsequently identified as a possible BLM homolog [94, 95]. Sgs1 function in

maintaining genomic stability is diverse and has been shown to work in both

recombinogenic and anti-recombinogenic capacity to promote repair and prevent

illegitimate recombination as well. Thus far, Sgs1 is known to play a role in both early

and late recombination repair of DNA breaks, the start of stalled replication forks,

telomere maintenance, and in meiotic recombination [96-99]. Cells lacking Sgs1 are

sensitive to irradiation (IR) damage, DNA damaging agents, have increased

accumulation of gross chromosomal rearrangements [100-104].

Sgs1 substrates and physical interaction partners.

Sgs1 preferentially binds specific DNA structures and physically interacts with

many DNA repair proteins. Sgs1 has been found to preferentially bind forked DNA,

DNA with 3′ ssDNA overhangs, and G4-quadruplexes; it also binds blunt-ended duplex

DNA with less affinity than the other DNA structures tested *in vitro* (Figure 1.2). Sgs1

can unwind these structures as well as Holliday junctions and DNA structures that

contain a bubble [97, 105-110]. Sgs1's ability to unwind these structures *in vitro*

demonstrates its enzymatic capabilities in both its recombinogenic and anti-recombinogenic functions.

RecQ helicases in other organisms demonstrate varying capability to unwind different DNA structures (Table 1.2). In humans, BLM has also been found to bind and unwind the same structures as Sgs1 and additionally been found to unwind D-loops, and Rad51-coated strand invasion structures *in vitro* [106]. The differences in the ability of different RecQ helicases in different organisms may be due to the differences in domains. For example, in humans, WRN has an exonuclease domain that appears to be absent in *C. elegans.* Wrn-1 in worms seems to have an additional function especially in the context of unwinding D-loops. Human WRN, in addition to unwinding, also recognizes the 3′ invading strand and the exonuclease domain can digest it independently of the helicase function. Much is left to be elucidated about the recombinogenic, and anti-recombinogenic functions in the RecQs across various organisms and additional analysis of their enzymatic activities on the same substrates would assist in the interpretation of phenotypes associated with genomic instability.
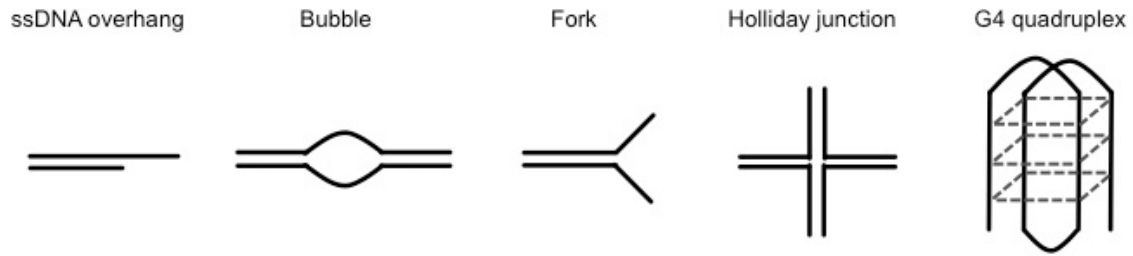
Figure 1.5 Sgs1 preferential DNA substrates.
Representative figures of DNA substrates Sgs1 has been shown to unwind. It has been reported that Sgs1 can most efficiently unwind the Holliday junction, followed by the forked and ssDNA overhangs. Sgs1 can also unwind bubble and G4 quadruplex structures. This figure has been adapted from (Larsen and Hickson, 2013).

Table 1.2. RecQ -like Helicases Unwind a Variety of DNA Structures

Substrate	*E.coli* RecQ	*S. pombe* Rqh1	*S. cerevisiae* Sgs1	*D. melanogaster* DmBlm	*C. elegans* Him-6	Wrn-1	*H. sapiens* BLM	WRN	RECQL1	RECQL4	RECQL5β
dsDNA	+	+	+	n.d.	-	+ RPA	-	-	-	n.d.	n.d.
3′ overhang	+	n.d.	+++	+	+	+	+	+	+ +	+	n.d.
3′ overhang DNA RNA hybrid	n.d.	n.d.	+	n.d	n.d.	n.d.	+	+	-	n.d	n.d.
5′ overhang	+	n.d.	+	~/-	-	-	n.d.	n.d.	~/-	-	n.d.
5′ flap	n.d.	n.d.	n.d.	n.d.	n.d.	+	n.d.	+	n.d	n.d	n.d.
Holliday Junction	+	n.d.	+++	n.d.	n.d.	+	+++	++	+	-	+RPA
Y structure	+	n.d.	+++	++	++	+	+RPA	+	++	+	+RPA
D-loop	++	n.d.	+++	n.d.	n.d.	+	+	+	n.d.	-	n.d.
Telomeric D-loop	n.d	n.d.	+	n.d.	n.d.	n.d.	+	+	+	+	-
G4 Quadraplex	+	n.d.	+	n.d.	n.d.	n.d.	+++	+++	-	-	n.d.
Bubble	n.d.	n.d.	+	n.d.	n.d.	+	+	+++	+	-	n.d.

Gray cells indicate an ability to bind the DNA structure with increased affinity from lightest to darkest gray.

White cells are structures not tested for binding affinity to that DNA structure.

n.d. – Ability to unwind was not determined.

~/- indicates a partial ability to unwind the DNA structure.

+RPA indicates unwinding was either only observed with the addition of RPA or is stimulated in the presence of RPA.

Table was compiled from supporting data from these sources [25, 32, 33, 40, 97, 105-151]

Sgs1 also interacts with many DNA metabolic factors involved in DNA repair. Mlh1, a factor involved in the repair of base mispairs generated during DNA replication has been found to physically interact with Sgs1, and this interaction is conserved in human BLM [152, 153]. The Mlh1 interaction was shown via yeast-two-hybrid with both human and yeast Mlh1.

The N-terminus of Sgs1 is unstructured and is not required for the catalytic function [242]. The N-terminus of Sgs1 has been implicated in strand exchange and physically interacts with Top3 in a complex with Rmi1. The complex of Sgs1/Top3/Rmi1 is conserved in humans as the BLM-TOP3α-RMI1/RMI2 [94, 154-157]. The Sgs1/Top3/Rmi1 complex is known to function late in homology-mediated repair to dissolve recombination intermediates to result in non-crossover products [97, 114, 158-160]. Sgs1 was initially found to suppress the slow growth phenotype of a *top3Δ* mutant and as has also been shown Sgs1 to help produce the recombination substrate that requires Top3 [94].

The single strand binding protein, RPA, has been shown to physically interact with Sgs1 *in vivo* and *in vitro* in the acidic region of the N-terminus [161]. RPA is known to stimulate BLM and WRN in humans [147] and Sgs1 in yeast *in vitro* [162] as well as preventing reannealing of ssDNA [163, 164].

Via yeast-two-hybrid and co-immunoprecipitation, it was found that another DNA helicase physically interacts with the N-terminus of Sgs1, the anti-recombinase Srs2 [165]. *SGS1* and *SRS2* also genetically interact as shown by the severe growth defect of cells lacking them both [166, 167], a defect that is dependent on recombination protein Rad51 [168]. It is thought that in the absence of Sgs1, recombination

17

intermediates accumulate and Srs2 dismantles the Rad51 filament that generates these recombination intermediates that if left unresolved are toxic [168-173]. Rad51 was also found to interact with the C-terminus of Sgs1 via yeast-two-hybrid, and in humans, this interaction also occurs between Rad51 and BLM at both the N- and C-terminus [174].

DNA double-strand break repair

Two pathways are known to repair dsDNA breaks, nonhomologous end-joining (NHEJ) and homologous recombination (HR). Sgs1 is known to function in both early and late steps of HR repair, and its function determines the end repair product. NHEJ repairs a break by ligating the two ends of the break indiscriminate of homology and loss or gain of a few nucleotides in this process together makes this process to be regarded as error-prone [175]. Repair by NHEJ is the preferred method of repair in G1 as there is no sister chromatid to use as a template for HR repair [176-179]; thus, HR repair is the preferred mechanism of repair during S/G2 phases.

Common early steps of HR repair of DNA double-strand breaks

In *S. cerevisiae*, once a DNA double-strand break occurs it is believed that there is competition between the non-homologous end joining pathway proteins (Ku70/80 from here on called Ku complex) and the Mre11-Rad50- Xrs2 (MRX) to bind to the break ends [180, 181]. The prevention of repair by NHEJ is achieved by the small range resection of the break by the MRX complex in yeast with the additional help from Sae2 to remove the Ku complex from the DNA ends [182-184]. Phosphorylation of Sae2 by cyclin-dependent kinase Cdc28 to promote MRX function in end resection has been

18

shown *in vitro* and *in vivo* although the exact mechanism of how Sae2 stimulates MRX function is yet to be elucidated [176, 177]. Resection by MRX/Sae2 leaves ~100-200 nucleotide 3′ overhangs that are then coated by ssDNA binding protein RPA to promote HR repair [185-188]. Stimulation of MRX activity has been suggested to also be necessary for the removal of MRX as it has been shown in the absence of Sae2, Mre11 is persistent at DNA ends and as a result regulation of the DNA damage checkpoint is defective [189, 190]. In humans, the MRX complex is MRN (Mre11-Rad50-Nbs1) and functions similarly to MRX, and defective Nbs1 is associated with the Nijmegen breakage syndrome [5-7].

Following short-range resection by MRX, Sgs1/Dna2, and Exo1 are recruited to the RPA coated 3′ single-strand DNA and redundantly resect leaving 2000-6000 nucleotide 3′ overhangs that will be used in the search for homology [162, 185, 191, 192]. Sgs1 acts a helicase providing the substrate for Dna2 endonuclease activity to cleave the unwound DNA while Exo1, a 5′-3′ exonuclease, redundantly resects the DNA ends without the need of a helicase [185, 193-195]. Sgs1 and Dna2 have also been shown to physically interact *in vitro.* The Sgs1/Dna2 physical interaction has not been mapped to specific domains of the proteins but the function if the interaction has been determined to be preferential degradation of the 5′ strand by Dna2 [196]. Loss of Sgs1 and Exo1 prevent any long-range resection, and the *sgs1Δ exo1Δ* mutant is hypersensitive to DNA damaging agents and has a high rate of gross chromosomal rearrangements as a result [192]. The long-range resection by Sgs1 and Exo1 produces the ssDNA substrate that allows for Rad51 filament strand invasion to continue homology-directed repair.

In the case of partial or incomplete long-range resection of HO-induced DNA breaks, recombination can still occur but can lead to aberrant repair by *de novo* telomere addition and break-induced replication [197, 198]. Recently, in the case of IR-induced breaks during the G2 cell cycle phase, repair by recombination still occurs in the absence of Sgs1 and Exo1 resection and is not repaired by *de novo* telomere addition [199]
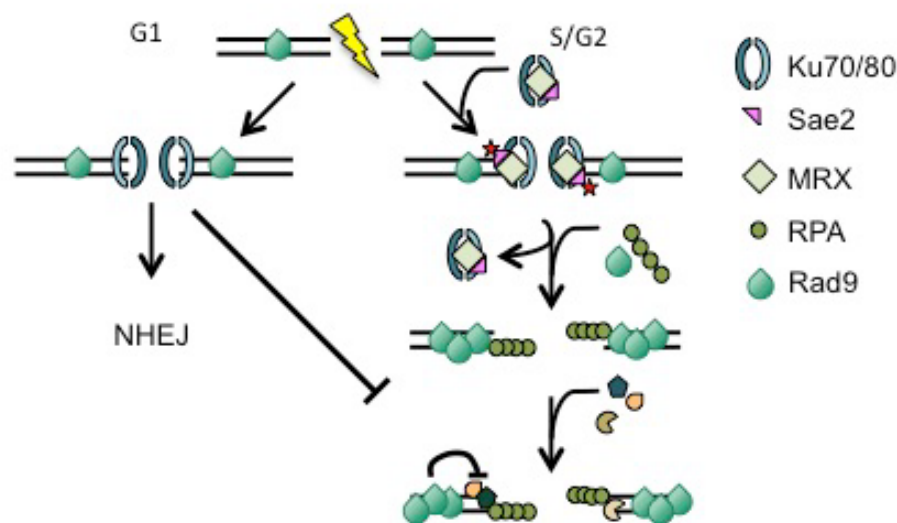
Figure 1.6 Early steps of DNA double-strand break repair. Rad9 is bound to DNA in the absence of DNA damage but accumulates at DNA breaks. In the event of a DSB during G1, Ku complex binds the DNA end, committing repair to NHEJ and preventing HR repair. During S/G2 both Ku and the MRX complex competitively bind the end of the DNA break. Sae2 is phosphorylated by Cdc28 (not shown) stimulating end processing by MRX, liberating both Ku and the MRX complex from the DNA ends. This end processing leaves a small 3′ DNA substrate that is quickly coated with single-strand binding protein RPA and is further processed by Sgs1/Dna2 and Exo1 leaving longer 3′ overhangs to be used in the homology search in HR repair. Rad9 accumulates following the DNA break and creates a physical obstacle that regulates Sgs1 mediated end resection.

Regulation of Sgs1 and Exo1 resection is still not well understood, but a few mechanisms stimulate and inhibit their role in end resection. Ku complex bound DNA ends have been found to prevent Exo1 mediated end resection *in vitro* and loss of Ku has been found to suppress resection defects in cells lacking resection by MRX/Sae2 [181, 183, 200]. It is also suggested that MRX and Sae2 recruit Exo1 to the break and in humans [201], BLM has been shown stimulates Exo1 activity [192, 202]. RPA is known to stimulate the resection activity of Sgs1 *in vitro* and is required for extensive end resection *in vivo* [196]. More recently in humans a novel protein, DNA helicase B (HELB), has been identified in control of resection during G1 through its physical interaction with RPA although the exact mechanism is yet to be determined [203]. The checkpoint adapter protein Rad9 is known to be bound to DNA even in the absence of DNA damage but in the event of a dsDNA breaks more Rad9 is recruited to the DNA ends and is suggested to create a physical barrier for Sgs1 function [204-206].

HR directed repair following Sgs1 and Exo1 resection of DNA ends

Sgs1 plays a role later in HR in promoting noncrossover repair products (Figure 1.4). Following resection, Rad51 displaces RPA on the 3′ single-strand DNA. Rad51 is recruited by Rad52 to form the presynaptic filament [207-209]. The Rad51 filament is then stabilized by Rad55/57 in preparation for strand invasion for the homology search [210, 211], which is assisted by Rad54 in stabilization in forming the D-loop [211, 212]. Srs2 can reverse strand invasion at this point to prevent aberrant repair, and this coincides with the genetic interaction observed in *sgs1Δ srs2Δ* mutant since recombination intermediates that are formed are unable to be reversed or dissolved

[166, 168, 213]. Following strand invasion, synthesis-dependent strand annealing can occur that requires Sgs1 to displace the new strand, a function dependent on its helicase function, to allow annealing and the removal of the flap [214]. If a second end is captured a double Holliday junction (dHJ) is formed and as the dHJs converge it forms a hemicatenane that is dissolved by the Sgs1/Top3/Rmi1 complex [114, 160] Dissolution of the HJ requires Top3, and *top3Δ* mutants are slow growing. Slow growth of *top3Δ* is suppressed with the loss of Sgs1 as it is involved in the early steps that allow for HJs for form [94]. In *C. elegans*, the loss of Top-3α in *him-6* worms rather than suppressing chromosomal aberrations resulted in more significant defects, including chromosomes in the gonad that appeared to be clumped together and first filial generation of worms were expectedly sterile. It was found by the same group that Top3-α and Him-6 physically interact and either the N- or C-terminus of Him-6 is enough for this interaction to occur. These similarities and differences from yeast and worm indicated that while these are conserved interactions, there are differences in how they function [215]. In the absence of Sgs1 endonucleases such as Yen1 can resolve the dHJ and this results in a half of the repair products as non-crossovers and half as crossovers [216, 217].

The role of Sgs1 at stalled replication forks

In *S. cerevisiae,* the *sgs1Δ* mutant is highly sensitive to the DNA damaging agents HU and MMS that stall replication forks [60]. It has been shown that Sgs1 physically interacts with Rad53 *in vitro* and *in vivo* [161, 218] in cells treated with hydroxyurea and this activates Rad53's kinase activity, an event independent of Sgs1

helicase function. The activation of the checkpoint in MMS treatment appears to be regulated differently than what is observed in HU-treated cells, as Top3 and Rmi1 were not required for this activation in HU but are necessary for full activation of Rad53 in MMS treated cells [169, 219]. Sgs1 is also implicated in error-free damage bypass at stalled replication forks by template switching and regressed forks as the intermediates resemble those Sgs1 is known to dissolve in the homology-mediated repair of double-strand breaks [220].
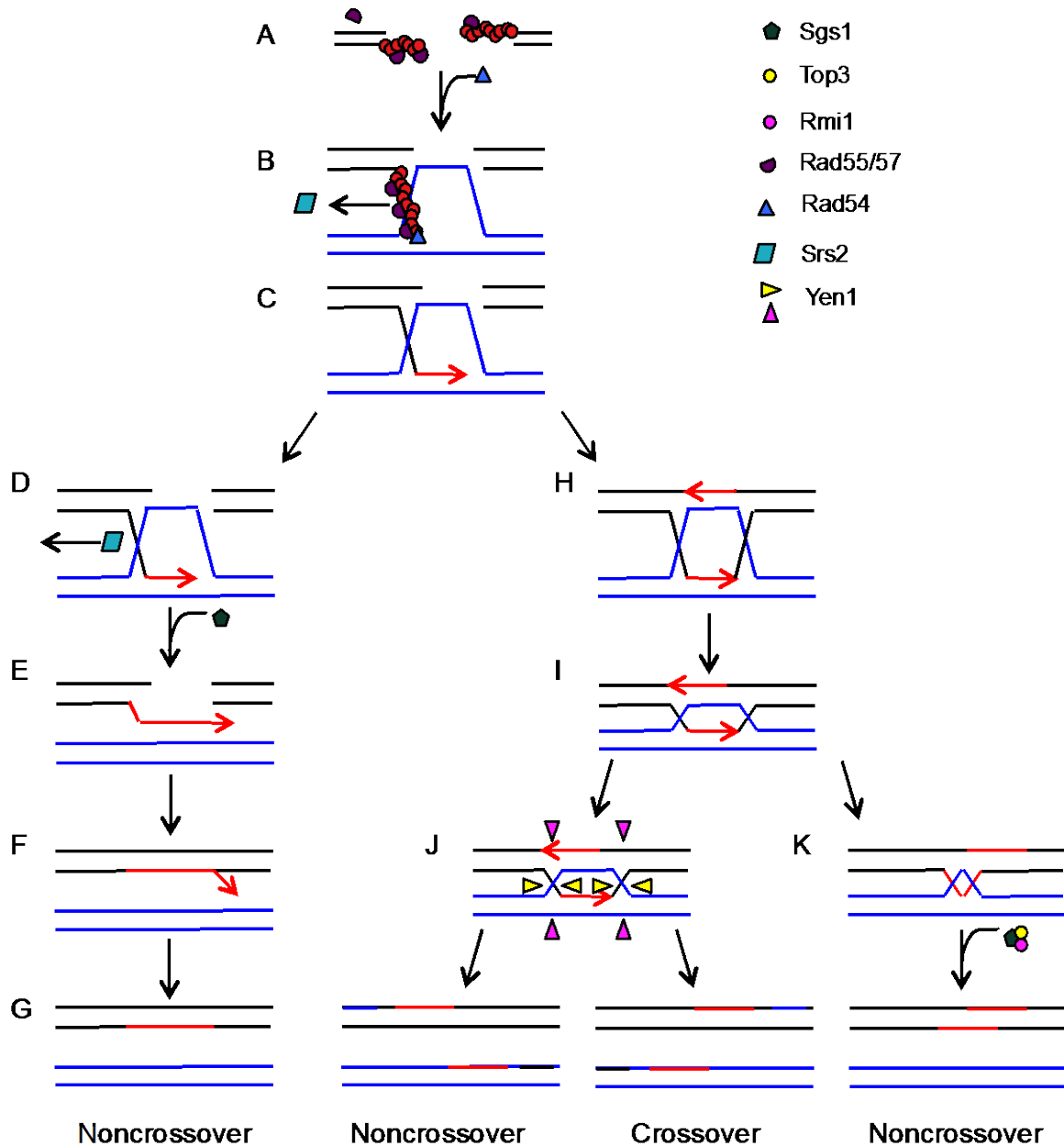
Figure 1.7 Role of Sgs1 in late steps of homology-mediated repair.
(A) The Rad51 filament coating the 3′ single-strand DNA ends are stabilized by Rad55 and Rad57 (B) which is then assisted by Rad54 to form the (C) D-loop for the search for homology and DNA synthesis can occur. The D-loop structure that can be reversed by Srs2 (D). (E) Synthesis-dependent strand annealing, Sgs1 can displace the invading strand which then can be annealed, the flap removed and ligated (F) to form a noncrossover repair product (G). If a second DNA end is captured, a double Holliday junction is formed (H). The two branches migrate toward each other (I) and can either be cut by an endonuclease such as Yen1 (J) resulting in half crossover and have noncrossover products or form a hemicatenane that is then dissolved by the Sgs1-Top3-Rmi1 complex.

24

The role of Sgs1 in meiosis

Sgs1 has a role in meiosis. Diploids homozygous for the deletion of *SGS1* can complete meiosis, but it takes a longer amount of time to complete meiosis than in wildtype cells and produces fewer viable tetrads, indicating a role for Sgs1 in meiosis [221, 222]. It was, also shown that there is an increase in nondisjunction in this mutant, as was observed in a red/white colony sectoring assay where the color of the colonies formed indicate chromosome loss and nondisjunction [222]. Truncation studies of the C-terminus have indicated that the helicase domain is dispensable for Sgs1 function in meiosis [103]. *SGS1* and *MLH1,* a gene encoding a protein involved in mismatch repair, have a genetic interaction indicating a role in the resolution of joint molecules in meiosis. In a recent study, it was shown that in conjunction with Exo1, Mlh1 promotes joint molecule resolution to produce crossover products with Sgs1 while Sgs1 alone produces non-crossover products. Interestingly, Mlh1 physically interacts with the C-terminus of Sgs1 in the region previously found to be dispensable for Sgs1's role in meiosis, indicating that the physical interaction of Sgs1 and Mlh1 is not required for its role in meiosis. Even with the loss of the nucleases known to act in joint molecule resolution into crossover and non-crossover products [152], Sgs1 could still carry out some of this function. In the absence of nucleases Yen1, Mus81-Mms4, Slx1-Slx4, crossover products still form but joint molecule resolution is dependent on Sgs1 in this context [223].

DNA repair exonuclease, Exo1

Functions of Exo1 in mismatch repair

Exo1 is a 5′→3′ exonuclease belonging to the Rad2p family of nucleases that are characterized by their N-terminal and Internal nuclease domains, sequence identity, and structure specificity. The Rad2p family is divided into three classes categorized by the amino acid identity and positions of the blocks of homology; *EXO1* is in the third class with the most amino acid similarity to the other family members contained in the N-terminal and Internal catalytic domain [224, 225].

Yeast Exo1 was initially discovered in *Schizosaccharomyces pombe* in a search for recombination proteins induced in cells undergoing meiosis and was subsequently found by the same group to be a protein involved in mismatch repair [225, 226]. While investigating Exo1's role in meiosis, Szankasi and colleagues observed a mutator phenotype in an *exo1Δ* mutant generated in an *ade6-* strain. The ade6- strains, grown on adenine limiting media typically appear as red colonies and the *exo1Δ* mutant had the frequent appearance of white colonies despite being confirmed as *ade6-*. The mutator phenotype seen in the *exo1Δ* mutant in the *ade6-* background implied mutations in genes upstream of *ade6-* in the adenine pathway, possibly due to a defect in mutation avoidance. At the time, no eukaryotic exonucleases had been found to play a role in mismatch repair. Following this discovery, the *S. cerevisiae* homolog of *S. pombe, EXO1,* was identified. Further identification of Exo1 in mismatch repair was found via Yeast-two-hybrid and co-immunoprecipitation as Exo1 physically interacts with Msh2 and Mlh1. There was also an epistatic relationship of the *exo1Δ msh2Δ* mutant in the rate of spontaneous mutations observed in the *msh2* mutant [152, 227]. Human *EXO1*

was identified, and the physical interaction of human Exo1 and Msh2 was observed and linked to mismatch repair [228, 229]. Following the discovery of *EXO1*'s role in mismatch repair, it was further characterized by Tran, Erdeniz, Dudley, and Liskay [194] by identifying phenotypes associated with the enzymatic function of Exo1. Th *exo1Δ* mutants were found to be sensitive to the DNA alkylating agent MMS, and a mutator phenotype was observed in the *exo1Δ* mutant as well as the nuclease deficient mutant that was dependent on Exo1's enzymatic function.

Regulation of Exo1 in response to DNA damage

Uncapped telomeres appear as a one-sided break, and the MRX complex binds the telomere preventing Ku from binding. MRX in this instance, unlike its role at double-strand breaks, instead of stimulating Exo1 activity it prevents Exo1 activity and recruits telomerase instead [230, 231]. It has been observed in yeast that Exo1 activity is negatively regulated by Mec1-dependent phosphorylation of four serine residues (372, 567, 587, 692) found in the C-terminus [232]. The serine residue 372 was also found in a screen for phosphorylated sites in response to MMS treatment [233]. In humans, nine phosphorylation sites (S376, S422, T581, S598, S623, S639, S660, S674, S746) have been identified in the C-terminus of Exo1 in cells that are untreated, and three (S454, T621, S714) that are suggested to reduce Exo1 protein stability in response to stalled replication forks, IR and CPT-induced DSBs [234, 235]. Phosphorylation of the C-terminus of Exo1 is also associated with regulation of Exo1 resection at stalled replication forks and sites of DNA damage by a physical interaction with 14-3-3 proteins in humans and yeast, and this inhibits the association of Exo1 at the site of damage

27

[236, 237]. In humans, it was found that PCNA physically interacts with the C-terminal end of Exo1 and this association contributes to the processivity of Exo1 resection at DNA double-strand breaks [238]. The stimulation of Exo1 mediated resection by RPA has also been proposed as a mechanism to promote repair [195, 199]; however, more recently it has been shown that other single-strand binding proteins regulate Exo1 resection differently. Other groups have looked at regulation of Exo1 resection and found, in humans, the single-strand DNA binding complex SOSS1 helps recruit Exo1 to DNA and RPA removes Exo1 [239, 240]. While both groups used *in vitro* assays one group looked at the cycling of these proteins over time on DNA through single-molecule imaging and found that the removal of Exo1 by RPA occurs with both human RPA and yeast RPA, and the recruitment of Exo1 by SSOS1 was observed only for human Exo1 [239].

In yeast, the loss of replication fork stability in *rad53Δ* mutants when challenged with DNA damaging agent requires Exo1 function for sensitivity. Exo1 resection could be responsible for additional damage from aberrant repair initiated by resection and excess single-strand DNA produced by Exo1 modulates the checkpoint response [241].

Hypothesis and Aims

Understanding the underlying mechanisms of proteins involved in protecting genomic integrity is essential in understanding the ability to prevent disease. As the genome is under constant stress from both endogenous and exogenous sources of DNA damage, the capacity to cope relies on DNA repair by many different enzymes that detect and repair the damage. Homology-directed repair is one of two repair pathways

that repair dsDNA breaks and can complete repair through various homology-dependent sub-pathways that share a common step, DNA break end resection. Sgs1 and Exo1 are essential for long-range resection of DNA DSBs and the loss of both leads to substantially increased genome instability. Here we hypothesize that with the loss or dysregulation of Sgs1 or Exo1, additional defects in other repair pathways and interactions will increase genomic instability.

Aim1- We seek to identify the DNA metabolic factors are required for the formation of translocations and characterize the domains of Exo1 in the suppression of GCRs.

Aim2- We seek to identify pathways that promote or suppress genomic instability in cells lacking Sgs1 and Exo1 and identify the role of Exo1 in cells under replication stress.

Aim3-We seek to determine the role of recombination factors in suppressing genomic instability through the physical interaction of Sgs1 and Rad51.

Significance

DNA double-strand breaks are one of the most toxic forms of DNA damage. If they are not repaired accurately this can lead to genome rearrangements, a hallmark of cancer. The exact mechanism of how large genome rearrangements occur and result in disease is not well understood. Determining defects in different repair pathways and the function of DNA metabolic factors in suppressing genomic instability will help

characterize the driving forces of cancer formation, allowing a better understanding of

genetic risk factors leading to disease.

REFERENCES

[1] R.L. Maher, A.M. Branagan, S.W. Morrical, Coordination of DNA replication and recombination activities in the maintenance of genome stability, Journal of Cellular Biochemistry, 112 (2011) 2672-2682.

[2] V.A. Zakian, ATM-related genes: what do they tell us about functions of the human gene?, Cell, 82 (1995) 685-687.

[3] K. Savitsky, S. Sfez, D.A. Tagle, Y. Ziv, A. Sartiel, F.S. Collins, Y. Shiloh, G. Rotman, The complete sequence of the coding region of the ATM gene reveals similarity to cell cycle regulators in different species, Human molecular genetics, 4 (1995) 2025-2032.

[4] K. Savitsky, A. Bar-Shira, S. Gilad, G. Rotman, Y. Ziv, L. Vanagaite, D.A. Tagle, S. Smith, T. Uziel, S. Sfez, M. Ashkenazi, I. Pecker, M. Frydman, R. Harnik, S.R. Patanjali, A. Simmons, G.A. Clines, A. Sartiel, R.A. Gatti, L. Chessa, O. Sanal, M.F. Lavin, N.G. Jaspers, A.M. Taylor, C.F. Arlett, T. Miki, S.M. Weissman, M. Lovett, F.S. Collins, Y. Shiloh, A single ataxia telangiectasia gene with a product similar to PI-3 kinase, Science (New York, N.Y.), 268 (1995) 1749-1753.

[5] R. Varon, C. Vissinga, M. Platzer, K.M. Cerosaletti, K.H. Chrzanowska, K. Saar, G. Beckmann, E. Seemanova, P.R. Cooper, N.J. Nowak, M. Stumm, C.M. Weemaes, R.A. Gatti, R.K. Wilson, M. Digweed, A. Rosenthal, K. Sperling, P. Concannon, A. Reis, Nibrin, a novel DNA double-strand break repair protein, is mutated in Nijmegen breakage syndrome, Cell, 93 (1998) 467-476.

[6] N.G. Jaspers, R.D. Taalman, C. Baan, Patients with an inherited syndrome characterized by immunodeficiency, microcephaly, and chromosomal instability: genetic relationship to ataxia telangiectasia, American journal of human genetics, 42 (1988) 66-73.

[7] C.M. Weemaes, T.W. Hustinx, J.M. Scheres, P.J. van Munster, J.A. Bakkeren, R.D. Taalman, A new chromosomal instability disorder: the Nijmegen breakage syndrome, Acta paediatrica Scandinavica, 70 (1981) 557-564.

[8] P.A. Mehta, J. Tolar, Fanconi Anemia, in: R.A. Pagon, M.P. Adam, H.H. Ardinger, S.E. Wallace, A. Amemiya, L.J.H. Bean, T.D. Bird, N. Ledbetter, H.C. Mefford, R.J.H. Smith, K. Stephens (Eds.) GeneReviews(R), University of Washington, Seattle. GeneReviews is a registered trademark of the University of Washington, Seattle, Seattle WA, 1993.

[9] W.K. Chu, I.D. Hickson, RecQ helicases: multifunctional genome caretakers, Nature reviews. Cancer, 9 (2009) 644-654.

[10] A.J. Ng, M.K. Walia, M.F. Smeets, A.J. Mutsaers, N.A. Sims, L.E. Purton, N.C. Walsh, T.J. Martin, C.R. Walkley, The DNA helicase recql4 is required for normal osteoblast expansion and osteosarcoma formation, PLoS genetics, 11 (2015) e1005160.

[11] C. Cunniff, J.A. Bassetti, N.A. Ellis, Bloom's Syndrome: Clinical Spectrum, Molecular Pathogenesis, and Cancer Predisposition, Molecular syndromology, 8 (2017) 4-23.

[12] D. Bloom, Congenital telangiectatic erythema resembling lupus erythematosus in dwarfs; probably a syndrome entity, A.M.A. American journal of diseases of children, 88 (1954) 754-758.

[13] J. German, R. Archibald, D. Bloom, CHROMOSOMAL BREAKAGE IN A RARE AND PROBABLY GENETICALLY DETERMINED SYNDROME OF MAN, Science (New York, N.Y.), 148 (1965) 506-507.

[14] J. German, L.P. Crippa, D. Bloom, Bloom's syndrome. III. Analysis of the chromosome aberration characteristic of this disorder, Chromosoma, 48 (1974) 361-366.

[15] R.S. Chaganti, S. Schonberg, J. German, A manyfold increase in sister chromatid exchanges in Bloom's syndrome lymphocytes, Proceedings of the National Academy of Sciences of the United States of America, 71 (1974) 4508-4512.

[16] M.M. Sanz, J. German, C. Cunniff, Bloom's Syndrome, in: R.A. Pagon, M.P. Adam, H.H. Ardinger, S.E. Wallace, A. Amemiya, L.J.H. Bean, T.D. Bird, N. Ledbetter, H.C. Mefford, R.J.H. Smith, K. Stephens (Eds.) GeneReviews(R), University of Washington, Seattle. GeneReviews is a registered trademark of the University of Washington, Seattle, Seattle WA, 1993.

[17] J. German, M.M. Sanz, S. Ciocci, T.Z. Ye, N.A. Ellis, Syndrome-causing mutations of the BLM gene in persons in the Bloom's Syndrome Registry, Human mutation, 28 (2007) 743-753.

[18] N.A. Ellis, S. Ciocci, M. Proytcheva, D. Lennon, J. Groden, J. German, The Ashkenazic Jewish Bloom syndrome mutation blmAsh is present in non-Jewish Americans of Spanish ancestry, American journal of human genetics, 63 (1998) 1685-1693.

[19] L. Li, C. Eng, R.J. Desnick, J. German, N.A. Ellis, Carrier frequency of the Bloom syndrome blmAsh mutation in the Ashkenazi Jewish population, Molecular genetics and metabolism, 64 (1998) 286-290.

[20] M.M. Grabowski, N. Svrzikapa, H.A. Tissenbaum, Bloom syndrome ortholog HIM-6 maintains genomic stability in C. elegans, Mechanisms of ageing and development, 126 (2005) 1314-1321.

[21] C. Wicky, A. Alpi, M. Passannante, A. Rose, A. Gartner, F. Muller, Multiple genetic pathways involving the Caenorhabditis elegans Bloom's syndrome genes him-6, rad-51, and top-3 are needed to maintain genome stability in the germ line, Molecular and cellular biology, 24 (2004) 5016-5027.

[22] N. Chester, F. Kuo, C. Kozak, C.D. O'Hara, P. Leder, Stage-specific apoptosis, developmental delay, and embryonic lethality in mice homozygous for a targeted disruption in the murine Bloom's syndrome gene, Genes & development, 12 (1998) 3382-3393.

[23] K.H. Goss, M.A. Risinger, J.J. Kordich, M.M. Sanz, J.E. Straughen, L.E. Slovek, A.J. Capobianco, J. German, G.P. Boivin, J. Groden, Enhanced tumor formation in mice heterozygous for Blm mutation, Science (New York, N.Y.), 297 (2002) 2051-2053.

[24] S.B. Gruber, N.A. Ellis, K.K. Scott, R. Almog, P. Kolachana, J.D. Bonner, T. Kirchhoff, L.P. Tomsho, K. Nafa, H. Pierce, M. Low, J. Satagopan, H. Rennert, H. Huang, J.K. Greenson, J. Groden, B. Rapaport, J. Shia, S. Johnson, P.K. Gregersen,

C.C. Harris, J. Boyd, G. Rennert, K. Offit, BLM heterozygosity and the risk of colorectal cancer, Science (New York, N.Y.), 297 (2002) 2013.

[25] J.K. Karow, R.K. Chakraverty, I.D. Hickson, The Bloom's syndrome gene product is a 3'-5' DNA helicase, The Journal of biological chemistry, 272 (1997) 30611-30614.

[26] S. Dutertre, M. Ababou, R. Onclercq, J. Delic, B. Chatton, C. Jaulin, M. Amor-Gueret, Cell cycle regulation of the endogenous wild type Bloom's syndrome DNA helicase, Oncogene, 19 (2000) 2731-2738.

[27] S. Kitao, I. Ohsugi, K. Ichikawa, M. Goto, Y. Furuichi, A. Shimamoto, Cloning of two new human helicase genes of the RecQ family: biological significance of multiple species in higher eukaryotes, Genomics, 54 (1998) 443-452.

[28] C. Barefield, J. Karlseder, The BLM helicase contributes to telomere maintenance through processing of late-replicating intermediate structures, Nucleic acids research, 40 (2012) 7358-7367.

[29] H. Kaneko, E. Matsui, T. Fukao, K. Kasahara, W. Morimoto, N. Kondo, Expression of the BLM gene in human haematopoietic cells, Clinical and experimental immunology, 118 (1999) 285-289.

[30] M.M. Sanz, M. Proytcheva, N.A. Ellis, W.K. Holloman, J. German, BLM, the Bloom's syndrome protein, varies during the cell cycle in its amount, distribution, and co-localization with other nuclear proteins, Cytogenetics and cell genetics, 91 (2000) 217-223.

[31] K.A. Manthei, J.L. Keck, The BLM dissolvasome in DNA replication and repair, Cellular and molecular life sciences : CMLS, 70 (2013) 4067-4084.

[32] C.Z. Bachrati, R.H. Borts, I.D. Hickson, Mobile D-loops are a preferred substrate for the Bloom's syndrome helicase, Nucleic acids research, 34 (2006) 2269-2279.

[33] A.J. van Brabant, T. Ye, M. Sanz, I.J. German, N.A. Ellis, W.K. Holloman, Binding and melting of D-loops by the Bloom syndrome helicase, Biochemistry, 39 (2000) 14617-14625.

[34] D.V. Bugreev, X. Yu, E.H. Egelman, A.V. Mazin, Novel pro- and anti-recombination activities of the Bloom's syndrome helicase, Genes & development, 21 (2007) 3085-3094.

[35] S.L. Davies, P.S. North, I.D. Hickson, Role for BLM in replication-fork restart and suppression of origin firing after replicative stress, Nature structural & molecular biology, 14 (2007) 677-679.

[36] V.A. Rao, A.M. Fan, L. Meng, C.F. Doe, P.S. North, I.D. Hickson, Y. Pommier, Phosphorylation of BLM, dissociation from topoisomerase IIIalpha, and colocalization with gamma-H2AX after topoisomerase I-induced replication damage, Molecular and cellular biology, 25 (2005) 8925-8937.

[37] H. Beamish, P. Kedar, H. Kaneko, P. Chen, T. Fukao, C. Peng, S. Beresten, N. Gueven, D. Purdie, S. Lees-Miller, N. Ellis, N. Kondo, M.F. Lavin, Functional link between BLM defective in Bloom's syndrome and the ataxia-telangiectasia-mutated protein, ATM, The Journal of biological chemistry, 277 (2002) 30515-30523.

[38] M. Ababou, S. Dutertre, Y. Lecluse, R. Onclercq, B. Chatton, M. Amor-Gueret, ATM-dependent phosphorylation and accumulation of endogenous BLM protein in response to ionizing radiation, Oncogene, 19 (2000) 5955-5963.

[39] C. Ralf, I.D. Hickson, L. Wu, The Bloom's syndrome helicase can promote the regression of a model replication fork, The Journal of biological chemistry, 281 (2006) 22839-22846.

[40] A. Machwe, L. Xiao, J. Groden, D.K. Orren, The Werner and Bloom syndrome proteins catalyze regression of a model replication fork, Biochemistry, 45 (2006) 13939-13946.

[41] C.J. Epstein, G.M. Martin, A.L. Schultz, A.G. Motulsky, Werner's syndrome a review of its symptomatology, natural history, pathologic features, genetics and relationship to the natural aging process, Medicine, 45 (1966) 177-221.

[42] H. Hoehn, On cataract in conjunction with scleroderma. Otto Werner, doctoral dissertation, 1904, Royal Ophthalmology Clinic, Royal Christian Albrecht University of Kiel, Advances in experimental medicine and biology, 190 (1985) 1-14.

[43] S. Kitao, A. Shimamoto, M. Goto, R.W. Miller, W.A. Smithson, N.M. Lindor, Y. Furuichi, Mutations in RECQL4 cause a subset of cases of Rothmund-Thomson syndrome, Nature genetics, 22 (1999) 82-84.

[44] M. Goto, Y. Ishikawa, M. Sugimoto, Y. Furuichi, Werner syndrome: a changing pattern of clinical manifestations in Japan (1917~2008), Bioscience trends, 7 (2013) 13-22.

[45] M. Takemoto, S. Mori, M. Kuzuya, S. Yoshimoto, A. Shimamoto, M. Igarashi, Y. Tanaka, T. Miki, K. Yokote, Diagnostic criteria for Werner syndrome based on Japanese nationwide epidemiological survey, Geriatrics & gerontology international, 13 (2013) 475-481.

[46] M. Eriksson, W.T. Brown, L.B. Gordon, M.W. Glynn, J. Singer, L. Scott, M.R. Erdos, C.M. Robbins, T.Y. Moses, P. Berglund, A. Dutra, E. Pak, S. Durkin, A.B. Csoka, M. Boehnke, T.W. Glover, F.S. Collins, Recurrent de novo point mutations in lamin A cause Hutchinson-Gilford progeria syndrome, Nature, 423 (2003) 293-298.

[47] P.L. Opresko, W.H. Cheng, V.A. Bohr, Junction of RecQ helicase biochemistry and human disease, The Journal of biological chemistry, 279 (2004) 18099-18102.

[48] K. Friedrich, L. Lee, D.F. Leistritz, G. Nurnberg, B. Saha, F.M. Hisama, D.K. Eyman, D. Lessel, P. Nurnberg, C. Li, F.V.M.J. Garcia, C.M. Kets, J. Schmidtke, V.T. Cruz, P.C. Van den Akker, J. Boak, D. Peter, G. Compoginis, K. Cefle, S. Ozturk, N. Lopez, T. Wessel, M. Poot, P.F. Ippel, B. Groff-Kellermann, H. Hoehn, G.M. Martin, C. Kubisch, J. Oshima, WRN mutations in Werner syndrome patients: genomic rearrangements, unusual intronic mutations and ethnic-specific alterations, Human genetics, 128 (2010) 103-111.

[49] L. Wang, C.E. Ogburn, C.B. Ware, W.C. Ladiges, H. Youssoufian, G.M. Martin, J. Oshima, Cellular Werner phenotypes in mice expressing a putative dominant-negative human WRN gene, Genetics, 154 (2000) 357-362.

[50] D.B. Lombard, C. Beard, B. Johnson, R.A. Marciniak, J. Dausman, R. Bronson, J.E. Buhlmann, R. Lipman, R. Curry, A. Sharpe, R. Jaenisch, L. Guarente, Mutations in the WRN gene in mice accelerate mortality in a p53-null background, Molecular and cellular biology, 20 (2000) 3286-3291.

[51] M. Lebel, P. Leder, A deletion within the murine Werner syndrome helicase induces sensitivity to inhibitors of topoisomerase and loss of cellular proliferative capacity,

Proceedings of the National Academy of Sciences of the United States of America, 95 (1998) 13097-13102.

[52] X. Du, J. Shen, N. Kugan, E.E. Furth, D.B. Lombard, C. Cheung, S. Pak, G. Luo, R.J. Pignolo, R.A. DePinho, L. Guarente, F.B. Johnson, Telomere shortening exposes functions for the mouse Werner and Bloom syndrome genes, Molecular and cellular biology, 24 (2004) 8437-8446.

[53] S. Chang, A.S. Multani, N.G. Cabrera, M.L. Naylor, P. Laud, D. Lombard, S. Pathak, L. Guarente, R.A. DePinho, Essential role of limiting telomeres in the pathogenesis of Werner syndrome, Nature genetics, 36 (2004) 877-882.

[54] G. Blander, J. Kipnis, J.F. Leal, C.E. Yu, G.D. Schellenberg, M. Oren, Physical and functional interaction between p53 and the Werner's syndrome protein, The Journal of biological chemistry, 274 (1999) 29463-29469.

[55] R.M. Brosh, Jr., P. Karmakar, J.A. Sommers, Q. Yang, X.W. Wang, E.A. Spillare, C.C. Harris, V.A. Bohr, p53 Modulates the exonuclease activity of Werner syndrome protein, The Journal of biological chemistry, 276 (2001) 35093-35102.

[56] J.A. Sommers, S. Sharma, K.M. Doherty, P. Karmakar, Q. Yang, M.K. Kenny, C.C. Harris, R.M. Brosh, Jr., p53 modulates RPA-dependent and RPA-independent WRN helicase activity, Cancer research, 65 (2005) 1223-1233.

[57] Q. Yang, R. Zhang, X.W. Wang, E.A. Spillare, S.P. Linke, D. Subramanian, J.D. Griffith, J.L. Li, I.D. Hickson, J.C. Shen, L.A. Loeb, S.J. Mazur, E. Appella, R.M. Brosh, Jr., P. Karmakar, V.A. Bohr, C.C. Harris, The processing of Holliday junctions by BLM and WRN helicases is regulated by p53, The Journal of biological chemistry, 277 (2002) 31980-31987.

[58] E. Gebhart, R. Bauer, U. Raub, M. Schinzel, K.W. Ruprecht, J.B. Jonas, Spontaneous and induced chromosomal instability in Werner syndrome, Human genetics, 80 (1988) 135-139.

[59] O. Imamura, K. Fujita, C. Itoh, S. Takeda, Y. Furuichi, T. Matsumoto, Werner and Bloom helicases are involved in DNA repair in a complementary fashion, Oncogene, 21 (2002) 954-963.

[60] K. Yamagata, J. Kato, A. Shimamoto, M. Goto, Y. Furuichi, H. Ikeda, Bloom's and Werner's syndrome genes suppress hyperrecombination in yeast sgs1 mutant: implication for genomic instability in human diseases, Proceedings of the National Academy of Sciences of the United States of America, 95 (1998) 8733-8738.

[61] N. Sasakawa, T. Fukui, S. Waga, Accumulation of FFA-1, the Xenopus homolog of Werner helicase, and DNA polymerase delta on chromatin in response to replication fork arrest, Journal of biochemistry, 140 (2006) 95-103.

[62] S. Liao, T. Toczylowski, H. Yan, Mechanistic analysis of Xenopus EXO1's function in 5'-strand resection at DNA double-strand breaks, Nucleic acids research, 39 (2011) 5967-5977.

[63] H. Yan, T. Toczylowski, J. McCane, C. Chen, S. Liao, Replication protein A promotes 5'-->3' end processing during homology-dependent DNA double-strand break repair, The Journal of cell biology, 192 (2011) 251-261.

[64] T. Suzuki, M. Shiratori, Y. Furuichi, T. Matsumoto, Diverged nuclear localization of Werner helicase in human and mouse cells, Oncogene, 20 (2001) 2551-2558.

[65] K. Yokote, S. Chanprasert, L. Lee, K. Eirich, M. Takemoto, A. Watanabe, N. Koizumi, D. Lessel, T. Mori, F.M. Hisama, P.D. Ladd, B. Angle, H. Baris, K. Cefle, S. Palanduz, S. Ozturk, A. Chateau, K. Deguchi, T.K. Easwar, A. Federico, A. Fox, T.A. Grebe, B. Hay, S. Nampoothiri, K. Seiter, E. Streeten, R.E. Pina-Aguilar, G. Poke, M. Poot, R. Posmyk, G.M. Martin, C. Kubisch, D. Schindler, J. Oshima, WRN Mutation Update: Mutation Spectrum, Patient Registries, and Translational Prospects, Human mutation, 38 (2017) 7-15.

[66] L. Larizza, G. Roversi, L. Volpi, Rothmund-Thomson syndrome, Orphanet journal of rare diseases, 5 (2010) 2.

[67] L.L. Wang, A. Gannavarapu, C.A. Kozinetz, M.L. Levy, R.A. Lewis, M.M. Chintagumpala, R. Ruiz-Maldanado, J. Contreras-Ruiz, C. Cunniff, R.P. Erickson, D. Lev, M. Rogers, E.H. Zackai, S.E. Plon, Association between osteosarcoma and deleterious mutations in the RECQL4 gene in Rothmund-Thomson syndrome, Journal of the National Cancer Institute, 95 (2003) 669-674.

[68] L. Lu, W. Jin, L.L. Wang, Aging in Rothmund-Thomson syndrome and related RECQL4 genetic disorders, Ageing research reviews, 33 (2017) 30-35.

[69] W.B. Taylor, Rothmund's syndrome; Thomson's syndrome; congenital poikiloderma with or without juvenile cataracts, A.M.A. archives of dermatology, 75 (1957) 236-244.

[70] A. Megarbane, I. Melki, N. Souraty, J. Gerbaka, V. El Ghouzzi, J. Bonaventure, A. Mornand, J. Loiselet, Overlap between Baller-Gerold and Rothmund-Thomson syndrome, Clinical dysmorphology, 9 (2000) 303-305.

[71] H.A. Siitonen, O. Kopra, H. Kaariainen, H. Haravuori, R.M. Winter, A.M. Saamanen, L. Peltonen, M. Kestila, Molecular defect of RAPADILINO syndrome expands the phenotype spectrum of RECQL diseases, Human molecular genetics, 12 (2003) 2837-2844.

[72] L. Van Maldergem, H.A. Siitonen, N. Jalkh, E. Chouery, M. De Roy, V. Delague, M. Muenke, E.W. Jabs, J. Cai, L.L. Wang, S.E. Plon, C. Fourneau, M. Kestila, Y. Gillerot, A. Megarbane, A. Verloes, Revisiting the craniosynostosis-radial ray hypoplasia association: Baller-Gerold syndrome caused by mutations in the RECQL4 gene, Journal of medical genetics, 43 (2006) 148-152.

[73] L. Van Maldergem, A. Verloes, L. Lejeune, Y. Gillerot, The Baller-Gerold syndrome, Journal of medical genetics, 29 (1992) 266-268.

[74] R.E. Cabral, S. Queille, C. Bodemer, Y. de Prost, J.B. Neto, A. Sarasin, L. Daya-Grosjean, Identification of new RECQL4 mutations in Caucasian Rothmund-Thomson patients and analysis of sensitivity to a wide range of genotoxic agents, Mutation research, 643 (2008) 41-47.

[75] M. Debeljak, A. Zver, J. Jazbec, A patient with Baller-Gerold syndrome and midline NK/T lymphoma, American journal of medical genetics. Part A, 149A (2009) 755-759.

[76] P. Reix, J. Derelle, H. Levrey-Hadden, H. Plauchu, G. Bellon, Bronchiectasis in two pediatric patients with Rothmund-Thomson syndrome, Pediatrics international : official journal of the Japan Pediatric Society, 49 (2007) 118-120.

[77] H.A. Siitonen, J. Sotkasiira, M. Biervliet, A. Benmansour, Y. Capri, V. Cormier-Daire, B. Crandall, K. Hannula-Jouppi, R. Hennekam, D. Herzog, K. Keymolen, M. Lipsanen-Nyman, P. Miny, S.E. Plon, S. Riedl, A. Sarkar, F.R. Vargas, A. Verloes, L.L. Wang, H. Kaariainen, M. Kestila, The mutation spectrum in RECQL4 diseases, European journal of human genetics : EJHG, 17 (2009) 151-158.

[78] Y. Hoki, R. Araki, A. Fujimori, T. Ohhata, H. Koseki, R. Fukumura, M. Nakamura, H. Takahashi, Y. Noda, S. Kito, M. Abe, Growth retardation and skin abnormalities of the Recql4-deficient mouse, Human molecular genetics, 12 (2003) 2293-2299.

[79] M.B. Mann, C.A. Hodges, E. Barnes, H. Vogel, T.J. Hassold, G. Luo, Defective sister-chromatid cohesion, aneuploidy and cancer predisposition in a mouse model of type II Rothmund-Thomson syndrome, Human molecular genetics, 14 (2005) 813-825.

[80] L. Bjergbaek, J.A. Cobb, S.M. Gasser, RecQ helicases and genome stability: lessons from model organisms and human disease, Swiss Med Wkly, 132 (2002) 433-442.

[81] K. Kusano, M.E. Berres, W.R. Engels, Evolution of the RECQ family of helicases: A drosophila homolog, Dmblm, is similar to the human bloom syndrome gene, Genetics, 151 (1999) 1027-1039.

[82] D.L. Croteau, V. Popuri, P.L. Opresko, V.A. Bohr, Human RecQ helicases in DNA repair, recombination, and replication, Annual review of biochemistry, 83 (2014) 519-552.

[83] A.E. Gorbalenya, E.V. Koonin, Helicases: amino acid sequence comparisons and structure-function relationships, Current Opinion in Structural Biology, 3 (1993) 419-429.

[84] H. Nakayama, K. Nakayama, R. Nakayama, N. Irino, Y. Nakayama, P.C. Hanawalt, Isolation and genetic characterization of a thymineless death-resistant mutant of Escherichia coli K12: identification of a new mutation (recQ1) that blocks the RecF recombination pathway, Molecular & general genetics : MGG, 195 (1984) 474-480.

[85] R.J. Bennett, J.L. Keck, Structure and function of RecQ DNA helicases, Critical reviews in biochemistry and molecular biology, 39 (2004) 79-97.

[86] A. Sato, M. Mishima, A. Nagai, S.Y. Kim, Y. Ito, T. Hakoshima, J.G. Jee, K. Kitano, Solution structure of the HRDC domain of human Bloom syndrome protein BLM, Journal of biochemistry, 148 (2010) 517-525.

[87] K. Kitano, N. Yoshihara, T. Hakoshima, Crystal structure of the HRDC domain of human Werner syndrome protein, WRN, The Journal of biological chemistry, 282 (2007) 2717-2728.

[88] D.A. Bernstein, J.L. Keck, Conferring substrate specificity to DNA helicases: role of the RecQ HRDC domain, Structure (London, England : 1993), 13 (2005) 1173-1182.

[89] Z. Liu, M.J. Macias, M.J. Bottomley, G. Stier, J.P. Linge, M. Nilges, P. Bork, M. Sattler, The three-dimensional structure of the HRDC domain and implications for the Werner and Bloom syndrome proteins, Structure (London, England : 1993), 7 (1999) 1557-1566.

[90] Y.M. Kim, B.S. Choi, Structure and function of the regulatory HRDC domain from human Bloom syndrome protein, Nucleic acids research, 38 (2010) 7764-7777.

[91] L. Wu, K.L. Chan, C. Ralf, D.A. Bernstein, P.L. Garcia, V.A. Bohr, A. Vindigni, P. Janscak, J.L. Keck, I.D. Hickson, The HRDC domain of BLM is required for the dissolution of double Holliday junctions, The EMBO journal, 24 (2005) 2679-2687.

[92] S. Samanta, P. Karmakar, Recruitment of HRDC domain of WRN and BLM to the sites of DNA damage induced by mitomycin C and methyl methanesulfonate, Cell biology international, 36 (2012) 873-881.

[93] C.F. Chen, S.J. Brill, An essential DNA strand-exchange activity is conserved in the divergent N-termini of BLM orthologs, The EMBO journal, 29 (2010) 1713-1725.

[94] S. Gangloff, J.P. McDonald, C. Bendixen, L. Arthur, R. Rothstein, The yeast type I topoisomerase Top3 interacts with Sgs1, a DNA helicase homolog: a potential eukaryotic reverse gyrase, Molecular and cellular biology, 14 (1994) 8391-8398.

[95] R. Rothstein, S. Gangloff, Hyper-recombination and Bloom's syndrome: microbes again provide clues about cancer, Genome research, 5 (1995) 421-426.

[96] A. De Muyt, L. Jessop, E. Kolar, A. Sourirajan, J. Chen, Y. Dayani, M. Lichten, BLM helicase ortholog Sgs1 is a central regulator of meiotic recombination intermediate metabolism, Mol Cell, 46 (2012) 43-53.

[97] P. Cejka, S.C. Kowalczykowski, The full-length Saccharomyces cerevisiae Sgs1 protein is a vigorous DNA helicase that preferentially unwinds holliday junctions, The Journal of biological chemistry, 285 (2010) 8290-8301.

[98] P.M. Watt, I.D. Hickson, R.H. Borts, E.J. Louis, SGS1, a homologue of the Bloom's and Werner's syndrome genes, is required for maintenance of genome stability in Saccharomyces cerevisiae, Genetics, 144 (1996) 935-945.

[99] F.O. Balogun, A.W. Truman, S.J. Kron, DNA resection proteins Sgs1 and Exo1 are required for G1 checkpoint activation in budding yeast, DNA Repair (Amst), 12 (2013) 751-760.

[100] B. Rockmill, J.C. Fung, S.S. Branda, G.S. Roeder, The Sgs1 helicase regulates chromosome synapsis and meiotic crossing over, Current biology : CB, 13 (2003) 1954-1962.

[101] K. Myung, A. Datta, C. Chen, R.D. Kolodner, SGS1, the Saccharomyces cerevisiae homologue of BLM and WRN, suppresses genome instability and homeologous recombination, Nature genetics, 27 (2001) 113-116.

[102] J. Saffi, V.R. Pereira, J.A. Henriques, Importance of the Sgs1 helicase activity in DNA repair of Saccharomyces cerevisiae, Current genetics, 37 (2000) 75-78.

[103] A. Miyajima, M. Seki, F. Onoda, A. Ui, Y. Satoh, Y. Ohno, T. Enomoto, Different domains of Sgs1 are required for mitotic and meiotic functions, Genes & genetic systems, 75 (2000) 319-326.

[104] F. Onoda, M. Seki, A. Miyajima, T. Enomoto, Elevation of sister chromatid exchange in Saccharomyces cerevisiae sgs1 disruptants and the relevance of the disruptants as a system to evaluate mutations in Bloom's syndrome gene, Mutation research, 459 (2000) 203-209.

[105] R.J. Bennett, J.A. Sharp, J.C. Wang, Purification and characterization of the Sgs1 DNA helicase activity of Saccharomyces cerevisiae, The Journal of biological chemistry, 273 (1998) 9644-9650.

[106] H. Sun, R.J. Bennett, N. Maizels, The Saccharomyces cerevisiae Sgs1 helicase efficiently unwinds G-G paired DNAs, Nucleic acids research, 27 (1999) 1978-1984.

[107] H. Han, R.J. Bennett, L.H. Hurley, Inhibition of unwinding of G-quadruplex structures by Sgs1 helicase in the presence of N,N'-bis[2-(1-piperidino)ethyl]-3,4,9,10-perylenetetracarboxylic diimide, a G-quadruplex-interactive ligand, Biochemistry, 39 (2000) 9311-9316.

[108] M.D. Huber, D.C. Lee, N. Maizels, G4 DNA unwinding by BLM and Sgs1p: substrate specificity and substrate-specific inhibition, Nucleic acids research, 30 (2002) 3954-3961.

[109] C.Z. Bachrati, I.D. Hickson, RecQ helicases: suppressors of tumorigenesis and premature aging, The Biochemical journal, 374 (2003) 577-606.

[110] K. Umezu, K. Nakayama, H. Nakayama, Escherichia coli RecQ protein is a DNA helicase, Proceedings of the National Academy of Sciences of the United States of America, 87 (1990) 5363-5367.

[111] H. Jung, J.A. Lee, S. Choi, H. Lee, B. Ahn, Characterization of the Caenorhabditis elegans HIM-6/BLM helicase: unwinding recombination intermediates, PloS one, 9 (2014) e102402.

[112] L.K. Ferrarelli, V. Popuri, A.K. Ghosh, T. Tadokoro, C. Canugovi, J.K. Hsu, D.L. Croteau, V.A. Bohr, The RECQL4 protein, deficient in Rothmund-Thomson syndrome is active on telomeric D-loops containing DNA metabolism blocking lesions, DNA Repair (Amst), 12 (2013) 518-528.

[113] M. Hyun, S. Park, E. Kim, D.H. Kim, S.J. Lee, H.S. Koo, Y.S. Seo, B. Ahn, Physical and functional interactions of Caenorhabditis elegans WRN-1 helicase with RPA-1, Biochemistry, 51 (2012) 1336-1345.

[114] P. Cejka, J.L. Plank, C.C. Dombrowski, S.C. Kowalczykowski, Decatenation of DNA by the S. cerevisiae Sgs1-Top3-Rmi1 and RPA complex: a mechanism for disentangling chromosomes, Mol Cell, 47 (2012) 886-896.

[115] M.L. Rossi, A.K. Ghosh, T. Kulikowicz, D.L. Croteau, V.A. Bohr, Conserved helicase domain of human RecQ4 is required for strand annealing-independent DNA unwinding, DNA Repair (Amst), 9 (2010) 796-804.

[116] X. Xu, Y. Liu, Dual DNA unwinding activities of the Rothmund-Thomson syndrome protein, RECQ4, The EMBO journal, 28 (2009) 568-577.

[117] A. Ghosh, M.L. Rossi, J. Aulds, D. Croteau, V.A. Bohr, Telomeric D-loops containing 8-oxo-2'-deoxyguanosine are preferred substrates for Werner and Bloom syndrome helicases and are bound by POT1, The Journal of biological chemistry, 284 (2009) 31074-31084.

[118] V. Popuri, C.Z. Bachrati, L. Muzzolini, G. Mosedale, S. Costantini, E. Giacomini, I.D. Hickson, A. Vindigni, The Human RecQ helicases, BLM and RECQ1, display distinct DNA substrate specificities, The Journal of biological chemistry, 283 (2008) 17766-17776.

[119] M. Hyun, V.A. Bohr, B. Ahn, Biochemical characterization of the WRN-1 RecQ helicase of Caenorhabditis elegans, Biochemistry, 47 (2008) 7583-7593.

[120] B.T. Weinert, D.C. Rio, DNA strand displacement, strand annealing and strand swapping by the Drosophila Bloom's syndrome helicase, Nucleic acids research, 35 (2007) 1367-1376.

[121] M.A. Macris, L. Krejci, W. Bussen, A. Shimamoto, P. Sung, Biochemical characterization of the RECQ4 protein, mutated in Rothmund-Thomson syndrome, DNA Repair (Amst), 5 (2006) 172-180.

[122] R.M. Brosh, Jr., P.L. Opresko, V.A. Bohr, Enzymatic mechanism of the WRN helicase/nuclease, Methods in enzymology, 409 (2006) 52-85.

[123] W. Wang, R.A. Bambara, Human Bloom protein stimulates flap endonuclease 1 activity by resolving DNA secondary structure, The Journal of biological chemistry, 280 (2005) 5391-5399.

[124] S. Sharma, J.A. Sommers, S. Choudhary, J.K. Faulkner, S. Cui, L. Andreoli, L. Muzzolini, A. Vindigni, R.M. Brosh, Jr., Biochemical analysis of the DNA unwinding and strand annealing activities catalyzed by human RECQ1, The Journal of biological chemistry, 280 (2005) 28072-28084.

[125] P.L. Garcia, Y. Liu, J. Jiricny, S.C. West, P. Janscak, Human RECQ5beta, a protein with DNA helicase and strand-annealing activities in a single polypeptide, The EMBO journal, 23 (2004) 2882-2891.

[126] S. Cui, R. Klima, A. Ochem, D. Arosio, A. Falaschi, A. Vindigni, Characterization of the DNA-unwinding activity of human RECQ1, a helicase specifically stimulated by human replication protein A, The Journal of biological chemistry, 278 (2003) 1424-1432.

[127] C. von Kobbe, P. Karmakar, L. Dawut, P. Opresko, X. Zeng, R.M. Brosh, Jr., I.D. Hickson, V.A. Bohr, Colocalization, physical, and functional interaction between Werner

and Bloom syndrome proteins, The Journal of biological chemistry, 277 (2002) 22035-22044.

[128] D.K. Orren, S. Theodore, A. Machwe, The Werner syndrome helicase/exonuclease (WRN) disrupts and degrades D-loops in vitro, Biochemistry, 41 (2002) 13483-13488.

[129] R.M. Brosh, Jr., J. Waheed, J.A. Sommers, Biochemical characterization of the DNA substrate specificity of Werner syndrome helicase, The Journal of biological chemistry, 277 (2002) 23236-23245.

[130] F. Ahmad, C.D. Kaplan, E. Stewart, Helicase activity is only partially required for Schizosaccharomyces pombe Rqh1p function, Yeast (Chichester, England), 19 (2002) 1381-1398.

[131] X. Wu, N. Maizels, Substrate-specific inhibition of RecQ helicase, Nucleic acids research, 29 (2001) 1765-1771.

[132] P.L. Opresko, J.P. Laine, R.M. Brosh, Jr., M.M. Seidman, V.A. Bohr, Coordinate action of the helicase and 3' to 5' exonuclease of Werner syndrome protein, The Journal of biological chemistry, 276 (2001) 44677-44687.

[133] P. Mohaghegh, J.K. Karow, R.M. Brosh, Jr., V.A. Bohr, I.D. Hickson, The Bloom's and Werner's syndrome proteins are DNA structure-specific helicases, Nucleic acids research, 29 (2001) 2843-2849.

[134] O. Imamura, K. Fujita, A. Shimamoto, H. Tanabe, S. Takeda, Y. Furuichi, T. Matsumoto, Bloom helicase is involved in DNA surveillance in early S phase in vertebrate cells, Oncogene, 20 (2001) 1143-1151.

[135] F.G. Harmon, S.C. Kowalczykowski, Biochemical characterization of the DNA helicase activity of the escherichia coli RecQ helicase, The Journal of biological chemistry, 276 (2001) 232-243.

[136] R. Freire, F. d'Adda Di Fagagna, L. Wu, G. Pedrazzi, I. Stagljar, I.D. Hickson, S.P. Jackson, Cleavage of the Bloom's syndrome gene product during apoptosis by caspase-3 results in an impaired interaction with topoisomerase IIIalpha, Nucleic acids research, 29 (2001) 3172-3180.

[137] R.M. Brosh, Jr., A. Majumdar, S. Desai, I.D. Hickson, V.A. Bohr, M.M. Seidman, Unwinding of a DNA triple helix by the Werner and Bloom syndrome helicases, The Journal of biological chemistry, 276 (2001) 3024-3030.

[138] J.K. Karow, A. Constantinou, J.L. Li, S.C. West, I.D. Hickson, The Bloom's syndrome gene product promotes branch migration of holliday junctions, Proceedings of the National Academy of Sciences of the United States of America, 97 (2000) 6504-6508.

[139] A. Constantinou, M. Tarsounas, J.K. Karow, R.M. Brosh, V.A. Bohr, I.D. Hickson, S.C. West, Werner's syndrome protein (WRN) migrates Holliday junctions and co-localizes with RPA upon replication arrest, EMBO reports, 1 (2000) 80-84.

[140] R.M. Brosh, Jr., J.L. Li, M.K. Kenny, J.K. Karow, M.P. Cooper, R.P. Kureekattil, I.D. Hickson, V.A. Bohr, Replication protein A physically interacts with the Bloom's syndrome protein and stimulates its helicase activity, The Journal of biological chemistry, 275 (2000) 23500-23508.

[141] N. Suzuki, M. Shiratori, M. Goto, Y. Furuichi, Werner syndrome helicase contains a 5'-->3' exonuclease activity that digests DNA and RNA strands in DNA/DNA and RNA/DNA duplexes dependent on unwinding, Nucleic acids research, 27 (1999) 2361-2368.

[142] N.F. Neff, N.A. Ellis, T.Z. Ye, J. Noonan, K. Huang, M. Sanz, M. Proytcheva, The DNA helicase activity of BLM is necessary for the correction of the genomic instability of bloom syndrome cells, Molecular biology of the cell, 10 (1999) 665-676.

[143] M. Fry, L.A. Loeb, Human werner syndrome DNA helicase unwinds tetrahelical structures of the fragile X syndrome repeat sequence d(CGG)n, The Journal of biological chemistry, 274 (1999) 12797-12802.

[144] R.M. Brosh, Jr., D.K. Orren, J.O. Nehlin, P.H. Ravn, M.K. Kenny, A. Machwe, V.A. Bohr, Functional and physical interaction between WRN helicase and human replication protein A, The Journal of biological chemistry, 274 (1999) 18341-18350.

[145] R.J. Bennett, J.L. Keck, J.C. Wang, Binding specificity determines polarity of DNA unwinding by the Sgs1 protein of S. cerevisiae, Journal of molecular biology, 289 (1999) 235-248.

[146] H. Sun, J.K. Karow, I.D. Hickson, N. Maizels, The Bloom's syndrome helicase unwinds G4 DNA, The Journal of biological chemistry, 273 (1998) 27587-27592.

[147] J.C. Shen, M.D. Gray, J. Oshima, L.A. Loeb, Characterization of Werner syndrome protein DNA helicase activity: directionality, substrate dependence and stimulation by replication protein A, Nucleic acids research, 26 (1998) 2879-2885.

[148] F.G. Harmon, S.C. Kowalczykowski, RecQ helicase, in concert with RecA and SSB proteins, initiates and disrupts DNA recombination, Genes & development, 12 (1998) 1134-1144.

[149] N. Suzuki, A. Shimamoto, O. Imamura, J. Kuromitsu, S. Kitao, M. Goto, Y. Furuichi, DNA helicase activity in Werner's syndrome gene product synthesized in a baculovirus system, Nucleic acids research, 25 (1997) 2973-2978.

[150] M.D. Gray, J.C. Shen, A.S. Kamath-Loeb, A. Blank, B.L. Sopher, G.M. Martin, J. Oshima, L.A. Loeb, The Werner syndrome protein is a DNA helicase, Nature genetics, 17 (1997) 100-103.

[151] K. Umezu, H. Nakayama, RecQ DNA helicase of Escherichia coli. Characterization of the helix-unwinding activity with emphasis on the effect of single-stranded DNA-binding protein, Journal of molecular biology, 230 (1993) 1145-1150.

[152] C. Dherin, E. Gueneau, M. Francin, M. Nunez, S. Miron, S.E. Liberti, L.J. Rasmussen, S. Zinn-Justin, B. Gilquin, J.B. Charbonnier, S. Boiteux, Characterization of a highly conserved binding site of Mlh1 required for exonuclease I-dependent mismatch repair, Molecular and cellular biology, 29 (2009) 907-918.

[153] G. Pedrazzi, C. Perrera, H. Blaser, P. Kuster, G. Marra, S.L. Davies, G.H. Ryu, R. Freire, I.D. Hickson, J. Jiricny, I. Stagljar, Direct association of Bloom's syndrome gene product with the human mismatch repair protein MLH1, Nucleic acids research, 29 (2001) 4378-4386.

[154] N.A. Ellis, J. Groden, T.Z. Ye, J. Straughen, D.J. Lennon, S. Ciocci, M. Proytcheva, J. German, The Bloom's syndrome gene product is homologous to RecQ helicases, Cell, 83 (1995) 655-666.

[155] J.K. Karow, L. Wu, I.D. Hickson, RecQ family helicases: roles in cancer and aging, Curr Opin Genet Dev, 10 (2000) 32-38.

[156] L. Wu, S.L. Davies, P.S. North, H. Goulaouic, J.F. Riou, H. Turley, K.C. Gatter, I.D. Hickson, The Bloom's syndrome gene product interacts with topoisomerase III, The Journal of biological chemistry, 275 (2000) 9636-9644.

[157] J.A. Kennedy, G.W. Daughdrill, K.H. Schmidt, A transient alpha-helical molecular recognition element in the disordered N-terminus of the Sgs1 helicase is critical for chromosome stability and binding of Top3/Rmi1, Nucleic acids research, 41 (2013) 10215-10227.

[158] J.R. Mullen, F.S. Nallaseth, Y.Q. Lan, C.E. Slagle, S.J. Brill, Yeast Rmi1/Nce4 controls genome stability as a subunit of the Sgs1-Top3 complex, Molecular and cellular biology, 25 (2005) 4476-4487.

[159] G. Ira, J.E. Haber, Characterization of RAD51-independent break-induced replication that acts preferentially with short homologous sequences, Molecular and cellular biology, 22 (2002) 6384-6392.

[160] P. Cejka, J.L. Plank, C.Z. Bachrati, I.D. Hickson, S.C. Kowalczykowski, Rmi1 stimulates decatenation of double Holliday junctions during dissolution by Sgs1-Top3, Nature structural & molecular biology, 17 (2010) 1377-1382.

[161] A.M. Hegnauer, N. Hustedt, K. Shimada, B.L. Pike, M. Vogel, P. Amsler, S.M. Rubin, F. van Leeuwen, A. Guenole, H. van Attikum, N.H. Thoma, S.M. Gasser, An N-terminal acidic region of Sgs1 interacts with Rpa70 and recruits Rad53 kinase to stalled forks, The EMBO journal, 31 (2012) 3768-3783.

[162] H. Niu, W.H. Chung, Z. Zhu, Y. Kwon, W. Zhao, P. Chi, R. Prakash, C. Seong, D. Liu, L. Lu, G. Ira, P. Sung, Mechanism of the ATP-dependent DNA end-resection machinery from Saccharomyces cerevisiae, Nature, 467 (2010) 108-111.

[163] A. Machwe, E.M. Lozada, L. Xiao, D.K. Orren, Competition between the DNA unwinding and strand pairing activities of the Werner and Bloom syndrome proteins, BMC molecular biology, 7 (2006) 1.

[164] C.Z. Bachrati, I.D. Hickson, RecQ helicases: guardian angels of the DNA replication fork, Chromosoma, 117 (2008) 219-233.

[165] I. Chiolo, W. Carotenuto, G. Maffioletti, J.H. Petrini, M. Foiani, G. Liberi, Srs2 and Sgs1 DNA helicases associate with Mre11 in different subcomplexes following

checkpoint activation and CDK1-mediated Srs2 phosphorylation, Molecular and cellular biology, 25 (2005) 5738-5751.

[166] S. Gangloff, C. Soustelle, F. Fabre, Homologous recombination is responsible for cell death in the absence of the Sgs1 and Srs2 helicases, Nature genetics, 25 (2000) 192-194.

[167] J.R. Mullen, V. Kaliraman, S.S. Ibrahim, S.J. Brill, Requirement for three novel protein complexes in the absence of the Sgs1 DNA helicase in Saccharomyces cerevisiae, Genetics, 157 (2001) 103-118.

[168] F. Fabre, A. Chan, W.D. Heyer, S. Gangloff, Alternate pathways involving Sgs1/Top3, Mus81/ Mms4, and Srs2 prevent formation of toxic recombination intermediates from single-stranded gaps created by DNA replication, Proceedings of the National Academy of Sciences of the United States of America, 99 (2002) 16887-16892.

[169] G. Liberi, G. Maffioletti, C. Lucca, I. Chiolo, A. Baryshnikova, C. Cotta-Ramusino, M. Lopes, A. Pellicioli, J.E. Haber, M. Foiani, Rad51-dependent DNA structures accumulate at damaged replication forks in sgs1 mutants defective in the yeast ortholog of BLM RecQ helicase, Genes & development, 19 (2005) 339-350.

[170] R. Chanet, M. Heude, A. Adjiri, L. Maloisel, F. Fabre, Semidominant mutations in the yeast Rad51 protein and their relationships with the Srs2 helicase, Molecular and cellular biology, 16 (1996) 4782-4789.

[171] G. Ira, A. Malkova, G. Liberi, M. Foiani, J.E. Haber, Srs2 and Sgs1-Top3 suppress crossovers during double-strand break repair in yeast, Cell, 115 (2003) 401-411.

[172] L. Krejci, S. Van Komen, Y. Li, J. Villemain, M.S. Reddy, H. Klein, T. Ellenberger, P. Sung, DNA helicase Srs2 disrupts the Rad51 presynaptic filament, Nature, 423 (2003) 305-309.

[173] X. Veaute, J. Jeusset, C. Soustelle, S.C. Kowalczykowski, E. Le Cam, F. Fabre, The Srs2 helicase prevents recombination by disrupting Rad51 nucleoprotein filaments, Nature, 423 (2003) 309-312.

[174] L. Wu, S.L. Davies, N.C. Levitt, I.D. Hickson, Potential role for the BLM helicase in recombinational repair via a conserved interaction with RAD51, The Journal of biological chemistry, 276 (2001) 19375-19381.

[175] K.K. Chiruvella, Z. Liang, T.E. Wilson, Repair of double-strand breaks by end joining, Cold Spring Harbor perspectives in biology, 5 (2013) a012757.

[176] G. Ira, A. Pellicioli, A. Balijja, X. Wang, S. Fiorani, W. Carotenuto, G. Liberi, D. Bressan, L. Wan, N.M. Hollingsworth, J.E. Haber, M. Foiani, DNA end resection, homologous recombination and DNA damage checkpoint activation require CDK1, Nature, 431 (2004) 1011-1017.

[177] P. Huertas, F. Cortes-Ledesma, A.A. Sartori, A. Aguilera, S.P. Jackson, CDK targets Sae2 to control DNA-end resection and homologous recombination, Nature, 455 (2008) 689-692.

[178] J.H. Barlow, M. Lisby, R. Rothstein, Differential regulation of the cellular response to DNA double-strand breaks in G1, Mol Cell, 30 (2008) 73-85.

[179] Y. Aylon, B. Liefshitz, M. Kupiec, The CDK regulates repair of double-strand breaks by homologous recombination during the cell cycle, The EMBO journal, 23 (2004) 4868-4875.

[180] J. Sun, K.J. Lee, A.J. Davis, D.J. Chen, Human Ku70/80 protein blocks exonuclease 1-mediated DNA resection in the presence of human Mre11 or Mre11/Rad50 protein complex, The Journal of biological chemistry, 287 (2012) 4936-4945.

[181] E.Y. Shim, W.H. Chung, M.L. Nicolette, Y. Zhang, M. Davis, Z. Zhu, T.T. Paull, G. Ira, S.E. Lee, Saccharomyces cerevisiae Mre11/Rad50/Xrs2 and Ku proteins regulate association of Exo1 and Dna2 with DNA breaks, The EMBO journal, 29 (2010) 3370-3380.

[182] P. Langerak, E. Mejia-Ramirez, O. Limbo, P. Russell, Release of Ku and MRN from DNA ends by Mre11 nuclease activity and Ctp1 is required for homologous recombination repair of double-strand breaks, PLoS genetics, 7 (2011) e1002271.

[183] S.S. Foster, A. Balestrini, J.H. Petrini, Functional interplay of the Mre11 nuclease and Ku in the response to replication-associated DNA damage, Molecular and cellular biology, 31 (2011) 4379-4389.

[184] E. Cannavo, P. Cejka, Sae2 promotes dsDNA endonuclease activity within Mre11-Rad50-Xrs2 to resect DNA breaks, Nature, 514 (2014) 122-125.

[185] Z. Zhu, W.H. Chung, E.Y. Shim, S.E. Lee, G. Ira, Sgs1 helicase and two nucleases Dna2 and Exo1 resect DNA double-strand break ends, Cell, 134 (2008) 981-994.

[186] E.P. Mimitou, L.S. Symington, Sae2, Exo1 and Sgs1 collaborate in DNA double-strand break processing, Nature, 455 (2008) 770-774.

[187] X. Wang, J.E. Haber, Role of Saccharomyces single-stranded DNA-binding protein RPA in the strand invasion step of double-strand break repair, PLoS biology, 2 (2004) E21.

[188] M.L. Nicolette, K. Lee, Z. Guo, M. Rani, J.M. Chow, S.E. Lee, T.T. Paull, Mre11-Rad50-Xrs2 and Sae2 promote 5' strand resection of DNA double-strand breaks, Nature structural & molecular biology, 17 (2010) 1478-1485.

[189] M. Clerici, D. Mantiero, G. Lucchini, M.P. Longhese, The Saccharomyces cerevisiae Sae2 protein negatively regulates DNA damage checkpoint signalling, EMBO reports, 7 (2006) 212-218.

[190] H. Chen, R.A. Donnianni, N. Handa, S.K. Deng, J. Oh, L.A. Timashev, S.C. Kowalczykowski, L.S. Symington, Sae2 promotes DNA damage resistance by removing the Mre11-Rad50-Xrs2 complex from DNA and attenuating Rad53 signaling, Proceedings of the National Academy of Sciences of the United States of America, 112 (2015) E1880-1887.

[191] W.H. Chung, Z. Zhu, A. Papusha, A. Malkova, G. Ira, Defective resection at DNA double-strand breaks leads to de novo telomere formation and enhances gene targeting, PLoS genetics, 6 (2010) e1000948.

[192] S. Gravel, J.R. Chapman, C. Magill, S.P. Jackson, DNA helicases Sgs1 and BLM promote DNA double-strand break resection, Genes & development, 22 (2008) 2767-2772.

[193] M.E. Budd, J.L. Campbell, Interplay of Mre11 nuclease with Dna2 plus Sgs1 in Rad51-dependent recombinational repair, PloS one, 4 (2009) e4267.

[194] P.T. Tran, N. Erdeniz, S. Dudley, R.M. Liskay, Characterization of nuclease-dependent functions of Exo1p in Saccharomyces cerevisiae, DNA Repair (Amst), 1 (2002) 895-912.

[195] E. Cannavo, P. Cejka, S.C. Kowalczykowski, Relationship of DNA degradation by Saccharomyces cerevisiae exonuclease 1 and its stimulation by RPA and Mre11-Rad50-Xrs2 to DNA end resection, Proceedings of the National Academy of Sciences of the United States of America, 110 (2013) E1661-1668.

[196] P. Cejka, E. Cannavo, P. Polaczek, T. Masuda-Sasa, S. Pokharel, J.L. Campbell, S.C. Kowalczykowski, DNA end resection by Dna2-Sgs1-RPA and its stimulation by Top3-Rmi1 and Mre11-Rad50-Xrs2, Nature, 467 (2010) 112-116.

[197] V.A. Marrero, L.S. Symington, Extensive DNA end processing by exo1 and sgs1 inhibits break-induced replication, PLoS genetics, 6 (2010) e1001007.

[198] J.R. Lydeard, Z. Lipkin-Moore, S. Jain, V.V. Eapen, J.E. Haber, G.P. Copenhaver, Sgs1 and Exo1 Redundantly Inhibit Break-Induced Replication and De Novo Telomere Addition at Broken Chromosome Ends, PLoS genetics, 6 (2010) e1000973.

[199] A.V. Nimonkar, J. Genschel, E. Kinoshita, P. Polaczek, J.L. Campbell, C. Wyman, P. Modrich, S.C. Kowalczykowski, BLM-DNA2-RPA-MRN and EXO1-BLM-RPA-MRN constitute two DNA end resection machineries for human DNA break repair, Genes & development, 25 (2011) 350-362.

[200] E.P. Mimitou, L.S. Symington, Ku prevents Exo1 and Sgs1-dependent resection of DNA ends in the absence of a functional MRX complex or Sae2, The EMBO journal, 29 (2010) 3358-3369.

[201] M. Granata, F. Lazzaro, D. Novarina, D. Panigada, F. Puddu, C.M. Abreu, R. Kumar, M. Grenon, N.F. Lowndes, P. Plevani, M. Muzi-Falconi, Dynamics of Rad9 Chromatin Binding and Checkpoint Function Are Mediated by Its Dimerization and Are Cell Cycle–Regulated by CDK1 Activity, PLoS genetics, 6 (2010).

[202] A.V. Nimonkar, A.Z. Ozsoy, J. Genschel, P. Modrich, S.C. Kowalczykowski, Human exonuclease 1 and BLM helicase interact to resect DNA and initiate DNA repair, Proceedings of the National Academy of Sciences of the United States of America, 105 (2008) 16906-16911.

[203] J. Tkac, G. Xu, H. Adhikary, J.T. Young, D. Gallo, C. Escribano-Diaz, J. Krietsch, A. Orthwein, M. Munro, W. Sol, A. Al-Hakim, Z.Y. Lin, J. Jonkers, P. Borst, G.W. Brown, A.C. Gingras, S. Rottenberg, J.Y. Masson, D. Durocher, HELB Is a Feedback Inhibitor of DNA End Resection, Mol Cell, (2016).

[204] V.V. Eapen, N. Sugawara, M. Tsabar, W.H. Wu, J.E. Haber, The Saccharomyces cerevisiae chromatin remodeler Fun30 regulates DNA end resection and checkpoint deactivation, Molecular and cellular biology, 32 (2012) 4727-4740.

[205] X. Chen, D. Cui, A. Papusha, X. Zhang, C.D. Chu, J. Tang, K. Chen, X. Pan, G. Ira, The Fun30 nucleosome remodeller promotes resection of DNA double-strand break ends, Nature, 489 (2012) 576-580.

[206] M. Ferrari, D. Dibitetto, G. De Gregorio, V.V. Eapen, C.C. Rawal, F. Lazzaro, M. Tsabar, F. Marini, J.E. Haber, A. Pellicioli, Functional interplay between the 53BP1-ortholog Rad9 and the Mre11 complex regulates resection, end-tethering and repair of a double-strand break, PLoS genetics, 11 (2015) e1004928.

[207] B. Song, P. Sung, Functional interactions among yeast Rad51 recombinase, Rad52 mediator, and replication protein A in DNA strand exchange, The Journal of biological chemistry, 275 (2000) 15895-15904.

[208] L. Krejci, V. Altmannova, M. Spirek, X. Zhao, Homologous recombination and its regulation, Nucleic acids research, 40 (2012) 5795-5818.

[209] A. Shinohara, H. Ogawa, T. Ogawa, Rad51 protein involved in repair and recombination in S. cerevisiae is a RecA-like protein, Cell, 69 (1992) 457-470.

[210] D.Y. Lui, T.L. Peoples-Holst, J.C. Mell, H.Y. Wu, E.W. Dean, S.M. Burgess, Analysis of close stable homolog juxtaposition during meiosis in mutants of Saccharomyces cerevisiae, Genetics, 173 (2006) 1207-1222.

[211] A.V. Mazin, O.M. Mazina, D.V. Bugreev, M.J. Rossi, Rad54, the motor of homologous recombination, DNA Repair (Amst), 9 (2010) 286-302.

[212] G. Petukhova, S. Stratton, P. Sung, Catalysis of homologous DNA pairing by yeast Rad51 and Rad54 proteins, Nature, 393 (1998) 91-94.

[213] P. Dupaigne, C. Le Breton, F. Fabre, S. Gangloff, E. Le Cam, X. Veaute, The Srs2 helicase activity is stimulated by Rad51 filaments on dsDNA: implications for crossover incidence during mitotic recombination, Mol Cell, 29 (2008) 243-254.

[214] C.L. Fasching, P. Cejka, S.C. Kowalczykowski, W.D. Heyer, Top3-Rmi1 dissolve Rad51-mediated D loops by a topoisomerase-based mechanism, Mol Cell, 57 (2015) 595-606.

[215] Y.C. Kim, M.H. Lee, S.S. Ryu, J.H. Kim, H.S. Koo, Coaction of DNA topoisomerase IIIalpha and a RecQ homologue during the germ-line mitosis in Caenorhabditis elegans, Genes to cells : devoted to molecular & cellular mechanisms, 7 (2002) 19-27.

[216] M.G. Blanco, J. Matos, U. Rass, S.C. Ip, S.C. West, Functional overlap between the structure-specific nucleases Yen1 and Mus81-Mms4 for DNA-damage repair in S. cerevisiae, DNA Repair (Amst), 9 (2010) 394-402.

[217] T.M. Ashton, H.W. Mankouri, A. Heidenblut, P.J. McHugh, I.D. Hickson, Pathways for Holliday junction processing during homologous recombination in Saccharomyces cerevisiae, Molecular and cellular biology, 31 (2011) 1921-1933.

[218] C. Frei, S.M. Gasser, The yeast Sgs1p helicase acts upstream of Rad53p in the DNA replication checkpoint and colocalizes with Rad53p in S-phase-specific foci, Genes & development, 14 (2000) 81-96.

[219] H.W. Mankouri, I.D. Hickson, Top3 processes recombination intermediates and modulates checkpoint activity after DNA damage, Molecular biology of the cell, 17 (2006) 4473-4483.

[220] X. Xu, S. Blackwell, A. Lin, F. Li, Z. Qin, W. Xiao, Error-free DNA-damage tolerance in Saccharomyces cerevisiae, Mutat Res Rev Mutat Res, 764 (2015) 43-50.

[221] S. Gangloff, B. de Massy, L. Arthur, R. Rothstein, F. Fabre, The essential role of yeast topoisomerase III in meiosis depends on recombination, The EMBO journal, 18 (1999) 1701-1711.

[222] P.M. Watt, E.J. Louis, R.H. Borts, I.D. Hickson, Sgs1: a eukaryotic homolog of E. coli RecQ that interacts with topoisomerase II in vivo and is required for faithful chromosome segregation, Cell, 81 (1995) 253-260.

[223] K. Zakharyevich, S. Tang, Y. Ma, N. Hunter, Delineation of joint molecule resolution pathways in meiosis identifies a crossover-specific resolvase, Cell, 149 (2012) 334-347.

[224] B.I. Lee, D.M. Wilson, 3rd, The RAD2 domain of human exonuclease 1 exhibits 5' to 3' exonuclease and flap structure-specific endonuclease activities, The Journal of biological chemistry, 274 (1999) 37763-37769.

[225] P. Szankasi, G.R. Smith, A role for exonuclease I from S. pombe in mutation avoidance and mismatch correction, Science (New York, N.Y.), 267 (1995) 1166-1169.

[226] P. Szankasi, G.R. Smith, A DNA exonuclease induced during meiosis of Schizosaccharomyces pombe, Journal of Biological Chemistry, 267 (1992) 3014-3023.

[227] D.X. Tishkoff, N.S. Amin, C.S. Viars, K.C. Arden, R.D. Kolodner, Identification of a human gene encoding a homologue of Saccharomyces cerevisiae EXO1, an exonuclease implicated in mismatch repair and recombination, Cancer research, 58 (1998) 5027-5031.

[228] C. Schmutte, R.C. Marinescu, M.M. Sadoff, S. Guerrette, J. Overhauser, R. Fishel, Human exonuclease I interacts with the mismatch repair protein hMSH2, Cancer research, 58 (1998) 4537-4542.

[229] C. Schmutte, M.M. Sadoff, K.S. Shim, S. Acharya, R. Fishel, The interaction of DNA mismatch repair proteins with human exonuclease I, The Journal of biological chemistry, 276 (2001) 33011-33018.

[230] L. Maringele, D. Lydall, EXO1 plays a role in generating type I and type II survivors in budding yeast, Genetics, 166 (2004) 1641-1649.

[231] M.K. Zubko, S. Guillard, D. Lydall, Exo1 and Rad24 differentially regulate generation of ssDNA at telomeres of Saccharomyces cerevisiae cdc13-1 mutants, Genetics, 168 (2004) 103-115.

[232] I. Morin, H.P. Ngo, A. Greenall, M.K. Zubko, N. Morrice, D. Lydall, Checkpoint-dependent phosphorylation of Exo1 modulates the DNA damage response, The EMBO journal, 27 (2008) 2400-2410.

[233] M.B. Smolka, C.P. Albuquerque, S.H. Chen, H. Zhou, Proteome-wide identification of in vivo targets of DNA damage checkpoint kinases, Proceedings of the National Academy of Sciences of the United States of America, 104 (2007) 10364-10369.

[234] M. El-Shemerly, D. Hess, A.K. Pyakurel, S. Moselhy, S. Ferrari, ATR-dependent pathways control hEXO1 stability in response to stalled forks, Nucleic acids research, 36 (2008) 511-519.

[235] E. Bolderson, N. Tomimatsu, D.J. Richard, D. Boucher, R. Kumar, T.K. Pandita, S. Burma, K.K. Khanna, Phosphorylation of Exo1 modulates homologous recombination repair of DNA double-strand breaks, Nucleic acids research, 38 (2010) 1821-1831.

[236] K. Engels, M. Giannattasio, M. Muzi-Falconi, M. Lopes, S. Ferrari, 14-3-3 Proteins regulate exonuclease 1-dependent processing of stalled replication forks, PLoS genetics, 7 (2011) e1001367.

[237] X. Chen, I.K. Kim, Y. Honaker, S.C. Paudyal, W.K. Koh, M. Sparks, S. Li, H. Piwnica-Worms, T. Ellenberger, Z. You, 14-3-3 proteins restrain the Exo1 nuclease to prevent overresection, The Journal of biological chemistry, 290 (2015) 12300-12312.

[238] X. Chen, S.C. Paudyal, R.I. Chin, Z. You, PCNA promotes processive DNA end resection by Exo1, Nucleic acids research, (2013).

[239] S.H. Yang, R. Zhou, J. Campbell, J. Chen, T. Ha, T.T. Paull, The SOSS1 single-stranded DNA binding complex promotes DNA end resection in concert with Exo1, The EMBO journal, (2012).

[240] L.R. Myler, I.F. Gallardo, Y. Zhou, F. Gong, S.H. Yang, M.S. Wold, K.M. Miller, T.T. Paull, I.J. Finkelstein, Single-molecule imaging reveals the mechanism of Exo1 regulation by single-stranded DNA binding proteins, Proceedings of the National Academy of Sciences of the United States of America, 113 (2016) E1170-1179.

[241] M. Segurado, J.F. Diffley, Separate roles for the DNA damage checkpoint protein kinases in stabilizing DNA replication forks, Genes & development, 22 (2008) 1816-1827.

[242] Mullen JR, Kaliraman V, Brill SJ, Bipartite structure of the SGS1 DNA helicase in Saccharomyces cerevisiae, Genetics,154 (2000) 1101-1114.

Chapter Two:

Differential genetic interactions between Sgs1, DNA-damage checkpoint

components and DNA repair factors in the maintenance of chromosome stability

Note to the reader: This chapter has been previously published with permission from the publisher as Lillian Doerfler, Lorena Harris, Emilie Viebranz and Kristina H Schmidt (2011). "Differential genetic interactions between Sgs1, DNA-damage checkpoint components and DNA repair factors in the maintenance of chromosome stability" *Genome Integrity*., 2:8. Research was designed by Kristina Schmidt with contributions from Lorena Harris and Lillian Doerfler. Permissions are found in appendix B. Lillian Doerfler and Lorena Harris contributed equally to experiments performed.

Corresponding author: Kristina Schmidt, Department of Cell Biology, Microbiology and Molecular Biology, University of South Florida, 4202 E. Fowler Avenue, ISA2015, Tampa, FL 33620. Phone: (813) 974-1592. Fax: (813) 974- 1614.; E-mail: kschmidt@usf.edu

ABSTRACT

Background: Genome instability is associated with human cancers and chromosome breakage syndromes, including Bloom's syndrome, caused by inactivation of BLM helicase. Numerous mutations that lead to genome instability are known, yet how they interact genetically is poorly understood.

Results: We show that spontaneous translocations that arise by nonallelic homologous recombination in DNA- damage-checkpoint-defective yeast lacking the BLM-related Sgs1 helicase (*sgs1Δ mec3Δ*) are inhibited if cells lack Mec1/ATR kinase. Tel1/ATM, in contrast, acts as a suppressor independently of Mec3 and Sgs1. Translocations are also inhibited in cells lacking Dun1 kinase, but not in cells defective in a parallel checkpoint branch defined by Chk1 kinase. While we had previously shown that *RAD51* deletion did not inhibit translocation formation, *RAD59* deletion led to inhibition comparable to the *rad52Δ* mutation. A candidate screen of other DNA metabolic factors identified Exo1 as a strong suppressor of chromosomal rearrangements in the sgs1Δ mutant, becoming even more important for chromosomal stability upon *MEC3* deletion. We determined that the C-terminal third of Exo1, harboring mismatch repair protein binding sites and phosphorylation sites, is dispensable for Exo1's roles in chromosomal rearrangement suppression, mutation avoidance and resistance to DNA-damaging agents.

Conclusions: Our findings suggest that translocations between related genes can form by Rad59-dependent, Rad51-independent homologous recombination, which is independently suppressed by Sgs1, Tel1, Mec3 and Exo1 but promoted by Dun1 and the telomerase-inhibitor Mec1. We propose a model for the functional interaction between mitotic recombination and the DNA-damage checkpoint in the suppression of chromosomal rearrangements in *sgs1Δ* cells.

INTRODUCTION

Eukaryotic cells have mechanisms at their disposal for the detection and repair of spontaneous and induced DNA lesions, thus preventing them from giving rise to potentially abnormal daughter cells. However, if these mechanisms are defective or overwhelmed by damage, deleterious chromosomal rearrangements can arise. A multitude of genes and genetic pathways for the maintenance of genome stability has been identified mostly using genetic screens in simple model organisms such as the yeast *Saccharomyces cerevisiae*. They include DNA damage checkpoints, DNA repair factors and proteins for processing of recombination substrates and intermediates [1-10]. The importance of the same mechanisms for maintaining genome stability in human cells is highlighted by the association of mutations in the human homologues of these yeast genes with chromosome breakage syndromes, which are characterized by signs of premature aging and/or cancer development. The syndromes include Nijmegen breakage syndrome associated with mutations in *NBS1*, the homologue of yeast *XRS2* [11-13]; Bloom's syndrome and Werner syndrome associated with mutations in *BLM* and *WRN*, respectively, both related to yeast SGS1 [14,15]; and ataxia telangiectasia associated with mutations in ATM [16], which is related to yeast *TEL1* [17].

Yeast *SGS1* encodes a 5' to 3' DNA helicase that preferentially unwinds three- and four-way junctions typical of replication and recombination intermediates and has recently been shown to collaborate with Exo1 in the long-range processing of double-strand breaks (DBSs) [18-21]. Without Sgs1, cells accumulate gross-chromosomal rearrangements (GCRs), exhibit elevated levels of mitotic recombination, have a reduced replicative lifespan and are sensitive to chemicals that alkylate DNA or slow

58

replication forks [2,22-26]. Among DNA- damage checkpoint components, Mec1 kinase, also considered the homolog of mammalian ATR [27-29], has been identified as one of the strongest suppressors of GCRs in yeast [3,4]. Other cellular phenotypes of *mec1Δ* mutants include increased sensitivity to DNA damaging agents and deficient DNA-damage checkpoint response [30], instability of stalled forks [31], accumulation of DNA breaks [32] and, in addition to these mitotic defects, deficiencies in meiotic checkpoint activation and recombination [33-35]. In contrast to Mec1, cells lacking the Tel1 checkpoint kinase, which is related to mammalian ATM [17,36], are not sensitive to DNA damaging agents [17], do not accumulate GCRs above wildtype levels [3], but show telomere erosion [36]. Synergistic interactions between *mec1Δ* and *tel1Δ* mutations have been reported for many phenotypes, suggesting a functional relationship and redundancy between the two kinases [3,17,37,38]. Other checkpoint components, such as those involved in sensing DNA damage (Mec3, Rad24), appear to have only small to moderate roles in suppressing GCRs in yeast [3,4]. In cells lacking the Sgs1 helicase, however, Mec3 and Rad24 strongly suppress overall genome instability [3,4] as well as the formation of spontaneous, recurring translocations between short identical sequences in non-allelic, but related, DNA sequences [10]. Utilizing the high susceptibility of the *sgs1Δ mec3Δ* mutant to recurring translocation formation between *CAN1*, *LYP1* and *ALP1*, we have in the current study conducted a candidate screen to identify two types of DNA metabolic factors those that are required for the formation of recurring translocations in the *sgs1Δ mec3Δ* mutant and those that act independently of Sgs1 and Mec3 to suppress translocations. For this purpose, *mec1Δ, tel1Δ, dun1Δ, chk1Δ* and *rad59Δ* mutations were introduced into the *sgs1Δ*

mec3Δ mutant and the accumulation of recurring translocations was assessed. We further determined how the lack of other DNA metabolic factors (*yen1Δ, lig4Δ, exo1Δ, rad1Δ, pol32Δ*) affects the accumulation of genome rearrangements, identifying a strong synergistic interaction between *sgs1Δ* and *exo1Δ*. We propose an integrated model for independent, functional interactions between Sgs1, HR subpathways and various DNA damage-checkpoint branches in the suppression of chromosomal rearrangements.

RESULTS AND DISCUSSION

Functional interaction between Sgs1 and DNA-damage checkpoint components Mec3, Mec1, Tel1, Dun1 and Chk1 in the suppression of chromosomal translocations

Chromosomal translocations between short stretches of homology in nonallelic sequences that are naturally present in the yeast genome, such as the highly similar, but diverged *CAN1* (on chromosome V), *ALP1* and *LYP1* genes (on chromosome XIV, 60-65% identity), are normally suppressed in yeast. However, they are recurrent in *sgs1Δ* mutants with certain additional DNA-metabolic defects, including *mec3Δ, rad24Δ, cac1Δ, asf1Δ* and *rfc5- 1* [10]. One of the mutants most susceptible to recurring translocations between the *CAN1, LYP1* and *ALP1* loci is the *sgs1Δ mec3Δ* mutant, whereas translocations are not found in the *sgs1Δ mec1Δ* mutant [10]. Here, we wanted to test whether the lack of *CAN1/LYP1/ALP1* translocations in the *sgs1Δ mec1Δ* mutant meant that Mec1 was not a suppressor of translocations and therefore its deletion had

60

no affect on translocation formation, or that Mec1 was actually required for the formation of viable chromosomal translocations. If the latter was true, we expected that introducing a *mec1Δ* mutation into the highly susceptible *sgs1Δ mec3Δ* strain should inhibit the accumulation *CAN1/LYP1/ALP1* translocations. Indeed, we found that while deleting *MEC1* led to a synergistic increase (~ 7-fold) in the rate of all GCR types compared to the *sgs1Δ mec3Δ* mutant (P < 0.0001), screening of GCR clones obtained from 431 individual *sgs1Δ mec3Δ mec1Δ* cultures failed to reveal a single *CAN1/LYP1/ALP1* translocation, signifying a > 7-fold decrease in the translocation rate compared to the *sgs1Δ mec3Δ* mutant (Table 1). The synergistic GCR rate increase in the *sgs1Δ mec3Δ mec1Δ* mutant shows that Mec1 can activate its targets through Mec3-independent sensing of DNA damage. This may occur by Mec1-Ddc2 itself recognizing and binding to DNA lesions [39,40] or through DNA- damage sensors other than the Mec3 clamp signaling to Mec1. The synergistic GCR rate increase in the *sgs1Δ mec3Δ mec1Δ* mutant also indicates that the failure to form *CAN1/LYP1/ALP1* translocations when *MEC1* is deleted is not due to an inability to form viable GCRs, but rather suggests that DNA lesions are channeled into GCR pathways other than homology-driven translocation. Most likely, Mec1 promotes chromosomal translocations by inhibiting *de novo* telomere synthesis at chromosome breaks [1], for example by phosphorylating the telomerase-inhibitor Pif1 [41] and by phosphorylating Cdc13 and thus preventing its accumulation at DNA breaks [42]. In a haploid wildtype cell, these chromosomal translocations are expected to be rare due to restraints placed on homologous recombination events by the need for relative long regions of sequence identity. However, when the restraints on homologous recombination are relaxed and

spontaneous DNA lesions are not properly detected by the DNA-damage checkpoint, as could be assumed for the *sgs1Δ mec3Δ* mutant, chromosomal translocations are promoted and occur between much shorter regions of sequence identity, such as the 5-41-bp segments present in *CAN1, LYP1* and *ALP1*.

Deleting *TEL1*, which encodes another DNA-damage checkpoint kinase that is considered at least partially functionally redundant with Mec1, had the same effect as deleting *MEC1* on the accumulation of all types of GCR (Table 1), as evidenced by the 44-fold increase in the overall GCR rate compared to the *sgs1Δ mec3Δ* mutant (5.7×10^{-6} versus 1.3×10^{-7}, P < 0.0001). However, deleting *TEL1* had the opposite effect on *CAN1/ LYP1/ALP1* translocation formation (Table 1). Instead of inhibiting *CAN1/LYP1/ALP1* translocations like the *mec1Δ* mutation, the *tel1Δ* mutation led to an increase (~15-fold) in *CAN1/LYP1/ALP1* translocations (Table 1). Unlike *mec1Δ* mutants, mutants lacking Tel1 are impaired in their ability to maintain telomeres [36] and may thus be unable to heal DNA breaks by *de novo* telomere addition. Thus, in the absence of Tel1, DNA breaks may be channeled into alternative pathways for repair, such as HR, and more frequently give rise to *CAN1/LYP1/ALP1* rearrangements under conditions that favor aberrant HR such as those in the *sgs1Δ mec3Δ* mutant. That failure to activate either Tel1 or Mec3-checkpoint pathways contributes independently to recurrent *CAN1/LYP1/ALP1* translocation formation suggests that both ssDNA overhangs or gaps, thought to be sensed in a Mec3-dependent manner, and DSBs, thought to be sensed in a Tel1-dependent manner, can lead to *CAN1/LYP1/ALP1* translocations and that they accumulate in unperturbed *sgs1Δ* cells spontaneously. The synergistic increase in overall genome instability in the *sgs1Δ mec3Δ tel1Δ* mutant

might also indicate that in the absence of lesion binding by the Mec3 clamp some lesions are further processed and eventually detected by the Tel1-dependent pathway. For example, a stalled replication fork might eventually be processed into double-stranded ends in an attempt at fork restart by fork regression or template-switching. Thus, both Tel1 and Mec1 act independently of Mec3 and Sgs1 to strongly suppress overall genome instability, but they affect *CAN1/LYP1/ALP1* translocation formation in opposite ways. The inhibition of *CAN1/LYP1/ALP1* translocations upon *MEC1* deletion as opposed to their increase upon *TEL1* deletion can most likely be explained by their opposite effects on telomere synthesis, with Mec1 inhibiting it and Tel1 promoting it. This is also consistent with the previous report of different GCR spectra in the *tel1Δ* and *mec1Δ* single mutants [1]. Apart from regulating telomere maintenance factors, it is also conceivable that the DNA-damage checkpoint dependent phosphorylation of homologous recombination factors, such as Rad55, Slx4 and Mus81 [43-47] contributes to differential regulation of translocation formation in the *sgs1Δ mec3Δ* mutant.

The opposing effects of Tel1 and Mec1 on *CAN1/ LYP1/ALP1* translocation formation led us to investigate other DNA-damage checkpoint components in *sgs1Δ* and *sgs1Δ mec3Δ* mutants. We found that deletion of either *CHK1* or *DUN1* led to a synergistic increase in overall genome instability when combined with an *sgs1Δ* mutation (P < 0.0001), however only the *dun1Δ* mutation caused a further significant GCR rate increase in the *sgs1Δ mec3Δ* mutant (P < 0.0001, Table 1) whereas the *chk1Δ* mutation did not (P = 0.1615, Table 1). Analysis of the GCR types revealed accumulation of *CAN1/ LYP1/ALP1* translocations in the Chk1-deficient *sgs1Δ mec3Δ* mutant at a similar rate as in the *sgs1Δ mec3Δ* mutant, but not in the Dun1-deficient

sgs1Δ mec3Δ mutant (Table 1), indicating that Dun1, like Mec1, promotes translocation events between *CAN1, LYP1* and *ALP1* whereas Chk1 does not. This is likely due to Mec1-mediated activation of Dun1 kinase, which in turn inactivates the transcription repressor Crt1, thus allowing transcription of several DNA-damage inducible genes [48,49]. Chk1 kinase is also activated through Mec1 in response to DNA damage and causes a transient G2/M arrest by blocking anaphase progression [50,51]. However, in contrast to Dun1, Chk1 is not thought to regulate DNA repair pathways, and its deletion did not inhibit translocation formation in the *sgs1Δ mec3Δ* mutant (Table 1). As expected, deletion of *RAD17*, which encodes another subunit of the Mec3/ Rad17/Ddc1 checkpoint clamp, had a similar effect on *CAN1/LYP1/ALP1* translocation formation in the *sgs1Δ tel1Δ* mutant as deletion of *MEC3* (Table 1). The detection of a *CAN1/LYP1/ALP1* translocation in two strains that expressed wildtype Sgs1 (*mec3Δ tel1Δ* (Table 1) and *mec3Δ tel1Δ rad17Δ* (not shown)) suggests that even in the presence of wildtype Sgs1 cells may accumulate *CAN1/LYP1/ALP1* translocations as long as they are deficient in at least two independent suppressors of translocation formation, such as Tel1 and Mec3 identified here.

Deletion of RAD59 inhibits spontaneous interchromosomal translocations between short repeats

We previously showed that translocations between *CAN1, LYP1* and *ALP1* in the *sgs1Δ mec3Δ* mutant are Rad52-dependent, but translocations still formed when Rad51 was absent [10]. To assess the role of other HR factors in translocation formation we deleted RAD59 in the highly susceptible *sgs1Δ mec3Δ* mutant and measured the rate of

accumulating all types of GCRs as well as *CAN1/LYP1/ALP1* translocations. One

CAN1/LYP1/ALP1 rearrangement was identified among GCR clones obtained from 158

independent cultures of the *sgs1Δ mec3Δ rad59Δ* mutant (Table 2), indicating a 10-fold

reduction in the *CAN1/LYP1/ALP1* translocation rate compared to the *sgs1Δ mec3Δ*

mutant. Thus, similar to Rad52, Rad59 is required for interchromosomal translocations

between short identical sequences in related genes. If Rad59 was indeed required for

translocation formation, we predicted that the formation of *CAN1/ LYP1/ALP1*

translocations in the *sgs1Δ mec3Δ rad51Δ* mutant would also be inhibited by a *rad59Δ*

mutation. Thus, we generated an *sgs1Δ mec3Δ rad51Δ rad59Δ* mutant and screened

for *CAN1/LYP1/ALP1* translocations. Among 168 independent GCR clones we identified

one *CAN1/LYP1/ALP1* translocation, indicative of a 28-fold reduction of the

translocation rate compared to the *sgs1Δ mec3Δ rad51Δ* mutant (Table 2). Thus

translocations between *CAN1, LYP1* and/or *ALP1* can form through Rad52/Rad59-

mediated HR that does not require Rad51. Rad59 has recently also been shown to

contribute to GCRs mediated by certain Ty-elements and to translocations involving

short DNA sequences of limited sequence identity [6,52].

While Rad52 is required for all HR in yeast, some DNA breaks can be repaired

by HR pathways that do not require Rad51, including single-strand annealing (SSA),

break-induced replication (BIR) and recombination-mediated telomere-lengthening Type

II [53-58]. SSA is a mechanism for the repair of a DSB between repeated DNA elements

and requires Rad59, but not Rad51 [59]. In order for the interchromosomal *CAN1/*

LYP1/ALP1 rearrangements to arise by SSA, however, at least two DSBs would have to

occur in the same cell one DSB within or downstream of *CAN1* on chromosome V and

one DSB near *ALP1* (or *LYP1*) on chromosome XIV. Resection would expose the short stretches of homology shared by *CAN1* and *ALP1* (or *LYP1*) [60], allowing them to anneal, followed by removal of the nonhomologous overhangs and ligation. Rad59-dependent, Rad51-independent interchromosomal translocation between *his3* fragments was recently shown after induction of HO-breaks in the two recombining chromosomes [61]. Such an interchromosomal SSA event could also produce the types of rearrangements we have observed between *CAN1, LYP1* and *ALP1*; however, the ends of chromosomes V and XIV not engaged in the SSA event would be left unrepaired and most likely would be lost after cell division unless the recombination event occurs in G2/M when sister-chromatids are present. Moreover, since we have shown that wildtype copies of *LYP1* and *ALP1* are still present in recombinants with *CAN1/LYP1/ALP1* rearrangements, indicative of a nonreciprocal translocation event [60], and the parts of chromosome XIV that would be lost after SSA contain essential genes, SSA is unlikely to be the main recombination mechanism that gives rise to *CAN1/ LYP1/ALP1* rearrangements.

Besides SSA, BIR also matches the genetic requirements for *CAN1/LYP1/ALP1* translocation formation. BIR is initiated by invasion of a duplex by a single- stranded 3'end of a one-sided DBS followed by replication to the chromosome end. Although Sgs1 has roles in recombination, specifically sister-chromatid exchange and resolution of recombination intermediates [2,9,62-64], it is not required for Rad51-independent BIR [57]. In contrast to SSA, the nonreciprocal nature of BIR events would maintain an intact copy of chromosome XIV in addition to the chromosome V/XIV translocation, suggesting that it is the more likely mechanism involved in *CAN1/LYP1/ALP1*

translocation. BIR has been implicated in the repair of one-sided DSBs, such as replication forks that collapsed at a single-strand break. BIR is also thought to allow telomerase-deficient cells (*tlc1Δ*), whose telomeres have shortened to a point where cells can no longer proliferate, to survive by extending what could be considered a one-sided DSB. Survivors can arise either by adding subtelomeric *Y'* elements in a Rad51-dependent mechanism (Type I) or by adding telomeric $(G_{1-3}T)_n$ repeats in a Rad51-independent, but Rad59-dependent mechanism (Type II) [53-55]. The differential requirement for Rad51 and Rad59 in these two pathways is thought to result from the differences in length and sequence identity of the recombination substrates for Type I and Type II [53]. The long, nearly identical (~1% variation within the same strain) *Y'* elements [65] are thought to be better substrates for Rad51-mediated strand invasion, whereas Rad59 is able to use the shorter stretches of homology likely to be found within the highly variable $(G_{1-3}T)_n$ repeats [53]. Besides BIR, evidence of homology-length dependency is also seen in gene conversion, with Rad59 becoming increasingly important as the length of sequence homology decreases [59]. This length-dependency may also explain our observation that *CAN1/ LYP1/ALP1* rearrangements, which show short regions of homology at the breakpoints [10,60], are inhibited by deletion of *RAD59*, but not by deletion of *RAD51*. Despite this differential effect on chromosome rearrangements between *CAN1, LYP1* and *ALP1*, we observed no difference in the rate of overall genome instability between *sgs1Δ mec3Δ rad51Δ* and *sgs1Δ mec3Δ rad59Δ* mutants (P = 0.6892, Table 2), suggesting that the DNA lesions that give rise to viable GCRs are accessible to multiple repair pathways.

Candidate screen reveals EXO1 as a strong suppressor of GCR formation in cells lacking Sgs1

To assess the possible role of other DNA metabolic factors in the suppression or formation of GCRs in cells lacking Sgs1, we introduced *exo1Δ, pol32Δ, rad1Δ, lig4Δ* and *yen1Δ* mutations into *sgs1Δ* and *sgs1Δ mec3Δ* mutants. Screening of the single, double and triple mutants revealed that *RAD1, POL32, LIG4* and *YEN1* are not strong suppressors of GCRs in wildtype cells, or in *sgs1Δ* or *sgs1Δ mec3Δ* mutants (Table 3). However, when we assessed the formation of *CAN1/LYP1/ALP1* translocations in *sgs1Δ mec3Δ* mutants with *pol32Δ* or *rad1Δ* mutations we found that in both triple mutants *CAN1/LYP1/ALP1* translocations were inhibited, revealing one *CAN1/LYP1* translocation among 98 independent GCR clones in the *sgs1Δ mec3Δ pol32Δ* mutant and none (0/55) in the *sgs1Δ mec3Δ rad1Δ* mutant. Pol32, a nonessential subunit of polymerase δ that promotes processivity of the polymerase, is not required for SSA, but for DNA repair processes that involve extensive DNA synthesis, such as BIR [66], consistent with BIR being a pathway for *CAN1/LYP1/ALP1* translocation formation. Although Rad1, a subunit of the Rad1-Rad10 nuclease critical for the removal of non-homologous overhangs from annealed single strands in processes such as SSA [67,68], has not been shown to be required for BIR, it has been implicated in the removal of nonhomologous overhangs during GCR formation [69] and in recombination events that combine BIR and SSA processes [70,71].

Deletion of *EXO1*, coding for a nuclease with 5' to 3' exonuclease and flap-endonuclease activities, which has roles in mitotic and meiotic recombination as well as mutation avoidance and is thought to cooperate with Sgs1 in the processing of DSBs

[19,72], induced the largest synergistic GCR rate increase we have observed to date in the *sgs1Δ* mutant. While *sgs1Δ* and *exo1Δ* single mutants exhibited moderately increased GCR rates compared to wildtype, the GCR rate of the *sgs1Δ exo1Δ* mutant was several hundred-fold higher than the rates of the single mutants (P < 0.0001, Table 3). This GCR rate increased another 26-fold upon deletion of MEC3 (P < 0.0001, Table 3). Screening of GCRs obtained from 66 independent cultures of the *sgs1Δ mec3Δ exo1Δ* mutant identified two *CAN1/LYP1/ALP1* translocations, indicating a ~ 200-fold increase in the *CAN1/LYP1/ ALP1* translocation rate compared to the *sgs1Δ mec3Δ* mutant (3.5×10^{-6} versus 1.7×10^{-8}).

Exo1 contains conserved N-terminal N- and I-nuclease domains, apparently separated by a short disordered linker, and binding sites for the mismatch repair (MMR) proteins Mlh1 and Msh2 have been located within the C-terminal half of Exo1 [72-74], which is predicted to be intrinsically disordered (Figure 1A). Four phosphorylation sites (S372, S567, S587, S692) required for the regulation of the DNA-damage response have also been located in the disordered C-terminus [75]. To determine if the C-terminus of Exo1 plays a role in the suppression of genome instability in the *sgs1Δ* mutant, we constructed a set of C-terminal deletions ranging from 100 to 400 residues (Figure 1A and 1B). We found that the C-terminal 260 residues of Exo1, making up 37% of the protein, play no major role in suppressing the accumulation of GCRs in the *sgs1Δ* mutant (Table 4). To test the possibility that the C-terminus with its binding sites for MMR proteins might be required for Exo1's role in mutation avoidance, but not for its role in suppressing GCRs, we utilized a fluctuation assay to determine the rate of accumulating canavanine resistance (Can^r) mutations in strains expressing the various

C-terminal Exo1 truncations (Table 5). As in the GCR assay, deletion of up to 260 residues had no effect on the Can^r mutation rate (P = 0.3524) whereas deletion of 280 or more residues caused a null phenotype (P = 0.0001). Similarly, only deletion of 280 or more residues caused sensitivity to methyl methanesulfonate (MMS) (Figure 1C). No sensitivity to 200 mM hydroxyurea was observed for any of the *exo1* mutants (Figure 1C). Thus, deletion of up to 260 residues caused a phenotype similar to wildtype in all assays tested here, whereas deletion of 280 or more residues caused a null (*exo1Δ*) phenotype.

In addition to providing MMR protein interaction sites, the C-terminus of Exo1 contains four phosphorylation sites (S372, S567, S587, S692), which were recently shown to be important for the regulation of the DNA damage checkpoint in response to uncapped telomeres in a *cdc13-1* mutant [75]. Unlike in a *cdc13-1* mutant, we did not detect Exo1 phosphorylation in the sgs1Δ mutant (data not shown), and deletion of the C-terminal third of Exo1 (*exo1-ΔC260*), which contains three of the four phosphorylation sites (S567, S587, S692), had no effect on Exo1 function in the assays used here (Can^r mutation rate, GCR assay, MMS sensitivity). The fourth phosphorylation site (S372) is present in both the *exo1-ΔC260* mutant and the *exo1-ΔC280* mutant and, therefore, is not responsible for the different phenotypes associated with the two alleles. Thus, the known phosphorylation sites in Exo1 do not appear to be required for Exo1's role in mutation avoidance, resistance to MMS or suppression of GCRs in a *sgs1Δ* mutant. Instead, it is likely that the *ΔC280* deletion affects Exo1 nuclease activity directly by disrupting intramolecular interactions with the N-terminus. The loss of yet unknown post-translational modifications in this segment of Exo1 or an indirect effect caused by

the loss of interaction with other cellular factors could also lead to the deficiency of the *exo1ΔC280* allele.

Besides the overall increase in genome instability, *CAN1/LYP1/ALP1* rearrangements seen in the *sgs1Δ mec3Δ* mutant were also present in the *sgs1Δ mec3Δ exo1Δ* mutant. Normally, Exo1 and Sgs1 function in independent end resection pathways that cooperate in the processing of DSBs, especially the long-range resection of the 5'-strand [19,20], and Marrero and Symington [21] recently showed that this extensive resection inhibits BIR in a plasmid-based assay. Besides upregulation of BIR, which was also accompanied by chromosome rearrangements, the *exo1Δ sgs1Δ* mutant was also more proficient in *de novo* telomere synthesis at HO- endonuclease-induced chromosome breaks [18,21]. The combination of increased BIR and more efficient *de novo* telomere addition, both of which have been identified as major mechanisms for the healing of chromosome V breaks in the GCR assay [76,77], likely also explains the remarkably strong accumulation of genome rearrangements originating from spontaneous DNA lesions in the *exo1Δ sgs1Δ* mutant studied here. Our study further adds that the *exo1Δ sgs1Δ* mutant has even greater potential for the accumulation of viable genome rearrangements, which is suppressed (~ 26-fold) in the *sgs1Δ exo1Δ* mutant by Mec3-dependent DNA- damage checkpoint functions (P < 0.0001). Nonhomologous end-joining does not appear to be a significant source for these genome rearrangements, as indicated by the lack of any effect of *LIG4* gene deletion in mutants with various combinations of *sgs1Δ, exo1Δ* and *mec3Δ* mutations (e.g., GCR rate of *sgs1Δ mec3Δ exo1Δ* compared to *sgs1Δ mec3Δ exo1Δ lig4Δ*, P =

0.3953, Table 3); however, it is also plausible that in the absence of one repair pathway DNA lesions simply become substrates for various other available repair pathways.

CONCLUSION

Our results indicate that spontaneous, interchromosomal translocations between short regions of sequence identity (5-41 bp), such as those present in the *CAN1, LYP1* and *ALP1* genes used in our assay, are promoted by Mec1/Dun1/Rad59-dependent pathways whereas Tel1, Mec3 and Sgs1 act as independent suppressors (Figure 2). The requirement for Pol32 and Rad1 in the translocation process further suggests the need for extensive DNA synthesis, such as seen in BIR, and the removal of nonhomologous overhangs from annealed single-strands, critical for SSA and implicated in GCR formation. Exo1 nuclease is a suppressor of overall genome rearrangements as well as *CAN1/LYP1/ALP1* translocations when cells lack Sgs1 or both Sgs1 and Mec3. That the disordered, C-terminal third is dispensable for Exo1 function in our assays further indicates that physical interaction with MMR proteins in this region and regulation of Exo1 function in response to DNA-damage are not important for Exo1's role in the suppression of spontaneous GCRs, mutation avoidance and resistance to MMS.

METHODS

Yeast strains and media

All strains used in this study are derived from KHSY802 (*MATa, ura3-52, trp1Δ63, his3Δ200, leu2Δ1, lys2Bgl, hom3-10, ade2Δ1, ade8, hxt13::URA3*) or the isogenic strain of the opposite mating type. Desired gene deletions were introduced by HR-mediated integration of PCR products containing a selectable marker cassette flanked by 50-nt sequences complementary to the target locus [78]. C-terminal truncations of Exo1 were constructed by replacing the desired DNA sequence at the chromosomal *EXO1* locus with a myc-epitope encoding sequence amplified from pFA-13Myc. His3MX6 (a gift from Mark Longtine, Washington University, St. Louis). Expression of Exo1 truncation alleles was confirmed by Western blotting using monoclonal anti-c-myc antibody (Covance). All haploid strains with multiple gene deletions were obtained by sporulating diploids heterozygous for the desired mutations to minimize the risk of obtaining suppressors. This was especially important for combinations of mutations known to cause fitness defects, such as *sgs1Δ* and *pol32Δ*. Spore isolation was followed by genotyping of meiotic pro- ducts by spotting on selective media or by PCR. All strains used in this study are listed in Table 6. Media for propagating yeast strains have been previously described [76,77].

Sensitivity to DNA damaging agents HU and MMS

Cell cultures were grown in yeast extract/peptone/dextrose (YPD) media and adjusted to $OD_{600} = 1$. Tenfold dilutions were spotted on YPD, YPD supplemented with

0.05% methyl-methanesulfonate (MMS) and YPD supplemented with 200 mM hydroxyurea (HU). Colony growth was documented after incubation at 30°C for 3 days.

Fluctuation Assays

Rates of accumulating spontaneous gross-chromosomal rearrangements (GCRs) were determined by fluctuation analysis and the method of the median as previously described [77,79]. Cells with GCRs were detected by their resistance to canavanine and 5-fluoro-orotic acid (Can[r] 5-FOA[r]) due to simultaneous inactivation of the *CAN1* and *URA3* genes, both located within a 12 kb nonessential region on the left arm of chromosome V. The median GCR rate is reported with 95% confidence intervals [80]. GCR clones were screened by PCR to identify clones with rearrangements between *CAN1* on chromosome V and *LYP1* and/or *ALP1* (collectively referred to as *CAN1/LYP1/ALP1* rearrangements in the text), located in opposite orientations on the same arm of chromosome XIV [10]. To determine the rate of accumulating spontaneous mutations that lead to inactivation of the *CAN1* gene, 3-ml YPD cultures expressing wildtype Exo1 or C-terminal truncations of Exo1 were grown overnight and aliquots were plated on synthetic media lacking arginine (US Biological) supplemented with 240 mg ml^{-1} canavanine (Sigma), and on YPD to obtain the viable cell count. Colonies were counted after two days of incubation at 30°C. At least twelve indepen-dent cultures from three isolates were analyzed per yeast strain. The median Can[r] mutation rate is reported with 95% confidence intervals [80]. Statistical significance of differences in GCR rates was evaluated by using the Mann-Whitney test and programs from Dr. R. Lowry at Vassar College http://faculty.vassar.edu/lowry/ VassarStats.html

74

Protein extraction and Western blot analysis

Cells were grown in YPD until they reached OD_{600} = 0.5. Whole cell extract was prepared from 5 ml of culture using a standard trichloroacetic acid (TCA) extraction. Briefly, cells were pelleted, vortexed with glass beads for 10 minutes in 200 μl of 20% TCA, followed by centrifugation for 2 minutes. The pellet was resuspended in sample buffer and pH was neutralized with 2 M Tris buffer (pH 7.6). Proteins were separated by PAGE, transferred to a PVDF membrane and incubated with monoclonal anti-c-myc antibody (Covance) to detect myc-tagged proteins. Bands were visualized using ECL Plus Chemiluminescence kit (GE Healthcare).

FIGURES AND TABLES
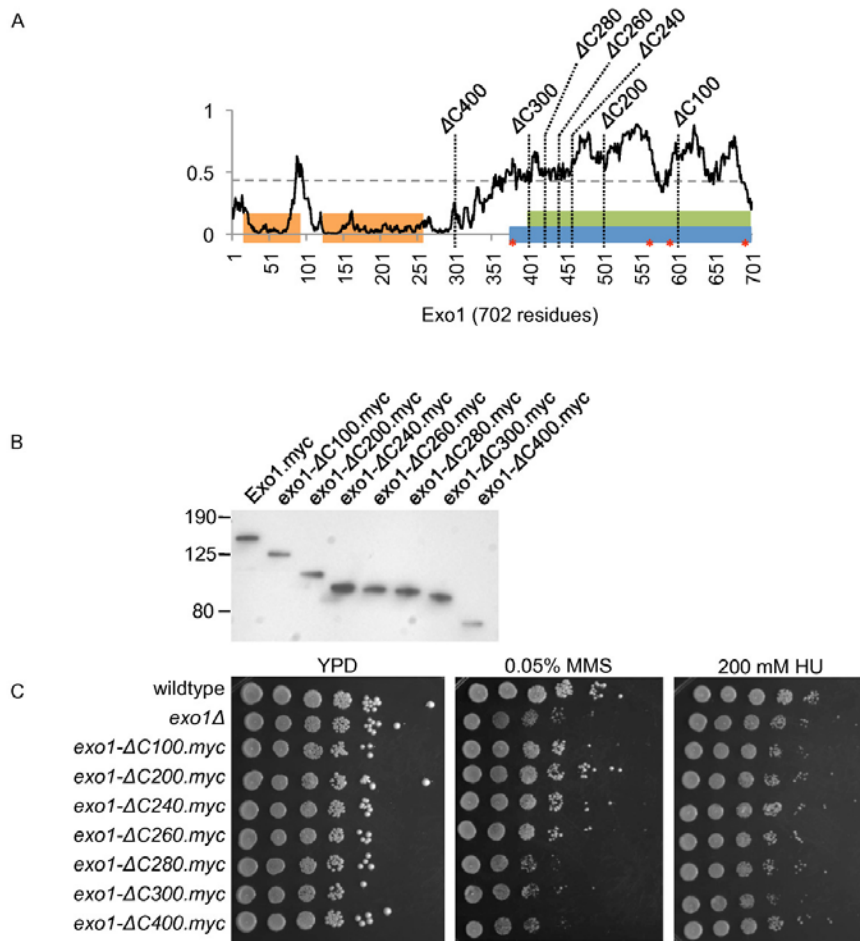
Figure 2.1 Expression of C-terminal truncations of Exo1 and sensitivity to DNA-damaging agents.
(A) Intrinsic disorder prediction of Exo1 using the IUPred algorithm in which values above 0.5 indicate residues predicted to be intrinsically disordered and values below 0.5 to be ordered. The N-terminus, harboring conserved N- and I-nuclease domains, is predicted to be ordered, whereas the C-terminus, which appears devoid of enzymatic activity but contains phosphorylation sites and sites for interaction with mismatch repair proteins, is disordered. The sites at which the Exo1 truncations examined in this study terminate are indicted by vertical dotted lines. The location of conserved domains was adapted from reference [71]: nuclease domains (orange boxes, 16-96 aa, 123-257 aa), Mlh1 interaction domain (green box, 400-702 aa) and the Msh2 interaction domain (blue box, 368-702 aa). Phosphorylation sites at S372, S567, S587 and S692, implicated in checkpoint regulation [74], are indicated by red asterisks. (B) Western blot analysis of expression of myc-epitope tagged exo1 truncations and wildtype Exo1. Molecular weight markers (kD) are indicated on the left. (C) Cells expressing Exo1 truncations lacking 280 or more C-terminal residues are as sensitive to 0.05% MMS as the *exo1Δ* mutant whereas cells expressing exo1 truncations lacking 260 or fewer C-terminal residues show wildtype levels of resistance to MMS. No sensitivity to 200 mM hydroxyurea was observed for any of the tested yeast strains.

76
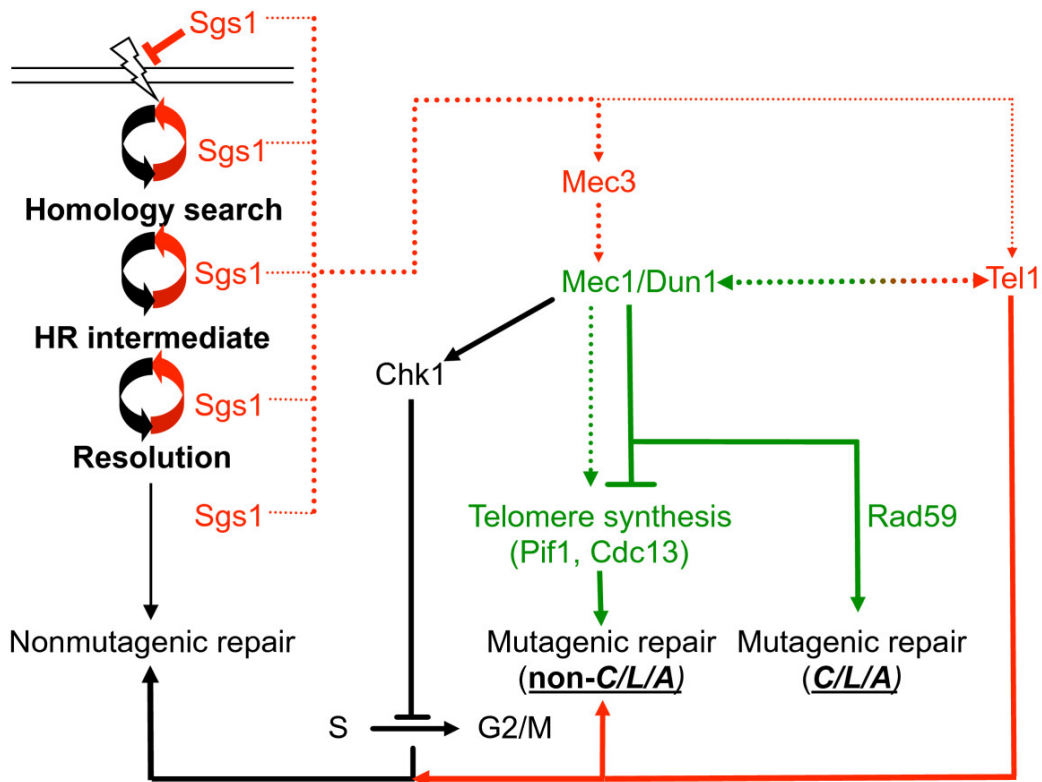
Figure 2.2 Factors affecting the suppression and promotion of chromosomal translocations between short segments of homology in *CAN1* , *LYP1* and *ALP1* in cells lacking Sgs1. In the absence of Sgs1, translocations between *CAN1, LYP1* and *ALP1* (referred to as *C/L/A*) are independently suppressed by the checkpoint components Mec3 and Tel1 (shown in red font), as suggested by the synergistic increases in the GCR rate and the *C/L/A* translocation rate of the *sgs1Δ* mutant upon deletion of *MEC3* (*sgs1Δ mec3Δ*) and subsequently *TEL1* (*sgs1Δ mec3Δ tel1Δ*). If Mec3 is absent (*sgs1Δ mec3Δ*), *C/L/A* translocations form through a pathway that requires Mec1, Dun1 and homologous recombination (HR) factors (shown in green font), especially Rad52 and Rad59. Mec1 most likely promotes translocations by inhibiting *de novo* telomere additions by regulating Pif1 and Cdc13. In addition to mutagenic repair that leads to *C/L/A* translocations, other types of mutagenic repair (e.g., translocations between other genes, *de novo* telomere additions, deletions, insertions, inversions) and most likely also nonmutagenic repair products are formed. If, in addition to Mec3, Tel1 is also absent (e.g., *sgs1Δ mec3Δ tel1Δ*), an even greater number of DNA lesions are channeled through the Mec1-dependent, *C/L/A*-promoting pathway. In contrast to *dun1Δ*, the *chk1Δ* mutation does not lead to a significant GCR rate increase in the *sgs1Δ mec3Δ* mutant and does not inhibit *C/L/A* translocation formation. Possibly, the inability to regulate cell cycle progression in the absence of Chk1 leads to increased formation of inviable GCRs. Dotted lines indicate events that occur in the absence of the protein from which the arrow originates; full lines indicate events that occur in the presence of the protein.

77

Table 2.1 Functional interaction between Sgs1 and components of the DNA-damage checkpoint in the suppression of GCRs and translocations between *CAN1, LYP1* and *ALP1* genes.

Relevant Genotyped[d]	All GCR types[a]		CAN1/LYP1/ALP1 translocations[b]		Frequency of CAN1/LYP1/ALP1 translocation types[c]		
	Rate	95% CI	Rate	Frequency	*CAN1-ALP1*	*CAN1-LYP1*	*CAN1-LYP1-ALP1*
wildtype	1.1	<1-6.2	ND	ND	ND	ND	ND
sgs1	220	144-276	<7.3	0/30	0/30	0/30	0/30
rad17	57	26-74	ND	ND	ND	ND	ND
mec3	46	18-75	<1.5	0/30	0/30	0/30	0/30
mec3 rad17	49	32-64	ND	ND	ND	ND	ND
sgs1 rad17	2515	903-4160	<101	0/25	0/25	0/25	0/25
sgs1 mec3	1297	1120-2030	173	20/150	7/150	3/150	7/150
sgs1 mec3 rad17	1690	1247-2230	75	2/45	1/45	1/45	0/45
tel1	2	ND	ND	ND	ND	ND	ND
tel1 mec3	453	340-638	15	1/30	1/30	0/30	0/30
tel1 rad17	129	72-246	<8.6	0/15	0/15	0/15	0/15
sgs1 tel1	227	46-418	ND[b]	ND	ND	ND	ND
sgs1 tel1 rad17	27600	22430-39653	4600	6/36	1/36	1/36	4/36
sgs1 tel1 mec3	57370	47157-76301	2674	11/236	0/236	6/236	4/236
sgs1 tel1 mec3 rad17	31960	23400-51800	ND	ND	ND	ND	ND
mec1	471	209-859	ND	ND	ND	ND	ND
sgs1 mec1	1930	960-2452	<10	0/190	0/190	0/190	0/190
sgs1 mec1 mec3	9628	5870-12100	<22	0/431	0/431	0/431	0/431
chk1	42	25-132	ND	ND	ND	ND	ND
sgs1 chk1	446	337-528	<15	0/30	0/30	0/30	0/30
sgs1 chk1 mec3	1099	725-1613	147	4/30	1/30	0/30	3/30
dun1	252	86-472	ND	ND	ND	ND	ND
sgs1 dun1	1145	698-1910	<23	0/50	0/50	0/50	0/50
sgs1 dun1 mec3	2800	2270-3570	<21	0/135	0/135	0/135	0/135

(a) GCR rate (Can[r] 5-FOA[r] × 10^{-10}). 95% confidence intervals (CIs) for median GCR rates were calculated according to Nair [80], where non-overlapping confidence intervals indicate statistically significant differences between median GCR rates. GCR rates of wildtype [81], *sgs1* [82], *mec3, sgs1 mec3* [60], *tel1* [3] were reported previously.

  (b) Rate of accumulating translocations between *CAN1, LYP1* and/or *ALP1* genes (x 10^{-10}). GCR clones from *sgs1, mec3, sgs1 mec3, sgs1 tel1* and *sgs1 mec1* were previously screened for *CAN1/LYP1/ALP1* translocations [10,60].

(C) Types of *CAN1/LYP1/ALP1* translocations were determined by sequencing. Of the 20 *CAN1/LYP1/ALP1* translocations identified among 150 GCR clones from the *sgs1 mec3* mutant, 17 were identified as being either *C/A, C/L/A* or *C/L* translocations and 3 clones had a mixture of multiple translocations [60].

(d) All mutants with a *mec1* deletion also contain a *sml1* deletion.

Table 2.2 Effect of homologous recombination mutations on the ability of the sgs1 mec3 mutant to accumulate GCRs and form rearrangements between the CAN1, LYP 1 and ALP1 genes.

Relevant genotype	All GCR types[a]		CAN1/LYP1/ALP1 translocations[b]	
	Rate	95% CI	Rate	Frequency
wildtype	1.1	<1-6.2	ND	ND
rad51[a]	<8	<7-15	ND	ND
rad52	138	16-267	ND	ND
rad59	24	13-50	ND	ND
sgs1[a]	220	144-276	<7.3	0/30
mec3[a]	46	18-75	<1.5	0/30
sgs1 rad59	126	107-300	ND	ND
sgs1 rad59 rad51	118	49-154	ND	ND
sgs1 mec3[a]	1297	1120-2030	173	20/150
sgs1 mec3 rad51[a]	1491	ND[c]	198	4/30
sgs1 mec3 rad52[a]	3168	ND[c]	<23	0/136
sgs1 mec3 rad59	2476	1595-3187	16	1/158
sgs1 mec3 rad59 rad51	1124	734-1460	7	1/168

(a) Median rate of cells resistant to canavanine and 5-FOA (Can[r] 5-FOA[r] $\times 10^{-10}$). 95% confidence intervals (CIs) for median GCR rates were calculated according to Nair [80], where non-overlapping confidence intervals indicate statistically significant differences between median GCR rates. GCR rates for wildtype [81], *sgs1* [82], *mec3, sgs1 mec3* [60], *rad51, sgs1 mec3 rad51* and *sgs1 mec3 rad52* mutants [10] were reported previously and are included for comparison.

(b) Rate of accumulating translocations between *CAN1, LYP1* and/or *ALP1* (Can[r] 5-FOA[r] $\times 10^{-10}$). GCR clones from *sgs1, mec3, sgs1 mec3, sgs1 mec3 rad51, sgs1 mec3 rad52* were previously screened for *CAN1/LYP1/ALP1* translocations [10,60]. ND, not determined.

(c) To determine 95% CIs for *sgs1 mec3 rad51* and *sgs1 mec3 rad52* mutants, GCR rates were re-measured for the current study. The GCR rate for the *sgs1 mec3 rad51* mutant was 1933×10^{-10} (95% CIs: $601\text{-}2240 \times 10^{-10}$) and the GCR rate for the *sgs1 mec3 rad52* mutant was 2220×10^{-10} ($951\text{-}3470 \times 10^{-10}$). The previously reported rates fall within the 95% CIs determined in the current study.

Table 2.3 Effect of *lig4Δ, exo1Δ, rad1Δ, pol32 Δ* and *yen1Δ* mutations on the accumulation of GCRs in checkpoint- proficient and checkpoint-deficient *sgs1Δ* mutants

Relevant genotype[a]	GCR rate[b]	95% CI[c]
wildtype	1.1	<1-6.2
exo1	24	7-79
sgs1	220	144-276
sgs1 mec3	1297	1120-2030
exo1 sgs1	43800	30400-186000
exo1 mec3	30	12-39
exo1 mec3 sgs1	1168498	549530-3251000
sgs1 mec3 exo1 lig4	895988	701149-1236740
lig4	16	ND
sgs1 lig4	80	35-254
sgs1 mec3 lig4	1335	948-2140
yen1	<5	<4-6
sgs1 yen1	81	57-265
sgs1 mec3 yen1	1089	254-2540
pol32	20	15-26
sgs1 pol32	25	<24-105
sgs1 mec3 pol32	2317	1800-3110
rad1	10	<9-23
sgs1 rad1	63	25-356
sgs1 mec3 rad1	1173	1020-1540

(a) Strains with multiple gene deletions were constructed by sporulation of the appropriate heterozygous diploids. GCR rates with 95% confidence intervals (CIs) for wildtype [81], *sgs1* [82], *sgs1 mec3* [60] and *lig4* [1] were reported previously and are included for comparison. Spores with both *sgs1Δ* and *pol32Δ* mutations grew very slowly and exhibited a low viable cell count on YPD in the GCR assay.

(b) The rate of accumulating gross-chromosomal rearrangements (GCRs) is calculated by selecting for cells resistant to canavanine (Can^r) and 5-fluoro-orotic acid (5-FOA^r) and is expressed as Can^r 5-FOA^r × 10^{-10} [77].

(c) 95% confidence intervals (CI) for median GCR rates were calculated according to Nair [80].

Table 2.4 Effect of exo1 mutations on the accumulation of GCRs in wildtype cells or cells lacking Sgs1 helicase.

Relevant genotype	GCR rate (Can^r 5-FOA^r × 10^{-10})	95% CI[a] (Can^r 5-FOA^r × 10^{-10})
sgs1Δ	89	57-177
exo1Δ	24	7-79
exo1Δ sgs1Δ	40484	31076-49848
EXO1.myc	5	4.4-5.3
exo1-ΔC100.myc	5	4-6
exo1-ΔC200.myc	< 4	< 3.8-4.8
exo1-ΔC260.myc	< 11	< 8-79
exo1-ΔC280.myc	< 11	< 8-29
exo1-ΔC300.myc	< 18	< 5-70
exo1-ΔC400.myc	13	5-41
sgs1Δ EXO1.myc	78	29-118
sgs1Δ exo1-ΔC100.myc	125	80-186
sgs1Δ exo1-ΔC200.myc	158	94-215
sgs1Δ exo1-ΔC260.myc	230	166-265
sgs1Δ exo1-ΔC280.myc	26840	22925-34036
sgs1Δ exo1-ΔC300.myc	31070	22871-33753
sgs1Δ exo1-ΔC400.myc	48190	39133-54471

(a) 95% confidence intervals (CI) for median GCR rates were calculated according to Nair [80].

Table 2.5 Effect of C-terminal deletions of Exo1 on the spontaneous mutation rate at the CAN1 locus.

Relvant genotype	*CAN1* (Can^r $\times$ 10^{-7})	95% CI^a (Can^r $\times$ 10^{-7})	Increase over wildtype
wildtype	3.27	2.50-5.82	1
exo1Δ	11.47	10.10-28.52	3.5
exo1-ΔC100.myc	3.64	2.92-4.70	1.1
exo1-ΔC200.myc	5.31	3.90-5.90	1.6
exo1-ΔC260.myc	3.89	2.89-5.92	1.2
exo1-ΔC280.myc	8.37	6.94-16.18	2.6
exo1-ΔC300.myc	10.72	8.55-19.88	3.3
exo1-ΔC400.myc	13.16	9.06-18.19	4.0

(a) 95% confidence intervals (CI) for median Canr rates were calculated according to Nair [80].

Table 2.6 *Saccharomyces cerevisiae* strains used in this study

Strain ID	Genotype
KHSY802	*MATa, ura3-52, trp1Δ63, his3Δ200, leu2Δ1, lys2Bgl, hom3-10, ade2Δ1, ade8, hxt13::URA3,*
RDKY 3721[a]	*MATa, ura3-52, trp1Δ63, his3Δ200, leu2Δ1, lys2Bgl, hom3-10, ade2Δ1, ade8, hxt13::URA3, rad17::HIS3*
RDKY 3739[a]	*MATa, ura3-52, trp1Δ63, his3Δ200, leu2Δ1, lys2Bgl, hom3-10, ade2Δ1, ade8, hxt13::URA3, dun1::HIS3*
RDKY 3745[a]	*MATa, ura3-52, trp1Δ63, his3Δ200, leu2Δ1, lys2Bgl, hom3-10, ade2Δ1, ade8, hxt13::URA3, chk1::HIS3*
RDKY 5209[a]	*MATa, ura3-52, trp1Δ63, his3Δ200, leu2Δ1, lys2Bgl, hom3-10, ade2Δ1, ade8, hxt13::URA3, tel1:G418*
KHSY 773	*MATa, ura3-52, trp1Δ63, his3Δ200, leu2Δ1, lys2Bgl, hom3-10, ade2Δ1, ade8, hxt13::URA3, sml1::TRP1, mec1::HIS3*
KHSY 884	*MATa, ura3-52, trp1Δ63, his3Δ200, leu2Δ1, lys2Bgl, hom3-10, ade2Δ1, ade8, hxt13::URA3, rad51::HIS3*
KHSY 906	*MATa, ura3-52, trp1Δ63, his3Δ200, leu2Δ1, lys2Bgl, hom3-10, ade2Δ1, ade8, hxt13::URA3, mec3::HIS3*
KHSY 1330	*MATa, ura3-52, trp1Δ63, his3Δ200, leu2Δ1, lys2Bgl, hom3-10, ade2Δ1, ade8, hxt13::URA3, sgs1::HIS3, mec1::TRP1, sml1::G418*
KHSY 1498	*MATa, ura3-52, trp1Δ63, his3Δ200, leu2Δ1, lys2Bgl, hom3-10, ade2Δ1, ade8, hxt13::URA3, sgs1::HIS3, mec1::TRP1, sml1::G418, mec3::G418*
KHSY 1524	*MATa, ura3-52, trp1Δ63, his3Δ200, leu2Δ1, lys2Bgl, hom3-10, ade2Δ1, ade8, hxt13::URA3, sgs1::TRP1*
KHSY 2260	*MATa, ura3-52, trp1Δ63, his3Δ200, leu2Δ1, lys2Bgl, hom3-10, ade2Δ1, ade8, hxt13::URA3, sgs1::TRP1, chk1::HIS3*
KHSY 2265	*MATa, ura3-52, trp1Δ63, his3Δ200, leu2Δ1, lys2Bgl, hom3-10, ade2Δ1, ade8, hxt13::URA3, sgs1::TRP1, rad17::HIS3*
KHSY 2280	*MATa, ura3-52, trp1Δ63, his3Δ200, leu2Δ1, lys2Bgl, hom3-10, ade2Δ1, ade8, hxt13::URA3, sgs1::TRP1, mec3::HIS3, rad59::G418*
KHSY 2283	*MATa, ura3-52, trp1Δ63, his3Δ200, leu2Δ1, lys2Bgl, hom3-10, ade2Δ1, ade8, hxt13::URA3, sgs1::TRP1, dun1::HIS3*
KHSY 2317	*MATa, ura3-52, trp1Δ63, his3Δ200, leu2Δ1, lys2Bgl, hom3-10, ade2Δ1, ade8, hxt13::URA3, tel1::G418, mec3::HIS3*
KHSY 2320	*MATa, ura3-52, trp1Δ63, his3Δ200, leu2Δ1, lys2Bgl, hom3-10, ade2Δ1, ade8, hxt13::URA3, sgs1::TRP1, mec3::HIS3*
KHSY 2330	*MATa, ura3-52, trp1Δ63, his3Δ200, leu2Δ1, lys2Bgl, hom3-10, ade2Δ1, ade8, hxt13::URA3, yen1::loxP-G418-loxP*
KHSY 2331	*MATa, ura3-52, trp1Δ63, his3Δ200, leu2Δ1, lys2Bgl, hom3-10, ade2Δ1, ade8, hxt13::URA3, lig4::loxP-G418-loxP*
KHSY 2336	*MATa, ura3-52, trp1Δ63, his3Δ200, leu2Δ1, lys2Bgl, hom3-10, ade2Δ1, ade8, hxt13::URA3, rad1::loxP-G418-loxP*
KHSY 2338	*MATa, ura3-52, trp1Δ63, his3Δ200, leu2Δ1, lys2Bgl, hom3-10, ade2Δ1, ade8, hxt13::URA3, exo1:loxp-G418-loxp*
KHSY 2388	*MATa, ura3-52, trp1Δ63, his3Δ200, leu2Δ1, lys2Bgl, hom3-10, ade2Δ1, ade8, hxt13::URA3, rad59::G418*
KHSY 2402	*MATa, ura3-52, trp1Δ63, his3Δ200, leu2Δ1, lys2Bgl, hom3-10, ade2Δ1, ade8, hxt13::URA3, sgs1::TRP1, exo1::loxP-G418-loxP*
KHSY 2408	*MATa, ura3-52, trp1Δ63, his3Δ200, leu2Δ1, lys2Bgl, hom3-10, ade2Δ1, ade8, hxt13::URA3, sgs1::TRP1, exo1::loxP-G418-loxP, mec3::HIS3*
KHSY 2424	*MATa, ura3-52, trp1Δ63, his3Δ200, leu2Δ1, lys2Bgl, hom3-10, ade2Δ1, ade8, hxt13::URA3, sgs1::TRP1, rad1::loxP-G418-loxP*
KHSY 2434	*MATa, ura3-52, trp1Δ63, his3Δ200, leu2Δ1, lys2Bgl, hom3-10, ade2Δ1, ade8, hxt13::URA3, sgs1::TRP1, rad1::loxP-G418-loxP, mec3::HIS3*

Table 2.6 *Saccharomyces cerevisiae* strains used in this study *(continued)*.

KHSY 2447   *MATa, ura3-52, trp1Δ63, his3Δ200, leu2Δ1, lys2Bgl, hom3-10, ade2Δ1, ade8, hxt13::URA3, sgs1::TRP1, lig4::loxP-G418-loxP*

KHSY 2448   *MATa, ura3-52, trp1Δ63, his3Δ200, leu2Δ1, lys2Bgl, hom3-10, ade2Δ1, ade8, hxt13::URA3, sgs1::TRP1, yen1::loxP-G418-loxP*

KHSY 2449   *MATa, ura3-52, trp1Δ63, his3Δ200, leu2Δ1, lys2Bgl, hom3-10, ade2Δ1, ade8, hxt13::URA3, sgs1::TRP1, yen1::loxP-G418-loxP, mec3::HIS3*

KHSY 2559   *MATa, ura3-52, trp1Δ63, his3Δ200, leu2Δ1, lys2Bgl, hom3-10, ade2Δ1, ade8, hxt13::URA3, mec3:: G418, rad17::HIS3*

KHSY 2565   *MATa, ura3-52, trp1Δ63, his3Δ200, leu2Δ1, lys2Bgl, hom3-10, ade2Δ1, ade8, hxt13::URA3, sgs1::TRP1, mec3::G418, rad17::HIS3*

KHSY 2579   *MATa, ura3-52, trp1Δ63, his3Δ200, leu2Δ1, lys2Bgl, hom3-10, ade2Δ1, ade8, hxt13::URA3, sgs1:: TRP1, lig4::G418, mec3::HIS3*

KHSY 2585   *MATa, ura3-52, trp1Δ63, his3Δ200, leu2Δ1, lys2Bgl, hom3-10, ade2Δ1, ade8, hxt13::URA3, sgs1::TRP1, tel1::G418, rad17::HIS3*

KHSY 2588   *MATa, ura3-52, trp1Δ63, his3Δ200, leu2Δ1, lys2Bgl, hom3-10, ade2Δ1, ade8, hxt13::URA3, tel1::G418, rad17::HIS3*

KHSY 2662   *MATa, ura3-52, trp1Δ63, his3Δ200, leu2Δ1, lys2Bgl, hom3-10, ade2Δ1, ade8, hxt13::URA3, sgs1::TRP1, mec3::HIS3, chk1::HIS3*

KHSY 2665   *MATa, ura3-52, trp1Δ63, his3Δ200, leu2Δ1, lys2Bgl, hom3-10, ade2Δ1, ade8, hxt13::URA3, sgs1::TRP1, mec3::HIS3, dun1::HIS3*

KHSY 2786   *MATa, ura3-52, trp1Δ63, his3Δ200, leu2Δ1, lys2Bgl, hom3-10, ade2Δ1, ade8, hxt13::URA3, sgs1::TRP1, exo1::loxP-G418-loxP, lig4::loxP-G418-loxP, mec3::HIS3*

KHSY 3086   *MATa, ura3-52, trp1Δ63, his3Δ200, leu2Δ1, lys2Bgl, hom3-10, ade2Δ1, ade8, hxt13::URA3, sgs1::TRP1, mec3::G418, rad17::HIS3, tel1::HIS3*

KHSY 3223   *MATa, ura3-52, trp1Δ63, his3Δ200, leu2Δ1, lys2Bgl, hom3-10, ade2Δ1, ade8, hxt13::URA3, sgs1::TRP1, mec3::HIS3, tel1::G418*

KHSY 3231   *MATa, ura3-52, trp1Δ63, his3Δ200, leu2Δ1, lys2Bgl, hom3-10, ade2Δ1, ade8, hxt13::URA3, rad17::H1S3, mec3::HIS3, tel1::G418*

KHSY 3265   *MATa, ura3-52, trp1Δ63, his3Δ200, leu2Δ1, lys2Bgl, hom3-10, ade2Δ1, ade8, hxt13::URA3, exo1ΔC300.MYC.HIS*

KHSY 3271   *MATa, ura3-52, trp1Δ63, his3Δ200, leu2Δ1, lys2Bgl, hom3-10, ade2Δ1, ade8, hxt13::URA3, exo1ΔC400.MYC.HIS*

KHSY 3274   *MATa, ura3-52, trp1Δ63, his3Δ200, leu2Δ1, lys2Bgl, hom3-10, ade2Δ1, ade8, hxt13::URA3, exo1ΔC200.MYC.HIS, sgs1::TRP1*

KHSY 3278   *MATa, ura3-52, trp1Δ63, his3Δ200, leu2Δ1, lys2Bgl, hom3-10, ade2Δ1, ade8, hxt13::URA3, exo1ΔC100.MYC.HIS, sgs1::TRP1*

KHSY 3282   *MATa, ura3-52, trp1Δ63, his3Δ200, leu2Δ1, lys2Bgl, hom3-10, ade2Δ1, ade8, hxt13::URA3, exo1ΔC100.MYC.HIS*

KHSY 3287   *MATa, ura3-52, trp1Δ63, his3Δ200, leu2Δ1, lys2Bgl, hom3-10, ade2Δ1, ade8, hxt13::URA3, EXO1.MYC.HIS, sgs1::TRP1*

KHSY 3395   *MATa, ura3-52, trp1Δ63, his3Δ200, leu2Δ1, lys2Bgl, hom3-10, ade2Δ1, ade8, hxt13::URA3, EXO1.MYC.HIS*

KHSY 3396   *MATa, ura3-52, trp1Δ63, his3Δ200, leu2Δ1, lys2Bgl, hom3-10, ade2Δ1, ade8, hxt13::URA3, exo1Δ200.MYC.HIS*

KHSY 3402   *MATa, ura3-52, trp1Δ63, his3Δ200, leu2Δ1, lys2Bgl, hom3-10, ade2Δ1, ade8, hxt13::URA3, exo1Δ300.MYC.HIS, sgs1::TRP1*

KHSY 3635   *MATa, ura3-52, trp1Δ63, his3Δ200, leu2Δ1, lys2Bgl, hom3-10, ade2Δ1, ade8, hxt13::URA3, exo1::loxP-G418-loxP, mec3::HIS3*

KHSY 3843   *MATa, ura3-52, trp1Δ63, his3Δ200, leu2Δ1, lys2Bgl, hom3-10, ade2Δ1, ade8, hxt13::URA3, exo1Δ400.MYC.HIS, sgs1::TRP1*

KHSY 3849   *MATa, ura3-52, trp1Δ63, his3Δ200, leu2Δ1, lys2Bgl, hom3-10, ade2Δ1, ade8, hxt13::URA3, exo1Δ280.MYC.HIS*

KHSY 3857   *MATa, ura3-52, trp1Δ63, his3Δ200, leu2Δ1, lys2Bgl, hom3-10, ade2Δ1, ade8, hxt13::URA3, exo1Δ280.MYC.HIS, sgs1::TRP1*

84

Table 2.6 *Saccharomyces cerevisiae* strains used in this study *(continued).*

KHSY 3860	*MATa, ura3-52, trp1Δ63, his3Δ200, leu2Δ1, lys2Bgl, hom3-10, ade2Δ1, ade8, hxt13::URA3, exo1Δ260.MYC.HIS*
KHSY 3866	*MATa, ura3-52, trp1Δ63, his3Δ200, leu2Δ1, lys2Bgl, hom3-10, ade2Δ1, ade8, hxt13::URA3, exo1Δ240.MYC.HIS*
KHSY 3868	*MATa, ura3-52, trp1Δ63, his3Δ200, leu2Δ1, lys2Bgl, hom3-10, ade2Δ1, ade8, hxt13::URA3, exo1Δ260.MYC.HIS*
KHSY 3869	*MATa, ura3-52, trp1Δ63, his3Δ200, leu2Δ1, lys2Bgl, hom3-10, ade2Δ1, ade8, hxt13::URA3, exo1Δ260.MYC.HIS, sgs1::TRP1*
KHSY 3875	*MATa, ura3-52, trp1Δ63, his3Δ200, leu2Δ1, lys2Bgl, hom3-10, ade2Δ1, ade8, hxt13::URA3, exo1Δ280.MYC.HIS, sgs1::TRP1*

(a) RDKY strains were a kind gift from Richard Kolodner (Ludwig Institute for Cancer Research, University of California - San Diego).

REFERENCES

1. Myung K, Chen C, Kolodner RD: Multiple pathways cooperate in the suppression of genome instability in Saccharomyces cerevisiae. *Nature* 2001, 411:1073-1076.

2. Myung K, Datta A, Chen C, Kolodner RD: SGS1, the Saccharomyces cerevisiae homologue of BLM and WRN, suppresses genome instability and homeologous recombination. *Nat Genet 2001*, 27:113-116.

3. Myung K, Datta A, Kolodner RD: Suppression of spontaneous chromosomal rearrangements by S phase checkpoint functions in Saccharomyces cerevisiae. *Cell* 2001, 104:397-408.

4. Myung K, Kolodner RD: Suppression of genome instability by redundant S-phase checkpoint pathways in Saccharomyces cerevisiae. *Proc Natl Acad Sci USA* 2002, 99:4500-4507.

5. Myung K, Pennaneach V, Kats ES, Kolodner RD: Saccharomyces cerevisiae chromatin-assembly factors that act during DNA replication function in the maintenance of genome stability*. Proc Natl Acad Sci USA* 2003, 100:6640-6645.

6. Putnam CD, Hayes TK, Kolodner RD: Specific pathways prevent duplication-mediated genome rearrangements. *Nature* 2009, 460:984-989.

7. Putnam CD, Jaehnig EJ, Kolodner RD: Perspectives on the DNA damage and replication checkpoint responses in Saccharomyces cerevisiae. *DNA Repair (Amst)* 2009, 8:974-982.

8. Putnam CD, Pennaneach V, Kolodner RD: Saccharomyces cerevisiae as a model system to define the chromosomal instability phenotype. *Mol Cell Biol* 2005, 25:7226-7238.

9. Schmidt KH, Kolodner RD: Suppression of spontaneous genome rearrangements in yeast DNA helicase mutants. *Proc Natl Acad Sci USA* 2006, 103:18196-18201.

10. Schmidt KH, Wu J, Kolodner RD: Control of Translocations between Highly Diverged Genes by Sgs1, the Saccharomyces cerevisiae Homolog of the Bloom's Syndrome Protein. *Mol Cell Biol* 2006, 26:5406-5420.

11. Antoccia A, Kobayashi J, Tauchi H, Matsuura S, Komatsu K: Nijmegen breakage syndrome and functions of the responsible protein, NBS1. *Genome Dyn* 2006, 1:191-205.

12. Carney JP, Maser RS, Olivares H, Davis EM, Le Beau M, Yates JR, Hays L, Morgan WF, Petrini JH: The hMre11/hRad50 protein complex and Nijmegen breakage syndrome: linkage of double-strand break repair to the cellular DNA damage response. *Cell* 1998, 93:477-486.

13. Varon R, Vissinga C, Platzer M, Cerosaletti KM, Chrzanowska KH, Saar K, Beckmann G, Seemanova E, Cooper PR, Nowak NJ, et al: Nibrin, a novel DNA

double-strand break repair protein, is mutated in Nijmegen breakage syndrome. *Cell* 1998, 93:467-476.

14. Ellis NA, Groden J, Ye TZ, Straughen J, Lennon DJ, Ciocci S, Proytcheva M, German J: The Bloom's syndrome gene product is homologous to RecQ helicases. *Cell* 1995, 83:655-666.

15. Yu CE, Oshima J, Fu YH, Wijsman EM, Hisama F, Alisch R, Matthews S, Nakura J, Miki T, Ouais S, et al: Positional cloning of the Werner's syndrome gene. *Science* 1996, 272:258-262.

16. Savitsky K, Bar-Shira A, Gilad S, Rotman G, Ziv Y, Vanagaite L, Tagle DA, Smith S, Uziel T, Sfez S, et al: A single ataxia telangiectasia gene with a product similar to PI-3 kinase. *Science* 1995, 268:1749-1753.

17. Morrow DM, Tagle DA, Shiloh Y, Collins FS, Hieter P: TEL1, an S. cerevisiae homolog of the human gene mutated in ataxia telangiectasia, is functionally related to the yeast checkpoint gene MEC1. *Cell* 1995, 82:831-840.

18. Lydeard JR, Lipkin-Moore Z, Jain S, Eapen VV, Haber JE: Sgs1 and exo1 redundantly inhibit break-induced replication and de novo telomere addition at broken chromosome ends. *PLoS Genet* 2010, 6:e1000973.

19. Mimitou EP, Symington LS: Sae2, Exo1 and Sgs1 collaborate in DNA double-strand break processing. *Nature* 2008, 455:770-774.

20. Zhu Z, Chung WH, Shim EY, Lee SE, Ira G: Sgs1 helicase and two nucleases Dna2 and Exo1 resect DNA double-strand break ends. *Cell* 2008, 134:981-994.

21. Marrero VA, Symington LS: Extensive DNA end processing by exo1 and sgs1 inhibits break-induced replication. *PLoS Genet* 2010, 6:e1001007.

22. Cobb JA, Bjergbaek L, Gasser SM: RecQ helicases: at the heart of genetic stability. *FEBS Lett* 2002, 529:43-48.

23. Frei C, Gasser SM: The yeast Sgs1p helicase acts upstream of Rad53p in the DNA replication checkpoint and colocalizes with Rad53p in S-phase- specific foci. *Genes Dev* 2000, 14:81-96.

24. Ira G, Malkova A, Liberi G, Foiani M, Haber JE: Srs2 and Sgs1-Top3 suppress crossovers during double-strand break repair in yeast. *Cell* 2003, 115:401-411.

25. Lee SK, Johnson RE, Yu SL, Prakash L, Prakash S: Requirement of yeast SGS1 and SRS2 genes for replication and transcription. Science 1999, 286:2339-2342.

26. Versini G, Comet I, Wu M, Hoopes L, Schwob E, Pasero P: The yeast Sgs1 helicase is differentially required for genomic and ribosomal DNA replication. *Embo J* 2003, 22:1939-1949.

27. Bentley NJ, Holtzman DA, Flaggs G, Keegan KS, DeMaggio A, Ford JC, Hoekstra M, Carr AM: The Schizosaccharomyces pombe rad3 checkpoint gene. *Embo J* 1996, 15:6641-6651.

28. Carr AM: Control of cell cycle arrest by the Mec1sc/Rad3sp DNA structure checkpoint pathway. *Curr Opin Genet Dev* 1997, 7:93-98.

29. Cimprich KA, Shin TB, Keith CT, Schreiber SL: cDNA cloning and gene mapping of a candidate human cell cycle checkpoint protein. *Proc Natl Acad Sci USA* 1996, 93:2850-2855.

30. Weinert TA, Kiser GL, Hartwell LH: Mitotic checkpoint genes in budding yeast and the dependence of mitosis on DNA replication and repair. *Genes Dev* 1994, 8:652-665.

31. Tercero JA, Diffley JF: Regulation of DNA replication fork progression through damaged DNA by the Mec1/Rad53 checkpoint. *Nature* 2001, 412:553-557.

32. Merrill BJ, Holm C: A requirement for recombinational repair in Saccharomyces cerevisiae is caused by DNA replication defects of mec1 mutants. *Genetics* 1999, 153:595-605.

33. Grushcow JM, Holzen TM, Park KJ, Weinert T, Lichten M, Bishop DK: Saccharomyces cerevisiae checkpoint genes MEC1, RAD17 and RAD24 are required for normal meiotic recombination partner choice. *Genetics* 1999, 153:607-620.

34. Kato R, Ogawa H: An essential gene, ESR1, is required for mitotic cell growth, DNA repair and meiotic recombination in Saccharomyces cerevisiae. *Nucleic Acids Res* 1994, 22:3104-3112.

35. Lydall D, Nikolsky Y, Bishop DK, Weinert T: A meiotic recombination checkpoint controlled by mitotic checkpoint genes. *Nature* 1996, 383:840-843.

36. Greenwell PW, Kronmal SL, Porter SE, Gassenhuber J, Obermaier B, Petes TD: TEL1, a gene involved in controlling telomere length in S. cerevisiae, is homologous to the human ataxia telangiectasia gene. *Cell* 1995, 82:823-829.

37. Ritchie KB, Mallory JC, Petes TD: Interactions of TLC1 (which encodes the RNA subunit of telomerase), TEL1, and MEC1 in regulating telomere length in the yeast Saccharomyces cerevisiae. *Mol Cell Biol* 1999, 19:6065-6075.

38. Sanchez Y, Desany BA, Jones WJ, Liu Q, Wang B, Elledge SJ: Regulation of RAD53 by the ATM-like kinases MEC1 and TEL1 in yeast cell cycle checkpoint pathways. *Science* 1996, 271:357-360.

39. Melo JA, Cohen J, Toczyski DP: Two checkpoint complexes are independently recruited to sites of DNA damage in vivo. *Genes Dev* 2001, 15:2809-2821.

40. Kondo T, Wakayama T, Naiki T, Matsumoto K, Sugimoto K: Recruitment of Mec1 and Ddc1 checkpoint proteins to double-strand breaks through distinct mechanisms. *Science* 2001, 294:867-870.

41. Makovets S, Blackburn EH: DNA damage signalling prevents deleterious telomere addition at DNA breaks. *Nat Cell Biol* 2009, 11:1383-1386.

42. Zhang W, Durocher D: De novo telomere formation is suppressed by the Mec1-dependent inhibition of Cdc13 accumulation at DNA breaks. *Genes Dev* 24:502-515.

43. Bashkirov VI, King JS, Bashkirova EV, Schmuckli-Maurer J, Heyer WD: DNA repair protein Rad55 is a terminal substrate of the DNA damage checkpoints. *Mol Cell Biol* 2000, 20:4393-4404.

44. Flott S, Alabert C, Toh GW, Toth R, Sugawara N, Campbell DG, Haber JE, Pasero P, Rouse J: Phosphorylation of Slx4 by Mec1 and Tel1 regulates the single-strand annealing mode of DNA repair in budding yeast. *Mol Cell Biol* 2007, 27:6433-6445.

45. Ehmsen KT, Heyer WD: Saccharomyces cerevisiae Mus81-Mms4 is a catalytic, DNA structure-selective endonuclease. *Nucleic Acids Res* 2008, 36:2182-2195.

46. Mordes DA, Nam EA, Cortez D: Dpb11 activates the Mec1-Ddc2 complex. *Proc Natl Acad Sci* USA 2008, 105:18730-18734.

47. Herzberg K, Bashkirov VI, Rolfsmeier M, Haghnazari E, McDonald WH, Anderson S, Bashkirova EV, Yates JR, Heyer WD: Phosphorylation of Rad55 on serines 2, 8, and 14 is required for efficient homologous recombination in the recovery of stalled replication forks. *Mol Cell Biol* 2006, 26:8396-8409.

48. Zhou Z, Elledge SJ: DUN1 encodes a protein kinase that controls the DNA damage response in yeast. *Cell* 1993, 75:1119-1127.

49. Huang M, Zhou Z, Elledge SJ: The DNA replication and damage checkpoint pathways induce transcription by inhibition of the Crt1 repressor. *Cell* 1998, 94:595-605.

50. Sanchez Y, Bachant J, Wang H, Hu F, Liu D, Tetzlaff M, Elledge SJ: Control of the DNA damage checkpoint by chk1 and rad53 protein kinases through distinct mechanisms. *Science* 1999, 286:1166-1171.

51. Gardner R, Putnam CW, Weinert T: RAD53, DUN1 and PDS1 define two parallel G2/M checkpoint pathways in budding yeast. *Embo J* 1999, 18:3173-3185.

52. Chan JE, Kolodner RD: A genetic and structural study of genome rearrangements mediated by high copy repeat Ty1 elements. *PLoS Genet* 7:e1002089.

53. Chen Q, Ijpma A, Greider CW: Two survivor pathways that allow growth in the absence of telomerase are generated by distinct telomere recombination events. *Mol Cell Biol* 2001, 21:1819-1827.

54. Teng SC, Chang J, McCowan B, Zakian VA: Telomerase-independent lengthening of yeast telomeres occurs by an abrupt Rad50p-dependent, Rif-inhibited recombinational process. *Mol Cell* 2000, 6:947-952.

55. Teng SC, Zakian VA: Telomere-telomere recombination is an efficient bypass pathway for telomere maintenance in Saccharomyces cerevisiae. *Mol Cell Biol* 1999, 19:8083-8093.

56. Malkova A, Ivanov EL, Haber JE: Double-strand break repair in the absence of RAD51 in yeast: a possible role for break-induced DNA replication. *Proc Natl Acad Sci USA* 1996, 93:7131-7136.

57. Signon L, Malkova A, Naylor ML, Klein H, Haber JE: Genetic requirements for RAD51- and RAD54-independent break-induced replication repair of a chromosomal double-strand break. *Mol Cell Biol* 2001, 21:2048-2056.

58. Symington LS: Role of RAD52 epistasis group genes in homologous recombination and double-strand break repair. *Microbiol Mol Biol Rev* 2002, 66:630-670, table of contents.

59. Sugawara N, Ira G, Haber JE: DNA length dependence of the single-strand annealing pathway and the role of Saccharomyces cerevisiae RAD59 in double-strand break repair. *Mol Cell Biol* 2000, 20:5300-5309.

60. Schmidt KH, Viebranz E, Doerfler L, Lester C, Rubenstein A: Formation of complex and unstable chromosomal translocations in yeast. *PLoS One* 2010, 5:e12007.

61. Pannunzio NR, Manthey GM, Bailis AM: RAD59 is required for efficient repair of simultaneous double-strand breaks resulting in translocations in Saccharomyces cerevisiae. *DNA Repair (Amst)* 2008, 7:788-800.

62. Onoda F, Seki M, Miyajima A, Enomoto T: Elevation of sister chromatid exchange in Saccharomyces cerevisiae sgs1 disruptants and the relevance of the disruptants as a system to evaluate mutations in Bloom's syndrome gene. *Mutat Res* 2000, 459:203-209.

63.   Ooi SL, Shoemaker DD, Boeke JD: DNA helicase gene interaction network defined using synthetic lethality analyzed by microarray. *Nat Genet* 2003, 35:277-286.64.

64. Watt PM, Hickson ID, Borts RH, Louis EJ: SGS1, a homologue of the Bloom's and Werner's syndrome genes, is required for maintenance of genome stability in Saccharomyces cerevisiae. *Genetics* 1996, 144:935-945. 65.

65. Louis EJ, Haber JE: The structure and evolution of subtelomeric Y' repeats in Saccharomyces cerevisiae. *Genetics* 1992, 131:559-574.66.

66. Lydeard JR, Jain S, Yamaguchi M, Haber JE: Break-induced replication and telomerase-independent telomere maintenance require Pol32. *Nature* 2007, 448:820-823.67.

67. Fishman-Lobell J, Haber JE: Removal of nonhomologous DNA ends in double-strand break recombination: the role of the yeast ultraviolet repair gene RAD1. *Science* 1992, 258:480-484.68.

68. Ivanov EL, Haber JE: RAD1 and RAD10, but not other excision repair genes, are required for double-strand break-induced recombination in Saccharomyces cerevisiae. *Mol Cell Biol* 1995, 15:2245-2251.69.

69. Hwang JY, Smith S, Myung K: The Rad1-Rad10 complex promotes the production of gross chromosomal rearrangements from spontaneous DNA damage in Saccharomyces cerevisiae. *Genetics* 2005, 169:1927-1937. 70.

70. Bartsch S, Kang LE, Symington LS: RAD51 is required for the repair of plasmid double-stranded DNA gaps from either plasmid or chromosomal templates. *Mol Cell Biol* 2000, 20:1194-1205.71.

71. Malagon F, Aguilera A: Yeast spt6-140 mutation, affecting chromatin and transcription, preferentially increases recombination in which Rad51p- mediated strand exchange is dispensable. *Genetics* 2001, 158:597-611. 72.

72. Tran PT, Erdeniz N, Symington LS, Liskay RM: EXO1-A multi-tasking eukaryotic nuclease. *DNA Repair (Amst)* 2004, 3:1549-1559.73.

73. Schmutte C, Sadoff MM, Shim KS, Acharya S, Fishel R: The interaction of DNA mismatch repair proteins with human exonuclease I. *J Biol Chem* 2001, 276:33011-33018.74.

74. Tishkoff DX, Boerger AL, Bertrand P, Filosi N, Gaida GM, Kane MF, Kolodner RD: Identification and characterization of Saccharomyces cerevisiae EXO1, a gene encoding an exonuclease that interacts with MSH2. *Proc Natl Acad Sci USA* 1997, 94:7487-7492.

75. Morin I, Ngo HP, Greenall A, Zubko MK, Morrice N, Lydall D: Checkpoint- dependent phosphorylation of Exo1 modulates the DNA damage response*. Embo J* 2008, 27:2400-2410.

76. Chen C, Umezu K, Kolodner RD: Chromosomal rearrangements occur in S. cerevisiae rfa1 mutator mutants due to mutagenic lesions processed by double-strand-break repair. *Mol Cell* 1998, 2:9-22.

77. Schmidt KH, Pennaneach V, Putnam CD, Kolodner RD: Analysis of gross-chromosomal rearrangements in Saccharomyces cerevisiae. *Methods Enzymol* 2006, 409:462-476.

78. Gietz RD, Woods RA: Yeast transformation by the LiAc/SS Carrier DNA/ PEG method. *Methods Mol Biol* 2006, 313:107-120.

79. Lea DE, Coulson CA: The distribution of the number of mutants in bacterial populations. *J Genet* 1949, 49:264-285.

80. Nair KR: Table of confidence intervals for the median in samples from any continuous population. *Sankhya* 1940, 4:551-558.

81. Mirzaei H, Syed S, Kennedy J, Schmidt KH: Sgs1 truncations inducegenome rearrangements but suppress detrimental effects of BLM overexpression in Saccharomyces cerevisiae. *J Mol Biol* 2011, 405:877-891.

82. Schmidt KH, Viebranz EB, Harris LB, Mirzaei-Souderjani H, Syed S, Medicus R: Defects in DNA lesion bypass lead to spontaneous chromosomal rearrangements and increased cell death. *Eukaryot Cell* 2010, 9:315-324.

Chapter Three:

Exo1 phosphorylation status controls the hydroxyurea sensitivity of cells lacking the Pol32 subunit of DNA polymerases delta and zeta.

 Corresponding author: Kristina Schmidt, Department of Cell Biology, Microbiology and Molecular Biology, University of South Florida, 4202 E. Fowler Avenue, ISA2015, Tampa, FL 33620. Phone: (813) 974-1592. Fax: (813) 974- 1614; E-mail: kschmidt@usf.edu

Abstract

Exo1 belongs to the Rad2 family of structure-specific nucleases and possesses 5′–3′ exonuclease activity on double-stranded DNA substrates. Exo1 interacts physically with the DNA mismatch repair (MMR) proteins Msh2 and Mlh1 and is involved in the excision of the mispaired nucleotide. Independent of its role in MMR, Exo1 contributes to long-range resection of DNA double-strand break (DSB) ends to facilitate their repair by homologous recombination (HR), and was recently identified as a component of error-free DNA damage tolerance pathways. Here, we show that Exo1 activity increases

the hydroxyurea sensitivity of cells lacking Pol32, a subunit of DNA polymerases δ and ζ. Both, phospho-mimicking and dephospho-mimicking exo1 mutants act as hypermorphs, as evidenced by an increase in HU sensitivity of *pol32Δ* cells, suggesting that they are trapped in an active form and that phosphorylation of Exo1 at residues S372, S567, S587, S692 is necessary, but insufficient, for the accurate regulation of Exo1 activity at stalled replication forks. In contrast, neither phosphorylation status is important for Exo1's role in MMR or in the suppression of genome instability in cells lacking Sgs1 helicase. This ability of an *EXO1* deletion to suppress the HU hypersensitivity of *pol32Δ* cells is in contrast to the negative genetic interaction between deletions of *EXO1* and *POL32* in MMS-treated cells as well as the role of *EXO1* in DNA-damage treated *rad53* and *mec1* mutants.

Introduction

Exo1 belongs to the Rad2-family of structure-specific nucleases and possesses 5′–3′ exonuclease activity on double-stranded DNA substrates as well as flap-endonuclease activity [1,2]. Exo1 has a catalytic role during the excision step of DNA mismatch repair (MMR) and has been shown to physically interact with the MMR proteins Msh2 and Mlh1 in yeast and humans [1,3–8]. Although missense mutations in *EXO1* from cancer patients have been shown to reduce binding to Msh2 in vitro, and disruption of *EXO1* function has been associated with somatic hypermutation and development of cancer in older mice, a causative association between *EXO1* mutations and hereditary nonpolyposis colorectal cancer (HNPCC), which is caused by MMR defects, remains unclear [9–15].

Independent of its role in MMR, *EXO1* plays a role in the resection of DNA double-strand breaks (DSBs). Formation of long, single- stranded 3′ overhangs is necessary for Rad51 filament formation and non-mutagenic repair of DSBs by homologous recombination (HR) [16]. Resection appears to be a two-step reaction that commits repair of the DSB to the HR pathway. The Mre11/Rad50/Xrs2 complex binds first to the unprocessed DSB and, with help from Sae2 endonuclease, resects a short stretch. In the second step, long-range 5′–3′ resection is accomplished by Sgs1 and Dna2, which, respectively, contribute 3′–5′ helicase and endonuclease activities to the reaction [17,18]. In addition to Sgs1/Dna2, Exo1 can carry out long-range resection by removing nucleotides from the 5′-ended strand [17–19]. Yeast cells that lack both Sgs1 and Exo1 exhibit severely retarded long-range resection and accumulate spontaneous chromosomal rearrangements at an extraordinarily high rate [20,21]. Analysis of rearranged chromosomes in *sgs1Δ exo1Δ* mutants where a DSB was induced by endonucleolytic cleavage revealed that incompletely processed DNA breaks become substrates for aberrant repair, predominantly de novo telomere addition and, to a lesser extent, break-induced replication [22,23].

Recently, *EXO1* was also identified in a genetic screen for components of the error-free DNA damage tolerance (DDT) pathway, which is engaged when the replisome encounters a blocking DNA lesion in the template strand [24]. As opposed to the error-prone pathway where a translesion DNA polymerase is recruited to monoubiquitinated proliferating cell nuclear antigen (PCNA) to replicate across a lesion, in the error-free pathway the replicative DNA polymerase is thought to switch from the damaged template to the undamaged sister chromatid in a HR-dependent reaction, also

referred to as template switching. Exo1 is thought to promote the HR-dependent steps in error-free DDT by extending the ssDNA gap behind the stalled replication fork [24]. Exo1-dependent ssDNA formation may also allow accumulation of enough replication protein A (RPA) at stalled forks to enhance the DNA-damage signal sufficiently for 9-1-1/Mec1-dependent checkpoint activation [25,26]. In addition to bypassing replication blocking lesions in the template strand, error-free DDT can be specifically induced by deleting POL32, which encodes a noncatalytic subunit of DNA polymerase [27]. Through physical interaction with the polymerase clamp PCNA, Pol32 increases the processivity of DNA polymerase and the efficiency of DNA synthesis [28]. The DNA polymerase subunits Pol32 and Pol31 also function as subunits of DNA polymerase, whose catalytic core is made up of Rev3 and Rev7 [29–31]. DNA polymerase is conserved in eukaryotes and plays a critical role in translesion DNA synthesis and mutagenesis [32–34]. Although cells that lack Pol32 are viable, they experience replication stress that leads to phosphorylation of the checkpoint kinase Rad53, S phase delay, accumulation in G2/M, and hypersensitivity to DNA damaging agents [24,27,35].

When replication forks stall due to exposure to the DNA damaging agents hydroxyurea (HU) or methyl methanesulfonate (MMS), which deplete the dNTP pool and generate base adducts in the template strand, respectively, activation of the replication checkpoint helps to maintain the activity of the replisome, possibly through phosphorylation, that permits fork restart after withdrawal of the genotoxin [36–38]. Although Exo1 has been found at these stalled forks the presence of the intact replisome is thought to prevent it from acting on the nascent strands [26]. In cells that

lack a functional replication checkpoint, components of the replisome, most notably DNA polymerase and the replicative helicase Mcm2-7, have been found to dissociate from stalled forks, which might make the ends of the nascent strands vulnerable to degradation by nucleases, including Exo1 [39–41]. Nascent strand degradation may contribute to the destabilization of stalled replication forks in checkpoint mutants and, possibly, provide sufficiently long ssDNA regions for recombination [26,42,43]. A recent comparison of the composition of replisomes in checkpoint-deficient cells and wildtype cells also raised the possibility that the inability to restart stalled forks in checkpoint-deficient cells may be due to a lack of phosphorylation of replisome components and accessory factors rather than their loss from the replication fork [44,45]. Exo1 has been found to be phosphorylated in a Mec1-dependent manner upon treatment of cells with HU or MMS [38,46]. In cells with uncapped telomeres (*cdc13-1*), four phosphorylated serine residues were identified in the C-terminal half of Exo1 [47,48]. Although the effect of mutating these serine residues on the viability of the *cdc13-1* mutant was small, it hinted that DNA-damage induced phosphorylation inhibits Exo1 activity.

To better understand Exo1 function in the DNA-damage response and the regulation of these functions by phosphorylation, we have determined the effect of defects in DNA repair and the replication stress response on DNA-damage sensitivity and accumulation of mutations in the *exo1Δ* mutant and cells harboring alleles that encode phospho-mimicking and dephospho-mimicking mutants of Exo1.

Materials and Methods

Yeast strains and media

Yeast strains used in DNA-damage sensitivity and mutation assays were all derived from KHSY802 (*MATa, ura3-52, trp1Δ63, his3Δ200, leu2Δ1, lys2Bgl, hom3-10, ade2Δ1, ade8, hxt13::URA3*). Gene deletions were carried out as described [49] using HR- mediated integration of a selectable cassette. Mutants containing more than one gene deletion or mutation were obtained by random spore isolation from diploids heterozygous for the desired mutations [50]. Residues S372, S567, S587, and S692 of Exo1 were changed to alanine (*exo1-SA*) or aspartic acid (*exo1-SD*) and residues E150 and D173 to aspartic acid and alanine, respectively (*exo1-ND, exo1-ND-SA, exo1-ND-SD*) by site-directed mutagenesis of the *EXO1* ORF in plasmid pKHS610. pKHS610 was generated by inserting *EXO1* into pXP320 [51] by gap-repair using yeast strain KHSY2331 (*lig4::kanMX6*) to promote HR-mediated insertion. The resulting plasmids with mutant *exo1* alleles were pKHS611 (*exo1- SD*), pKHS612 (*exo1-SA*), pKHS613 (*exo1-ND-SA*), and pKHS614 (*exo1-ND-SD*). The exo1 alleles, including a HIS3MX6 cassette were amplified from the appropriate plasmids and integrated at the chromosomal *EXO1* locus in KHSY2338 (*exo1::KANMX6*) using the lithium acetate method [49]. Yeast strains used in this study are listed in Supplemental Table S1. Yeast was grown at 30◦C in yeast extract (10g/l), peptone (20 g/l), dextrose (20 g/l), media (YPD) with or without Bacto agar, or in synthetic complete (SC) media (yeast nitrogen base 6.7 g/l, dextrose 20g/l) supplemented with the appropriate amino acid mix.

Gross-chromosomal rearrangement (GCR) assay

GCR rates were determined by fluctuation analysis by taking the median rate of at least 15 cultures from at least two isolates [52,53] and are shown with 95% confidence intervals [54]. Cells with GCRs were identified by their resistance to canavanine and 5-fluoro-orotic acid (Can^r 5-FOA^r), which is indicative of simultaneous inactivation of *CAN1* and *URA3* on chromosome V. Selective media for the GCR assay was prepared as previously described [55].

Fluctuation assays and *CAN1* mutation spectrum analysis

Forward mutation rates were determined by fluctuation analysis by method of the median as previously described [53,56] and are shown with 95% confidence intervals [54]. Five cultures from at least two different isolates were grown overnight in 3–5 ml of YPD media. Dilutions were plated on YPD agar plates to determine the viable cell count, and either 500 l or 1000 l were plated on synthetic media supplemented with 60 g/ml canavanine, but lacking arginine (SC-ARG/canavanine) to select for *can1* mutants. To select for Thr+ (*hom3-10*) revertants, 250–4000 l were plated on synthetic media lacking threonine. Semi-quantitative assessment of accumulation of *CAN1* mutations was performed by a patch assay. Briefly, three independent colonies of each mutant were spread over approximately 1-inch squares on YPD agar or YPD agar containing 10mM HU. Patches were allowed to grow for five days at 30 ◦ C and replica plated onto SC-ARG/canavanine. Formation of papillae was documented each day for four days of incubation at 30 ◦ C. To determine the *CAN1* mutation spectrum, the *CAN1* open

102

reading frame (ORF) and 50 bp upstream as well as 43bp downstream of the ORF were amplified by PCR from canavanine-resistant colonies and sequenced.

Hydroxyurea (HU) and methylmethanesulfonate (MMS) sensitivity assays

Cultures of single colonies grown overnight at 30°C in YPD liquid media were adjusted to OD_{600} =0.2 and grown at 30°C to OD_{600} = 0.5. Ten-fold serial dilutions were spotted on YPD, and YPD supplemented with the indicated concentrations of MMS and HU. Colony formation was documented each day for 5 days of incubation at 30°C

Results

Functional interactions between Exo1, DNA repair and DNA-damage response

Exo1 and Sgs1/Dna2 act in parallel in long-range 5′ end resection during DSB repair by HR [18]. When both pathways are disrupted (*sgs1Δ exo1Δ*) the accumulation of gross-chromosomal rearrangements (GCRs) increases synergistically to 450-fold over the rate of the *sgs1Δ* single mutant [20,21]. Here we report that this rapid accumulation of GCRs in the *sgs1Δ exo1Δ* mutant can be further accelerated by increasing replication stress either by impairing DNA polymerase δ (*pol32Δ*) or by failure to complete repair (*apn1Δ, rad1Δ*) or bypass (*rev3Δ, pol32Δ*) of spontaneous DNA lesions (Table 1). Disruption of these activities in the *exo1Δ* single mutant (Table 2), but not in the *sgs1Δ* single mutant (Table S2), also caused significant increases in genome instability, with the strongest synergistic increases caused by the *rev3Δ* and *pol32Δ*

103

mutations. Deletion of *TEL1* also caused a significant increase in GCR accumulation in the *sgs1Δ exo1Δ* mutant, but to a lesser extent than the 28-fold increase observed upon deletion of *MEC3* [20], suggesting that the Mec3-Ddc1-Rad17-mediated replication stress response plays a significantly greater role in the suppression of genome instability in the *sgs1Δ exo1Δ* mutant than the Tel1-mediated checkpoint response to DNA breaks.

The small, but significant, increases in genome instability in the *sgs1Δ exo1Δ* mutant upon deletion of either *TEL1, REV3* or *APN1* were accompanied by increases in sensitivity to hydroxyurea (HU), which impedes replisome progression by depleting the dNTP pool, whereas no such increase was observed upon deletion of *RAD1* (Fig. 1A–D). Combining *sgs1Δ* and *pol32Δ* mutations caused a clear fitness defect on rich media, which was not further exacerbated by deletion of *EXO1* (Fig. 1E). However, deletion of *EXO1* appeared to slightly suppress the HU hypersensitivity of the *sgs1Δ pol32Δ* mutant, but not its hypersensitivity to methyl methanesulfonate (MMS), which impairs replisome progression by generating DNA lesions (e.g., base adducts) in the template strand (Fig. 1E). Since insensitivity to HU (200 mM) and sensitivity to MMS (0.05%) are characteristic of an *exo1Δ* mutant [20], we next evaluated the HU sensitivity of *sgs1Δ* and *pol32Δ* single mutants in the presence and the absence of *EXO1*. We increased the HU concentration from 10 to 55 mM – a level at which *sgs1Δ* and *pol32Δ* mutants display significantly higher HU sensitivity than the wildtype strain. We found that the *exo1Δ* mutation suppressed the HU hypersensitivity of the *pol32Δ* mutant to a level comparable to the wildtype strain, but had no effect on the *sgs1Δ* mutant (Fig. 1F). Disrupting the nuclease activity of Exo1 (*exo1-ND*) achieved the same level of

suppression of HU hypersensitivity in the *pol32Δ* mutant as deletion of EXO1 (Fig. 2A).

Disruption of Exo1, however, had no effect on the viability of *pol32Δ* cells treated with

high concentrations of HU (200 mM) (Fig. 2 B). These findings suggest that under low

replication stress Exo1-dependent events, most likely ssDNA formation at stalled

replication forks, are the major contributor to the inviability of *pol32Δ* cells, whereas

under conditions when DNA synthesis is grossly impeded by high concentrations of HU

Exo1-independent lesions, such as DNA breaks, are the major cause of *pol32Δ*

inviability.

In contrast to HU, Exo1 was not found to be toxic to MMS-treated *pol32Δ* cells at

the tested concentrations. In fact, when the *pol32Δ* mutant was exposed to MMS we

observed the opposite response: while *exo1, exo1-ND* and *pol32Δ* single mutants grew

almost like wildtype cells on 0.01% MMS, combining the *pol32Δ* mutation with *exo1Δ* or

exo1-ND mutations increased MMS sensitivity synergistically (Fig. 2A). This is

consistent with the recent finding that *EXO1* is required for the bypass of MMS-induced

DNA lesions by error-free DNA-damage tolerance pathways [24].

Phosphorylation-site mutants of Exo1 are hypermorphic in HU-treated

pol32Δ cells

In yeast cells with a defective telomere capping complex (*cdc13-1*), the C-

terminal half of Exo1 has been found to be phosphorylated in a Mec1-dependent

manner at four dispersed sites (S372, S567, S587, S692) [47]. To determine how

phosphorylation contributes to the adverse effect of Exo1 on HU-treated *pol32Δ* cells we

crossed *pol32Δ* cells with *exo1* mutants that either mimicked constitutive Exo1

phosphorylation (*exo1-SD*) or were refractory to phosphorylation at these four sites (*exo1-SA*). Although we expected that mutating the phosphorylation sites would affect Exo1 activity and therefore affect the viability of *pol32Δ* cells on HU we were surprised to find that both alleles, *exo1-SA* and *exo1-SD*, led to increases in HU hypersensitivity that clearly exceeded that of the pol32 mutant with an EXO1 wildtype allele (Fig. 2A). Since the nuclease activity of Exo1 appears to sensitize *pol32Δ* cells to HU, the strong synergistic increases in HU sensitivity in the *pol32Δ exo1-SA* and *pol32Δ exo1-SD* mutants could indicate that the *exo1-SA* and *exo1-SD* alleles code for hyperactive nucleases. To test this, we inactivated the nuclease activity of the *exo1-SA* and *exo1-SD* mutants by introducing E150D and D173A mutations. Consistent with our hypothesis we observed suppression of HU hypersensitivity for both alleles (Fig. 2C). To determine if the *exo1-SA* and the *exo1-SD* alleles were equally toxic to HU-treated *pol32Δ* cells we lowered the HU concentration to a level at which the *pol32Δ* mutant was no more sensitive than wildtype (20 mM) and compared the growth of *exo1-SA pol32Δ* and *exo1-SD pol32Δ* cells. We observed that the dephospho-mimicking *exo1-SA* allele was slightly more damaging than the phospho-mimicking *exo1-SD* allele (Fig. 2D). This difference disappeared at higher HU concentrations (≥40 mM).

In contrast to the *exo1Δ* mutation, expression of the *exo1-SA* and *exo1-SD* alleles had no effect on the viability of *pol32Δ* cells exposed to MMS (Fig. 2A). As expected from the phenotype of *exo1-ND pol32Δ* cells, mutation of the nuclease domain of *exo1-SA* or *exo1-SD* alleles in *pol32Δ* cells caused a synergistic increase in MMS-hypersensitivity (Fig. 2C).

Since Pol32 not only plays a major role as the processivity factor for DNA polymerase δ, but also functions as a subunit of the translesion DNA polymerase ζ , we wanted to determine if the effect of the *pol32Δ* mutation on HU and MMS sensitivity could be due to disruption of Pol ζ activity. We found that deletion of *REV3*, which encodes the catalytic subunit of Pol ζ, did not cause an increase in sensitivity to 55 mM HU, a concentration to which the *pol32Δ* mutant is hypersensitive (Fig. 2E), or 100 mM HU (Supplemental Figure S1). Opposite to the effect in the *pol32Δ* mutant, deletion of *EXO1* had no effect on the HU sensitivity of the *rev3Δ* mutant at 55 mM HU and increased its sensitivity when exposed to 100 mM HU (Fig. 2E, Supplemental Figure S1). Also in contrast to the *pol32Δ* mutant, the *exo1-SA* and *exo1-SD* alleles had no effect on the HU sensitivity of the *rev3Δ* mutant, even at 100 mM HU (Supplemental Figure S1). These differences between *rev3Δ* and *pol32Δ* mutations suggest that the genetic interactions between *pol32Δ* and *exo1* mutations on HU are largely caused by the role of Pol32 as a subunit of Pol δ. On 0.01% MMS, deletion of *REV3* did not increase the sensitivity of the *exo1Δ* or *pol32Δ* mutant, but led to a further increase in the sensitivity of the *pol32Δ exo1Δ* double mutant, suggesting that Pol32, Exo1 and Rev3 play at least partially redundant roles in the response to MMS (Fig. 2A and E). Similar to the *rev3Δ* mutant, we observed no difference in the HU sensitivity between *sgs1Δ* or *tel1Δ* mutants expressing the *exo1-SA* or the *exo1-SD* allele or the *EXO1* wildtype allele (Supplemental Figure S1). Using the gross-chromosomal rearrangement (GCR) assay [55,57], which measures the rate of accumulating viable outcomes of chromosome break repair, we found that the loss of Exo1 activity in untreated *pol32Δ*

cells caused a significant (8-fold) increase in chromosomal instability whereas expression of the *exo1-SA* or *exo1-SD* allele had no effect (Table 3). These results mirror the role of *EXO1* in MMS-treated *pol32Δ* cells. Although, *EXO1* is the strongest known suppressor of spontaneous chromosome rearrangements in *sgs1Δ* cells [20,21], the four phospho-sites are also dispensable for this suppressor function (Table 3).

Mismatch repair activity partially contributes to Exo1 toxicity in *pol32Δ* cells

In addition to its role in DSB processing, Exo1 performs a late step in MMR, most likely degradation of the mismatch-containing nascent strand, and binds to the MMR factors Msh2 and Mlh1 through its C-terminus [1,58]. Thus, one way in which Exo1 could localize to replicating DNA is through interaction with the MMR machinery, whose subunits Msh6 and Msh3 interact with the replication machinery by binding to PCNA [59,60]. Once there, Exo1 is thought to be able to degrade nascent DNA strands by acting on the 5′ ends of Okazaki fragments [61,62]. In addition to these pre-existing 5′ ends, the MMR factor MutLα is thought to make incisions in the nascent strand [63]. Disruption of the MMR pathway by deletion of *MSH2* would disrupt one avenue for recruitment of Exo1 to replicating DNA and prevent the formation of MutLα-dependent strand nicks for Exo1 entry and increased ssDNA formation. To test the possibility that MMR factors contribute to Exo1 toxicity in HU-treated *pol32Δ* cells, we assessed the HU sensitivity of *pol32Δ msh2Δ* cells expressing either *exo1Δ*, *EXO1, exo1-SA* or *exo1-SD* alleles. We observed that a *msh2Δ* mutation had no effect on the HU sensitivity of the *pol32Δ* and *pol32Δ exo1-SA* mutants, but suppressed the HU sensitivity of the *pol32Δ*

exo1-SD mutant (Fig. 3A). These results show that MMR activity contributes

significantly to the hypertoxicity of the phospho-mimicking *exo1-SD* allele in *pol32Δ*

cells. It also suggests that MMR-independent functions of Exo1 are mostly responsible

for the toxicity of the dephospho-mimicking *exo1-SA* allele in HU-treated *pol32Δ* cells.

That the impact of Exo1 activity in the *pol32Δ* mutant exceeds its role in MMR is also

suggested by the different responses of the *exo1Δ pol32Δ* and *msh2Δ pol32Δ* mutants

to MMS; whereas the *exo1Δ pol32Δ* mutant shows an increase in MMS sensitivity

compared to the single mutants, sensitivity of the *msh2Δ pol32Δ* mutant is

indistinguishable from that of the *pol32Δ* single mutant (Fig. 3B). Additionally, *exo1Δ*,

but not *msh2Δ*, caused a statistically significant increase in the accumulation of GCRs in

the *pol32Δ* mutant (Table 2).

　　Since the four phosphorylation sites are located in the C-terminal half of Exo1

where Mlh1 and Msh2 have been reported to bind we tested if the *exo1-SA* and *exo1-*

SD alleles were associated with a mutator phenotype. Three single colonies of wildtype,

pol32Δ, or *sgs1Δ* cells with either *EXO1, exo1Δ, exo1-SA* or *exo1-SD* alleles were

grown into thick, 1-inch squares on nonselective rich media (YPD) and replica-plated

onto synthetic media containing canavanine to select for clones that had spontaneously

acquired inactivating mutations in the *CAN1* gene. In contrast to *exo1Δ*, neither the

exo1-SA nor the *exo1-SD* mutation affected the *CAN1* mutation rate in wildtype, *sgs1Δ*

or *pol32Δ* cells (Fig. 4A, Supplemental Figure S2), mirroring the lack of effect of these

exo1 alleles on GCR accumulation (Table 3). A more accurate determination of the

CAN1 mutation rate using a fluctuation assay confirmed the previously reported weak

mutator phenotype of the *exo1Δ* cells [1], but did not reveal statistically significant

differences between the *exo1Δ pol32Δ* mutant and the single mutants, or the *exo1-SA pol32Δ* or *exo1-SD pol32Δ* mutants and the single mutants (Fig. 4C). These findings indicate that the phosphorylation site mutations do not affect the function of Exo1 in mutation avoidance at the *CAN1* locus. However, when we determined the mutation rate of the *hom3-10* allele (Thr−), which detects mutations that revert a +1T insertion in a mononucleotide (T10) run, we observed a synergistic (24-fold) increase in Thr+ reversion events in the *pol32Δ exo1Δ* mutant (Fig. 4C), consistent with a previously reported synergistic mutation rate increase in the *lys2-10A* assay, which detects mutations that revert +1A insertions [64]. In the *hom3-10* assay, we also detected a small (2.8-fold), but significant increase of Thr$^+$ revertants in the *exo1-SD* mutant; but no synergistic interaction when the *exo1-SD* and *pol32Δ* mutations were combined (Fig. 4C). Finally, growing the cells in the presence of 10mM HU before replica-plating onto canavanine media did not lead to noticeable changes in mutation rates, except in the *exo1-SA pol32Δ* mutant, which exhibited a markedly reduced number of papillae compared to the single mutants (Fig. 4B). The slow growth of *pol32Δ exo1-SA* cells even in the presence of a very low concentration of HU (Fig. 2C) is the most likely cause of the lower number of Can^r papillae in this mutant.

When we analyzed the *CAN1* mutation spectrum in Can^r clones (Supplemental Table S3) we found that the majority (89.5%) of mutations in the *exo1Δ* mutant were base substitutions and small (≤3 bp) insertions/deletions, whereas larger insertions/deletions ranging from 18 to 72bp dominated (52.6%) in *pol32Δ* mutant. Upon deletion of *EXO1* in the *pol32Δ* mutant these large deletions decreased to 20% whereas small insertions/deletions increased (40%), with a similar fraction of base substitutions

110

(30%) as in the *pol32Δ* mutant (36.8%). We also identified rare complex

rearrangements that consist of large deletions (8–233 bp) that contain small insertions

(2–36 bp).

Discussion

In wildtype cells, the nuclease activity of Exo1 is important for 5′ end resection of

DSB ends during HR, for the excision step of MMR and for HR-mediated template

switching during error-free bypass of DNA lesions. Exo1 has also been shown to

counteract fork reversal in checkpoint-deficient cells and is thought to promote template

switching by contributing to the extension of ssDNA behind stalled replication forks [25–

27,65–67]. We have shown here that Exo1 nuclease activity is toxic to HU-treated

pol32Δ cells and that this toxicity can be further increased by mutating four serine

residues in the C-terminal tail of Exo1 that have previously been shown to be

phosphorylated in response to telomere uncapping [47]. That the viability of HU-treated

pol32Δ cells could be rescued by disruption of the nuclease activity of Exo1 suggests

that phosphorylated Exo1, which forms in response to HU [46], is still a potent nuclease,

but at a level that is compatible with normal growth of HU-treated wildtype cells. Only

when replication fork stalling due to HU treatment is combined with another event that

independently impairs DNA synthesis (*pol32Δ*), do Exo1 nuclease-dependent events,

most likely ssDNA formation, reach toxic levels. This could suggest that there is a

balance between the speed of ssDNA formation at replication forks and the speed of

DNA synthesis, which does not allow ssDNA to accumulate at deleterious levels. If the

speed of DNA synthesis is reduced (HU treatment), this balance may be restored by

111

reducing Exo1 activity through Mec1-dependent phosphorylation of Exo1. However, this reduced level of Exo1 activity might be damaging if DNA synthesis is inhibited further (e.g., HU-treatment of the *pol32Δ* mutant) and DNA resection exceeds DNA synthesis. That Exo1 phosphorylation also occurs in MMS-treated cells [38], which depend on Exo1 activity for viability, also supports a model in which phosphorylation reduces, rather than deactivates, Exo1 nuclease function. This model is also consistent with the finding that the C-terminal tail of Exo1, where the phosphorylation sites are located, is dispensable for normal function of Exo1 in MMS-treated cells [20] and the finding in this study that expression of *exo1-SA* and *exo1-SD* alleles has no effect on the viability of MMS-treated wildtype or *pol32Δ* cells, leading us to suggest that downregulation of Exo1 activity by phosphorylation is tolerated in MMS-treated cells, but not necessary. As in HU-treated *pol32Δ* cells, endogenous Exo1 activity was previously shown to inhibit proliferation of the *cdc13-1* mutant [47]. In these cells, which accumulate uncapped telomeres, a phospho-mimicking *exo1* allele led to a minor increase in cell viability whereas a dephospho-mimicking allele had no effect. Although the effect was subtle, it suggested that phosphorylation inhibits Exo1 activity. Unlike in the *cdc13-1* mutant, however, we did not observe a rescue of cell viability upon expression of the phospho-mimicking *exo1-SD* allele in HU-treated *pol32Δ* cells. Instead, *exo1-SD* and *exo1-SA* inhibited proliferation more strongly than wildtype *EXO1*. For both alleles this negative effect was dependent on the nuclease activity, suggesting that *exo1-SA* and *exo1-SD* encode functional exonucleases that are trapped in an active state. The hyperactivity of both alleles further suggests that both, phosphorylated and the non-phosphorylated forms of Exo1, and possibly the ability to convert one form into the other, are necessary

for the proper response of *pol32Δ* cells to HU. Although Pol32 functions as a subunit of

Pol δ and Pol ζ, the different effects of *pol32Δ* and *rev3Δ* mutations, the latter of which

disrupts the catalytic activity of Pol ζ, suggest that the observed genetic interactions

between *pol32Δ* and *exo1Δ* mutations on hydroxyurea are dominated by the role of

Pol32 as a processivity factor of Pol δ.

     The inability to phosphorylate serine residues 372, 567, 587 and 692 could

explain the unrestrained activity of the exo1-SA mutant, which appears to exceed that of

the exo1-SD mutant slightly. Whereas hypertoxicity of exo1-SA suggests that

phosphorylation of the four serine residues is necessary for the proper regulation of

Exo1 activity, hypertoxicity of the exo1-SD mutant could suggest that it is insufficient.

That the aspartic acid substitutions in the exo1-SD mutant, which mimic the negative

charge of phosphorylated serine residues, do not inactivate, even partially, Exo1,

argues that irreversible negative charges at residues 372, 567, 587, and 692 may

interfere with additional events that are required for the downregulation of Exo1 activity

at stalled replication forks, such as additional phosphorylation events or conformational

changes. In addition to phosphorylation, the activity of Exo1 could be affected by

binding to proteins that modulate its activity through conformational changes,

recruitment to DNA substrates, subcellular relocalization, or sequestration. The proteins

that are currently known to bind to yeast Exo1 are the MMR factors Msh2 and Mlh1 [1],

the 14-3-3 proteins Bmh1 and Bmh2 [46], and Mec3, a subunit of the Ddc1/Rad17/Mec3

(9-1-1) checkpoint clamp [24]. All could affect Exo1 activity. First, we show here that

deletion of *MSH2* significantly suppresses the detrimental effects of the hyperactive

exo1-SD allele, suggesting that constitutive phosphorylation of the Exo1 C-terminus

113

might lead to a dysregulation of its physical interaction with Msh2. MMR factors, which travel with the replisome via interaction with PCNA [59,60], could be involved in recruiting Exo1 to replication forks and provide additional 5′ ends for Exo1 to resect, thereby contributing to increased Exo1-dependent ssDNA formation at stalled replication forks. Recent evidence in yeast indeed suggests a role for MMR activity and Exo1 in checkpoint activation through promoting ssDNA formation at stalled replication forks and DNA repair-induced gaps [68,69]. Second, 14-3-3 proteins can modulate protein activity through affecting access to substrates by changing a protein's subcellular localization, by inducing conformational changes that either increase or decrease activity, or by bridging interaction with another protein [70]. Although the vast majority of 14-3-3 proteins interact with phosphorylated targets, the question whether Bmh1/2 interacts with a phosphorylated or a unphosphorylated form of Exo1 is currently unresolved, as is the molecular mechanism by which Bmh1/2 affects Exo1 activity [46]. Third, as Exo1 phosphorylation occurs in a Mec1-dependent manner in response to HU and MMS [38,46], it is plausible that phosphorylation-dependent binding of Exo1 to the Mec3/Ddc1/Rad17 checkpoint clamp, which loads onto the ds/ssDNA junctions at ssDNA gaps, could control Exo1 activity during the DNA-damage response. Whereas Rad27 activity is strongly stimulated through physical interaction with PCNA [71–73], it is not known if Exo1 activity at replication forks is regulated by another protein. The interaction of Exo1 with the Mec3 checkpoint clamp, however, could provide such regulation during the DNA damage response – analogous to the interaction between Rad27 and PCNA during DNA replication.

114

The ability of an *EXO1* deletion to rescue *pol32Δ* cells treated with a low dose of HU (55 mM), but not those exposed to a high dose of HU (200mM) might be due to a difference in the types of DNA lesions and their quantity induced by low and high doses of HU. For instance, deletion of *EXO1* may have a positive effect on viability by preventing excessive ssDNA formation at slowed or stalled forks, which are likely to dominate in *pol32Δ* cells exposed to low HU concentrations. In contrast, deletion of *EXO1* is unlikely to prevent the formation DNA breaks, which may be more typical in cells exposed to high HU concentrations. Similarly, the different extent by which the dephospho-mimicking and phospho-mimicking *exo1* alleles affect the viability of the *cdc13-1* mutant [47] and HU-treated *pol32Δ* cells could indicate that the DNA-damage response is differently regulated for different regions of the genome. Specifically, differences in the sets of proteins and DNA structures found at telomeres versus those found at replicating DNA could cause differences in the regulation of Exo1 activity and the extent of DNA resection at those sites. In an *cdc13-1* mutant, for instance, Exo1 is responsible for the majority of new ssDNA formation at the unprotected telomeres and for the initiation of Mec1-dependent checkpoint activation [74,75] reviewed in [76], whereas Exo1 appears to be redundant with other nuclease functions during 5′ end resection elsewhere in the genome, most notably in the processing of DSB ends during HR [18] and degradation of the mismatch-containing strand in MMR [1]. Finally, the differences between the effect of the exo1 phosphorylation mutants in *pol32Δ* and *cdc13-1* mutants could also suggest that phosphorylation is more important for regulating Exo1 activity at slowed and stalled replication forks than at uncapped telomeres.

Although in the absence of Exo1 excessive ssDNA formation and loss of cell viability could be prevented during increased fork stalling, other aberrant structures may still form due to lack of resection by Exo1, leading to genome instability. This is supported by the synergistic increase in the GCR rate in the *exo1Δ pol32Δ* mutant. Lack of resection in the absence of Exo1 could also provide an explanation for the rare complex mutations we observed at the *CAN1* locus, which appear to be a combination of deletion and insertion events. They could, for example, arise if ends of the nascent strands dissociate from their templates, misanneal in a chickenfoot structure and then dissociate after limited DNA synthesis to reanneal with their template strands.

Our findings are consistent with the report in cells with uncapped telomeres that phosphorylation inhibits Exo1 activity, but they do, on their own, not exclude the possibility that phosphorylation upregulates Exo1 activity at stalled replication forks. Upregulation of Exo1 activity by phosphorylation is consistent with our finding that disruption of the nuclease activity of Exo1 rescues the viability of HU-treated *pol32Δ* cells. It would also provide an explanation for the hypertoxicity of the phospho-mimicking exo1-SD mutant in HU-treated *pol32Δ* cells and the normal function of the allele in MMS-treated *pol32Δ* cells, whose viability depends on functional Exo1. The hypertoxicity of the exo1-SA mutant, which is refractory to phosphorylation at the previously identified four serine residues, could be explained if activating phosphorylation events shift to other residues. Since the C-terminal half of Exo1 is predicted to be unstructured [20], other serine residues in this 331-residue region should be easily accessible to phosphorylation. Indeed, Western blot analysis has shown that the exo1-SA mutant can still be phosphorylated in the presence of DNA

damage [47]. Additional analyses of Exo1 post-translational modifications will therefore be needed to determine if Exo1 activity is regulated differently in response to varying DNA damage-inducing agents, genetic mutations, or types of DNA lesions, and how these modifications affect the binding of Exo1 to proteins that might modulate its activity.

Figures and Tables
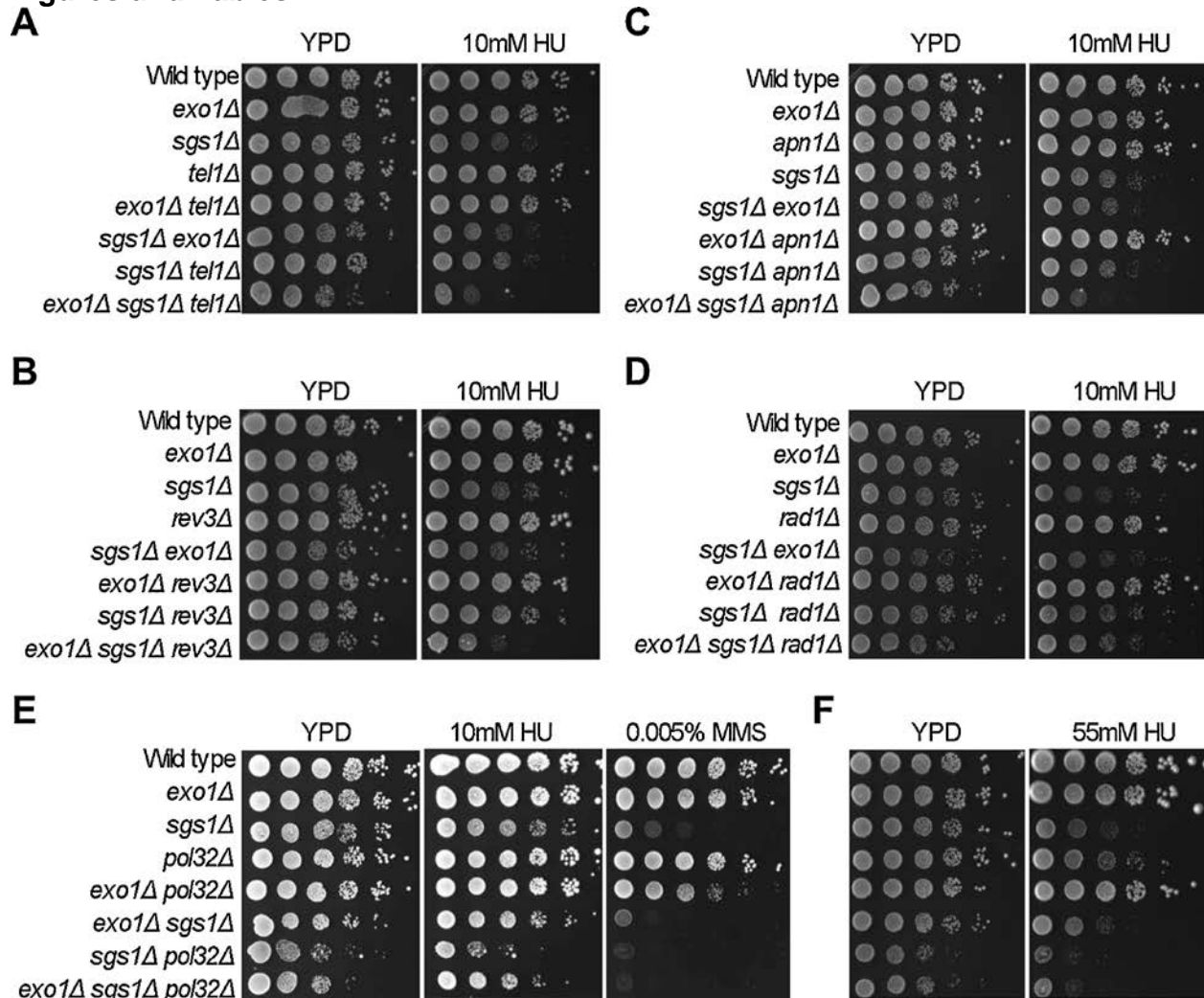
Figure 3.1. Effect of DNA repair and checkpoint mutations on DNA-damage sensitivity of *sgs1Δ, exo1Δ* and *sgs1Δ exo1Δ* cells. (A–D) At 10 mM HU, the *tel1Δ, rad1Δ, rev3Δ* and *apn1Δ* mutations do not affect the viability of *sgs1Δ* and *exo1Δ* mutants, but inhibit growth of the *sgs1Δ exo1Δ* mutant. (E) The *exo1Δ* mutation suppresses the hypersensitivity of the *pol32Δ sgs1Δ* mutant to HU, but not to MMS. (F) Hypersensitivity of the *pol32Δ* mutant to higher concentrations of HU (55 mM) is suppressed by *exo1Δ*.
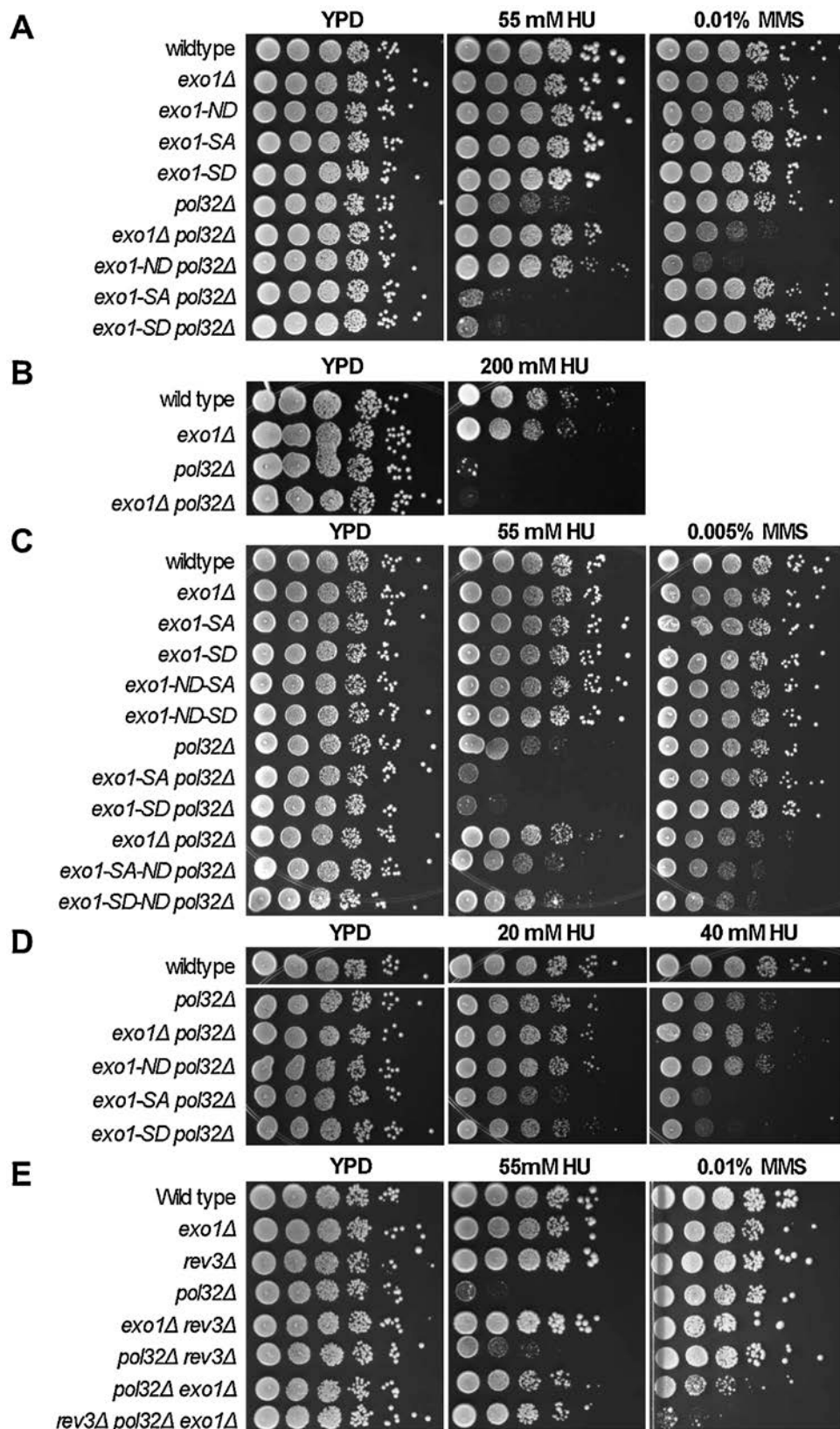
Figure 3.2. Sensitivity of *pol32Δ* cells to HU and MMS is differently affected by nuclease-dead and phosphorylation site mutants of *EXO1*. (A) Toxicity of Exo1 in

HU-treated *pol32Δ* cells is due to the nuclease activity of Exo1. exo1 mutants with four serine residues substituted with either alanine (exo1-SA, dephospho-mimic) or aspartic acid (exo1-SD, phospho-mimic) are more toxic to HU-treated *pol32Δ* cells than wildtype Exo1. In MMS-treated pol32 cells, deletion of Exo1 activity causes a decrease of viability whereas the phospho-site mutants of Exo1 have no effect. (B) Deletion of *EXO1* does not improve viability of *pol32Δ* cells exposed to a high concentration of HU. (C) The hypertoxicity of *exo1-SA* and *exo1-SD* in HU-treated *pol32Δ* cells depends on the nuclease activity of Exo1. (D) The dephospho-mimicking *exo1-SA* allele is more toxic to HU-treated *pol32Δ* cells than the phospho-mimicking *exo1-SD* allele. (E) The *rev3Δ* mutation does not affect the sensitivity of the *exo1Δ pol32Δ* mutant to 55 mM HU, but increases its sensitivity to 0.01% MMS. Unlike the *exo1Δ* mutation, the *rev3Δ* mutation is not a major suppressor of the hypersensitivity of the *pol32Δ* mutant to 55 mM HU.
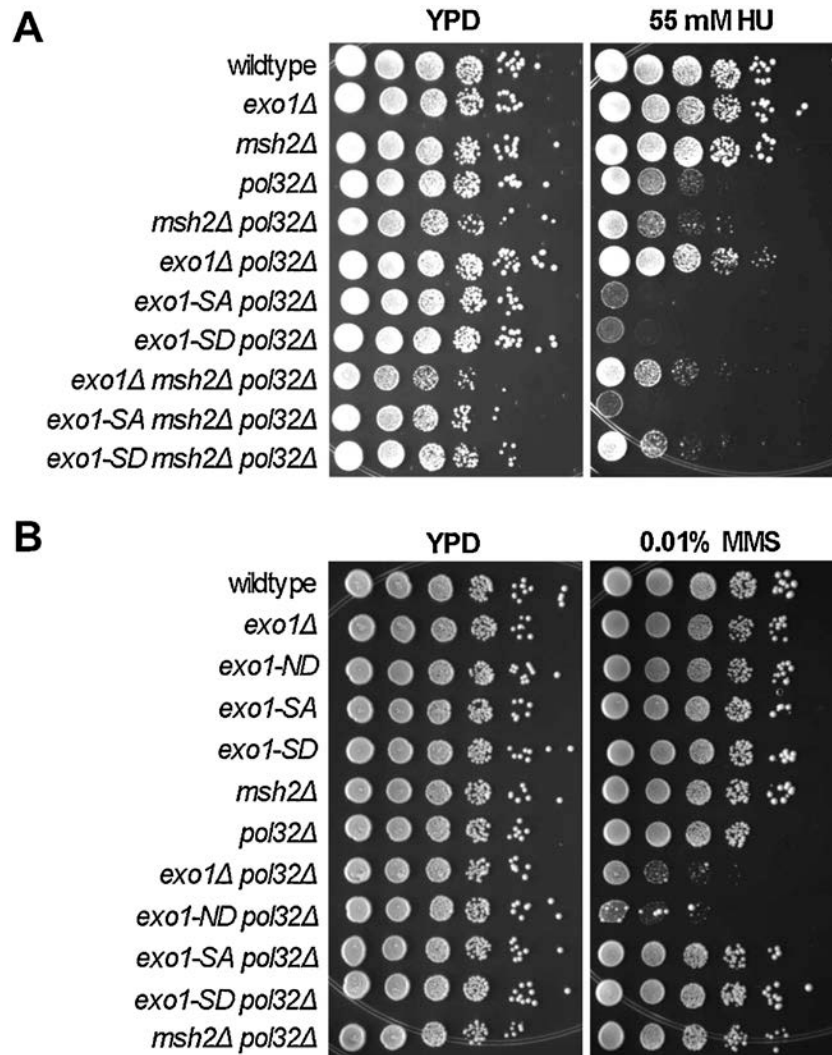
Figure 3.3. Effect of DNA mismatch repair on DNA damage sensitivity of *pol32Δ* and *exo1Δ* mutants. (A) Deletion of *MSH2* does not affect the HU hypersensitivity of the *pol32Δ* mutant or the *pol32Δ exo1-SA* mutant, but suppresses the hypertoxicity of the phospho-mimic *exo1-SD* allele in HU-treated *pol32Δ* cells. (B) In contrast to inactivation of *EXO1* (*exo1Δ*, *exo1-ND*), deletion of *MSH2* does not increase the sensitivity of the *pol32Δ* mutant to 0.01% MMS.

A -HU

wildtype   exo1Δ pol32Δ
exo1Δ   exo1-SA pol32Δ
exo1-SA   exo1Δ sgs1Δ
pol32Δ   exo1-SA sgs1Δ
sgs1Δ   msh2Δ

B + 10 mM HU

wildtype   msh2Δ
pol32Δ   msh2Δ pol32Δ
exo1Δ   exo1Δ pol32Δ
exo1-SA   exo1-SA pol32Δ
exo1-SD   exo1-SD pol32Δ

C

Genotype	Can^r (x10^{-7})		Thr$^+$ (x10^{-9})	
	Mutation rate	95% CI	Mutation rate	95% CI
wildtype	3.3	2.5-5.8	2.2	1.8-2.8
exo1Δ	10.9	9.9-13.4	9.5	6.5-10.0
exo1-SA	1.3	0.7-4.8	3.1	2.7-4.0
exo1-SD	1.5	1.0-2.4	6.2	4.7-11.8
pol32Δ	2.1	1.1-3.4	8.7	5.1-12.1
exo1Δ pol32Δ	14.4	11.1-17.1	235.8	147.9-313.4
exo1-SA pol32Δ	1.9	1.5-2.2	7.7	3.9-10.0
exo1-SD pol32Δ	2.4	1.8-2.7	5.8	3.2-9.8

Figure 4.4. Effect of phosphorylation site mutations on the function of Exo1 in mutation avoidance. Patches were grown from individual colonies of the indicated mutants to allow accumulation of mutations at the *CAN1* locus. Patches were then replica-plated onto media supplemented with canavanine to select Can^r mutants. The *exo1-SA* and *exo1-SD* alleles do not exhibit a mutator phenotype when grown in the absence of HU (A) or presence of 10 mM HU (B) prior to replica-plating onto canavanine media (see Supplemental Figure S4.2. for the *exo1-SD* allele). (C)

Compared to the single mutants, the *exo1Δ pol32Δ* mutant exhibits a synergistic (24-fold) increase in Thr$^+$ reversion events (*hom3-10* allele), but no increase in the accumulation of Can^r mutants (*CAN1* locus). Whereas the *exo1-SA* allele exhibits a wildtype mutation rate, the *exo1-SD* allele causes a small (2.8-fold), but significant, increase in the accumulation of Thr$^+$ revertants.
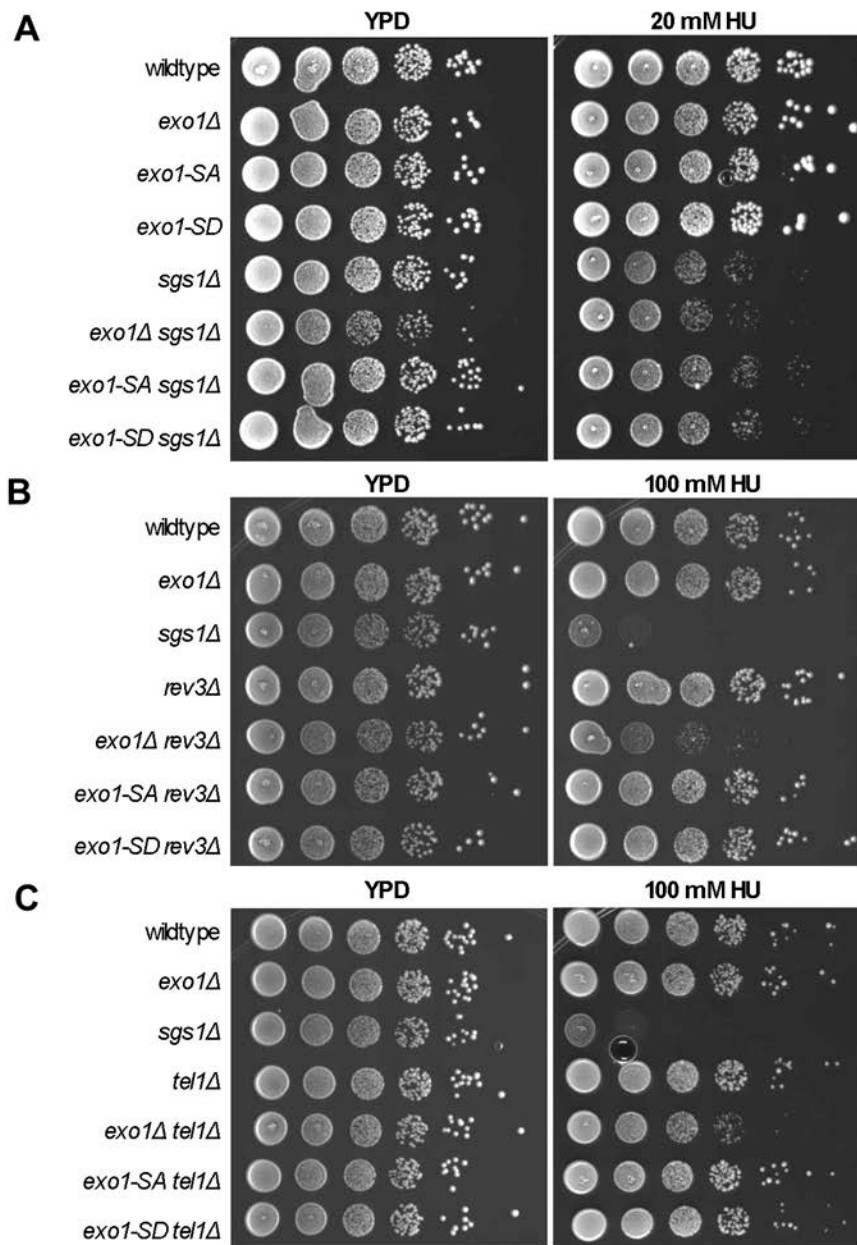
Fig. S3.1. Effects of *exo1Δ* and *exo1* phosphorylation site mutants *exo1-SA* and *exo1-SD* on HU sensitivity of *sgs1Δ, rev3Δ,* and *tel1Δ* mutants.
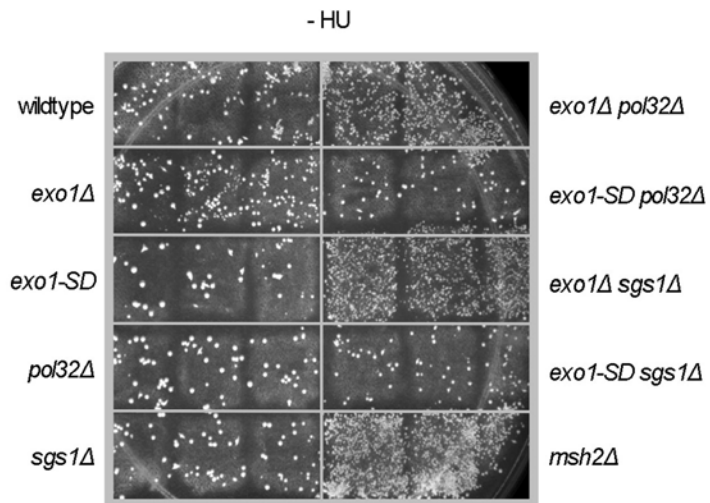
Figure S4.2. Effect of the phospho-mimicking *exo1-SD* allele on the spontaneous mutation rate at the *CAN1* locus in the *pol32Δ* and the *sgs1Δ* mutant. The mismatch-repair-defective *msh2Δ* mutant is included as a positive control.

Table 3.1 Gross-chromosomal rearrangements (GCRs) in the *sgs1Δ exo1Δ* mutant.

Relevant genotype	GCR rate (Can^r 5-FOA^r × 10^-10)	95% CI[a] (Can^r 5-FOA^r × 10^-10)	Fold increase over *sgs1Δ exo1Δ*
Wildtype	1.1	<1-6.2	_
exo1Δ	14	7-28	_
sgs1Δ	89	57-177	_
exo1Δ sgs1Δ	40,500	31,000-49,800	_
exo1Δ sgs1Δ rev3Δ	176,000	148,000-210,000	4.4
exo1Δ sgs1Δ pol32Δ	141,000	107,000-166,000	3.5
exo1Δ sgs1Δ tel1Δ	140,000	126,000-174,000	3.4
exo1Δ sgs1Δ rad1Δ	96,600	74,500-180,000	2.4
exo1Δ sgs1Δ apn1Δ	78,500	57,000-131,000	1.9

(a) 95% confidence intervals (CI) were calculated according to Ref. [54].

Table 3.2 *EXO1-* dependent suppression of gross-chromosomal rearrangements (GCRs) in DNA repair and DNA-damage checkpoints mutants.

Relevant genotype	GCR rate[a] (Can^r 5-FOA^r × 10^{-10})	95% CI[b] (Can^r 5-FOA^r × 10^{-10})	Increase over single mutant[c]
Wildtype	1.1	<1-6.2	
exo1Δ	14	7-28	
rad1Δ	10	<9-23	
exo1Δ rad1Δ	45	30-66	3.2
apn1Δ	19	14-41	
exo1Δ apn1Δ	64	42-224	3.3
tel1Δ	2	1.8-2.2	
exo1Δ tel1Δ	95	46-180	6.7
pol32Δ	20	15-26	
exo1Δ pol32Δ	173	94-273	8.6
rev3Δ	13	8-20	
exo1Δ rev3Δ	205	127-304	14.6
msh2Δ	40	n.d.	
msh2Δ pol32Δ	41	25-102	1

(a) GCR rates for *msh2Δ* and *tel1Δ* are from Refs. [77,78].
(b) 95% confidence intervals (CI) were calculated according to Ref. [54]. n.d., not determined.
(c) The increase in the GCR rate of the double mutant was calculated by dividing the GCR rate of the double mutant by the higher GCR rate of the two single mutants.

Table 3.3. Effect of nuclease-dead and phosphosite mutaitons in *EXO1* on the accumulation of gross-chromosomal rearrangements.

Relevant genotype	GCR rate (Can^r 5-FOA^r × 10^{-10})	95% CI^a (Can^r 5-FOA^r × 10^{-10})
Wildtype	1.1	<1-6.2
exo1Δ	14	7–28
exo1-ND	58	12-100
exo1-ND sgs1Δ	69,000	45,000-79,000
exo1Δ sgs1Δ	40,500	31,000-50,000
pol32Δ	20	15-26
exo1-ND pol32Δ	270	110-650
exo1Δ pol32Δ	170	94-270
exo1-SA	23	16-85
exo1-SA sgs1Δ	33	<12-119
exo1-SD sgs1Δ	43	<22-140
exo1-SA pol32Δ	<20	<17-33
exo1-SD pol32Δ	<8	<7-19

(a) 95% confidence intervals (CI) were calculated according to Ref. [54].

TABLE S3.1. *Saccharomyces cerevisiae* strains used in this study

Strain ID	Genotype
KSHY 802	*MATa, ura3-52, leu2Δ1, trp1Δ63, his3Δ200, lys2Bgl, hom3-10, ade2Δ1, ade8, hxt13::URA3*
KHSY 1338	*MATa, ura3-52, trp1Δ63, his3Δ200, leu2Δ1, lys2Bgl, hom3-10, ade2Δ1, ade8, hxt13::URA3, sgs1::TRP1*
KHSY 1954	*MATa, ura3-52, trp1Δ63, his3Δ200, leu2Δ1, lys2Bgl, hom3-10, ade2Δ1, ade8, hxt13::URA3, rev3::TRP1*
KHSY 1957	*MATa, ura3-52, trp1Δ63, his3Δ200, leu2Δ1, lys2Bgl, hom3-10, ade2Δ1, ade8, hxt13::URA3, apn1::TRP1*
KHSY 2311	*MATa, ura3-52, trp1Δ63, his3Δ200, leu2Δ1, lys2Bgl, hom3-10, ade2Δ1, ade8, hxt13::URA3, sgs1::TRP1, tel1::G418*
KHSY 2316	*MATa, ura3-52, trp1Δ63, his3Δ200, leu2Δ1, lys2Bgl, hom3-10, ade2Δ1, ade8, hxt13::URA3, tel1::G418*
KHSY 2333	*MATa, ura3-52, trp1Δ63, his3Δ200, leu2Δ1, lys2Bgl, hom3-10, ade2Δ1, ade8, hxt13::URA3, pol32::loxP-G418-loxP*
KHSY 2338	*MATa, ura3-52, trp1Δ63, his3Δ200, leu2Δ1, lys2Bgl, hom3-10, ade2Δ1, ade8, hxt13::URA3, exo1::loxP-G418-loxP*
KHSY 2402	*MATa, ura3-52, trp1Δ63, his3Δ200, leu2Δ1, lys2Bgl, hom3-10, ade2Δ1, ade8, hxt13::URA3, exo1::loxP-G418-loxP, sgs1::TRP1*
KHSY 2425	*MATa, ura3-52, trp1Δ63, his3Δ200, leu2Δ1, lys2Bgl, hom3-10, ade2Δ1, ade8, hxt13::URA3, rad1::loxP-G418-loxP, sgs1::TRP1*
KHSY 2430	*MATa, ura3-52, trp1Δ63, his3Δ200, leu2Δ1, lys2Bgl, hom3-10, ade2Δ1, ade8, hxt13::URA3, rad1::loxP-G418-loxP*
KHSY 2437	*MATa, ura3-52, trp1Δ63, his3Δ200, leu2Δ1, lys2Bgl, hom3-10, ade2Δ1, ade8, hxt13::URA3, pol32::loxP-G418-loxP, sgs1::TRP1*
KHSY 3782	*MATa, ura3-52, trp1Δ63, his3Δ200, leu2Δ1, lys2Bgl, hom3-10, ade2Δ1, ade8, hxt13::URA3, msh2::TRP1*
KHSY 4394	*MATa, ura3-52, trp1Δ63, his3Δ200, leu2Δ1, lys2Bgl, hom3-10, ade2Δ1, ade8, hxt13::URA3, apn1::TRP1, exo1::loxP-G418-loxP*
KHSY 4398	*MATa, ura3-52, trp1Δ63, his3Δ200, leu2Δ1, lys2Bgl, hom3-10, ade2Δ1, ade8, hxt13::URA3, exo1::loxP-G418-loxP, rad1::loxP-G418-loxP, sgs1::TRP1*
KHSY 4402	*MATa, ura3-52, trp1Δ63, his3Δ200, leu2Δ1, lys2Bgl, hom3-10, ade2Δ1, ade8, hxt13::URA3, exo1::loxP-G418-loxP, rev3::TRP1*
KHSY 4417	*MATa, ura3-52, trp1Δ63, his3Δ200, leu2Δ1, lys2Bgl, hom3-10, ade2Δ1, ade8, hxt13::URA3, apn1::TRP1, exo1::loxP-G418-loxP*
KHSY 4421	*MATa, ura3-52, trp1Δ63, his3Δ200, leu2Δ1, lys2Bgl, hom3-10, ade2Δ1, ade8, hxt13::URA3, exo1::loxP-G418-loxP, rev3::TRP1 sgs1::TRP1*
KHSY 4430	*MATa, ura3-52, trp1Δ63, his3Δ200, leu2Δ1, lys2Bgl, hom3-10, ade2Δ1, ade8, hxt13::URA3, exo1::loxP-G418-loxP, sgs1::TRP1, tel1::G418*
KHSY 4438	*MATa, ura3-52, trp1Δ63, his3Δ200, leu2Δ1, lys2Bgl, hom3-10, ade2Δ1, ade8, hxt13::URA3, exo1-E150D-D173A.HIS3, sgs1::TRP1*
KHSY 4454	*MATa, ura3-52, trp1Δ63, his3Δ200, leu2Δ1, lys2Bgl, hom3-10, ade2Δ1,*

TABLE S3.1. *Saccharomyces cerevisiae* strains used in this study *(continued).*

	ade8, hxt13::URA3, exo1::loxP-G418-loxP, tel1::G418
KHSY 4458	*MATa, ura3-52, trp1Δ63, his3Δ200, leu2Δ1, lys2Bgl, hom3-10, ade2Δ1, ade8, hxt13::URA3, exo1::loxP-G418-loxP, pol32::loxP-G418-loxP*
KHSY 4460	*MATa, ura3-52, trp1Δ63, his3Δ200, leu2Δ1, lys2Bgl, hom3-10, ade2Δ1, ade8, hxt13::URA3, exo1-E150D-D173A.HIS3*
KHSY 4701	*MATa, ura3-52, trp1Δ63, his3Δ200, leu2Δ1, lys2Bgl, hom3-10, ade2Δ1, ade8, hxt13::URA3, exo1-S392A, S567A, S587A, S692A.HIS3*
KHSY 4710	*MATa, ura3-52, trp1Δ63, his3Δ200, leu2Δ1, lys2Bgl, hom3-10, ade2Δ1, ade8, hxt13::URA3 exo1-S392A, S567A, S587A, S692A.HIS3, pol32::loxP-G418-loxP*
KHSY 4803	*MATa, ura3-52, trp1Δ63, his3Δ200, leu2Δ1, lys2Bgl, hom3-10, ade2Δ1, ade8, hxt13::URA3, exo1::loxP-G418-loxP, pol32::loxP-G418-loxP, sgs1::TRP1*
KHSY 4836	*MATa, ura3-52, trp1Δ63, his3Δ200, leu2Δ1, lys2Bgl, hom3-10, ade2Δ1, ade8, hxt13::URA3, exo1-S392A, S567A, S587A, S692A.HIS3, sgs1::TRP1*
KHSY 4839	*MATa, ura3-52, trp1Δ63, his3Δ200, leu2Δ1, lys2Bgl, hom3-10, ade2Δ1, ade8, hxt13::URA3, apn1::TRP1, exo1::loxP-G418-loxP, sgs1::TRP1*
KHSY 4844	*MATa, ura3-52, trp1Δ63, his3Δ200, leu2Δ1, lys2Bgl, hom3-10, ade2Δ1, ade8, hxt13::URA3, exo1::loxP-G418-loxP, rad1::loxP-G418-loxP*
KHSY 4847	*MATa, ura3-52, trp1Δ63, his3Δ200, leu2Δ1, lys2Bgl, hom3-10, ade2Δ1, ade8, hxt13::URA3, exo1-E150D-D173A.HIS3, pol32::loxP-G418-loxP*
KHSY 4852	*MATa, ura3-52, trp1Δ63, his3Δ200, leu2Δ1, lys2Bgl, hom3-10, ade2Δ1, ade8, hxt13::URA3, rev3::TRP1, sgs1::HIS3*
KHSY 4888	*MATa, ura3-52, trp1Δ63, his3Δ200, leu2Δ1, lys2Bgl, hom3-10, ade2Δ1, ade8, hxt13::URA3, msh2::TRP1, pol32::loxP-G418-loxP*
KHSY 4892	*MATa, ura3-52, trp1Δ63, his3Δ200, leu2Δ1, lys2Bgl, hom3-10, ade2Δ1, ade8, hxt13::URA3, exo1-S392A, S567A, S587A, S692A.HIS3, sgs1::TRP1*
KHSY 4896	*MATa, ura3-52, trp1Δ63, his3Δ200, leu2Δ1, lys2Bgl, hom3-10, ade2Δ1, ade8, hxt13::URA3, exo1-S392A, S567A, S587A, S692A.HIS3*
KHSY 4897	*MATa, ura3-52, trp1Δ63, his3Δ200, leu2Δ1, lys2Bgl, hom3-10, ade2Δ1, ade8, hxt13::URA3 exo1-S392A, S567A, S587A, S692A.HIS3, pol32::loxP-G418-loxP*
KHSY 4963	*MATa, ura3-52, trp1Δ63, his3Δ200, leu2Δ1, lys2Bgl, hom3-10, ade2Δ1, ade8, hxt13::URA3, exo1-S392A, S567A, S587A, S692A.HIS3, sgs1::TRP1, tel1::G418*
KHSY 4968	*MATa, ura3-52, trp1Δ63, his3Δ200, leu2Δ1, lys2Bgl, hom3-10, ade2Δ1, ade8, hxt13::URA3, exo1-S392A, S567A, S587A, S692A.HIS3, sgs1::TRP1, tel1::G418*
KHSY 4969	*MATa, ura3-52, trp1Δ63, his3Δ200, leu2Δ1, lys2Bgl, hom3-10, ade2Δ1, ade8, hxt13::URA3, exo1-E150D-D173A-S392D-S567D-S587D-S692D.HIS3*

130

TABLE S3.1. *Saccharomyces cerevisiae* strains used in this study *(continued)*.

KHSY 4986	*MATa, ura3-52, trp1Δ63, his3Δ200, leu2Δ1, lys2Bgl, hom3-10, ade2Δ1, ade8, hxt13::URA3, exo1-S392A, S567A, S587A, S692A.HIS3, rev3::TRP1, sgs1::HIS3*
KHSY 4987	*MATa, ura3-52, trp1Δ63, his3Δ200, leu2Δ1, lys2Bgl, hom3-10, ade2Δ1, ade8, hxt13::URA3, exo1-S392A, S567A, S587A, S692A.HIS3, rev3::TRP1, sgs1::HIS3*
KHSY 4989	*MATa, ura3-52, trp1Δ63, his3Δ200, leu2Δ1, lys2Bgl, hom3-10, ade2Δ1, ade8, hxt13::URA3, exo1-E150D-D173A-S392D-S567D-S587D-S692D.HIS3*
KHSY 4993	*MATa, ura3-52, trp1Δ63, his3Δ200, leu2Δ1, lys2Bgl, hom3-10, ade2Δ1, ade8, hxt13::URA3, exo1-E150D-D173A-S392D-S567D-S587D-S692D.HIS3, HIS3, pol32::loxP-G418-loxP*
KHSY 5004	*MATa, ura3-52, trp1Δ63, his3Δ200, leu2Δ1, lys2Bgl, hom3-10, ade2Δ1, ade8, hxt13::URA3, exo1-S392D-S567D-S587D- S692D.HIS3, msh2::TRP1, pol32::loxP-G418-loxP*
KHSY 5008	*MATalpha, ura3-52, trp1Δ63, his3Δ200, leu2Δ1, lys2Bgl, hom3-10, ade2Δ1, ade8, hxt13::URA3, exo1-S392A, S567A, S587A, S692A.HIS3, msh2::TRP1, pol32::loxP-G418-loxP*
KHSY 5014	*MATa, ura3-52, trp1Δ63, his3Δ200, leu2Δ1, lys2Bgl, hom3-10, ade2Δ1, ade8, hxt13::URA3, exo1-E150D-D173A-S392D-S567D-S587D-S692D.HIS3, pol32::loxP-G418-loxP*
KHSY 5037	*MATa, ura3-52, trp1Δ63, his3Δ200, leu2Δ1, lys2Bgl, hom3-10, ade2Δ1, ade8, hxt13::URA3, exo1::loxP-G418-loxP, msh2::TRP1, pol32::loxP-G418-loxP*
KHSY 5043	*MATa, ura3-52, trp1Δ63, his3Δ200, leu2Δ1, lys2Bgl, hom3-10, ade2Δ1, ade8, hxt13::URA3, exo1::loxP-G418-loxP, pol32::loxP-G418-loxP, rev3::TRP1*
KHSY 5044	*MATa, ura3-52, trp1Δ63, his3Δ200, leu2Δ1, lys2Bgl, hom3-10, ade2Δ1, ade8, hxt13::URA3, pol32::loxP-G418-loxP, rev3::TRP1*

TABLE S3.2. *SGS1*-dependent suppression of gross-chromosomal rearrangements.

Relevant Genotype	GCR Rate[i] (Can^r 5-FOA^r x 10^{-10})	95% CI[ll] (Can^r 5-FOA^r x 10^{-10})
wildtype	1.1	< 1 – 6.2
sgs1Δ	89	57-177
tel1Δ	2	1.8–2.2
sgs1Δ tel1Δ	227	46-418
rev3Δ	13	8-20
sgs1Δ rev3Δ	195	75-279
pol32Δ	20	15-26
sgs1Δ pol32Δ	25	<24-105
rad1Δ	10	< 9-23
sgs1Δ rad1Δ	63	25-356
apn1Δ	19	14-41
sgs1Δ apn1Δ	141	72-362

(i) GCR rate for *tel1Δ* is from reference [75].
(ii) 95% confidence intervals (CI) were calculated according to reference [51].

Table S3.3. Spontaneous *CAN1* mutations identified in *exo1Δ, pol32Δ* and *exo1Δ pol32Δ* mutants.

Genotype	Mutation type[a]	Mutation	Frequency (%)
wildtype	base substitution	C→T	17/20 (85)
		A→T	
		G→T	
		T→C	
		G→A	
		C→G	
		T→G	
		A→C	
		G→C	
		C→A	
	≤ 3 bp insertion/deletion	$T_3 \rightarrow T_2$	1/20 (5)
	> 3 bp insertion/deletion	148 bp deletion	1/20 (5)
	complex	24 bp del/ 2 bp ins	1/20 (5)
exo1Δ	base substitution	A → T	14/19 (73.7)
		G → C	
		C → A	
		T → G	
		T→C	
		G→T	
		C→A	
		G→C	
		A→T	
		C→G	
		C→T	
	≤ 3 bp insertion/deletion	GCT → GT	3/19 (15.8)
		$T_2 \rightarrow T_3$	
	> 3 bp insertion/deletion	53 bp deletion	1/19 (5.3)
	complex	233 bp del/36 bp ins	1/19 (5.3)
pol32Δ	Base substitution	G→C	7/19 (36.8)
		C→G	
		G→A	
		G→T	
		T→A	
		A→C	
	≤ 3 bp insertion/deletion	ATG →AG	2/19 (5.3)
		$T_4 \rightarrow T_2$	
	> 3 bp insertion/deletion	8 bp deletion	10/19 (52.6)
		18 bp deletion	
		22 bp deletion	
		24 bp deletion	
		31 bp deletion	
		36 bp deletion	
		38 bp deletion	
		41 bp deletion	
		72 bp deletion	
		32 bp insertion	
	complex		0/19 (0)

Table S3.3. Spontaneous *CAN1* mutations identified in *exo1Δ*, *pol32Δ* and *exo1Δ pol32Δ* mutants (*continued*).

Genotype	Mutation type	Mutation	Frequency (%)
exo1Δ pol32Δ	base substitution	G → A	6/20 (30)
		T → C	
		T → G	
		C→A	
	≤ 3 bp insertion/deletion	$A_6 → A_5$	8/20 (40)
		$T_3 → T_2$	
		$T_4 → T_3$	
		$T_6 → T_5$	
		$G_4 → G_3$	
		$T_6 → T_7$	
		2 bp insertion (TC)	
	> 3 bp insertion/deletion	8 bp deletion	4/20 (20)
		26 bp deletion	
		94 bp deletion	
		586 bp deletion	
	complex	8 bp del/5 bp ins	2/20 (10)
		27 bp del/3 bp ins	

(a) The *CAN1* open reading frame was amplified by PCR from independent canavanine-resistant colonies and sequenced. The identified mutations were divided into four groups: base substitutions, insertions/deletions ≤ 3 bp), insertions/deletions (> 3 bp), and complex mutations. Complex mutations were deletions (8-233 bp) that contained a small insertion (2-36 bp).

References

[1] D.X. Tishkoff, A.L. Boerger, P. Bertrand, N. Filosi, G.M. Gaida, M.F. Kane, R.D. Kolodner, Identification and characterization of *Saccharomyces cerevisiae* EXO1, a gene encoding an exonuclease that interacts with MSH2, Proc. Natl. Acad. Sci. U. S. A. 94 (1997) 7487–7492.

[2] P.T. Tran, N. Erdeniz, S. Dudley, R.M. Liskay, Characterization of nuclease-dependent functions of Exo1p in *Saccharomyces cerevisiae*, DNA Repair 1 (2002) 895–912.

[3] P. Fiorentini, K.N. Huang, D.X. Tishkoff, R.D. Kolodner, L.S. Symington, Exonuclease I of *Saccharomyces cerevisiae* functions in mitotic recombination in vivo and in vitro, Mol. Cell. Biol. 17 (1997) 2764–2773.

[4] C. Rudolph, O. Fleck, J. Kohli, *Schizosaccharomyces pombe* exo1 is involved in the same mismatch repair pathway as msh2 and pms1, Curr. Genet. 34 (1998) 343–350.

[5] C. Schmutte, M.M. Sadoff, K.S. Shim, S. Acharya, R. Fishel, The interaction of DNA mismatch repair proteins with human exonuclease I, J. Biol. Chem. 276 (2001) 33011–33018.

[6] T. Sokolsky, E. Alani, EXO1 and MSH6 are high-copy suppressors of conditional mutations in the MSH2 mismatch repair gene of *Saccharomyces cerevisiae*, Genetics 155 (2000) 589–599.

[7] P. Szankasi, G.R. Smith, A role for exonuclease I from S. pombe in mutation avoidance and mismatch correction, Science 267 (1995) 1166–1169.

[8] P.T. Tran, J.P. Fey, N. Erdeniz, L. Gellon, S. Boiteux, R.M. Liskay, A mutation in EXO1 defines separable roles in DNA mismatch repair and post-replication repair, DNA Repair 6 (2007) 1572–1583.

[9] K. Wei, A.B. Clark, E. Wong, M.F. Kane, D.J. Mazur, T. Parris, N.K. Kolas, R. Russell, H. Hou, B. Kneitz Jr., G. Yang, T.A. Kunkel, R.D. Kolodner, P.E. Cohen, W. Edelmann, Inactivation of exonuclease 1 in mice results in DNA mismatch repair defects, increased cancer susceptibility, and male and female sterility, Genes Dev. 17 (2003) 603–614.

[10] Y. Wu, M.J. Berends, J.G. Post, R.G. Mensink, E. Verlind, T. Van Der Sluis, C. Kempinga, R.H. Sijmons, A.G. van der Zee, H. Hollema, J.H. Kleibeuker, C.H. Buys, R.M. Hofstra, Germline mutations of EXO1 gene in patients with hereditary nonpolyposis colorectal cancer (HNPCC) and atypical HNPCC forms, Gastroenterology 120 (2001) 1580–1587.

[11] N.A. Alam, P. Gorman, E.E. Jaeger, D. Kelsell, I.M. Leigh, R. Ratnavel, M.E. Murdoch, R.S. Houlston, L.A. Aaltonen, R.R. Roylance, I.P. Tomlinson, Germline deletions of EXO1 do not cause colorectal tumors and lesions which are null for EXO1 do not have microsatellite instability, Cancer Genet. Cytogenet. 147 (2003) 121–127.

[12] S. Jagmohan-Changur, T. Poikonen, S. Vilkki, V. Launonen, F. Wikman, T.F. Orntoft, P. Moller, H. Vasen, C. Tops, R.D. Kolodner, J.P. Mecklin, H. Jarvinen, S. Bevan, R.S. Houlston, L.A. Aaltonen, R. Fodde, J. Wijnen, A. Karhu, EXO1 variants occur commonly in normal population: evidence against a role in hereditary nonpolyposis colorectal cancer, Cancer Res. 63 (2003) 154–158.

[13] E. Thompson, C.J. Meldrum, R. Crooks, M. McPhillips, L. Thomas, A.D. Spigelman, R.J. Scott, Hereditary non-polyposis colorectal cancer and the role of hPMS2 and hEXO1 mutations, Clin. Genet. 65 (2004) 215–225.

[14] X. Sun, L. Zheng, B. Shen, Functional alterations of human exonuclease 1 mutants identified in atypical hereditary nonpolyposis colorectal cancer syndrome, Cancer Res. 62 (2002) 6026–6030.

[15] P.D. Bardwell, C.J. Woo, K. Wei, Z. Li, A. Martin, S.Z. Sack, T. Parris, W. Edelmann, M.D. Scharff, Altered somatic hypermutation and reduced class-switch recombination in exonuclease 1-mutant mice, Nat. Immunol. 5 (2004) 224–229.

[16] B.O. Krogh, L.S. Symington, Recombination proteins in yeast, Annu. Rev. Genet. 38 (2004) 233–271.

[17] Z. Zhu, W.H. Chung, E.Y. Shim, S.E. Lee, G. Ira, Sgs1 helicase and two nucleases Dna2 and Exo1 resect DNA double-strand break ends, Cell 134 (2008) 981–994.

[18] E.P. Mimitou, L.S. Symington, Sae2, Exo1 and Sgs1 collaborate in DNA double-strand break processing, Nature 455 (2008) 770–774.

[19] L.K. Lewis, G. Karthikeyan, J.W. Westmoreland, M.A. Resnick, Differential suppression of DNA repair deficiencies of Yeast rad50, mre11 and xrs2 mutants by EXO1 and TLC1 (the RNA component of telomerase), Genetics 160 (2002) 49–62.

[20] L. Doerfler, L. Harris, E. Viebranz, K.H. Schmidt, Differential genetic interactions between Sgs1, DNA-damage checkpoint components and DNA repair factors in the maintenance of chromosome stability, Genome Integr. 2 (2011) 8.

[21] S. Gravel, J.R. Chapman, C. Magill, S.P. Jackson, DNA helicases Sgs1 and BLM promote DNA double-strand break resection, Genes Dev. 22 (2008) 2767–2772.

[22] J.R. Lydeard, Z. Lipkin-Moore, S. Jain, V.V. Eapen, J.E. Haber, Sgs1 and exo1 redundantly inhibit break-induced replication and de novo telomere addition at broken chromosome ends, PLoS Genet. 6 (2010) e1000973.

[23] V.A.Marrero,L.S.Symington,D.N.A.Extensive,endprocessingbyexo1andsgs1 inhibits break-induced replication, PLoS Genet. 6 (2010) e1001007.

[24] G.I.Karras,M.Fumasoni,G.Sienski,F.Vanoli,D.Branzei,S.Jentsch,Noncanonical role of the 9-1-1 clamp in the error-free DNA damage tolerance pathway, Mol. Cell 49 (2013) 536–546.

[25] F. Vanoli, M. Fumasoni, B. Szakal, L. Maloisel, D. Branzei, Replication and recombination factors contributing to recombination-dependent bypass of DNA lesions by template switch, PLoS Genet. 6 (2010) e1001205.

[26] C. Cotta-Ramusino, D. Fachinetti, C. Lucca, Y. Doksani, M. Lopes, J. Sogo, M. Foiani, Exo1 processes stalled replication forks and counteracts fork reversal in checkpoint-defective cells, Mol. Cell 17 (2005) 153–159.

[27] G.I. Karras, S. Jentsch, The RAD6 DNA damage tolerance pathway operates uncoupled from the replication fork and is functional beyond S phase, Cell 141 (2010) 255–267.

[28] E. Johansson, P. Garg, P.M. Burgers, ThePol32subunitofDNApolymerasedelta contains separable domains for processive replication and proliferating cell nuclear antigen (PCNA) binding, J. Biol. Chem. 279 (2004) 1907–1915.

[29] A.G. Baranovskiy, A.G. Lada, H.M. Siebler, Y. Zhang, Y.I. Pavlov, T.H. Tahirov, DNA polymerase delta and zeta switch by sharing accessory subunits of DNA polymerase delta, J. Biol. Chem. 287 (2012) 17281–17287.

[30] A.V. Makarova, J.L. Stodola, P.M. Burgers, A four-subunit DNA polymerase zeta complex containing Pol delta accessory subunits is essential for PCNA-mediated mutagenesis, Nucleic Acids Res. 40 (2012) 11618–11626.

[31] H.M. Siebler, A.G. Lada, A.G. Baranovskiy, T.H. Tahirov, Y.I. Pavlov, A novel variant of DNA polymerase zeta, Rev3DeltaC, highlights differential regulation of Pol32 as a subunit of polymerase delta versus zeta in *Saccharomyces cerevisiae*, DNA Repair (2014).

[32] P.E. Gibbs, W.G. McGregor, V.M. Maher, P. Nisson, C.W. Lawrence, A human homolog of the *Saccharomyces cerevisiae* REV3 gene, which encodes the catalytic subunit of DNA polymerase zeta, Proc. Natl. Acad. Sci. U. S. A. 95 (1998) 6876–6880.

[33] C.W. Lawrence, V.M. Maher, Eukaryotic mutagenesis and translesion replication dependent on DNA polymerase zeta and Rev1 protein, Biochem. Soc. Trans. 29 (2001) 187–191.

[34] A. Morrison, R.B. Christensen, J. Alley, A.K. Beck, E.G. Bernstine, J.F. Lemontt, C.W. Lawrence, REV3, a *Saccharomyces cerevisiae* gene whose function is required for induced mutagenesis, is predicted to encode a nonessential DNA polymerase, J. Bacteriol. 171 (1989) 5659–5667.

[35] M.E. Huang, E. Cadieu, J.L. Souciet, F. Galibert, Disruption of six novel yeast genes reveals three genes essential for vegetative growth and one required for growth at low temperature, Yeast 13 (1997) 1181–1194.

[36] S.H. Chen, C.P. Albuquerque, J. Liang, R.T. Suhandynata, H. Zhou, A proteome-wide analysis of kinase-substrate network in the DNA damage response, J. Biol. Chem. 285 (2010) 12803–12812.

[37] J.C. Randell, A. Fan, C. Chan, L.I. Francis, R.C. Heller, K. Galani, S.P. Bell, Mec1 is one of multiple kinases that prime the Mcm2-7 helicase for phosphorylation by Cdc7, Mol. Cell 40 (2010) 353–363.

[38] M.B. Smolka, C.P. Albuquerque, S.H. Chen, H. Zhou, Proteome-wide identification of in vivo targets of DNA damage checkpoint kinases, Proc. Natl. Acad. Sci. U. S. A. 104 (2007) 10364–10369.

[39] J.A. Cobb, L. Bjergbaek, K. Shimada, C. Frei, S.M. Gasser, DNA polymerase stabilization at stalled replication forks requires Mec1 and the RecQ helicase Sgs1, EMBO J. 22 (2003) 4325–4336.

[40] J.A. Cobb, T. Schleker, V. Rojas, L. Bjergbaek, J.A. Tercero, S.M. Gasser, Replisome instability, fork collapse, and gross chromosomal rearrangements arise synergistically from Mec1 kinase and RecQ helicase mutations, Genes Dev. 19 (2005) 3055–3069.

[41] C. Lucca, F. Vanoli, C. Cotta-Ramusino, A. Pellicioli, G. Liberi, J. Haber, M. Foiani, Checkpoint-mediated control of replisome-fork association and signalling in response to replication pausing, Oncogene 23 (2004) 1206–1213.

[42] P. McGlynn, R.G. Lloyd, Recombinational repair and restart of damaged replication forks, Nat. Rev. Mol. Cell Biol. 3 (2002) 859–870.

[43] M. Segurado, J.F. Diffley, Separate roles for the DNA damage checkpoint protein kinases in stabilizing DNA replication forks, Genes Dev. 22 (2008) 1816–1827.

[44] G. De Piccoli, Y. Katou, T. Itoh, R. Nakato, K. Shirahige, K. Labib, Replisome stability at defective DNA replication forks is independent of S phase checkpoint kinases, Mol. Cell 45 (2012) 696–704.

[45] K. Labib, G. De Piccoli, Surviving chromosome replication: the many roles of the S-phase checkpoint pathway, Philos. Trans. R. Soc. Lond. B: Biol. Sci. 366 (2011) 3554–3561.

[46] K. Engels, M. Giannattasio, M. Muzi-Falconi, M. Lopes, S. Ferrari, 14-3-3 Proteins regulate exonuclease 1-dependent processing of stalled replication forks, PLoS Genet. 7 (2011) e1001367.

[47] I. Morin, H.P. Ngo, A. Greenall, M.K. Zubko, N. Morrice, D. Lydall, Checkpoint-dependent phosphorylation of Exo1 modulates the DNA damage response, EMBO J. 27 (2008) 2400–2410.

[48] X. Jia, T. Weinert, D. Lydall, Mec1 and Rad53 inhibit formation of single-stranded DNA at telomeres of *Saccharomyces cerevisiae* cdc13-1 mutants, Genetics 166 (2004) 753–764.

[49] R.D. Gietz, R.A. Woods, Transformation of yeast by lithium acetate/single-stranded carrier DNA/polyethylene glycol method, Methods Enzymol. 350 (2002) 87–96.

[50] B. Rockmill, E.J. Lambie, G.S. Roeder, Spore enrichment, Methods Enzymol. 194 (1991) 146–149.

[51] F. Fang, K. Salmon, M.W.Y. Shen, K.A. Aeling, E. Ito, B. Irwin, U.P.C. Tran, G.W. Hatfield, N.A. Da Silva, S. Sandmeyer, A vector set for systematic metabolic engineering in *Saccharomyces cerevisiae*, Yeast (Chichester, England) 28 (2011) 123–136.

[52] K.H. Schmidt, V. Pennaneach, C.D. Putnam, R.D. Kolodner, Analysis of gross chromosomal rearrangements in *Saccharomyces cerevisiae*, in: L.C. Judith, M. Paul (Eds.), Methods in Enzymology, Academic Press, 2006, pp. 462–476.

[53] D.E. Lea, C.A. Coulson, The distribution of the numbers of mutants in bacterial populations, J. Genet. 49 (1949) 264–285.

[54] K. Nair, Table of confidence intervals for the median in samples from any con tinous population, Sankhya (1940) 551–558.

[55] K.H. Schmidt, V. Pennaneach, C.D. Putnam, R.D. Kolodner, Analysis of gross-chromosomal rearrangements in *Saccharomyces cerevisiae*, Methods Enzymol. 409 (2006) 462–476.

[56] R.A. Reenan, R.D. Kolodner, Characterization of insertion mutations in the *Saccharomyces cerevisiae* MSH1 and MSH2 genes: evidence for separate mitochondrial and nuclear functions, Genetics 132 (1992) 975–985.

[57] A. Motegi, K. Myung, Measuring the rate of gross chromosomal rearrangements in *Saccharomyces cerevisiae*: a practical approach to study genomic rearrangements observed in cancer, Methods 41 (2007) 168–176.

[58] P.T. Tran, J.A. Simon, R.M. Liskay, Interactions of Exo1p with components of MutLalpha in *Saccharomyces cerevisiae*, Proc. Natl. Acad. Sci. U. S. A. 98 (2001) 9760–9765.

[59] H. Flores-Rozas, D. Clark, R.D. Kolodner, Proliferating cell nuclear antigen and Msh2p-Msh6p interact to form an active mispair recognition complex, Nat. Genet. 26 (2000) 375–378.

[60] H.E. Kleczkowska, G. Marra, T. Lettieri, J. Jiricny, hMSH3 and hMSH6 interact with PCNA and colocalize with it to replication foci, Genes Dev. 15 (2001) 724–736.

[61] Y.I. Pavlov, I.M. Mian, T.A. Kunkel, Evidence for preferential mismatch repair of lagging strand DNA replication errors in yeast, Curr. Biol. 13 (2003) 744–748.

[62] S.E. Liberti, A.A. Larrea, T.A. Kunkel, Exonuclease 1 preferentially repairs mismatches generated by DNA polymerase alpha, DNA Repair 12 (2013) 92–96

[63] F.A. Kadyrov, S.F. Holmes, M.E. Arana, O.A. Lukianova, M. O'Donnell, T.A. Kunkel, P. Modrich, *Saccharomyces cerevisiae* MutLalpha is a mismatch repair endonuclease, J. Biol. Chem. 282 (2007) 37181–37190.

[64] N.S. Amin, M.N. Nguyen, S. Oh, R.D. Kolodner, exo1-Dependent mutator mutations: model system for studying functional interactions in mismatch repair, Mol. Cell. Biol. 21 (2001) 5142–5155.

[65] A. Blastyak, L. Pinter, I. Unk, L. Prakash, S. Prakash, L. Haracska, Yeast Rad5 protein required for postreplication repair has a DNA helicase activity specific for replication fork regression, Mol. Cell 28 (2007) 167–175.

[66] B. Michel, M.J. Flores, E. Viguera, G. Grompone, M. Seigneur, V. Bidnenko, Rescue of arrested replication forks by homologous recombination, Proc. Natl. Acad. Sci. U. S. A. 98 (2001) 8181–8188.

[67] D. Branzei, M. Foiani, The checkpoint response to replication stress, DNA Repair 8 (2009) 1038–1046.

[68] L.J. Reha-Krantz, M.S. Siddique, K. Murphy, A. Tam, M. O'Carroll, S. Lou, A. Schultz, C. Boone, Drug-sensitive DNA polymerase delta reveals a role for mismatch repair in checkpoint activation in yeast, Genetics 189 (2011) 1211–1224.

[69] M. Giannattasio, C. Follonier, H. Tourriere, F. Puddu, F. Lazzaro, P. Pasero, M. Lopes, P. Plevani, M. Muzi-Falconi, Exo1 competes with repair synthesis, converts NER intermediates to long ssDNA gaps, and promotes checkpoint activation, Mol. Cell 40 (2010) 50–62.

[70] M. Uhart, D.M. Bustos, Protein intrinsic disorder and network connectivity. The case of 14-3-3 proteins, Front Genet. 5 (2014) 10.

[71] G. Frank, J. Qiu, L. Zheng, B. Shen, Stimulation of eukaryotic flap endonuclease-1 activities by proliferating cell nuclear antigen (PCNA) is independent of its in vitro interaction via a consensus PCNA binding region, J. Biol. Chem. 276 (2001) 36295–36302.

[72] X.V. Gomes, P.M. Burgers, Two modes of FEN1 binding to PCNA regulated by DNA, EMBO J. 19 (2000) 3811–3821.

[73] Z.O. Jonsson, R. Hindges, U. Hubscher, Regulation of DNA replication and repair proteins through interaction with the front side of proliferating cell nuclear antigen, EMBO J. 17 (1998) 2412–2425.

[74] L. Maringele, D. Lydall, EXO1-dependent single-stranded DNA at telomeres acti-vates subsets of DNA damage and spindle checkpoint pathways in budding yeast yku70Delta mutants, Genes Dev. 16 (2002) 1919–1933.

[75] M.K. Zubko, S. Guillard, D. Lydall, Exo1, Rad24 differentially regulate generation of ssDNA at telomeres of *Saccharomyces cerevisiae* cdc13-1 mutants, Genetics 168 (2004) 103–115.

[76] J.M. Dewar, D. Lydall, Similarities and differences between uncapped telomeres and DNA double-strand breaks, Chromosoma 121 (2012) 117–130.

[77] K. Myung, A. Datta, C. Chen, R.D. Kolodner, SGS1, the *Saccharomyces cerevisiae* homologue of BLM and WRN, suppresses genome instability and homeologous recombination, Nat. Genet. 27 (2001) 113–116.

[78] K. Myung, A. Datta, R.D. Kolodner, Suppression of spontaneous chromosomal rearrangements by S phase checkpoint functions in *Saccharomyces cerevisiae*, Cell 104 (2001) 397–408.

Chapter Four :

Sgs1 binding to Rad51 stimulates homology-dependent DNA repair in
Saccharomyces cerevisiae

Note to the reader: This chapter has been submitted for publication in the journal

Genetics. The research was designed by K. Schmidt with contributions from Lillian

Campos-Doerfler. All genetic analysis was performed by Lillian Doerfler, and

biochemical analysis was conducted by Salahuddin Syed. Corresponding author:

Kristina Schmidt, Department of Cell Biology, Microbiology and Molecular Biology,

University of South Florida, 4202 E. Fowler Avenue, ISA2015, Tampa, FL 33620.

Phone: (813) 974-1592. Fax: (813) 974- 1614; E-mail: kschmidt@usf.edu

ABSTRACT

Accurate repair of DNA breaks is essential for maintaining genome integrity and

cellular fitness. Sgs1, the sole member of the RecQ family of DNA helicases in

Saccharomyces cerevisiae, plays important roles in both early and late stages of

homology-dependent repair of DNA lesions. Its large number of physical and genetic

interactions with cellular factors that play roles in DNA recombination, repair and

replication have established Sgs1 as a key player in the maintenance of genome

integrity. To determine the significance of Sgs1 binding to the strand exchange factor

Rad51 we have identified a single amino acid change in an unstructured linker C-

terminal of the helicase core of Sgs1 that disrupts Rad51 binding. In contrast to an

SGS1 deletion or a helicase-defective *sgs1* allele, this new separation-of-function allele,

sgs1-FD, does not cause DNA damage hypersensitivity or genome instability but

exhibits negative and positive genetic interactions with *sae2Δ, mre11Δ, exo1Δ, srs2Δ,*

rrm3Δ, and *pol32Δ* that are distinct from those of known sgs1 mutants. Our findings

suggest a role for the Sgs1-Rad51 interaction in stimulating homologous recombination

(HR). However, unlike sgs1 mutations that impair the resection of DNA double-strand

ends, negative genetic interactions of the *sgs1-FD* allele are not suppressed by *YKU70*

deletion. We, therefore, propose that the Sgs1-Rad51 interaction stimulates HR by

facilitating the formation of the presynaptic Rad51filament, possibly by Sgs1 competing

with replication protein A for single-strand DNA binding during resection.

INTRODUCTION

DNA double-strand breaks (DSBs) can be induced exogenously by DNA

damaging agents or form endogenously if the replisome collapses at a break in the

template strand or encounters a physical barrier that blocks progression of the

replisome, such as a bound protein, DNA adduct, interstrand crosslink, or unusual DNA

structure. Cells can repair such DSBs by homologous recombination (HR) or non-

homologous end-joining (NHEJ). In the event of a DSB, the NHEJ proteins Ku70/Ku80

(Ku) and HR proteins Mre11-Rad50-Xrs2 (MRX) initiate the repair process by binding to

the DSB ends [1]. NHEJ is preferred in G1 as there is no sister chromatid whereas HR

is preferred during S phase and G2 [2-4]. In S phase, Ku and MRX bind to the DSB first

and recruitment of Sae2 activates short range resection, removing Ku and MRX and

leaving a small 3' single-stranded DNA (ssDNA) overhang [1, 5-9]. These trimmed DNA

ends are then more extensively resected by the 5'- 3' exonuclease Exo1 or by Dna2

nuclease, which works with the 3'- 5' helicase Sgs1 [9-11]. Rad52, an essential HR factor in budding yeast, then allows a recombinogenic Rad51 filament to assemble on the replication protein A (RPA) coated 3'-overhang [12, 13]. Regulation of HR at this stage relies on the antirecombinase Srs2, which can disassemble Rad51 filaments [14-16]. If Rad51-mediated homology search is successful, the 3' end of the invading strand is used as a priming site for DNA synthesis and thus extended. In classic DSB repair (DSBR) the second end of the DNA break is also captured to form a double-Holliday Junction (dHJ), which can either be resolved by endonucleases Mus81/Mms4 or Yen1 to produce both crossovers and noncrossovers, or the HJs are converged and decatenated by the Sgs1/Top3/Rmi1 complex, resulting in only noncrossovers [17-19]. Homology-directed repair of DSBs in mitotic cells often occurs in ways other than by DSBR, such as synthesis-dependent strand annealing (SDSA), single-strand annealing (SSA) and break-induced replication (BIR) [20-22]. In SDSA the invading strand is extended by DNA synthesis, but then displaced before capture and annealed to complementary sequences on the other side of the DSB; since this process does not lead to the formation of HJs, it always results in noncrossover products [23]. In contrast to DSBR and SDSA, SSA and BIR are error-prone. SSA occurs when regions of sequence homology are recognized during resection, annealed and then ligated, resulting in the loss of the DNA sequence between the repeats [24, 25]. BIR is used for homology-directed repair of one-ended DSBs, such as those that arise when a replication fork collapses at a nick in the template strand or when a stalled replication fork is cut [26-30].

Resection of the DSB ends is essential for all HR. After initial trimming by MRX/Sae2, long-range resection by Sgs1/Dna2 and Exo1 is redundant, with loss of both activities resulting in a severe resection defect and mutagenic repair [9, 10, 31]. Exo1 and Dna2 differ in that Exo1 can degrade the 5' strand in double-strand DNA (dsDNA) whereas Dna2 requires the Sgs1 helicase to unwind the dsDNA to provide ssDNA on which Dna2 can act [11, 32]. In a yeast-two-hybrid assay, Sgs1 was found to interact with Mre11, and it has been proposed that this helps to recruit Sgs1/Dna2 to the DSB after initial resection [33, 34]. Sgs1 is a member of the highly conserved family of RecQ-like DNA helicases, which interact with a large number of proteins with functions in genome maintenance. Sgs1 not only interacts with Dna2, Mre11, Top3/Rmi1 but also contains acidic regions in its long unstructured N-terminal tail that are required for binding the ssDNA binding protein RPA [35-39]. Rad53 kinase, Top2 topoisomerase and the nucleotide excision repair factor Rad16 have also been shown to physically interact with the N-terminal tail of Sgs1, whereas Rad51 and Mlh1 binding has been narrowed down to the region C-terminal of the helicase core [38, 40-44].

Lack of Sgs1 results in increased sensitivity to DNA damaging agents, shortened lifespan, missegregated chromosomes, and moderate accumulation of gross-chromosomal rearrangements (GCRs), including characteristic recurrent translocations between short homologous, but non-allelic, sequences [29, 45-48]. Cells lacking Sgs1 exhibit growth defects or die in the absence of structure-specific endonucleases Mus81/Mms4 and Slx1/4 that resolve recombination intermediates and stalled replication forks, the HR factors MRX or Sae2, the antirecombinase Srs2, or the Rrm3 helicase, which regulates replisome progression [45, 49-54].

149

This multitude of physical and genetic interactions has established Sgs1 as a key player in the maintenance of genome integrity. The molecular basis and functional significance of some of the physical interactions for HR are increasingly well understood, especially the interaction of Sgs1 with Top3/Rmi1 in dHJ dissolution, with Dna2 in DSB resection, and with mismatch repair factors in the suppression of mitotic and meiotic homeologous recombination [11, 39, 46, 55-57]. Here, to understand the role of the physical interaction of Sgs1 with Rad51 in homology-dependent DNA repair, we set out to identify a separation-of-function allele of SGS1 that disrupts Sgs1-Rad51 binding and to characterize the genetic interactions of this sgs1 allele in cells with replication-dependent DNA lesions.

Materials and Methods

Yeast Strains and Media

Yeast strains were derived from S288C strain KHSY802 (*MATa, ura3-52, trp1Δ63, his3Δ200, leu2Δ1, lys2Bgl, hom3-10, ade2Δ1, ade8, hxt13:: URA3*). *SGS1* mutant alleles for amino acid changes K706A (*sgs1-HD*, pKHS787) and F1192D (*sgs1-FD*, pKHS786) were generated by site-directed mutagenesis (QuikChange, Stratagene) of wildtype *SGS1* in pKHS360 (pRS405-*SGS1.TRP1*) and integrated into the chromosome under control of the endogenous SGS1 promoter by LiAc-mediated transformation as described [58]. Haploid strains with multiple mutant alleles were obtained by sporulating diploids heterozygous for the desired mutations and genotyping spores on selective media or PCR. All yeast strains used in this study are listed in Supplementary Table S1. Yeast were grown at 30° in yeast extract, peptone, and

150

dextrose (YPD) or synthetic complete (SC) media as previously described [59]. Solid media was supplemented with 20 g/l agar (US Biological).

DNA-damage sensitivity assays

Sensitivity of yeast cells in exponential growth phase to HU and MMS was tested by spot assays as previously described [60]. Briefly, cell cultures were grown in liquid YPD medium OD600=0.5 and ten-fold serial dilutions were spotted on YPD containing the indicated concentration of HU (US Biological) or MMS (Sigma-Aldrich). Images of colony growth were acquired every 24 hours for five days of incubation at 30° with a GelCam 315 CCD camera mounted on a Gel-Doc IT Imaging system (UVP) and VisionWorks software.

Gross-Chromosomal Rearrangement (GCR) Assay

Cells with GCRs were identified by simultaneous inactivation of *CAN1* and *URA3* on chromosome V indicated by resistance to canavanine and 5-fluoro-orotic acid (Can^r 5-FOA^r). Cultures were grown for two days in at least 10 ml of YPD media. Viable cell counts were determined by plating dilutions on YPD agar plates, and cells with GCRs were identified by plating 0.25 ml-15 ml on synthetic media lacking arginine and uracil and supplemented with 60 mg/l canavanine (Sigma) and 1 g/l 5-fluoro-orotic acid (US Biological). The rate of accumulating GCRs was calculated as previously described [61].

Mutator Assays and Mutation Spectrum Analysis

Rates of accumulating mutations at the *CAN1* locus or reversion mutations in the *hom3-10* or *lys2-BgI* alleles were determined by fluctuation analysis by the method of the median [62] in at least fourteen cultures from at least two different isolates as previously described [63]. Cultures were grown overnight in 3 - 6 ml of YPD media. Viable cell counts were determined by plating dilutions on YPD agar plates and 250 µl - 6 ml were plated on synthetic media lacking arginine and supplemented with 60 µg/ml canavanine for selection of inactivation of *CAN1*, or on SC media lacking threonine or lysine to select for threonine (*hom3-10*) or lysine (*lys2-BgI*) revertants, respectively. Median rates are reported with 95% confidence intervals [64]. The spectrum of inactivating mutation at the *CAN1* locus was determined by sequence analysis of *CAN1* from canavanine-resistant colonies using primer pairs that anneal 50 bp upstream and 43 bp downstream of the *CAN1* ORF.

Tetrad analysis

Diploid strains for tetrad dissection were derived from S288C strains provided by Richard Kolodner (UC San Diego) and are listed in Supplementary Table S1. To generate the diploid heterozygous for *sgs1Δ, rad52Δ,* and *exo1Δ* mutations (KHSY4810) RDKY5290 was crossed to KHSY4805, a spore obtained from a cross between RDKY2614 and RDKY2710. *RAD59* and *RAD51* deletions were obtained by HR-mediated integration of a selectable marker at these loci in RDKY2666 using the LiAc method [58] and diploids heterozygous for *sgs1Δ, exo1Δ,* and *rad51Δ* or *rad59Δ* were obtained by crossing as described above. For tetrad dissections, diploids were

grown overnight in YPD at 30° and starved of nitrogen in 0.1% potassium acetate. Asci

were briefly incubated with zymolase and dissected on YPD agar plates using a

micromanipulator mounted on an Axioscop 40 (Zeiss). YPD plates were incubated for 4

days at 30° and spore germination and colony growth were documented at 24 hour

intervals with a CCD camera mounted on a GelDoc-IT Imager (UVP).

Pull-Down Assay and Western Blotting

Plasmid pKHS657, expressing GST-Sgs1647-1447, was created by inserting the

last 2400 bp of SGS1 into pGEX-6p-2 (GE Healthcare) using BamHI and XhoI

restriction sites. Stop codons and F1192A and F1192D mutations were introduced at

the indicated positions by site-directed mutagenesis (Quikchange, Agilent Genomics).

Sgs1 fragments were expressed in *E. coli* BL21 (DE) in LB media (10 g/l tryptone, 5 g/l

NaCl, 5 g/l Yeast extract) supplemented with 1.5 µg/ml ampicillin for 3 hours in the

presence of 1 mM IPTG. Cells were resuspended in 100 µl GST buffer (125mM Tris,

150mM NaCl, pH 8.0) plus HALT protease inhibitor cocktail (Pierce), lysed using glass

beads with a BeadBeater (Biospec Products, Inc.) at 4° and lysate cleared by

centrifugation at 14000 rpm for 10 min at 4°. Lysate was treated with benzonase

(Sigma) and 1mg of lysate was added to glutathione magnetic beads (Pierce) and

incubated for 1 h at 4°C before beads were washed three times with GST buffer.

Similarly, yeast cells expressing endogenous levels of VSV-tagged Rad51 (Open

Biosystems) were resuspended in Rad51 buffer (50 mM Tris, pH 7.5, 0.01% NP-40, 5

mM β-glycerol phosphate, 2 mM magnesium acetate, 120 mM NaCl) with HALT

protease inhibitor cocktail (Pierce), lysed with glass beads in a BeadBeater and cleared

153

by centrifugation at 14000 rpm for 20 min at 4°. Lysate was treated with benzonase (Sigma) and 10 mg of lysate were incubated with Sgs1-bound magnetic beads for 120 min at room temperature while rotating. Beads were washed five times with Rad51 buffer plus HALT protease inhibitor cocktail (Pierce) and then boiled in Laemmli buffer (BioRad) for 10 min. The eluate was separated by 10% SDS-polyacrylamide gel electrophoresis. Sgs1 fragments and Rad51 were detected by Western blotting using monoclonal antibodies against GST (Covance) and VSV (Sigma) epitopes.

Data and reagent availability: Yeast strains are available upon request. Table S1 contains a list of yeast strains used in this study and detailed genotype descriptions.

RESULTS

Rad51 binds to the loop that connects the helicase core of Sgs1 to the HRDC domain

SGS1 and *RAD51* are epistatic and the gene products interact physically [40, 51]. Using a yeast-two-hybrid assay, the physical interaction with Rad51 was mapped to the last 469-residues of Sgs1 (residues 978-1447). This region flanks the ATPase domain and contains the conserved RQC domain, which is essential for the helicase activity of Sgs1, as well as other conserved sites, including the HRDC domain and a Mlh1 binding site [40, 65]. Thus, disrupting Rad51 binding by deleting this 469-residue region disrupts multiple other Sgs1 functions. Therefore, to enable elucidation of the biological importance of the interaction between Sgs1 and Rad51 for HR, we sought to

154

identify a separation-of-function mutation in Sgs1 that specifically disrupts Rad51 binding but leaves other functional sites intact.

To narrow down the Rad51 binding region we purified fragments of Sgs1 as GST-fusions from *E. coli* and tested their ability to pull-down endogenous VSV-epitope tagged Rad51 from yeast whole cell extract. We determined that deleting up to 240 C-terminal residues of Sgs1 did not impair its ability to bind Rad51, whereas a deletion of 260 residues abolished it (Figure 1A and 1B). This critical 20-residue region maps to residues 1187 to 1207 immediately C-terminal of the WH-domain and contains a phenylalanine at position 1192. Mutating this hydrophobic residue to aspartic acid (F1192D) disrupted Rad51 binding, whereas mutating it to alanine did not have a major effect (F1192A) (Figure 1B).

Unlike loss of Sgs1 helicase activity, loss of Sgs1-Rad51 binding does not cause DNA damage sensitivity and genome instability in haploid cells

To determine how the loss of Rad51 binding affects Sgs1 function in vivo we integrated the *sgs1-F1192D* allele (hereafter *sgs1-FD*) at the chromosomal locus under control of the *SGS1* promoter. Unlike an *SGS1* deletion, the *sgs1-FD* mutation did not lead to an increase in genome instability (Table 1) or an increase in sensitivity to hydroxyurea (HU), which induces replication stress by inhibiting ribonucleotide reductase, or methyl methanesulfonate (MMS), an alkylating agent that directly damages bases (Figure 1C). Since the *sgs1-FD* mutation is disrupting a link between Sgs1 and HR, we also tested its effect on DNA-damage sensitivity in diploids, which depend more strongly on HR for repair of DNA breaks than haploids [66, 67]. Diploids were indeed more sensitive to 0.025% MMS if they were homozygous for the *sgs1-FD*

mutation than if they were heterozygous for *sgs1-FD* or homozygous for the wildtype allele (Figure 1D), indicating a mild DNA repair defect in the *sgs1-FD* mutant.

Rad51 binding to Sgs1 is required for normal growth, DNA damage tolerance, and genome stability in the absence of Sae2, but not Mre11: To identify Sgs1 functions that are impacted by its binding to Rad51, we first investigated genetic interactions between *sgs1-FD* and HR genes. In HR, Sgs1 acts in addition to Exo1 in the resection of DSBs after their initial nucleolytic processing by Sae2 and the MRX complex [9]. In cells lacking *SGS1*, deletion of *EXO1* causes a fitness defect and one of the largest known synergistic increases in genomic instability (>500-fold) [31, 68, 69] whereas a deletion of *SAE2* or *MRE11* is synthetically lethal with *sgs1Δ* [53, 70]. These reported phenotypic similarities between Sae2 and Mre11 deficiency, however, did not apply to the *sgs1-FD* mutant. The *sgs1-FD* mutation caused a significant fitness defect in the *sae2Δ* mutant but had no detrimental effect on the growth of the *mre11Δ* mutant (Figure 2A). The *sgs1-FD* allele also increased hypersensitivity of the *sae2Δ* mutant to HU and MMS but exhibited a wildtype phenotype in the *mre11Δ* mutant (Figure 2B-C). Moreover, the *sgs1-FD* allele led to a synergistic (25-fold) increase in the GCR rate in the *sae2Δ* mutant but did not affect the accumulation of genome rearrangements in the *mre11Δ* mutant (Figure 2E).

In the current model of DSB end processing, MRX and Sae2 bind to the unprocessed ends, trimming off a few nucleotides and causing their own release from the DNA [9, 10]. These trimmed ends are poor substrates for Ku binding, but good substrates for extensive nucleolytic processing by Exo1 and Sgs1/Dna2 to produce the

long 3' terminated overhangs for Rad51-mediated homology search [9, 10]. When initial

trimming and long-range resection are impaired due to absence of Sae2 and Sgs1 cells

die [71, 72]. However, these cells are rescued by deleting *YKU70*, suggesting that

preventing Ku from binding to the DSB ends makes them accessible to the alternative,

Exo1-mediated pathway for long-range resection, thus bypassing the requirement of

Sae2 for removal of Ku and that of Sgs1 for long-range resection [1]. Based on this

finding, any sgs1 mutation that causes a resection defect and a synthetic growth defect

with *sae2Δ* should be suppressed by deletion of *YKU70*. Indeed, the defects of the

sgs1-D664Δ mutant, which include a severe fitness defect with *sae2Δ* and a resection

defect, are bypassed in cells lacking Ku [73, 74]. However, we observed that neither the

severe fitness defect the *sgs1-FD sae2Δ* mutant nor its DNA damage sensitivity was

suppressed by deleting *YKU70* (Figure 2C), suggesting that the *sgs1-FD* mutation does

not cause a resection defect.

To test the possibility that the requirement of Sae2 in the *sgs1-FD* mutant was

related to a MRX-related function of Sae2, we next deleted *MRE11* in the *sae2Δ sgs1-*

FD mutant. We observed that the *mre11Δ* mutation suppressed the growth defect and

the associated HU/MMS sensitivity of the *sgs1-FD sae2Δ* mutant to levels observed in

the *mre11Δ sae2Δ* mutant (Figure 2A and 2C), indicating that unlike in the *sgs1Δ* mutant

MRX is not required in the *sgs1-FD* mutant and that, in fact, the inability to remove MRX

from the DSB ends is toxic in the *sgs1-FD mutant.*

157

sgs1-FD increases genome instability and DNA damage hypersensitivity in cells lacking Exo1

The need in the sgs1-FD mutant for SAE2 prompted us to further investigate the requirement of EXO1, which cooperates with Sgs1/Dna2 during more extensive resection of DSB after Sae2. The exo1Δ mutant is mildly sensitive to high concentrations of MMS, but not HU [69]. The sgs1-FD allele increased the sensitivity of the exo1Δ mutant to MMS and caused sensitivity to 200 mM HU, but remained far below the effect of an SGS1 deletion (Figure 3A and 3B). The sgs1-FD allele also caused a significant (6-fold) increase in the accumulation of genome rearrangements in the exo1Δ mutant albeit this, too, was much milder than the 500-fold increase in GCR accumulation previously reported for the SGS1 deletion [31, 68].

Suppression of the severe growth defect of the top3Δ mutant by the sgs1-FD mutation

In addition to interacting with Dna2 and RPA during DSB resection, Sgs1 forms a complex with Top3/Rmi1 to dissolve dHJ [35, 37, 75]. In vitro, Top3 also stimulates Sgs1 activity in DSB resection and resolves protein-bound D-loops [76, 77]. Both, deletion of *SGS1* or loss of Sgs1 helicase activity, suppress the severe growth defect of the *top3Δ* mutant, which has been interpreted to mean that Sgs1 produces HR intermediates that then require Top3 for dissolution [37]. We found that the *sgs1-FD* allele, too, suppressed the severe slow growth phenotype of the top3Δ mutant to a similar extent as the *sgs1Δ* or *sgs1-HD* alleles and improved growth during exposure to HU or MMS (Figures 2D and 2E), suggesting that the interaction between Sgs1 and

158

Rad51 drives the formation of recombination intermediates and thereby significantly contributes to the severe growth defect of the *top3Δ* mutant.

Opposite effects of the *sgs1-FD* mutation on the DNA-damage sensitivity of *srs2Δ* and *rrm3Δ* mutants: Srs2 acts as an inhibitor of HR through its ability to disrupt the Rad51 presynaptic filament [14, 15]. In the absence of Srs2, cells become hyper-recombinogenic, hypersensitive to exogenous DNA damage and replication stress, as well as dependent on Sgs1 for viability [14, 15, 54]. The negative genetic interactions of the *sgs1-FD* allele with *sae2Δ* and *exo1Δ* mutations, and the positive interaction with *top3Δ* suggest that *sgs1-FD* is a hypo-recombination allele of *SGS1*. To further explore this possibility, we introduced *sgs1-FD* into the *srs2Δ* mutant, which we expected to benefit from a reduction in HR. Indeed, in stark contrast to a deletion of *SGS1* or loss of Sgs1 helicase activity, which are both lethal to *srs2Δ* cells, the *sgs1-FD* allele had no detrimental effect on the growth of *srs2Δ* cells and in fact suppressed the hypersensitivity of *srs2Δ* cells to HU and MMS by more than 10-fold (Figure 3B), consistent with *sgs1-FD* being a hypo-recombination allele.

We also investigated the importance of the Sgs1-Rad51 interaction in the *rrm3Δ* mutant. Replisomes pause frequently at many sites throughout the genome when the Rrm3 helicase is absent, generating DNA lesions that are substrates for Sgs1 and Rad51-dependent repair [50, 51, 78]. Like a deletion of *SRS2*, deletion of *RRM3* causes a severe growth defect in *sgs1Δ* cells that can be suppressed by deleting *RAD51* [50, 51]. The *sgs1-FD* mutation did not cause a growth defect in *rrm3Δ* cells; however, cells

became highly sensitive to both HU and MMS (Figure 3B). Despite the increased DNA damage sensitivity, the *rrm3Δ sgs1-FD* mutant did not accumulate genome rearrangements (Figure 3D, Table 1) in contrast to the *rrm3Δ sgs1Δ* mutant [30]. This genetic interaction between *rrm3Δ* and a hypomorphic allele of *SGS1* further underscores the strong dependence of the repair of the replication-associated DNA lesions in *rrm3Δ* cells on homology-directed replication fork restart and rescue [52].

Sgs1-Rad51 interaction promotes large deletions and contributes to DNA damage hypersensitivity of cells lacking Pol32: In the absence of *POL32*, which codes for the structural subunit of polymerase δ that attaches the polymerase to the processivity factor PCNA, DNA replication is inefficient and prone to pausing and mutations [79-81]. Since an *SGS1* deletion causes a fitness defect and increased HU and MMS sensitivity in the *pol32Δ* mutant, we decided to assess the effect of the *sgs1-FD* allele in this mutant. Surprisingly, we found that the *sgs1-FD* mutation had the opposite effect of the *SGS1* deletion and the helicase-defective *sgs1-HD* allele, suppressing the HU hypersensitivity of the *pol32Δ* mutant (Figure 4A, and 4C). Since the HU hypersensitivity of the *pol32Δ* mutant is also suppressed by deletion of *EXO1* [69], we next tested the combined effect of *exo1Δ* and *sgs1-FD* mutations on HU sensitivity of the *pol32Δ* mutant (Figure 4D). Instead of suppression, however, we observed an increase in HU and MMS sensitivity even at low drug concentrations, suggesting that Exo1 and the Sgs1-Rad51 interaction cooperate in a pathway that is required in the absence of Pol32. Since both Sgs1 and Exo1 act in DSB end processing to initiate HR, we investigated the effect of a *RAD51* deletion on the HU/MMS sensitivity

160

of the *pol32Δ* mutant and observed a strong increase in sensitivity (Figure 4E). This suggests that *pol32Δ* cells depend on a Rad51-dependent HR pathway for the survival of replication stress and that Exo1 and the Sgs1-Rad51 interaction independently promote this pathway.

The accumulation of large deletions between short repeats in *CAN1* or other genomic loci is characteristic of *pol32Δ* cells and has been explained by an increased propensity of the nascent strands to dissociate from their templates as a result of frequent pausing, followed by error-prone reannealing [80]. When we combined the *pol32Δ* mutation with the *sgs1-FD* mutation, there was no significant change in the mutation rate at *CAN1* (Supplemental Table S2), but the rate of large deletions was reduced 4-fold similar to the 6-fold reduction when *SGS1* was deleted, suggesting that the interaction of Sgs1 with Rad51 contributes to the formation of large deletions in the absence of Pol32 (Figure 4B). In contrast, when we deleted *EXO1* in the *pol32Δ* mutant, the rate of large deletions increased 4-fold (Figure 4B). These observations indicate that, in contrast to their cooperative roles in DSB end resection, Exo1 and Sgs1 have opposite effects at impaired replication forks. For example, Exo1 could prevent deletions by degrading the mutagenic substrate, whereas Sgs1 and the Sgs1-Rad51 interaction might help generate deletions by facilitating DNA slippage by misannealing at nearby repeats.

Rad52/Rad59-mediated DNA repair, but not Rad51, is essential for cells with compromised DNA resection due to lack of Sgs1 and Exo1: Cells lacking Sgs1 and Exo1 show minimal resection of DSBs and accumulate GCRs at an extreme level [9, 31, 68]. Because of the failure to sufficiently resect DSB ends we expected that DSBs

161

would not be suitable for repair by HR. Surprisingly, however, we found that deleting

RAD52 was lethal in the *sgs1Δ exo1Δ* mutant, and deletion of *RAD59* caused an

extreme growth defect (Figure 5A). In contrast, deleting *RAD51* caused only a mild

fitness defect (Figure 5A), consistent with the ability of other groups to readily obtain

and characterize the *sgs1Δ exo1Δ rad51Δ* mutant [9, 73, 82].

When we analyzed the effect of HR mutations on chromosome rearrangements

in the *sgs1Δ exo1Δ* mutant, we found that deleting *RAD51* significantly suppressed (3.1-

fold) their accumulation (Figure 5C, Table 2). We also analyzed GCR formation in the

sgs1Δ exo1Δ rad59Δ mutant. Because of the severe growth defect of this mutant and

the associated risk of obtaining suppressors with prolonged propagation, we set up all

cell cultures from colonies immediately after they formed from meiotic products of the

heterozygous diploid. In contrast to the decrease upon *RAD51* deletion, *RAD59* deletion

doubled (2.4-fold) the GCR rate of *sgs1Δ exo1Δ* cells (Figure 5C, Table 2).

The dramatic decrease in viability of the *sgs1Δ exo1Δ* mutant upon *RAD59* and *RAD52*

deletion suggests that a Rad59-dependent HR pathway repairs DNA lesions in this

mutant. The decrease in GCR formation upon *RAD51* deletion and the opposite effect

of a *RAD59* deletion further suggest that Rad51 and Rad59 compete for repair of these

incompletely processed DNA lesions in the *sgs1Δ exo1Δ* mutant and that repair by

Rad51, but not Rad59, is mutagenic.

Interestingly, we observed that the effect of *RAD51* and *RAD59* deletions on the

accumulation of GCRs is the same in *sgs1Δ* cells with *EXO1* intact as in cells with

EXO1 deleted; that is, a *RAD51* deletion led to a significant (5.1-fold) decrease in the

GCR rate of *sgs1Δ* cells (versus 3.1-fold decrease in *sgs1Δ exo1Δ*) and *RAD59* deletion

to a significant (1.8-fold) increase (versus a 2.3-fold increase in *sgs1Δ exo1Δ*) (Figure

5B and 5C, Table 2). Essentially, deleting *EXO1* increased all GCR rates by ~ 700-fold,

but had no effect on the genetic interactions between *sgs1Δ, rad51Δ*, and *rad59Δ*

(compare the last three columns in Figures 5B with 5C).

DISCUSSION

We have identified a novel separation-of-function mutant of Sgs1 (*sgs1-FD*) that

fails to bind Rad51 but does not cause the severe sensitivity to DNA-damaging agents

seen in cells lacking Sgs1 or expressing helicase-defective Sgs1. Novel positive and

negative genetic interactions between this *sgs1-FD* allele and mutations in genes with

roles in HR (*mre11Δ, sae2Δ, srs2, exo1Δ, top3Δ*) or replisome progression (*pol32Δ,

rrm3Δ*) suggest that the physical interaction between Sgs1 and Rad51 stimulates

homology-dependent DNA repair.

We observed the strongest genetic interaction of the *sgs1-FD* allele with a *SAE2*

deletion (Figure 2). Sae2 removes MRX from DSB ends and prevents yKu binding,

making the DSB accessible to extensive resection by Sgs1/Dna2 and Exo1 [1]. YKU70

deletion suppresses resection defects in cells that lack Sae2 and Sgs1 activities by

allowing the alternative Exo1 pathway access to the DSB ends for resection [1, 73, 74,

83]. In addition to suppressing the DNA-damage sensitivity and fitness defect of the

sgs1Δ sae2Δ mutant, the resection-defective *sgs1-D664Δ* mutant was found to benefit

from deleting *YKU70* [73, 74]. In contrast, deleting *YKU70* had no effect on the *sgs1-FD*

sae2Δ mutant identified here, indicating that the *sgs1-FD* mutant does not benefit from

increased Exo1 activity at DSBs and, thus, that *sgs1-FD* is proficient for resection.

Surprisingly, even though Sae2 acts with MRX in the initial processing step and sgs1Δ

is synthetically lethal with both *sae2Δ* and *mre11Δ,* disruption of the Sgs1-Rad51

interaction was not detrimental to *mre11Δ* cells. In fact, the *MRE11* deletion suppressed

the detrimental effects of the *sgs1-FD* mutation in *sae2Δ* cells, suggesting that the Sae2

function that is critical in *sgs1-FD* cells is the removal of MRX from DSB ends. If MRX

stays bound, the DNA-damage checkpoint is activated and oligomers of the Rad9

checkpoint adaptor accumulate nearby [84-87]. Disrupting the DNA damage checkpoint

alleviates the requirement for Sae2 at DSBs [88]. Although this suggests that Sgs1 can

compensate for the lack of initial resection by Sae2, more extensive resection and

Rad51 filament formation are still impaired by MRX stuck on the DSB ends [88, 89].

Recent findings have indicated that Sgs1 can eventually remove MRX and analysis of

the *sgs1-D664Δ* mutant linked this ability to long-range resection by Sgs1 [73, 88].

Because of the resection defect of the *sgs1-D664Δ* mutant, defects of the *sgs1-D664Δ*

sae2Δ mutant could be suppressed by deleting *YKU70.* That the *YKU70* deletion had no

effect on the *sgs1-FD sae2Δ* mutant indicates that the suppression by *MRE11* deletion

is not related to a resection defect in the *sgs1-FD* mutant. We propose, therefore, that

the disruption of Sgs1-Rad51 interaction by the *sgs1-FD* mutation reduces the efficiency

of Rad51 filament formation, and thus repair by HR. Removing *MRE11* from the DSB

ends and, consequently, preventing Rad9 accumulation around the DSB ends could

compensate for this deficiency in the *sae2Δ sgs1-FD* mutant by increasing the efficiency

of long-range resection due to increased access of sgs1-FD/Dna2 to the DSB ends.

Thus, when DNA end processing is impaired because of the lack of Sae2, and

persistent MRX binding and resulting checkpoint activation inhibit Sgs1/Dna2 function in

resection, HR increasingly depends on the stimulation of Rad51 filament formation by

Sgs1.

All other genetic interactions of the *sgs1-FD* allele investigated here are also in

agreement with a role of the Sgs1-Rad51 interaction in stimulating HR, such as the

positive interactions of the *sgs1-FD* mutation with *top3Δ, pol32Δ* and *srs2Δ* and the

negative interaction with *rrm3Δ*. Especially the suppression of the DNA damage

sensitivity of the *srs2Δ* mutant strengthens our hypothesis that the Sgs1-Rad51

interaction stimulates Rad51 filament formation. Based on the ability of Srs2 to

disassemble Rad51 filaments [14], suppression of *srs2Δ sgs1Δ* synthetic lethality by

RAD51 deletion [90] could be interpreted in two ways: either Sgs1 acts like Srs2 by

disassembling presynaptic Rad51 filaments, or Sgs1 in complex with Top3/Rmi1 is

needed to dissolve the accumulating recombination intermediates that overwhelm the

cell because Rad51 filaments are no longer disrupted by Srs2. Our findings suggest the

second explanation to be true; if the Sgs1-Rad51 interaction indeed promoted the

disassembly of presynaptic Rad51 filaments, then the disruption of the Sgs1-Rad51

interaction by the *sgs1-FD* mutation would not have suppressed the DNA-damage

sensitivity of the *srs2Δ* mutant (Figure 3B).

Thus, taken together, the genetic interactions of the *sgs1-FD* allele are distinct from

those of the *sgs1Δ* and helicase-defective *sgs1-hd* alleles (Figure 6B) and consistent

with a model (Figure 6A) whereby Sgs1 is not only responsible for the resection of DSB

ends and the formation of ssDNA overhangs but, through binding Rad51, promotes HR

by stimulating formation of the Rad51 presynaptic filament. As DNA ends are resected,

RPA binding to the newly formed ssDNA overhangs limits the initiation of the Rad51

filament. Rad52 is essential to overcome this limitation and form a productive Rad51

presynaptic filament on RPA-coated ssDNA. In addition to binding Rad51 C-terminal of

the helicase core, Sgs1 binds RPA N-terminal of the helicase core [38]. However, the

biological significance of this interaction has remained unclear. We propose that the

acidic regions in the N-terminus of Sgs1 to which RPA binds serve as a DNA mimic,

and that via this DNA mimic Sgs1 can compete with the ssDNA overhang for RPA

binding, thereby freeing up ssDNA locally for Rad51 and stimulating filament initiation

(Figure 6A). Such a role for Sgs1 is reminiscent of the function of *E. coli* RecBCD not

only in resection but also in assembling the RecA filament [91]. Moreover, the ability of

BRCA2 to load Rad51 onto ssDNA in vitro was recently shown to be aided by

interaction with a protein, DSS1, that appears to act as a DNA mimic and targets RPA

on ssDNA [92].

　　　We also observed a stimulatory effect of the Sgs1-Rad51 interaction on the

formation of the direct-repeat mediated, large deletions characteristic of *pol32Δ* cells.

Unlike in DSB resection, however, Sgs1 had the opposite effect of Exo1: the Sgs1-

Rad51 interaction promoted the deletions, and Exo1 suppressed them, both to

approximately the same extent (4-fold). The large deletions in *pol32Δ* cells most likely

form during inefficient replisome progression, which makes the nascent DNA strands

prone to dissociation, followed by misannealing at a repeated downstream sequence,

thus deleting the sequence between the repeats. We propose a model (Figure 6A)

whereby Exo1 prevents large deletions through its ability to degrade the nascent lagging DNA strand at stalled forks [93] and the Sgs1-Rad51 interaction, in contrast, promotes annealing of dissociated nascent strands with downstream repeated sequences on both, the leading and the lagging strand.

Finally, our study also provided new insight into the repair of DSBs in cells where long-range resection by Sgs1/Dna2 and Exo1 is disrupted. It is thought that for HR, the ends need to be resected extensively by Sgs1/Dna2 or Exo1 before the Rad51 filament can form and initiate a homology search. Hence, *sgs1Δ exo1Δ* mutants should not be able to rely on HR as a major pathway for DNA lesion repair. It was therefore surprising that *sgs1Δ exo1Δ* cells depend on *RAD52* for their survival. That the fitness of these cells was more dependent on Rad59 than Rad51 suggests that the minimally resected DSB ends in *sgs1Δ exo1Δ* cells are mainly repaired by Rad59/Rad52-dependent HR. This is consistent with a preference of Rad59 for the repair of short substrates, including by Rad51-independent BIR [25, 26, 94]. Interestingly, we also found that Rad59 suppressed genome rearrangements in *sgs1Δ exo1Δ* mutants whereas Rad51 increased them, suggesting that both Rad51 and Rad59 can act on minimally resected ends, but with Rad59 leading to proper repair, whereas Rad51 is mutagenic. That the genetic interactions between *SGS1, RAD51*, and *RAD59* were the same in the presence or absence of *EXO1* – that is, Rad59 suppressed GCRs in the absence of Sgs1 whereas Rad51 generated them – further indicates that *sgs1Δ* and *sgs1Δ exo1Δ* cells simply differ in the abundance of the lesions, but the lesions are of the same type and accessed in the same manner by Rad59 and Rad51 whether Exo1 is present or not.

167

In addition to Rad51, Sgs1 interacts with numerous other DNA repair factors, including

Top2, Top3, RPA, Mre11, Rad16, and Mlh1, and the checkpoint kinase Rad53.

However, determining the significance of these interactions for Sgs1 function has

remained challenging due to the lack of point mutations that disrupt individual

interactions. Identifying the binding sites on Sgs1 for these other interacting partners will

allow to further dissect the well-characterized, but pleiotropic, effect of an *SGS1* deletion

on DNA break repair and provide a more precise understanding of the specific roles of
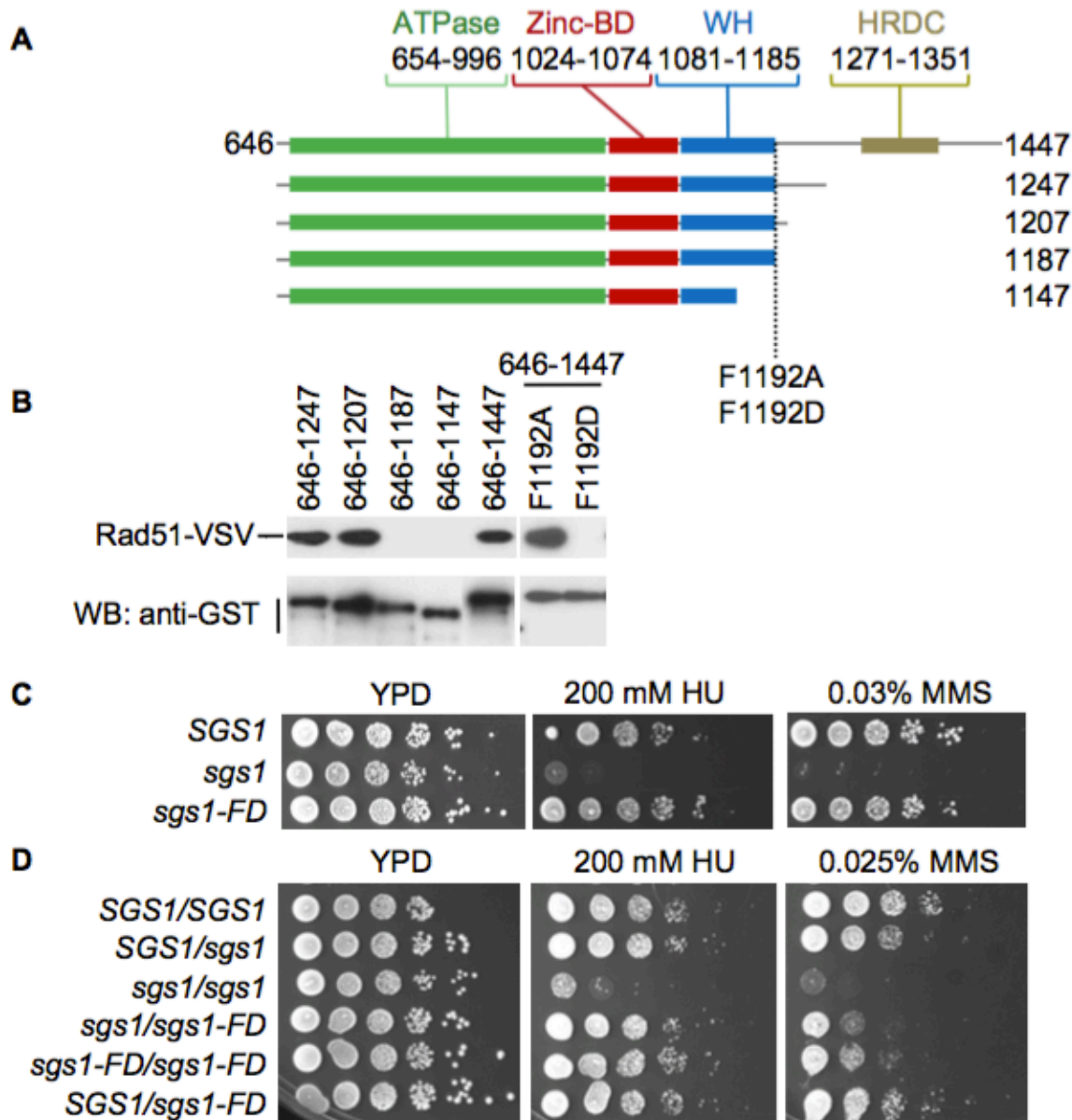
Sgs1 in promoting genome integrity.

Figure 4.1. **Rad51 binds to Sgs1 downstream of the winged-helix domain. (A) Domain structure of Sgs1.** The helicase core of Sgs1 consists of the ATPase domain, which is formed by two RecA-like lobes, and the RecQ-C terminal (RQC) domain, which consists of a zinc-binding (Zinc-BD) and a winged-helix (WH) domain. The helicase- and RNaseD C-terminal (HRDC) domain are separated from the helicase core by a proline/glycine-rich loop. The 645-residue unstructured N-terminal tail is omitted. (B) Pulldown of Rad51-V5-3XVSV with GST-tagged Sgs1 fragments and sgs1-FD and sgs1-FA mutants. (C) Unlike an *SGS1* deletion, the *sgs1-FD* allele does not cause hypersensitivity to MMS or HU in haploid cells. Homozygosity for the sgs1-FD mutation causes mild sensitivity to HU and MMS in diploid cells.
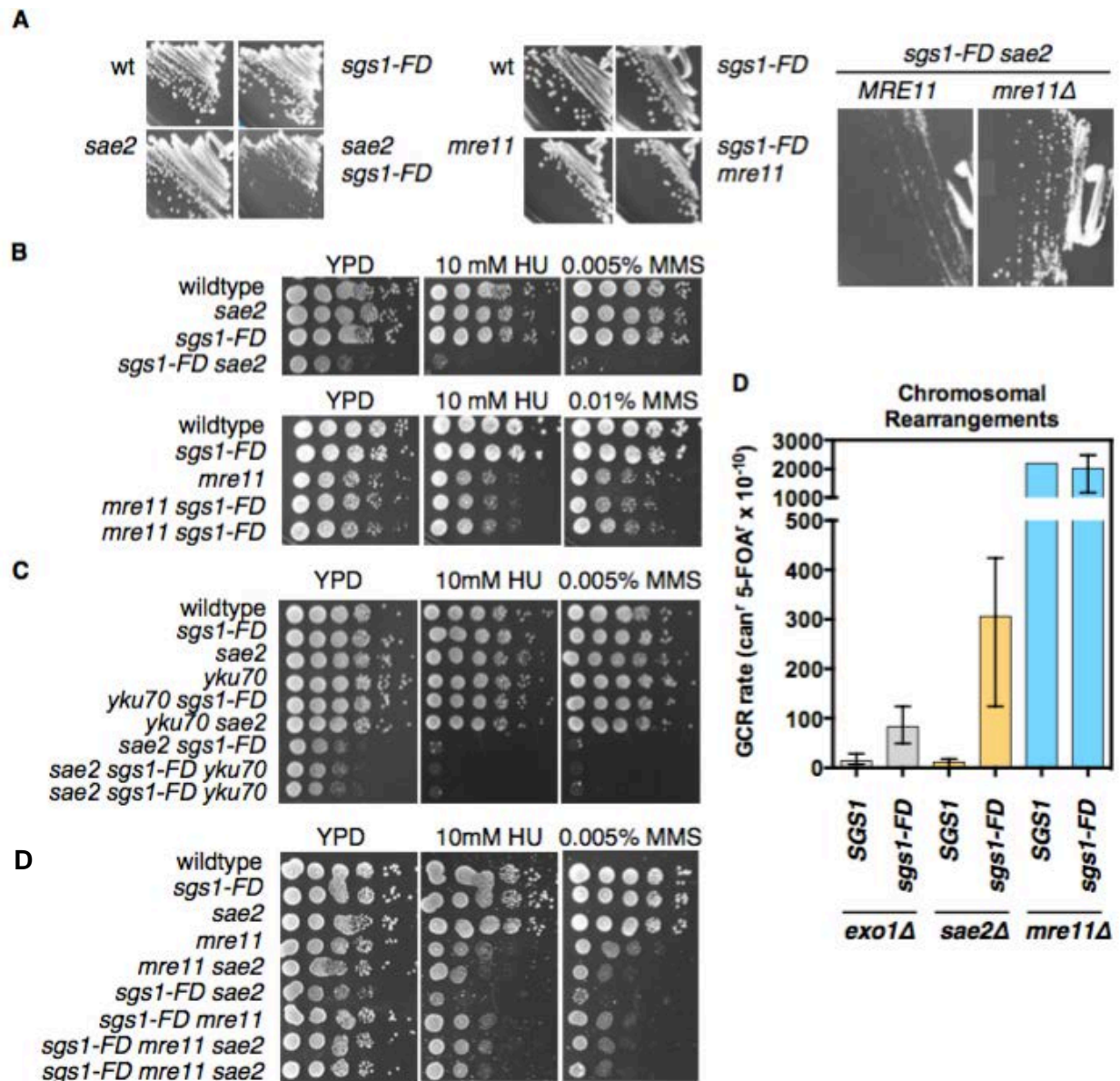
169

Figure 4.2. Effect of the *sgs1-FD* mutation on fitness, DNA-damage sensitivity and genome stability of *sae2Δ*, *mre11Δ* and *yku70Δ* mutants. (A) *sgs1-FD* causes a severe growth defect in the *sae2Δ* mutant, but not the *mre11Δ* mutant. Deletion of *MRE11* suppresses the growth defect of *sgs1-FD sae2Δ*. (B) *sgs1-FD* increases the HU/MMS sensitivity of the *sae2Δ* mutant, but not the *mre11Δ* mutant. (C) Unlike *mre11Δ, yku70Δ* does not the suppress growth defect and HU/MMS hypersensitivity of the *sgs1-FD sae2Δ* mutant. (D) *sgs1-FD* causes synergistic GCR rate increases in *sae2Δ* and *exo1Δ* mutants but has no effect on GCR accumulation in the *mre11Δ* mutant. Median GCR rate is shown with 95% confidence intervals (see also Table 1).
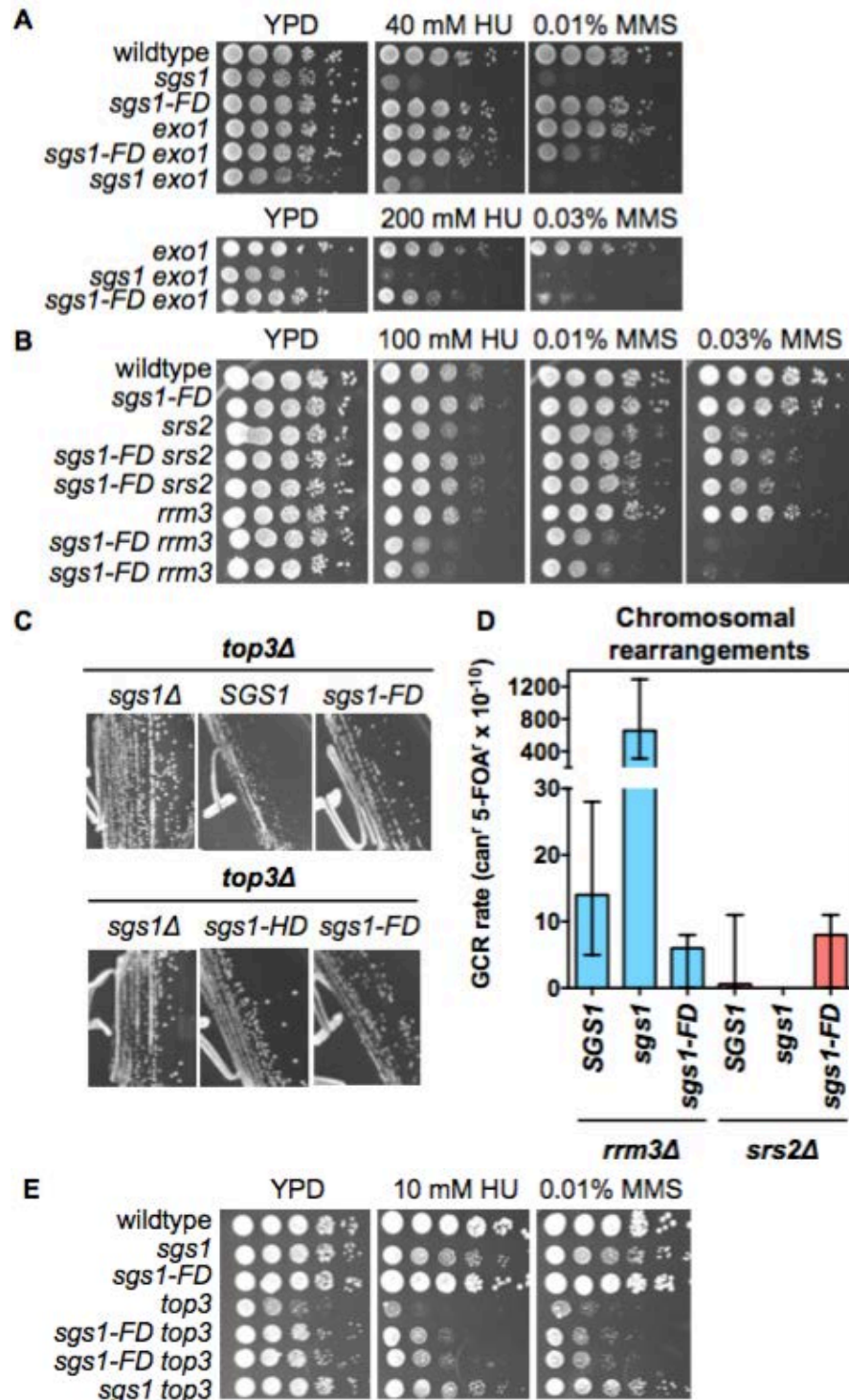
170

Figure 4.3. **Effect of the *sgs1-FD* mutation on fitness and DNA-damage sensitivity of *exo1Δ, srs2Δ, rrm3Δ* and *top3Δ* mutants.** (A) *sgs1-FD* sensitizes the *exo1Δ* mutant to MMS and, to a lesser extent, HU. (B) *sgs1-FD* suppresses HU/MMS sensitivity of the *srs2Δ* mutant and increases HU/MMS sensitivity of the *rrm3Δ* mutant. (C) *sgs1-FD* suppresses *top3Δ* slow growth nearly as effectively as a deletion of *SGS1* or helicase-dead *sgs1-HD*. (D) Unlike deletion of *SGS1*, *sgs1-FD* does not cause a GCR rate

171

increase in the *rrm3Δ* mutant. *sgs1-FD* does not affect GCR formation in the *srs2Δ* mutant (see also Table 1). (E) Improved growth of *sgs1-FD top3Δ* in the presence of HU and MMS correlates with partial suppression of the *top3Δ* fitness defect by *sgs1-FD*.
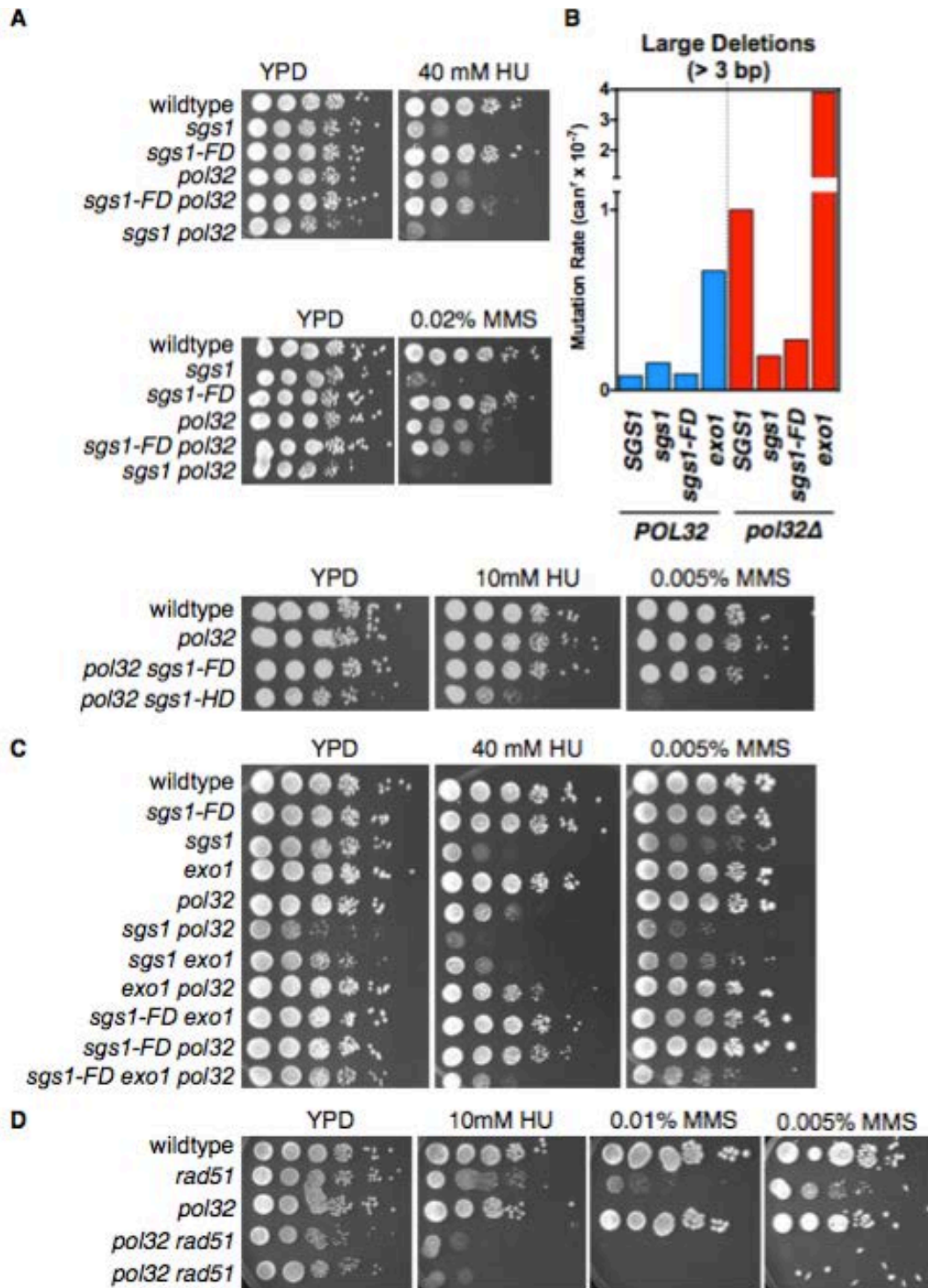
Figure 4.4. Effect of *sgs1-FD* on DNA-damage sensitivity and large deletion formation in the absence of Pol32. (A) Suppression of hydroxyurea sensitivity of the *pol32Δ* mutant by *sgs1-FD*. In contrast, *SGS1* deletion or helicase-defective *sgs1-HD* increase DNA-damage sensitivity of *pol32Δ* cells. (B) Accumulation of large deletions (> 3 bp) in *CAN1*, characteristic of cells lacking the Pol32 subunit of polymerase δ, is suppressed by *sgs1-FD* or by deletion of *SGS1* but stimulated by deletion of *EXO1*. (C)

173

Whereas *exo1Δ* and *sgs1-FD* suppress HU sensitivity of the *pol32Δ* mutant, the combination of both *exo1Δ* and *sgs1-FD* mutations increases DNA damage sensitivity of the *pol32Δ* mutant. (D) Deletion of *RAD51* in the *pol32Δ* mutant causes severe hypersensitivity to HU and MMS.
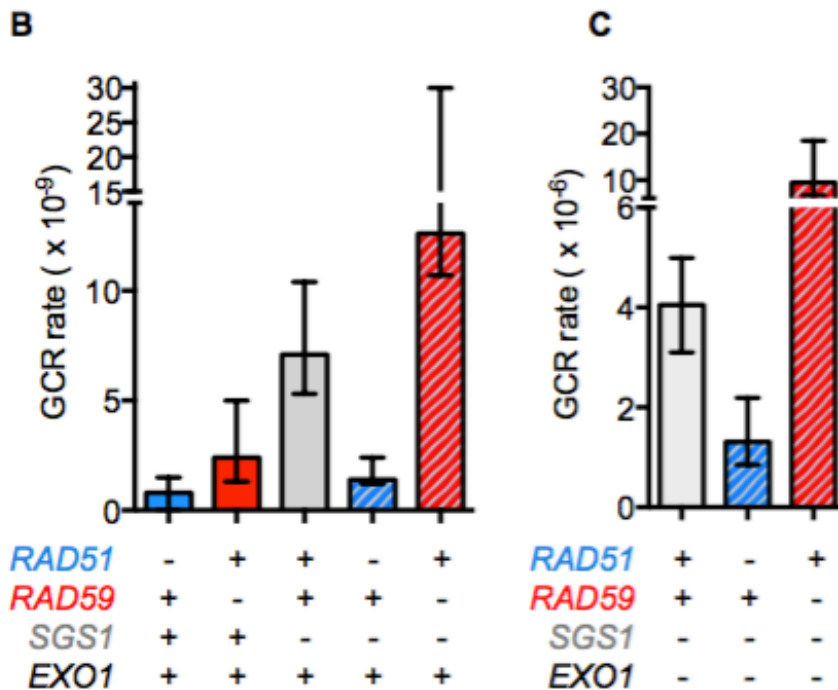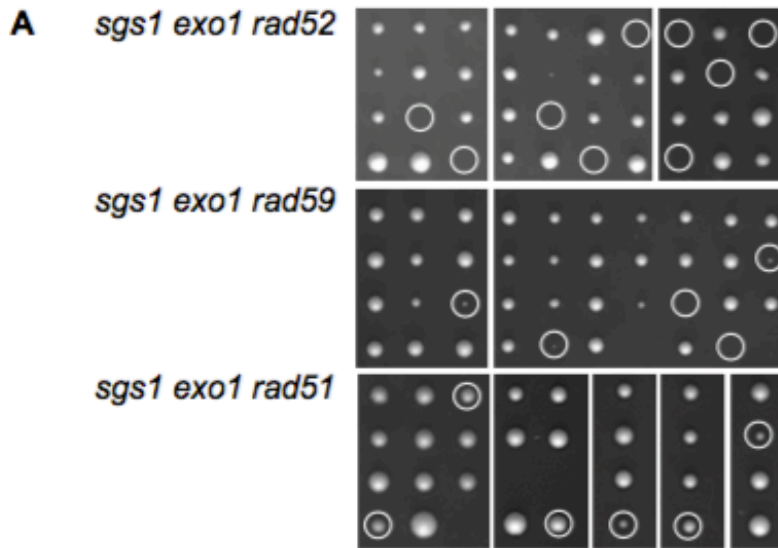
Figure 4.5. Effect of *RAD52, RAD51* and *RAD59* deletions on viability and genome stability of the *sgs1Δ exo1Δ* mutant. (A) As shown by tetrad dissections, deletion of *RAD52* in the *sgs1Δ exo1Δ* mutant is lethal, and deletion of *RAD59* causes a severe growth defect. In contrast, deletion of *RAD51* causes only a mild growth defect. Triple mutant spores are indicated by a white circle. (B) Deletion of *RAD51* suppresses gross-chromosomal rearrangements (GCRs) in the *sgs1Δ* mutant whereas deletion of *RAD59* stimulates GCR formation in the *sgs1Δ* mutant. (C) Deletion of *EXO1* increases GCR formation in the *sgs1Δ* mutant ~700-fold, but does not affect the genetic interactions of *sgs1Δ* with *rad51Δ* and *rad59Δ*.

175

Figure 4.6. Model for a stimulatory role of the Sgs1-Rad51 interaction in homology-dependent repair of spontaneous DNA lesions. (A) Replication stress, exogenous DNA damage, or disruption of factors with roles in replisome progression (e.g., *rrm3Δ, pol32Δ*) can impair replication forks and give rise to mutations (left) and DSBs (right). Right panel: Unprocessed DNA breaks can be bound by Ku and MRX. The nuclease activity of MRX/Sae2 trims the ends, which are then extensively resected by Exo1 and Sgs1/Dna2. Bound Ku and MRX inhibit long-range resection by Exo1 and Sgs1/Dna2, respectively. As the *sgs1-FD* mutant does not benefit from *YKU70* deletion, suggesting it does not have a significant resection defect, we propose that the Sgs1-Rad51 interaction could instead stimulate HR by linking Sgs1's role in long-range resection to Rad51 filament formation. Specifically, the acidic regions (AR) in the unstructured N-terminal tail of Sgs1, through their capacity to bind RPA, could act as a DNA mimic, allowing Sgs1 to compete with ssDNA for RPA binding, thereby facilitating deposition of Sgs1-bound Rad51 onto ssDNA during resection. Note: Ku, MRX, Exo1 and Sgs1/Dna2 can act on the same DSB end; two ends are shown to separate their activities for clarity only. Left panel: In the absence of Pol32, cells are known to accumulate large deletions of sequences flanked by direct short repeats. We propose a model whereby Sgs1, through its interaction with Rad51, stimulates the formation of these deletions (Figure 4B) by mediating misannealing of the nascent strands with

downstream repeated sequences, whereas the 5'-3' exonuclease Exo1 reduces deletion formation (Figure 4B) by degrading nascent DNA on the lagging strand from its accessible 5' end. (B) Summary of differential genetic interactions of the *sgs1-FD* allele and the *SGS1* deletion with mutations in DNA recombination and replication factors (n.a., not available; n.d., not determined).

Table 4.1. Effect of the *sgs1-FD* mutation on the rate of accumulation of gross-chromosomal rearrangements (GCRs).

Relevant genotype	GCR rate[i] (Can[r] 5-FOA[r] x 10^{-10})	95% CI[ii] (Can[r] 5-FOA[r] x 10^{-10})
wildtype	1.1	< 1 – 6.2
sgs1	71	53-104
sgs1-FA	<9	<7-9
sgs1-FD	<7	<6-8
exo1	14	7-28
sgs1 exo1	40500	31000-49900
sgs1-FD exo1	83	49-124
sae2	12	<7-18
sgs1-FD sae2	306	(124-424)
mre11	2200	n.d.
mre11 sgs1-FD	2030	1170-2480
top3	27	17-96
top3 sgs1-FD	12	9-36
rad24	23	9-37
sgs1 rad24	136	117-216
sgs1-FD rad24	26	10-69
pol32	20	15-26
sgs1 pol32	25	<24-105
sgs1-FD pol32	<8	<7-19
rrm3	14	5-28
sgs1 rrm3	656	311-1290
sgs1-FD rrm3	<6	<5-8
srs2	0.6	<2-11
sgs1-FD srs2	8	<7-11

[i] Gross-chromosomal rearrangement (GCR) rates for *mre11* and *top3* mutants are from (48); for *sgs1 rrm3* from Schmidt and Kolodner (30); for *sgs1 exo1* and *exo1* from Doerfler, 2014 (69); and for *srs2* from Schmidt *et al.* 2010 (61).
[ii]95% confidence intervals (CI) were calculated according to Nair *et al.* 1940 (64).

Table 4.2. Differential effects of *RAD51* and *RAD59* deletions on gross-chromosomal rearrangement (GCR) formation in *sgs1* and *sgs1 exo1* mutants

Genotype	GCR Rate[i] (Can^r 5-FOA^r x 10^{-10})	95% CI[ii] (Can^r 5-FOA^r x 10^{-10})
wildtype	1.1	< 1 – 6.2
sgs1	71	53-104
exo1	14	7-28
rad51	< 8	< 7-15
rad59	24	13-50
rad52	138	16-267
sgs1 exo1	40500	31000-49900
sgs1 rad51	14	12-24
sgs1 rad59	126	107-300
sgs1 rad52	308	140-452
sgs1 rad51 exo1	13100	8520-21900
sgs1 rad59 exo1	94900	67400-185000

[i]Gross-chromosomal rearrangement (GCR) rate for *sgs1 rad59* is from DOERFLER *et al.* 2011 (31).

[ii]95% confidence intervals (CI) were calculated according to NAIR *et al.* 1940 (64).

Table S4.1. *Saccharomyces cerevisiae* strains used in this study

Strain ID[i]	Genotype
KSHY802	*MATa, ura3-52, leu2Δ1, trp1Δ63, his3Δ200, lys2Bgl, hom3-10, ade2Δ1, ade8, hxt13::URA3*
KHSY978	*MATa, ura3-52, trp1Δ63, his3Δ200, leu2Δ1, lys2Bgl, hom3-10, ade2Δ1, ade8, hxt13::URA3, srs2::G418*
KHSY1256	*MATa, ura3-52, trp1Δ63, his3Δ200, leu2Δ1, lys2Bgl, hom3-10, ade2Δ1, ade8, hxt13::URA3, rrm3::G418*
KHSY1338	*MATa, ura3-52, trp1Δ63, his3Δ200, leu2Δ1, lys2Bgl, hom3-10, ade2Δ1, ade8, hxt13::URA3, sgs1::TRP1*
KHSY2295	*MATa, ura3-52, trp1Δ63, his3Δ200, leu2Δ1, lys2Bgl, hom3-10, ade2Δ1, ade8, hxt13::URA3, rad59::G418, sgs1::TRP1*
KHSY2333	*MATa, ura3-52, trp1Δ63, his3Δ200, leu2Δ1, lys2Bgl, hom3-10, ade2Δ1, ade8, hxt13::URA3, pol32::loxP-G418-loxP*
KHSY2338	*MATa, ura3-52, trp1Δ63, his3Δ200, leu2Δ1, lys2Bgl, hom3-10, ade2Δ1, ade8, hxt13::URA3, exo1::loxP-G418-loxP*
KHSY2385	*MATα, ura3Δ0, leu2Δ0, his3Δ1, lys2Δ0, RAD51.V5.3xVSV.KANMX6*
KHSY2402	*MATa, ura3-52, trp1Δ63, his3Δ200, leu2Δ1, lys2Bgl, hom3-10, ade2Δ1, ade8, hxt13::URA3, exo1::loxP-G418-loxP, sgs1::TRP1*
KHSY2437	*MATa, ura3-52, trp1Δ63, his3Δ200, leu2Δ1, lys2Bgl, hom3-10, ade2Δ1, ade8, hxt13::URA3, pol32::loxP-G418-loxP, sgs1::TRP1*
KHSY4458	*MATa, ura3-52, trp1Δ63, his3Δ200, leu2Δ1, lys2Bgl, hom3-10, ade2Δ1, ade8, hxt13::URA3, exo1::loxP-G418-loxP, pol32::loxP-G418-loxP*
KHSY4484	*MATa, ura3-52, trp1Δ63, his3Δ200, leu2Δ1, lys2Bgl, hom3-10, ade2Δ1, ade8, hxt13::URA3 exo1::loxP-G418-loxP, rad59::G418*
KHSY4716	*MATa, ura3-52, trp1Δ63, his3Δ200, leu2Δ1, lys2Bgl, hom3-10, ade2Δ1, ade8, hxt13::URA3, top3::G418*
KHSY4800	*ura3-52/ura3-52, trp1Δ63/trp1Δ63, hisΔ200/hisΔ200, EXO1/exo1::HIS3, RAD52/rad52::URA*
KHSY4805	*MATα, ura3-52, trp1Δ63, hisΔ200, exo1::HIS3, rad52::URA*
KHSY4810	*ura3-52/ura3-52, trp1Δ63/trp1Δ63, hisΔ200/hisΔ200, EXO1/exo1::HIS3, RAD52/rad52::URA, SGS1/sgs1::TRP1*
KHSY5049	*MATa, ura3-52, trp1Δ63, hisΔ200, rad59::HIS3*
KHSY5051	*MATα, ura3-52, trp1Δ63, hisΔ200, exo1::HIS3, rad59::HIS3*
KHSY5052	*ura3-52/ura3-52, trp1Δ63/trp1Δ63, hisΔ200/hisΔ200, EXO1/exo1::HIS3, RAD59/rad59::HIS3*
KHSY5055	*MATa, ura3-52, trp1Δ63, hisΔ200, rad51::HIS3*
KHSY5056	*ura3-52/ura3-52, trp1Δ63/trp1Δ63, hisΔ200/hisΔ200, EXO1/exo1::HIS3, RAD51/rad51::HIS3*

Table S4.1. *Saccharomyces cerevisiae* strains used in this study *(continued)*.

KHSY5057   *MATα, ura3-52, trp1Δ63, hisΔ200, exo1::HIS3, rad51::HIS3*

KHSY5059   *ura3-52/ura3-52, trp1Δ63/trp1Δ63, hisΔ200/hisΔ200, EXO1/exo1::HIS3, RAD51/rad51::HIS3, SGS1/sgs1::TRP1*

KHSY5060   *ura3-52/ura3-52, trp1Δ63/trp1Δ63, hisΔ200/hisΔ200, EXO1/exo1::HIS3, RAD59/rad59::HIS3, SGS1/sgs1::TRP1*

KHSY5067   *MATa, ura3-52, trp1Δ63, his3Δ200, leu2Δ1, lys2Bgl, hom3-10, ade2Δ1, ade8, hxt13::URA3, rad59::HIS3*

KHSY5068   *MATa, ura3-52, trp1Δ63, his3Δ200, leu2Δ1, lys2Bgl, hom3-10, ade2Δ1, ade8, hxt13::URA3, rad51::HIS3*

KHSY5095   *MATa, ura3-52, trp1Δ63, his3Δ200, leu2Δ1, lys2Bgl, hom3-10, ade2Δ1, ade8, hxt13::URA3, rad51::HIS3, sgs1::TRP1*

KHSY5098   *MATa, ura3-52, trp1Δ63, his3Δ200, leu2Δ1, lys2Bgl, hom3-10, ade2Δ1, ade8, hxt13::URA3, exo1::loxP-G418-loxP, rad59::HIS3, sgs1::TRP1*

KHSY5099   *MATa, ura3-52, trp1Δ63, his3Δ200, leu2Δ1, lys2Bgl, hom3-10, ade2Δ1, ade8, hxt13::URA3, exo1::loxP-G418-loxP, rad51::HIS3*

KHSY5099   *MATa, ura3-52, trp1Δ63, his3Δ200, leu2Δ1, lys2Bgl, hom3-10, ade2Δ1, ade8, hxt13::URA3, exo1::loxP-G418-loxP, rad51::HIS3*

KHSY5102   *MATa, ura3-52, trp1Δ63, his3Δ200, leu2Δ1, lys2Bgl, hom3-10, ade2Δ1, ade8, hxt13::URA3, exo1::loxP-G418-loxP, rad51::HIS3, sgs1::TRP1*

KHSY5109   *MATa, ura3-52, trp1Δ63, his3Δ200, leu2Δ1, lys2Bgl, hom3-10, ade2Δ1, ade8, hxt13::URA3, sgs1-F1192D.TRP1*

KHSY5132   *MATa, ura3-52, trp1Δ63, his3Δ200, leu2Δ1, lys2Bgl, hom3-10, ade2Δ1, ade8, hxt13::URA3, exo1::loxP-G418-loxP, sgs1-F1192D.TRP1*

KHSY5222   *MATa, ura3-52, trp1Δ63, his3Δ200, leu2Δ1, lys2Bgl, hom3-10, ade2Δ1, ade8, hxt13::URA3, rrm3::G418, sgs1-F1192D.TRP1*

KHSY5225   *MATa, ura3-52, trp1Δ63, his3Δ200, leu2Δ1, lys2Bgl, hom3-10, ade2Δ1, ade8, hxt13::URA3, sgs1-F1192D.TRP1, srs2::G418*

KHSY5229   *ura3-52/ura3-52, leu2Δ1/ leu2Δ1, trp1Δ63/trp1Δ63, his3Δ200/his3Δ200, lys2ΔBgl/ lys2ΔBgl, hom3-10/ hom3-10, ade2Δ1/ade2Δ1, ade8/ade8, YEL069C::URA3/YEL069C::URA3, sgs1::TRP1/sgs1-F1192D.TRP1*

KHSY5233   *MATa, ura3-52, trp1Δ63, his3Δ200, leu2Δ1, lys2Bgl, hom3-10, ade2Δ1, ade8, hxt13::URA3, pol32::loxP-G418-loxP, sgs1-F1192D.TRP1*

KHSY5253   *ura3-52/ura3-52, leu2Δ1/ leu2Δ1, trp1Δ63/trp1Δ63, his3Δ200/his3Δ200, lys2ΔBgl/ lys2ΔBgl, hom3-10/ hom3-10, ade2Δ1/ade2Δ1, ade8/ade8, YEL069C::URA3/YEL069C::URA3, sgs1::TRP1/sgs1::TRP1*

KHSY5255   *ura3-52/ura3-52, leu2Δ1/ leu2Δ1, trp1Δ63/trp1Δ63, his3Δ200/his3Δ200, lys2ΔBgl/ lys2ΔBgl, hom3-10/*

Table S4.1. *Saccharomyces cerevisiae* strains used in this study *(continued)*.

	hom3-10, ade2Δ1/ade2Δ1, ade8/ade8, YEL069C::URA3/YEL069C::URA3, SGS1/sgs1-F1192D.TRP1
KHSY5257	*MATa, ura3-52, trp1Δ63, his3Δ200, leu2Δ1, lys2Bgl, hom3-10, ade2Δ1, ade8, hxt13::URA3, sae2::TRP1*
KHSY5262	*ura3-52/ura3-52, leu2Δ1/ leu2Δ1, trp1Δ63/trp1Δ63, his3Δ200/his3Δ200, lys2ΔBgl/ lys2ΔBgl, hom3-10/ hom3-10, ade2Δ1/ade2Δ1, ade8/ade8, YEL069C::URA3/YEL069C::URA3*
KHSY5265	*ura3-52/ura3-52, leu2Δ1/ leu2Δ1, trp1Δ63/trp1Δ63, his3Δ200/his3Δ200, lys2ΔBgl/ lys2ΔBgl, hom3-10/ hom3-10, ade2Δ1/ade2Δ1, ade8/ade8, YEL069C::URA3/YEL069C::URA3, SGS1/sgs1::TRP1*
KHSY5274	*MATa, ura3-52, trp1Δ63, his3Δ200, leu2Δ1, lys2Bgl, hom3-10, ade2Δ1, ade8, hxt13::URA3, mre11::HIS3 , sgs1-F1192D.TRP1*
KHSY5289	*ura3-52/ura3-52, leu2Δ1/ leu2Δ1, trp1Δ63/trp1Δ63, his3Δ200/his3Δ200, lys2ΔBgl/ lys2ΔBgl, hom3-10/ hom3-10, ade2Δ1/ade2Δ1, ade8/ade8, YEL069C::URA3/YEL069C::URA3, sgs1-F1192D.TRP1/sgs1-F1192D.TRP1*
KHSY5304	*MATa, ura3-52, trp1Δ63, his3Δ200, leu2Δ1, lys2Bgl, hom3-10, ade2Δ1, ade8, hxt13::URA3, sae2::TRP1, sgs1-F1192D.TRP1*
KHSY5312	*MATa, ura3-52, trp1Δ63, his3Δ200, leu2Δ1, lys2Bgl, hom3-10, ade2Δ1, ade8, hxt13::URA3, sgs1-F1192D.TRP1, top3::G418*
KHSY5315	*MATa, ura3-52, trp1Δ63, his3Δ200, leu2Δ1, lys2Bgl, hom3-10, ade2Δ1, ade8, hxt13::URA3, exo1::loxP-G418-loxP, pol32::loxP-G418-loxP, sgs1-F1192D.TRP1*
KHSY5320	*MATa, ura3-52, trp1Δ63, his3Δ200, leu2Δ1, lys2Bgl, hom3-10, ade2Δ1, ade8, hxt13::URA3, sgs1-K706A, F1192D.TRP1*
KHSY5321	*MATa, ura3-52, trp1Δ63, his3Δ200, leu2Δ1, lys2Bgl, hom3-10, ade2Δ1, ade8, hxt13::URA3, sgs1-K706A.TRP1*
KHSY5335	*MATa, ura3-52, trp1Δ63, his3Δ200, leu2Δ1, lys2Bgl, hom3-10, ade2Δ1, ade8, hxt13::URA3, pol32::loxP-G418-loxP, rad51::HIS3*
KHSY5354	*MATa, ura3-52, trp1Δ63, his3Δ200, leu2Δ1, lys2Bgl, hom3-10, ade2Δ1, ade8, hxt13::URA3, mre11::HIS3*
KHSY5356	*MATa, ura3-52, trp1Δ63, his3Δ200, leu2Δ1, lys2Bgl, hom3-10, ade2Δ1, ade8, hxt13::URA3, sgs1::TRP1, top3::G418*
KHSY5363	*MATa, ura3-52, trp1Δ63, his3Δ200, leu2Δ1, lys2Bgl, hom3-10, ade2Δ1, ade8, hxt13::URA3, pol32::loxP-G418-loxP, sgs1-K706A, F1192D.TRP1*
KHSY5365	*MATa, ura3-52, trp1Δ63, his3Δ200, leu2Δ1, lys2Bgl, hom3-10, ade2Δ1, ade8, hxt13::URA3, pol32::loxP-G418-loxP, sgs1-K706A.TRP1*
KHSY5373	*MATa, ura3-52, trp1Δ63, his3Δ200, leu2Δ1, lys2Bgl, hom3-10, ade2Δ1, ade8, hxt13::URA3, mre11::HIS3 , sae2::TRP1*

Table S4.1. *Saccharomyces cerevisiae* strains used in this study *(continued)*.

KHSY5377	*MATa, ura3-52, trp1Δ63, his3Δ200, leu2Δ1, lys2Bgl, hom3-10, ade2Δ1, ade8, hxt13::URA3, mre11:HIS3: , sae2::TRP1, sgs1-F1192D.TRP1*
RDKY2614	*MATα, ura3-52, trp1Δ63, hisΔ200, exo1::HIS3*
RDKY2666	*MATa, ura3-52, trp1Δ63, hisΔ200*
RDKY2710	*MATa, ura3-52, trp1Δ63, hisΔ200, rad52::URA*
RDKY5290	*MATa, ura3-52, trp1Δ63, hisΔ200, sgs1::TRP1*

[i] RDKY strains are a gift from Richard Kolodner (University of California, San Diego).

Table S4.2. Rates of accumulating spontaneous mutations at *CAN1*, *hom3-10*, and *lys2-BgI* loci

Genotype	Mutation rate					
	Can^r (x 10^{-7})	95% CI[i]	Hom$^+$ (x 10^{-9})	95% CI	Lys$^+$ (x 10^{-9})	95% CI
wildtype	**1.5**	0.9-2	**2.2**	1.8-2.8	**4.7**	2.3-6.3
sgs1	**2.7**	1.8-4	**1.7**	1.1-2.4	**11**	7.6-12
sgs1-FD	**1.4**	1.2-1.6	**4.1**	3.3-5.3	**6.0**	4.6-11.9
pol32	**2.1**	1.1-3.4	**8.7**	5.1-12.1	**6.9**	4.5-8.9
pol32 sgs1	**1.5**	0.9-2.4	**10.0**	8.0-16.0	**10.0**	6.0-14.0

[i] 95% confidence intervals (CI) were calculated according to Nair *et al.* 1940 (64).

REFERENCES

[1] E.P. Mimitou, L.S. Symington, Ku prevents Exo1 and Sgs1-dependent resection of DNA ends in the absence of a functional MRX complex or Sae2, The EMBO journal, 29 (2010) 3358-3369.

[2] G. Ira, A. Pellicioli, A. Balijja, X. Wang, S. Fiorani, W. Carotenuto, G. Liberi, D. Bressan, L. Wan, N.M. Hollingsworth, J.E. Haber, M. Foiani, DNA end resection, homologous recombination and DNA damage checkpoint activation require CDK1, Nature, 431 (2004) 1011-1017.

[3] P. Huertas, F. Cortes-Ledesma, A.A. Sartori, A. Aguilera, S.P. Jackson, CDK targets Sae2 to control DNA-end resection and homologous recombination, Nature, 455 (2008) 689-692.

[4] J.H. Barlow, M. Lisby, R. Rothstein, Differential regulation of the cellular response to DNA double-strand breaks in G1, Mol Cell, 30 (2008) 73-85.

[5] K.M. Trujillo, D.H. Roh, L. Chen, S. Van Komen, A. Tomkinson, P. Sung, Yeast xrs2 binds DNA and helps target rad50 and mre11 to DNA ends, J Biol Chem, 278 (2003) 48957-48964.

[6] H. Niu, W.H. Chung, Z. Zhu, Y. Kwon, W. Zhao, P. Chi, R. Prakash, C. Seong, D. Liu, L. Lu, G. Ira, P. Sung, Mechanism of the ATP-dependent DNA end-resection machinery from Saccharomyces cerevisiae, Nature, 467 (2010) 108-111.

[7] M.L. Nicolette, K. Lee, Z. Guo, M. Rani, J.M. Chow, S.E. Lee, T.T. Paull, Mre11-Rad50-Xrs2 and Sae2 promote 5' strand resection of DNA double-strand breaks, Nature structural & molecular biology, 17 (2010) 1478-1485.

185

[8] E. Cannavo, P. Cejka, Sae2 promotes dsDNA endonuclease activity within Mre11-Rad50-Xrs2 to resect DNA breaks, Nature, 514 (2014) 122-125.

[9] E.P. Mimitou, L.S. Symington, Sae2, Exo1 and Sgs1 collaborate in DNA double-strand break processing, Nature, 455 (2008) 770-774.

[10] Z. Zhu, W.H. Chung, E.Y. Shim, S.E. Lee, G. Ira, Sgs1 helicase and two nucleases Dna2 and Exo1 resect DNA double-strand break ends, Cell, 134 (2008) 981-994.

[11] M. Levikova, C. Pinto, P. Cejka, The motor activity of DNA2 functions as an ssDNA translocase to promote DNA end resection, Genes Dev, 31 (2017) 493-502.

[12] B. Song, P. Sung, Functional interactions among yeast Rad51 recombinase, Rad52 mediator, and replication protein A in DNA strand exchange, The Journal of biological chemistry, 275 (2000) 15895-15904.

[13] J.H. New, T. Sugiyama, E. Zaitseva, S.C. Kowalczykowski, Rad52 protein stimulates DNA strand exchange by Rad51 and replication protein A, Nature, 391 (1998) 407-410.

[14] L. Krejci, S. Van Komen, Y. Li, J. Villemain, M.S. Reddy, H. Klein, T. Ellenberger, P. Sung, DNA helicase Srs2 disrupts the Rad51 presynaptic filament, Nature, 423 (2003) 305-309.

[15] X. Veaute, J. Jeusset, C. Soustelle, S.C. Kowalczykowski, E. Le Cam, F. Fabre, The Srs2 helicase prevents recombination by disrupting Rad51 nucleoprotein filaments, Nature, 423 (2003) 309-312.

[16] J. Liu, L. Renault, X. Veaute, F. Fabre, H. Stahlberg, W.D. Heyer, Rad51 paralogues Rad55-Rad57 balance the antirecombinase Srs2 in Rad51 filament formation, Nature, 479 (2011) 245-248.

[17] P. Cejka, J.L. Plank, C.Z. Bachrati, I.D. Hickson, S.C. Kowalczykowski, Rmi1 stimulates decatenation of double Holliday junctions during dissolution by Sgs1-Top3, Nature structural & molecular biology, 17 (2010) 1377-1382.

[18] L. Wu, I.D. Hickson, The Bloom's syndrome helicase suppresses crossing over during homologous recombination, Nature, 426 (2003) 870-874.

[19] P. Cejka, J.L. Plank, C.C. Dombrowski, S.C. Kowalczykowski, Decatenation of DNA by the S. cerevisiae Sgs1-Top3-Rmi1 and RPA complex: a mechanism for disentangling chromosomes, Mol Cell, 47 (2012) 886-896.

[20] L.S. Symington, Role of RAD52 epistasis group genes in homologous recombination and double-strand break repair, Microbiology and molecular biology reviews : MMBR, 66 (2002) 630-670, table of contents.

[21] A. Mehta, J.E. Haber, Sources of DNA double-strand breaks and models of recombinational DNA repair, Cold Spring Harbor perspectives in biology, 6 (2014) a016428.

[22] E.L. Ivanov, N. Sugawara, J. Fishman-Lobell, J.E. Haber, Genetic requirements for the single-strand annealing pathway of double-strand break repair in Saccharomyces cerevisiae, Genetics, 142 (1996) 693-704.

[23] P. Sung, H. Klein, Mechanism of homologous recombination: mediators and helicases take on regulatory functions, Nature reviews. Molecular cell biology, 7 (2006) 739-750.

[24] N.R. Pannunzio, G.M. Manthey, A.M. Bailis, RAD59 and RAD1 cooperate in translocation formation by single-strand annealing in Saccharomyces cerevisiae, Current genetics, 56 (2010) 87-100.

[25] N. Sugawara, G. Ira, J.E. Haber, DNA length dependence of the single-strand annealing pathway and the role of Saccharomyces cerevisiae RAD59 in double-strand break repair, Mol Cell Biol, 20 (2000) 5300-5309.

[26] G. Ira, J.E. Haber, Characterization of RAD51-independent break-induced replication that acts preferentially with short homologous sequences, Molecular and cellular biology, 22 (2002) 6384-6392.

[27] A.P. Davis, L.S. Symington, RAD51-dependent break-induced replication in yeast, Molecular and cellular biology, 24 (2004) 2344-2351.

[28] C.E. Smith, B. Llorente, L.S. Symington, Template switching during break-induced replication, Nature, 447 (2007) 102-105.

[29] K.H. Schmidt, E. Viebranz, L. Doerfler, C. Lester, A. Rubenstein, Formation of complex and unstable chromosomal translocations in yeast, PloS one, 5 (2010) e12007.

[30] K.H. Schmidt, J. Wu, R.D. Kolodner, Control of translocations between highly diverged genes by Sgs1, the Saccharomyces cerevisiae homolog of the Bloom's syndrome protein, Molecular and cellular biology, 26 (2006) 5406-5420.

[31] L. Doerfler, L. Harris, E. Viebranz, K.H. Schmidt, Differential genetic interactions between Sgs1, DNA-damage checkpoint components and DNA repair factors in the maintenance of chromosome stability, Genome integrity, 2 (2011) 8.

[32] E. Cannavo, P. Cejka, S.C. Kowalczykowski, Relationship of DNA degradation by Saccharomyces cerevisiae exonuclease 1 and its stimulation by RPA and Mre11-Rad50-Xrs2 to DNA end resection, Proceedings of the National Academy of Sciences of the United States of America, 110 (2013) E1661-1668.

[33] M. Lisby, J.H. Barlow, R.C. Burgess, R. Rothstein, Choreography of the DNA damage response: spatiotemporal relationships among checkpoint and repair proteins, Cell, 118 (2004) 699-713.

[34] I. Chiolo, W. Carotenuto, G. Maffioletti, J.H. Petrini, M. Foiani, G. Liberi, Srs2 and Sgs1 DNA helicases associate with Mre11 in different subcomplexes following checkpoint activation and CDK1-mediated Srs2 phosphorylation, Molecular and cellular biology, 25 (2005) 5738-5751.

[35] J.R. Mullen, F.S. Nallaseth, Y.Q. Lan, C.E. Slagle, S.J. Brill, Yeast Rmi1/Nce4 controls genome stability as a subunit of the Sgs1-Top3 complex, Molecular and cellular biology, 25 (2005) 4476-4487.

[36] A. Ui, M. Seki, H. Ogiwara, R. Onodera, S. Fukushige, F. Onoda, T. Enomoto, The ability of Sgs1 to interact with DNA topoisomerase III is essential for damage-induced recombination, DNA Repair (Amst), 4 (2005) 191-201.

[37] S. Gangloff, J.P. McDonald, C. Bendixen, L. Arthur, R. Rothstein, The yeast type I topoisomerase Top3 interacts with Sgs1, a DNA helicase homolog: a potential eukaryotic reverse gyrase, Molecular and cellular biology, 14 (1994) 8391-8398.

[38] A.M. Hegnauer, N. Hustedt, K. Shimada, B.L. Pike, M. Vogel, P. Amsler, S.M. Rubin, F. van Leeuwen, A. Guenole, H. van Attikum, N.H. Thoma, S.M. Gasser, An N-terminal acidic region of Sgs1 interacts with Rpa70 and recruits Rad53 kinase to stalled forks, The EMBO journal, 31 (2012) 3768-3783.

[39] J.A. Kennedy, G.W. Daughdrill, K.H. Schmidt, A transient alpha-helical molecular recognition element in the disordered N-terminus of the Sgs1 helicase is critical for

chromosome stability and binding of Top3/Rmi1, Nucleic acids research, 41 (2013) 10215-10227.

[40] L. Wu, S.L. Davies, N.C. Levitt, I.D. Hickson, Potential role for the BLM helicase in recombinational repair via a conserved interaction with RAD51, The Journal of biological chemistry, 276 (2001) 19375-19381.

[41] J. Saffi, H. Feldmann, E.L. Winnacker, J.A. Henriques, Interaction of the yeast Pso5/Rad16 and Sgs1 proteins: influences on DNA repair and aging, Mutation research, 486 (2001) 195-206.

[42] P.M. Watt, E.J. Louis, R.H. Borts, I.D. Hickson, Sgs1: a eukaryotic homolog of E. coli RecQ that interacts with topoisomerase II in vivo and is required for faithful chromosome segregation, Cell, 81 (1995) 253-260.

[43] W.M. Fricke, V. Kaliraman, S.J. Brill, Mapping the DNA topoisomerase III binding domain of the Sgs1 DNA helicase, The Journal of biological chemistry, 276 (2001) 8848-8855.

[44] C. Dherin, E. Gueneau, M. Francin, M. Nunez, S. Miron, S.E. Liberti, L.J. Rasmussen, S. Zinn-Justin, B. Gilquin, J.B. Charbonnier, S. Boiteux, Characterization of a highly conserved binding site of Mlh1 required for exonuclease I-dependent mismatch repair, Molecular and cellular biology, 29 (2009) 907-918.

[45] W.M. Fricke, S.J. Brill, Slx1-Slx4 is a second structure-specific endonuclease functionally redundant with Sgs1-Top3, Genes & development, 17 (2003) 1768-1778.

[46] J.R. Mullen, V. Kaliraman, S.J. Brill, Bipartite structure of the SGS1 DNA helicase in Saccharomyces cerevisiae, Genetics, 154 (2000) 1101-1114.

[47] D.A. Sinclair, K. Mills, L. Guarente, Accelerated aging and nucleolar fragmentation in yeast sgs1 mutants, Science (New York, N.Y.), 277 (1997) 1313-1316.

[48] K. Myung, A. Datta, C. Chen, R.D. Kolodner, SGS1, the Saccharomyces cerevisiae homologue of BLM and WRN, suppresses genome instability and homeologous recombination, Nature genetics, 27 (2001) 113-116.

[49] J.R. Mullen, V. Kaliraman, S.S. Ibrahim, S.J. Brill, Requirement for three novel protein complexes in the absence of the Sgs1 DNA helicase in Saccharomyces cerevisiae, Genetics, 157 (2001) 103-118.

[50] K.H. Schmidt, R.D. Kolodner, Requirement of Rrm3 helicase for repair of spontaneous DNA lesions in cells lacking Srs2 or Sgs1 helicase, Molecular and cellular biology, 24 (2004) 3213-3226.

[51] J.Z. Torres, S.L. Schnakenberg, V.A. Zakian, Saccharomyces cerevisiae Rrm3p DNA helicase promotes genome integrity by preventing replication fork stalling: viability of rrm3 cells requires the intra-S-phase checkpoint and fork restart activities, Molecular and cellular biology, 24 (2004) 3198-3212.

[52] S. Syed, C. Desler, L.J. Rasmussen, K.H. Schmidt, A Novel Rrm3 Function in Restricting DNA Replication via an Orc5-Binding Domain Is Genetically Separable from Rrm3 Function as an ATPase/Helicase in Facilitating Fork Progression, PLoS genetics, 12 (2016) e1006451.

[53] X. Pan, P. Ye, D.S. Yuan, X. Wang, J.S. Bader, J.D. Boeke, A DNA integrity network in the yeast Saccharomyces cerevisiae, Cell, 124 (2006) 1069-1081.

[54] S.K. Lee, R.E. Johnson, S.L. Yu, L. Prakash, S. Prakash, Requirement of yeast SGS1 and SRS2 genes for replication and transcription, Science (New York, N.Y.), 286 (1999) 2339-2342.

[55] R.M. Spell, S. Jinks-Robertson, Examination of the roles of Sgs1 and Srs2 helicases in the enforcement of recombination fidelity in Saccharomyces cerevisiae, Genetics, 168 (2004) 1855-1865.

[56] T.F. Wang, W.M. Kung, Supercomplex formation between Mlh1-Mlh3 and Sgs1-Top3 heterocomplexes in meiotic yeast cells, Biochemical and biophysical research communications, 296 (2002) 949-953.

[57] A.D. Amin, A.B. Chaix, R.P. Mason, R.M. Badge, R.H. Borts, The roles of the Saccharomyces cerevisiae RecQ helicase SGS1 in meiotic genome surveillance, PloS one, 5 (2010) e15380.

[58] R.D. Gietz, R.A. Woods, Yeast transformation by the LiAc/SS Carrier DNA/PEG method, Methods Mol Biol, 313 (2006) 107-120.

[59] H. Mirzaei, S. Syed, J. Kennedy, K.H. Schmidt, Sgs1 truncations induce genome rearrangements but suppress detrimental effects of BLM overexpression in Saccharomyces cerevisiae, Journal of molecular biology, 405 (2011) 877-891.

[60] H. Mirzaei, K. Schmidt, Non-Bloom-syndrome-associated partial and total loss-of-function variants of BLM helicase, Proc Natl Acad Sci U S A, (2012).

[61] K.H. Schmidt, E.B. Viebranz, L.B. Harris, H. Mirzaei-Souderjani, S. Syed, R. Medicus, Defects in DNA lesion bypass lead to spontaneous chromosomal rearrangements and increased cell death, Eukaryot Cell, 9 (2010) 315-324.

[62] D.E. Lea, C.A. Coulson, The distribution of the numbers of mutants in bacterial populations, Journ. of Genetics, 49 (1949) 264-285.

[63] R.A. Reenan, R.D. Kolodner, Characterization of insertion mutations in the Saccharomyces cerevisiae MSH1 and MSH2 genes: evidence for separate mitochondrial and nuclear functions, Genetics, 132 (1992) 975-985.

[64] K.R. Nair, Table of confidence intervals for the median in samples from any continuous population., Sankhya, (1940) 551-558.

[65] G. Pedrazzi, C. Perrera, H. Blaser, P. Kuster, G. Marra, S.L. Davies, G.H. Ryu, R. Freire, I.D. Hickson, J. Jiricny, I. Stagljar, Direct association of Bloom's syndrome gene product with the human mismatch repair protein MLH1, Nucleic acids research, 29 (2001) 4378-4386.

[66] M. Frank-Vaillant, S. Marcand, NHEJ regulation by mating type is exercised through a novel protein, Lif2p, essential to the ligase IV pathway, Genes Dev, 15 (2001) 3005-3012.

[67] X.C. Li, B.K. Tye, Ploidy dictates repair pathway choice under DNA replication stress, Genetics, 187 (2011) 1031-1040.

[68] S. Gravel, J.R. Chapman, C. Magill, S.P. Jackson, DNA helicases Sgs1 and BLM promote DNA double-strand break resection, Genes Dev, 22 (2008) 2767-2772.

[69] L. Doerfler, K.H. Schmidt, Exo1 phosphorylation status controls the hydroxyurea sensitivity of cells lacking the Pol32 subunit of DNA polymerases delta and zeta, DNA Repair (Amst), 24 (2014) 26-36.

[70] E. Shor, S. Gangloff, M. Wagner, J. Weinstein, G. Price, R. Rothstein, Mutations in homologous recombination genes rescue top3 slow growth in Saccharomyces cerevisiae, Genetics, 162 (2002) 647-662.

[71] A.H. Tong, M. Evangelista, A.B. Parsons, H. Xu, G.D. Bader, N. Page, M. Robinson, S. Raghibizadeh, C.W. Hogue, H. Bussey, B. Andrews, M. Tyers, C. Boone, Systematic genetic analysis with ordered arrays of yeast deletion mutants, Science (New York, N.Y.), 294 (2001) 2364-2368.

[72] S.L. Ooi, D.D. Shoemaker, J.D. Boeke, DNA helicase gene interaction network defined using synthetic lethality analyzed by microarray, Nature genetics, 35 (2003) 277-286.

[73] K.A. Bernstein, E.P. Mimitou, M.J. Mihalevic, H. Chen, I. Sunjaveric, L.S. Symington, R. Rothstein, Resection activity of the Sgs1 helicase alters the affinity of DNA ends for homologous recombination proteins in Saccharomyces cerevisiae, Genetics, 195 (2013) 1241-1251.

[74] K.A. Bernstein, E. Shor, I. Sunjevaric, M. Fumasoni, R.C. Burgess, M. Foiani, D. Branzei, R. Rothstein, Sgs1 function in the repair of DNA replication intermediates is separable from its role in homologous recombinational repair, The EMBO journal, 28 (2009) 915-925.

[75] M. Chang, M. Bellaoui, C. Zhang, R. Desai, P. Morozov, L. Delgado-Cruzata, R. Rothstein, G.A. Freyer, C. Boone, G.W. Brown, RMI1/NCE4, a suppressor of genome instability, encodes a member of the RecQ helicase/Topo III complex, The EMBO journal, 24 (2005) 2024-2033.

[76] C.L. Fasching, P. Cejka, S.C. Kowalczykowski, W.D. Heyer, Top3-Rmi1 dissolve Rad51-mediated D loops by a topoisomerase-based mechanism, Mol Cell, 57 (2015) 595-606.

[77] P. Cejka, E. Cannavo, P. Polaczek, T. Masuda-Sasa, S. Pokharel, J.L. Campbell, S.C. Kowalczykowski, DNA end resection by Dna2-Sgs1-RPA and its stimulation by Top3-Rmi1 and Mre11-Rad50-Xrs2, Nature, 467 (2010) 112-116.

[78] A.S. Ivessa, J.Q. Zhou, V.P. Schulz, E.K. Monson, V.A. Zakian, Saccharomyces Rrm3p, a 5' to 3' DNA helicase that promotes replication fork progression through telomeric and subtelomeric DNA, Genes & development, 16 (2002) 1383-1396.

[79] P.M. Burgers, K.J. Gerik, Structure and processivity of two forms of Saccharomyces cerevisiae DNA polymerase delta, J Biol Chem, 273 (1998) 19756-19762.

[80] M.E. Huang, A.G. Rio, M.D. Galibert, F. Galibert, Pol32, a subunit of Saccharomyces cerevisiae DNA polymerase delta, suppresses genomic deletions and is involved in the mutagenic bypass pathway, Genetics, 160 (2002) 1409-1422.

[81] E. Johansson, P. Garg, P.M. Burgers, The Pol32 subunit of DNA polymerase delta contains separable domains for processive replication and proliferating cell nuclear antigen (PCNA) binding, J Biol Chem, 279 (2004) 1907-1915.

[82] L. Signon, M.N. Simon, The analysis of S. cerevisiae cells deleted for mitotic cyclin Clb2 reveals a novel requirement of Sgs1 DNA helicase and Exonuclease 1 when replication forks break in the presence of alkylation damage, Mutation research, 769 (2014) 80-92.

[83] E.Y. Shim, W.H. Chung, M.L. Nicolette, Y. Zhang, M. Davis, Z. Zhu, T.T. Paull, G. Ira, S.E. Lee, Saccharomyces cerevisiae Mre11/Rad50/Xrs2 and Ku proteins regulate association of Exo1 and Dna2 with DNA breaks, The EMBO journal, 29 (2010) 3370-3380.

[84] H. Chen, R.A. Donnianni, N. Handa, S.K. Deng, J. Oh, L.A. Timashev, S.C. Kowalczykowski, L.S. Symington, Sae2 promotes DNA damage resistance by removing the Mre11-Rad50-Xrs2 complex from DNA and attenuating Rad53 signaling, Proceedings of the National Academy of Sciences of the United States of America, 112 (2015) E1880-1887.

[85] M. Clerici, D. Mantiero, G. Lucchini, M.P. Longhese, The Saccharomyces cerevisiae Sae2 protein negatively regulates DNA damage checkpoint signalling, EMBO reports, 7 (2006) 212-218.

[86] F. Puddu, T. Oelschlaegel, I. Guerini, N.J. Geisler, H. Niu, M. Herzog, I. Salguero, B. Ochoa-Montano, E. Vire, P. Sung, D.J. Adams, T.M. Keane, S.P. Jackson, Synthetic viability genomic screening defines Sae2 function in DNA repair, The EMBO journal, 34 (2015) 1509-1522.

[87] T. Usui, H. Ogawa, J.H. Petrini, A DNA damage response pathway controlled by Tel1 and the Mre11 complex, Mol Cell, 7 (2001) 1255-1266.

[88] M. Ferrari, D. Dibitetto, G. De Gregorio, V.V. Eapen, C.C. Rawal, F. Lazzaro, M. Tsabar, F. Marini, J.E. Haber, A. Pellicioli, Functional interplay between the 53BP1-ortholog Rad9 and the Mre11 complex regulates resection, end-tethering and repair of a double-strand break, PLoS genetics, 11 (2015) e1004928.

[89] E. Gobbini, M. Villa, M. Gnugnoli, L. Menin, M. Clerici, M.P. Longhese, Sae2 Function at DNA Double-Strand Breaks Is Bypassed by Dampening Tel1 or Rad53 Activity, PLoS genetics, 11 (2015) e1005685.

[90] S. Gangloff, C. Soustelle, F. Fabre, Homologous recombination is responsible for cell death in the absence of the Sgs1 and Srs2 helicases, Nature genetics, 25 (2000) 192-194.

[91] D.G. Anderson, S.C. Kowalczykowski, The translocating RecBCD enzyme stimulates recombination by directing RecA protein onto ssDNA in a chi-regulated manner, Cell, 90 (1997) 77-86.

[92] W. Zhao, S. Vaithiyalingam, J. San Filippo, D.G. Maranon, J. Jimenez-Sainz, G.V. Fontenay, Y. Kwon, S.G. Leung, L. Lu, R.B. Jensen, W.J. Chazin, C. Wiese, P. Sung, Promotion of BRCA2-Dependent Homologous Recombination by DSS1 via RPA Targeting and DNA Mimicry, Mol Cell, 59 (2015) 176-187.

[93] K. Engels, M. Giannattasio, M. Muzi-Falconi, M. Lopes, S. Ferrari, 14-3-3 Proteins regulate exonuclease 1-dependent processing of stalled replication forks, PLoS genetics, 7 (2011) e1001367.

[94] N.R. Pannunzio, G.M. Manthey, A.M. Bailis, RAD59 is required for efficient repair of simultaneous double-strand breaks resulting in translocations in Saccharomyces cerevisiae, DNA Repair (Amst), 7 (2008) 788-800.

CHAPTER FIVE: IMPLICATIONS AND FUTURE DIRECTIONS

Proper repair of DNA lesions is essential for cell survival and prevention of disease. Defects in a variety of proteins involved in DNA repair have been shown to directly impact humans as illustrated by the increased predisposition to develop cancer. While only a small portion of cancers are hereditary, accounting only for ~10% of all cancers, the ability of the cell to respond to DNA damage plays a major role in all tumorigenesis and late-stage tumors that have become chemoresistant [1-4]. Hereditary defects in DNA repair proteins can lead to severe syndromes where patients have a higher propensity to develop cancer at an early age. Such is seen in defects in RecQ-helicases (Bloom's syndrome, Werner's syndrome, Rothmund-Thompson syndrome), mismatch repair (Lynch syndrome), and nucleotide excision repair (xeroderma pigmentosum) [5]. Increased prevalence of cancer is not exclusively linked to defects that result in syndromes, defects in some homologous recombination factors increase the risk of development of breast and ovarian cancer (BRCA1, BRCA2, BARD1, ATM, CDH1, CHEK2, PALB2, PTEN, STK11, and TP53) [1]. Understanding the role of components of the DNA damage response in maintaining genomic integrity is essential to understanding cancer risk, development, and in the advancement of drugs to treat cancer. We have, in these studies, used yeast as a model to study the role *SGS1* and *EXO1* in maintaining genomic stability. We have characterized their genetic interactions with other repair pathways and checkpoints, and

identified the domains of Exo1 required for these genetic interactions. We have also described the importance of a physical interaction site of Sgs1 with the homologous recombination factor Rad51 [6, 7]. Understanding *SGS1* and *EXO1* function is informative as both have human homologs, *BLM* and *EXO1*, respectively that have been shown to have similar functions [8, 9].

Chromosomal translocations in cells lacking Sgs1 are dependent on Rad52 paralog, Rad59.

In chapter two of this dissertation we have identified, through a candidate screen, checkpoint and DNA metabolic factors that suppress the formation of gross chromosomal rearrangements. We assessed the candidate's ability to promote or suppress a chromosomal translocation event between *CAN1, LYP1,* and *ALP1 (C/L/A)* that is observed in the absence of the Sgs1 helicase and the DNA damage checkpoint sensor, Mec3. It was previously found that the translocations between *C/L/A* in the *sgs1Δ mec3Δ* depend on the presence of the homologous recombination factor Rad52 [10]. We additionally found that these translocations that use short regions of homology rely on the Rad52 paralog Rad59 and checkpoint components Mec1 and Dun1. Rad51, the homologous recombination component that searches for homology in this study has been identified to be dispensable for translocations in the absence of Sgs1, the only RecQ helicase in *S. cerevisiae.* A defect in BLM in humans is associated with the genomic instability that is also observed in yeast lacking the BLM homolog Sgs1 [10]. Although the rate of GCRs did not differ between *sgs1Δ mec3Δ rad51Δ* and *sgs1Δ mec3Δ rad59Δ,* this has distinguished the role of Rad59 in the formation of the types of

199

GCRs as opposed to the rate of accumulation. The absence of Rad59 preventing the

formation *C/L/A* translocations but not change the accumulation of GCRs leaves other

repair mechanisms that must generate other forms of GCRs. The other types of repair

in the absence of Rad59 leave the open questions, what pathways contribute the

genome instability rate and what kind of GCR is formed to understand better what other

mechanisms contribute to genome instability.

In chapter four we investigated further the role of Rad51 and Rad59 in the

suppression of genome rearrangements. We found that Exo1 is a strong suppressor of

genome rearrangements in cells lacking Sgs1 and that both of these proteins are

required for long-range resection of DNA double-strand break ends. Through a

candidate screen of DNA metabolic factors, we found that Rad52 is essential in

resection deficient *sgs1Δ exo1Δ* mutants. The synthetic lethality of the *sgs1Δ exo1Δ*

rad52Δ mutant indicates that homology-mediated repair is necessary for cells that are

lacking Sgs1 and Exo1 resection. When we assessed the role of two sub-pathways of

Rad52 mediated repair we found that Rad59 rather than Rad51 was required for the

fitness of cells defective in the resection. We found that this role of Rad59 in preventing

mutagenic Rad51 mediated HR repair is also important in cells that just lack Sgs1,

indicating a larger role than previously thought for Rad59 in the prevention of genome

rearrangements. Determining what type of repair Rad59 engages in to prevent

illegitimate recombination by Rad51 still needs to be resolved. Assessing the

rearrangement type by mapping the breakpoint that is assessed in the GCR assay

would help determine how repair by Rad51 or Rad59 prevent these rearrangements

from occurring and will help elucidate the mechanism by which Rad59 prevents

genomic instability. Mutant alleles of *RAD59* have been identified that reduce Rad52 association with double-strand breaks (*rad59-K166A),* have an effect on homologous recombination (*rad59-K174A*and *rad59-F180A*), and affect homologous recombination without diminishing Rad52 association to DNA breaks (*rad59-Y92A)* [11]. To help identify the role of Rad59 in preventing aberrant recombination the mutant alleles of *RAD59* in the *sgs1Δ* mutants could combined and assessed for types of genome rearrangements.

Characterization of the Exo1 C-terminus in the prevention of genome instability

Sgs1 and Exo1 are known to redundantly resect DNA double-strand breaks to generate 3′-overhangs used for the homology search in homology-driven repair [12, 13]. We have shown that the loss of both Sgs1 and Exo1 substantially increase the accumulation of GCRs. Exo1 contains an N-terminal and enzymatic domain, and the C-terminus (predicted to unstructured) has been characterized to harbor physical interaction sites with mismatch repair proteins Msh2 and Mhl1. There are four phosphorylation sites implicated in the inhibition of its enzymatic function [14-16]. The role of the C-terminus of Exo1 in the formation of GCRs had not yet been determined. To better characterize the genetic interaction of *SGS1* and *EXO1,* we investigated what domains of Exo1 are required for the suppression of GCRs. We created systematic truncations from the C-terminus of Exo1 to determine what was necessary to maintain genome stability and challenged these cells with DNA damaging agents and measured the accumulation of GCRs. We show that the loss of phosphorylation sites and domains

required for the physical interaction of mismatch repair proteins of Exo1 is dispensable

for its function in the suppression of GCRs in the absence of Sgs1 and only its

enzymatic function is essential. The loss of Exo1 function occurs from the loss of 260 to

280 amino acids of the C-terminus, where three of the known phosphorylation sites are

lost, and the fourth remains intact in both truncations. The loss of the phosphorylation

sites that were found to modulate Exo1 function did not affect the formation of GCRs.

These phosphorylation sites were found to be important in the context of uncapped

telomeres where regulation single strand DNA produced by Exo1 is important for

modulating the checkpoint response [16]. The inhibition of Exo1 nuclease function is

not required in suppressing spontaneous mutations or GCRs. The enzymatic domain of

the *exo1ΔC280* allele is still intact, although this truncation still impacts the enzymatic

function of Exo1 [7]; this could be due to the loss of another post-translational

modification that occurs in this region or protein interaction site not yet identified. The

structure prediction program IUPRED has shown this domain may not be structured, but

a single amino acid changes the prediction drastically to a more structured prediction

[7]. While testing this change would not explain the significance of this region it could be

used to determine if the structure of that region is enough to challenge its enzymatic

function. Additionally, upon analysis of the amino acid sequence, there is a motif that

resembles a nuclear localization signal, which could be verified by mutating the motif

and determining the effect on Exo1 subcellular localization. Purified wildtype Exo1 and

exo1 truncation mutants could be analyzed by mass spectrometry for additional physical

interactions with unknown factors that may play a role in regulating Exo1 function. For

example, in humans, RPA may play a role in displacing Exo1 as a form of regulation,

but a physical interaction with RPA has not been identified in yeast or humans [17]. Also, PCNA was found to interact at a PCNA interaction motif (PIP box) located at the end of the C-terminus of human Exo1 and is thought to contribute to Exo1's resection processivity [18].

In chapter three we identify a role for the Exo1 phosphorylation sites in the cellular response to replication stress. Phosphorylation of Exo1 was found to play a role in inhibiting its enzymatic function at uncapped telomeres where it has been shown to be the principle exonuclease responsible for generating ssDNA at these sites [16, 19]. Here, we find a new role for the previously described phosphorylation sites at stalled replication forks where Exo1 is also known to generate ssDNA preventing fork reversal in Rad53 checkpoint-deficient cells to promote error-free repair by template switching [20]. We show by using Exo1 mutants that mimic constitutive phosphorylation and a mutant that is not able to be phosphorylated, that this post-translational modification does not necessarily inhibit Exo1 activity but may be in an active state, which is detrimental at stalled forks. It has not yet been determined if just a single phosphorylation site out of the four identified is required rather than in combination; testing this could reveal the cause for the difference in Exo1 regulation at replication intermediates versus uncapped telomeres. The possibility of additional post-translational modifications of Exo1 and these exo1 mutants, both in the presence and absence of HU, could be assessed by mass-spectrometry.

Moreover, measuring the amount of single-strand DNA in the phospho-mutants of Exo1 in a *pol32Δ* mutant challenged with HU using electron-micrographs would help

determine if there is more Exo1 mediated resection, whereas 2D gel analysis could reveal the accumulation of replication-dependent recombination intermediates.

A new separation of function allele of Sgs1 reveals a role in stimulating HR repair

In chapter four we have described a new function of Sgs1 dependent on the physical interaction with HR repair factor Rad51. We previously determined that the loss of the C-terminal 260 amino acids of Sgs1 causes defects similar to that of the complete loss of Sgs1 with regard to sensitivity to DNA damaging agents and the accumulation of genome rearrangements [21]. It was also shown that Rad51 physically interacts with Sgs1 in that region although the significance of this physical interaction had not been determined [22]. We hypothesized that loss of the physical interaction of Sgs1 and Rad51 might be contributing to the defects seen in the sgs1 truncation mutant, as this truncation did not impinge on the enzymatic domain. We identified a single amino acid change (F1192D) that disrupts the physical interaction of Sgs1 and Rad51 (*sgs1-FD* allele*).* Unexpectedly we found that the *sgs1-FD* mutant did not exhibit any of the defects seen in the *sgs1ΔC260* truncation mutant. However, when combined with the loss of DNA repair factors known to have a genetic interaction with *SGS1* we observed phenotypes unique to recombination defects. We found a separation of function allele where we propose the physical interaction of Sgs1 and Rad51 promotes homology-mediated repair, possibly by helping mediate the exchange of RPA and Rad51 at DNA breaks. Assessing association of Rad51 with an HO-induced DSB in wildtype cells and in the sgs1-FD mutant by chromatin-immunoprecipitation could test

204

whether Sgs1 promotes HR by helping Rad51 load on the ssDNA. The difference in RPA affinity for single-strand DNA in the presence of the Sgs1/Rad51 complex could also be assessed to determine Sgs1 does help remove RPA and help promote Rad51 filament formation.

Together, these findings add to the functions of Sgs1 and Exo1 in protecting the genome.

REFERENCES

[1] N. Romero-Laorden, E. Castro, Inherited mutations in DNA repair genes and cancer risk, Current problems in cancer, 41 (2017) 251-264.

[2] P.A. Jeggo, L.H. Pearl, A.M. Carr, DNA repair, genome stability and cancer: a historical perspective, Nature reviews. Cancer, 16 (2016) 35-42.

[3] V.G. Gorgoulis, L.V. Vassiliou, P. Karakaidos, P. Zacharatos, A. Kotsinas, T. Liloglou, M. Venere, R.A. Ditullio, Jr., N.G. Kastrinakis, B. Levy, D. Kletsas, A. Yoneta, M. Herlyn, C. Kittas, T.D. Halazonetis, Activation of the DNA damage checkpoint and genomic instability in human precancerous lesions, Nature, 434 (2005) 907-913.

[4] J. Bartkova, Z. Horejsi, K. Koed, A. Kramer, F. Tort, K. Zieger, P. Guldberg, M. Sehested, J.M. Nesland, C. Lukas, T. Orntoft, J. Lukas, J. Bartek, DNA damage response as a candidate anti-cancer barrier in early human tumorigenesis, Nature, 434 (2005) 864-870.

[5] J. German, M.M. Sanz, S. Ciocci, T.Z. Ye, N.A. Ellis, Syndrome-causing mutations of the BLM gene in persons in the Bloom's Syndrome Registry, Human mutation, 28 (2007) 743-753.

[6] L. Doerfler, K.H. Schmidt, Exo1 phosphorylation status controls the hydroxyurea sensitivity of cells lacking the Pol32 subunit of DNA polymerases delta and zeta, DNA Repair (Amst), 24 (2014) 26-36.

[7] L. Doerfler, L. Harris, E. Viebranz, K.H. Schmidt, Differential genetic interactions between Sgs1, DNA-damage checkpoint components and DNA repair factors in the maintenance of chromosome stability, Genome integrity, 2 (2011) 8.

[8] K. Yamagata, J. Kato, A. Shimamoto, M. Goto, Y. Furuichi, H. Ikeda, Bloom's and Werner's syndrome genes suppress hyperrecombination in yeast sgs1 mutant: implication for genomic instability in human diseases, Proceedings of the National Academy of Sciences of the United States of America, 95 (1998) 8733-8738.

[9] D.X. Tishkoff, N.S. Amin, C.S. Viars, K.C. Arden, R.D. Kolodner, Identification of a human gene encoding a homologue of Saccharomyces cerevisiae EXO1, an exonuclease implicated in mismatch repair and recombination, Cancer research, 58 (1998) 5027-5031.

[10] K.H. Schmidt, J. Wu, R.D. Kolodner, Control of translocations between highly diverged genes by Sgs1, the Saccharomyces cerevisiae homolog of the Bloom's syndrome protein, Molecular and cellular biology, 26 (2006) 5406-5420.

[11] L.C. Liddell, G.M. Manthey, S.N. Owens, B.X. Fu, A.M. Bailis, Alleles of the homologous recombination gene, RAD59, identify multiple responses to disrupted DNA replication in Saccharomyces cerevisiae, BMC Microbiol, 13 (2013) 229.

[12] E.P. Mimitou, L.S. Symington, Sae2, Exo1 and Sgs1 collaborate in DNA double-strand break processing, Nature, 455 (2008) 770-774.

[13] Z. Zhu, W.H. Chung, E.Y. Shim, S.E. Lee, G. Ira, Sgs1 helicase and two nucleases Dna2 and Exo1 resect DNA double-strand break ends, Cell, 134 (2008) 981-994.

[14] P.T. Tran, J.A. Simon, R.M. Liskay, Interactions of Exo1p with components of MutLalpha in Saccharomyces cerevisiae, Proceedings of the National Academy of Sciences of the United States of America, 98 (2001) 9760-9765.

[15] D.X. Tishkoff, A.L. Boerger, P. Bertrand, N. Filosi, G.M. Gaida, M.F. Kane, R.D. Kolodner, Identification and characterization of Saccharomyces cerevisiae EXO1, a gene encoding an exonuclease that interacts with MSH2, Proceedings of the National Academy of Sciences of the United States of America, 94 (1997) 7487-7492.

[16] I. Morin, H.P. Ngo, A. Greenall, M.K. Zubko, N. Morrice, D. Lydall, Checkpoint-dependent phosphorylation of Exo1 modulates the DNA damage response, The EMBO journal, 27 (2008) 2400-2410.

[17] L.R. Myler, I.F. Gallardo, Y. Zhou, F. Gong, S.H. Yang, M.S. Wold, K.M. Miller, T.T. Paull, I.J. Finkelstein, Single-molecule imaging reveals the mechanism of Exo1 regulation by single-stranded DNA binding proteins, Proceedings of the National Academy of Sciences of the United States of America, 113 (2016) E1170-1179.

[18] X. Chen, S.C. Paudyal, R.I. Chin, Z. You, PCNA promotes processive DNA end resection by Exo1, Nucleic acids research, (2013).

[19] X. Jia, T. Weinert, D. Lydall, Mec1 and Rad53 inhibit formation of single-stranded DNA at telomeres of Saccharomyces cerevisiae cdc13-1 mutants, Genetics, 166 (2004) 753-764.

[20] C. Cotta-Ramusino, D. Fachinetti, C. Lucca, Y. Doksani, M. Lopes, J. Sogo, M. Foiani, Exo1 processes stalled replication forks and counteracts fork reversal in checkpoint-defective cells, Mol Cell, 17 (2005) 153-159.

[21] H. Mirzaei, S. Syed, J. Kennedy, K.H. Schmidt, Sgs1 truncations induce genome rearrangements but suppress detrimental effects of BLM overexpression in Saccharomyces cerevisiae, Journal of molecular biology, 405 (2011) 877-891.

[22] L. Wu, S.L. Davies, N.C. Levitt, I.D. Hickson, Potential role for the BLM helicase in recombinational repair via a conserved interaction with RAD51, The Journal of biological chemistry, 276 (2001) 19375-19381.

Appendix A:

Phosphoproteomics Reveals Distinct Modes of Mec1/ATR Signaling during DNA Replication

ABSTRACT

The Mec1/Tel1 kinases (human ATR/ATM) play numerous roles in the DNA replication stress response. Despite the multi-functionality of these kinases, studies of their *in vivo* action have mostly relied on a few well-established substrates. Here we employed a combined genetic-phosphoproteomic approach to monitor Mec1/Tel1 signaling in a systematic, unbiased, and quantitative manner. Unexpectedly, we find that Mec1 is highly active during normal DNA replication, at levels comparable or higher than Mec1's activation state induced by replication stress. This "replication-correlated"

mode of Mec1 action requires the 9-1-1 clamp and the Dna2 lagging-strand factor and is distinguishable from Mec1's action in activating the downstream kinase Rad53. We propose that Mec1/ATR performs key functions during ongoing DNA synthesis that are distinct from their canonical checkpoint role during replication stress.

INTRODUCTION

During DNA replication, cells are prone to accumulate genomic instabilities. Progression of the replication machinery is often impeded by barriers such as DNA adducts, DNA-RNA hybrids, and protein-DNA complexes (Lambert and Carr, 2013). Replication forks often stall upon encountering these hard-to-replicate regions, leading to exposure of single-stranded DNA (ssDNA), which, in turn, is a major signal for the activation of the evolution- arily conserved PI3K-like sensor kinase ATR (yeast Mec1) (Mac- Dougall et al., 2007). Once activated, ATR and Mec1 initiate a signaling response that induces key effects such as cell-cycle arrest, inhibition of origin firing, and stabilization of stalled replica- tion forks (Branzei and Foiani, 2010; Santocanale and Diffley, 1998). The importance of ATR is highlighted by the fact that deletion or mutations that affect its activity are associated with embryonic lethality, chromosomal fragmentation, and increasing sensitivity to genotoxic drugs (Brown and Baltimore, 2000; Wright et al., 1998). In budding yeast, strains with *mec1* mutations were shown to accumulate gross chromosomal rearrangements (GCRs) (Myung et al., 2001) and be exquisitely sensitive to genotoxic drugs that induce replication stress (Weinert et al., 1994). Like ATR, the PI3K-like sensor kinase ATM (yeast Tel1) is also important during DNA damage responses. Cells lacking ATM show sensitivity to DNA-damaging agents

and elevated levels of mitotic recombination (Meyn, 1993), but differently from ATR, which is a sensor for ssDNA accumulation, ATM responds mainly to DNA double-strand breaks (DSBs) (Shiloh and Ziv, 2013). In yeast, *tel1Δ* mutants are viable and show no significant sensitivity to DNA-damaging agents. However, *mec1Δ tel1Δ* double mutants are more sensitive to replication stress and display a more severe growth defect than the single deletion mutants, revealing functionally redundant roles for these kinases (Morrow et al., 1995).

Over the last decade, others and we have identified many candidate substrates of Mec1/Tel1 and ATR/ATM using large- scale mass spectrometry (MS)-based approaches (Chen et al., 2010; Matsuoka et al., 2007; Smolka et al., 2007). However, our understanding of how these kinases promote a systemic cellular response that safeguards genomic integrity and allows cells to better cope with the effects of replication stress is still limited. A major limitation toward a more comprehensive charac-terization of Mec1/Tel1 and ATR/ATM action is posed by the difficulty of reproducibly and quantitatively monitoring the many substrates identified by MS. Consequently, the use of anti- body-based approaches to monitor well-established substrates remains the method of choice. Substrates commonly monitored using western blotting techniques include the histone variant H2AX (yeast H2A) and the downstream checkpoint kinases CHK1 and CHK2 (yeast Rad53). Despite the biological relevance of these substrates, the use of their phosphorylation as readouts for the checkpoint response has introduced a marked bias in studies aiming at characterizing Mec1/Tel1 action. To address this problem, here we employed a combined genetic-proteomic approach (which we refer to as quantitative mass-spectrometry analysis of phospho-substrates [QMAPS]) for

identifying and monitoring multiple *in vivo* kinase substrates in a systematic, unbiased, and quantitative manner. Using QMAPS, we show that Mec1 is robustly activated during unperturbed DNA replication, in a manner that correlates with the extent of DNA replication and that is distinct from a canonical checkpoint. Collectively, our results demonstrate the importance of unbiased and quantitative analysis of kinase substrates to comprehensively characterize the *in vivo* action of multi-functional kinases.

RESULTS

Unbiased Delineation of Mec1 and Tel1 Action Using a Genetic-Proteomic Approach

Our current understanding of Mec1 and Tel1 action is biased toward the use of a few established substrates as reporters of the *in vivo* activity of these kinases. In particular, the activation state of the major downstream kinase Rad53 has been extensively used as a key indicator of Mec1 and Tel1 activation status. To circumvent this bias and be able to comprehensively characterize the action of Mec1 and Tel1, we used quantitative MS analysis of kinase mutant strains to identify and monitor as many candidate substrates of these kinases as possible. First, we performed a proteomic screen to globally define the set of Mec1 and Tel1 candidate targets. Building on our previously published work (Smolka et al., 2007), we used quantitative MS to compare the phosphoproteome of wild-type (WT) and *mec1Δ tel1Δ* cells treated with methyl methanesulfonate (MMS) or hydroxyurea (HU) to induce replication stress. To facilitate the classification of Mec1/Tel1-dependent phosphorylation sites into direct or indirect Mec1/Tel1 phosphorylation events, we also quantified the relative abundance of the

212

phosphopeptides in cells lacking Rad53, the major kinase downstream of Mec1/ Tel1.

We were able to identify and quantify more than 6,000 phosphopeptides over distinct

biological replicates (Figure 1A; Table S1). Of interest, the abundance of 232 of the

identified phosphopeptides was significantly reduced in cells lacking Mec1 and Tel1,

and we refer to them as Mec1/Tel1-dependent events. Among the 232 Mec1/Tel1-

dependent targets, 115 were found to be dependent on Rad53, and thus considered as

indirect Mec1/Tel1-dependent events (Figure 1B). In our strategy, direct targets of

Mec1/Tel1 should be present in the group of phosphopeptides carrying a Mec1/Tel1-

dependent and Rad53-independent phospho-site. As shown in Figure 1C (Table S1),

analysis of the amino acid in the +1 position of Mec1/Tel1- dependent and Rad53-

independent phospho-sites revealed a strong enrichment of the S/T-Q motif, consistent

with previous work indicating this preferential motif for Mec1 and Tel1 (Kim et al., 1999;

Smolka et al., 2007). Of the 117 Mec1/Tel1-depen- dent and Rad53-independent

phosphorylation events, 97 are in the preferred S/T-Q motif, and we considered them as

directly targeted by Mec1 or Tel1. On the other hand, Rad53 showed a bias toward the

S/T-bulky amino acid (c) motif (Figure 1B; Table S1). For more than 60% of the proteins

found to have a Mec1/Tel1-dependent phosphorylation, we were able to also detect at

least one Mec1/Tel1-independent phosphorylation event, supporting that most of the

observed changes are not due to changes in protein abundance (Figure S1; Table S1).

To sort out the relative contribution of Mec1 or Tel1 in the response, we performed

similar analyses as described above, but comparing WT cells to cells lacking either

Mec1 or Tel1 (Figure 1D). Of the Mec1 and Tel1 direct phospho-events identified

above, 67% were found to heavily depend mostly on Mec1 (Fig- ure 1E; Table S1). Only

four phospho-sites were found to heavily depend exclusively on Tel1, consistent with the fact that cells lacking Tel1 don't exhibit significant sensitivity to replication stress-inducing agents (Morrow et al., 1995). Importantly, about 29% of Mec1/Tel1-dependent sites were found to remain robustly phosphorylated in cells lacking either Mec1 or Tel1 and represent a set of common candidate substrates of these kinases (Figures 1D–1F; Table S1). These results establish a large set of Mec1 and Tel1 targets and define their relative level of dependency for each of these kinases. This defined set of phosphorylation sites targeted by Mec1 and/or Tel1 forms the basis of our unbiased strategy to characterize the action of these kinases in different growth conditions and genetic backgrounds. The output of this analysis of substrates is a quantitative map, herein named QMAPS, revealing the relative levels of phosphorylation of identified phosphopeptides in two different conditions being tested (see Figure 2A).

QMAPS Reveals Robust Activation of Mec1 during Normal DNA Replication

It is currently accepted that activation of Mec1 is strongly induced by replication stress. This notion is mainly based on the fact that HU-induced replication fork stalling leads to a robust activation of Rad53 (Tercero et al., 2003). To test if our unbiased QMAPS approach could reveal new insights into the action of Mec1 or Tel1, we compared the phosphorylation level of Mec1/Tel1 candidate substrates in cells undergoing normal S-phase with cells treated with HU. In both cases, cells were arrested in G1 with α-factor and then released from the arrest in media containing HU or not for 45 min. As shown in Figure 2A and Table S2, nearly all phosphopeptides

carrying a Rad53- dependent phosphorylation site were induced by HU. Unexpectedly,

only a minor fraction of Mec1 and/or Tel1 candidate substrates was induced by HU

treatment. This fraction included a phosphorylation site in Rad53 (serine 24) and a

phosphorylation in the Mrc1 protein (serine 189), the adaptor known to transduce

signals from Mec1 to Rad53 in response to HU. Most phosphorylation events in Mec1

and/or Tel1 targets were either only slightly induced by HU or did not change at all when

comparing cells going through normal replication with cells experiencing HU-induced

replication stress. Remarkably, a Mec1 autophosphorylation site (serine 38) and

phosphorylation of Rfa1 and Rfa2 (serines 178 and 122, respectively), which are highly

dependent on Mec1, were in fact inhibited by HU. Targeted analysis of purified Mec1

complexes further confirmed that the Mec1 auto- phosphorylation site and

phosphorylation of Rfa1 are indeed induced during normal S-phase and accumulate as

more DNA is replicated, following a similar trend observed for the acetylation of H3K56,

which is a well-established replication mark (Fig- ure 2B) (Masumoto et al., 2005). To

test if Mec1 activation in normal S-phase is dependent on DNA replication, we used

QMAPS to compare the phosphorylation levels of its targets in WT cells as well as in

cells lacking the S-phase cyclins Clb5 and Clb6, which display delayed replication

initiation due to delayed CDK activation but undergo normal budding dynamics as they

progress through S-phase (Figures 2C and 2D) (Donaldson et al., 1998). As shown in

Figure 2D, several Mec1 candidate substrates are highly induced during S-phase in WT

cells but are not induced in *clb5Δ clb6Δ* cells at the 35 min time point, when only limited

DNA replication had occurred in the mutant (Figures 2C and 2D; Table S2). Taken

together, these results show that Mec1 action in normal S-phase depends, at least

partially, on DNA replication. While the MS analysis could detect many Mec1/Tel1-dependent phosphopeptides in G1 in *clb5Δ clb6Δ* cells (Figure 2D), we attributed this basal phosphorylation level to the potential accumulation of these phospho-events in the extended and deregulated S-phase from the previous cell cycle. Very few Rad53-dependent phosphopeptides were detected in the absence of drug-induced replication stress (data not shown). Even in cells lacking three phosphatases known to act on Rad53, namely Ptc2, Ptc3, and Pph3 (Heideker et al., 2007), we were not able to detect robust Rad53 action during a normal S-phase as we still identified a very limited set of targets (Figure S2). Nonetheless, we were able to observe an increase in the level of phosphorylation of the detected Rad53 targets in *ptc2Δ ptc3Δ pph3Δ* triple mutant cells compared to WT cells, suggesting that phosphatases play a role in counteracting Rad53 activation during normal DNA replication.

Collectively, the QMAPS results shown in Figure 2 reveal that Mec1 is robustly activated during normal DNA replication and that this mode of Mec1 signaling is partially uncoupled from Rad53 activation. On the other hand, HU-induced replication stress leads to an increase in the phosphorylation of most Rad53 targets but to minor changes in the phosphorylation of a large fraction of Mec1 targets, or even inhibition of some of them. We therefore propose that Mec1 can operate in two distinct modes of signaling during DNA replication, one correlated with ongoing DNA synthesis ("replication-correlated") and another correlated with the extent of replication stress that involves strong Rad53 activation (canonical checkpoint response).

The 9-1-1 Clamp and the Lagging-Strand Factor Dna2 Are Important

for ''Replication-Correlated'' Mec1 Activation

Recent work revealed that activation of the Mec1 kinase in response to replication stress or DNA damage requires the action of factors such as Ddc1, Dna2, and Dpb11, all of which possess an unstructured region that can tether Mec1 for activation (Kumar and Burgers, 2013; Navadgi-Patil and Burgers, 2009; Puddu et al., 2008). To test if the replication-correlated mode of Mec1 action also requires these factors for activation, we used QMAPS to compare phosphorylation of substrates in WT and mutants of Mec1-activating factors. As shown in Figure 3A and Table S3, mutation of two residues (W128A and Y130A) in Dna2 previously shown to be required for the ability of Dna2 to activate Mec1 has mild effects on the ability of Mec1 to target some of its specific targets, such as Rfa1, Spt7, and Dad1. Deletion of *DDC1* had almost no effect in most targets (Figure 3A; Table S3), suggesting that Dna2 has a more prominent role in activating Mec1 during normal DNA replication. Importantly, deletion of *DDC1* also prevents the recruitment of Dpb11 and its ability to activate Mec1 (Navadgi-Patil and Burgers, 2009). Finally, combination of the *dna2 WY-AA* mutation (herein referred as *dna2-AA*) with *DDC1* deletion had a significant impact on the phosphorylation levels of targets that highly depend on Mec1, suggesting that Dna2 and Ddc1 function redundantly to activate Mec1 during normal DNA repli- cation (Figure 3A; Table S3). This is consistent with the fact that these proteins are known to localize and function on the lagging strand of the replication fork. These results suggest that Mec1 may be activated mostly at the lagging strand of a moving replication fork during normal DNA replication.

Tel1 Phosphorylates a Specific Group of Mec1 Targets to Prevent GCR and Support Robust DNA Replication in the Absence of Mec1

Analysis of GCRs revealed that activation of Mec1 via Dna2 or Ddc1 during replication becomes particularly important in the absence of Tel1, as shown by the dramatic increase in GCR in *tel1Δ ddc1Δ dna2-AA* cells (Figure 3B). This result highlights the key role of Tel1 in compensating for the loss of Mec1 during normal DNA replication. Consistent with this data, while *ddc1Δ dna2-AA* cells exhibit a major loss of phosphorylation of most Mec1-specific phosphorylation, we could still observe robust phosphorylation of targets common to Mec1 and Tel1 during an unchallenged S-phase (Figure 3A). We interpret this result as Tel1 acting in the absence of Mec1 activation during a normal S-phase. Similar to Mec1's "replication-correlated" mode, the action of Tel1 during normal S-phase (and in the absence of Mec1 activation) does not result in higher phosphorylation of Rad53 targets (Figure S3). Of importance, while *ddc1Δ dna2-AA* cells can still replicate DNA and progress through S-phase at WT rates (data not shown), *ddc1Δ dna2-AA* cells lacking *TEL1* display severe replication defects (Kumar and Burgers, 2013). These results suggest that phosphorylation events in one, or several, common Mec1 and Tel1 targets play an important role in promoting robust DNA replication and prevent- ing the accumulation of GCRs. As shown in Table S3, most of these targets are proteins involved in transcription, RNA processing, and chromatin regulation, and several of them are either essential or required for efficient S-phase progression. These results reveal that Tel1 also plays a role during replication-correlated signaling, in a manner that is uncoupled from Rad53 activation. But

differently from Mec1, Tel1 does not rely on Ddc1 and Dna2 for activation during replication, so it remains unclear how Tel1 engages and becomes active at sites of ongoing DNA replication. Taken together, this analysis uncovers a subset of Mec1 targets (common to Tel1) whose phosphorylations are correlated with the ability of cells to suppress GCRs and maintain robust DNA replication.

Dna2 and Ddc1 Are Not Essential for Activation of the Canonical Mec1-Rad53 Signaling Response Following Replication Stress

To determine the extent in which Dna2 and Ddc1 are necessary for activation of the canonical Mec1-Rad53 response during replication stress, we performed QMAPS analysis comparing WT cells versus *ddc1Δ dna2-AA* cells treated with MMS, which leads to robust Rad53 activation. As shown in Figure 4A (Table S4), *ddc1Δ dna2-AA* cells exhibit strong defects in Mec1 activation during MMS treatment, but unexpectedly, activation of Rad53 under this condition does not seem to be greatly affected. On the other hand, similar QMAPS analysis comparing WT and *mec1Δ* cells revealed a strong impact in the phosphorylation of Rad53 targets in the absence of Mec1. These results show that *ddc1Δ dna2-AA* cells do not phenocopy *mec1Δ* cells regarding Rad53 activation and suggest the existence of additional factors that may activate Mec1 to specifically activate Rad53, consistent with a recent paper (Bandhu et al., 2014). In support of the idea of additional Mec1 activator(s), *ddc1Δdna2-AA* cells are not as sensitive to MMS or HU as *mec1Δ* cells (Figure 4B). Also, while *mec1Δ* and *rad53Δ* cells are well known to require deletion of the ribonucleotide reductase inhibitor *SML1* for viability (Zhao et al., 1998), we found that *ddc1Δ dna2-AA* cells do not require *SML1*

deletion for viability (Figure 4C). Of note, even *tel1Δ ddc1Δ dna2-AA* cells do not require

SML1 deletion for viability, despite these cells showing the dramatic increase in GCR

rates that is characteristic of *mec1Δ tel1Δ* cells. We could exclude the possibility of a

Ddc1- independent role for Dpb11 in the activation of Mec1 under MMS in *ddc1Δ dna2-*

AA cells as removal of the C-terminal region of Dpb11, which is required for its ability to

activate Mec1 (Navadgi-Patil and Burgers, 2008), did not cause loss of viability or major

growth defect (Figure 4D). As shown in the working model in Figure 4E, we propose two

distinct modes of Mec1 action during DNA replication, one correlated with DNA

replication and another correlated with the extent of replication stress as part of a

canonical checkpoint signaling. In our model, the replication-correlated mode of Mec1

action functions redundantly with Tel1 to ensure robust DNA replication and prevent

GCR. On the other hand, the canonical checkpoint mode leads to the well-established

effects of inhibition of DNA replication and increased production of dNTPs.

DISCUSSION

The ATR and ATM kinases, and their yeast orthologs, regulate hundreds of

substrates, but our ability to fully capture their multi-functional action *in vivo* has been

hampered by the common use of one or a few classical substrates as readouts of their

activity. Here we used a quantitative MS approach to monitor *in vivo* Mec1/Tel1 kinase

action in a systematic, unbiased, and quantitative manner. Our analysis revealed

surprising insights into how Mec1 functions during DNA replication and provided

evidence of a non-canonical mode of Mec1 action, which we propose is distinct from

Mec1's established role in the checkpoint response (see model in Figure 4E).

By quantitatively monitoring the phospho-status of dozens of Mec1 candidate

substrates, we found that Mec1 is highly active during normal DNA replication. In fact,

genetic data support the idea that Mec1 functions during normal DNA replication. For

example, cells lacking *MEC1* and *TEL1* exhibit high rates of GCR in an assay

performed in the absence of any exogenously-induced DNA damage (Myung et al.,

2001). But the prevailing hypothesis has been that the ability of Mec1 to suppress

spontaneous GCR accumulation is attributed to a residual action of Mec1 in response to

spontaneous DNA damage generated during DNA replication. Distinct from the notion of

residual Mec1 activation during normal replication, our work supports a model in which

Mec1 is highly engaged onto sites of ongoing DNA synthesis to become activated in a

"replication-correlated" manner. Also, distinct from the established role of Mec1 in

checkpoint signaling, our results reveal that the action of Mec1 during normal DNA

replication is partially uncoupled from the action of the downstream kinase Rad53. Our

results are consistent with the idea that Mec1 is either continuously activated during

ongoing DNA synthesis or is activated at many sites in the genome that pose moderate

level of difficulty for replication forks to pass. At these sites, forks would only

dynamically pause, allowing sufficient ssDNA exposure for Mec1 recruitment and

activation but not for robust Rad53 activation, which requires further recruitment and/or

phosphorylation of mediator proteins to mount a full checkpoint response. Nonetheless,

it is important to mention that Rad53 also needs to be activated during normal DNA

replication. Cells lacking Rad53 are not viable, unless the RNR inhibitor *SML1* is also

deleted (Zhao et al., 1998). But contrary to Mec1's action, our quantitative analysis

reveals that the activity of Rad53 in normal DNA replication is significantly lower than

drug-induced Rad53 activity (Figure 2A). We speculate that during normal DNA replication, Rad53 becomes preferentially activated at specific genomic sites that pose major challenges for replication, such as hard-to-replicate transcriptional barriers. Interestingly, our results suggest that phosphatases such as Pph3, Ptc2, and Ptc3 may also function during normal S-phase to prevent excess Rad53 activation, consistent with a recent report showing a constitutive Mec1-Pph3 interaction (Hustedt et al., 2015). The identification of a replication-correlated mode of Mec1 action leads to a paradox, as Rad53 has established roles in inhibiting DNA synthesis as part of a canonical checkpoint response to replication stress (Santocanale and Diffley, 1998). We hypothesize that Mec1 positively regulates DNA replication when functioning uncoupled from Rad53 activation in the replication-correlated mode (Figure 4E). Consistent with this hypothesis, the Bell lab has shown that Mec1 phosphorylates the MCM complex to prime it for activation (Randell et al., 2010). We further speculate that the replication-correlated mode of Mec1 signaling plays a major role in facilitating the movement of replication forks by preemptively opening chromatin and/or removing RNA and transcriptional machineries from DNA.

Consistent with this notion, we found that Mec1 targets several proteins involved in transcription, RNA processing, and chromatin remodeling during unchallenged DNA replication. Also, we showed that during normal DNA replication Tel1 partially compensates for the lack of Mec1 by targeting substrates involved in transcription and chromatin regulation. The fact that cells lacking both Mec1 and Tel1 are extremely slow growing further strengthens the idea that the set of Mec1 substrates that can also be phosphorylated by Tel1 comprise a critical set of proteins involved in promoting robust

222

DNA replication. Previous reports have functionally connected Mec1 to chromatin and transcription regulation (Rodriguez and Tsukiyama, 2013; Seeber et al., 2013). Our work suggests that regulation of these processes by Mec1 is actually part of the normal replication program that positively controls ongoing DNA synthesis. The delineation of which substrates are common to Mec1 and Tel1 should provide the framework of targets that will help better understand the mechanisms by which Mec1 and Tel1 positively impact DNA synthesis. Finally, the observation that replication- correlated mode of Mec1 and Tel1 action does not efficiently relay signaling to Rad53 activation is consistent with these ideas, as it is well known that Rad53 activation leads to outputs that would antagonize the potential role of Mec1 as a positive regulator of DNA replication.

EXPERIMENTAL PROCEDURES

Cell Culture

Yeast strains used in this study are listed in Table S5. For stable isotope labeling of amino acids in cell culture (SILAC), auxotrophic yeast strains for lysine and arginine were grown in -Arg -Lys synthetic dropout media supplemented with either normal L-arginine and L-lysine (light culture) or L-lysine $^{13}C_6$, $^{15}N_2$ and L-arginine $^{13}C_6$, $^{15}N_4$ (heavy culture) as describe in Ohouo et al. (2013).

ACCESSION NUMBERS

The MS proteomics data have been deposited to the Peptide Atlas database (http://www.peptideatlas.org/) with the data set identifier PASS00651 and PASS00652.

Plasmid

DNA2 sequence was amplified from genomic DNA and cloned into pFA6a plasmid (pMBS 538) followed by site-directed mutagenesis reactions for W128A and Y130A mutations. The plasmid generated contains a 50bp upstream region of *DNA2* (from positions -50bp to -1bp of start codon), the *DNA2-AA* ORF and a 214bp downstream region of *DNA2* (from positions +1bp to +214bp of stop codon) cloned with *Pac*I and *Asc*I. Plasmid pMBS 538 also contains a 500bp downstream region of *DNA2* (from positions +215bp to +715bp of stop codon) (cloned with *Pme*I and *EcoR*I) for subsequent integration into the endogenous *DNA2* locus. *DNA2-AA* was integrated into the endogenous *DNA2* locus in a diploid strain preserving the *DNA2* promoter and 3' UTR sequences. After sporulation, haploid strains containing *DNA2-AA* mutant were isolated by tetrad dissection and genotyped based on PCR and analysis of auxotrophic markers. Plasmid pMBS 538 is available upon request.

Cell Synchronization

For synchronization, yeast cells were arrested in G1 with α-factor and released in α-factor-free media for allowing cells to progress into S-phase. Efficiency of cell cycle arrest and release was monitored by FACS analysis.

FACS analysis

Cells sample were collected at appropriate time points, fixed in 70% ethanol and stored at -20° C. Yeast cells were harvested by centrifugation, ethanol was removed, cell pellet was resuspended in 50mM sodium citrate followed by treatement with 200µg/ml of RNase A (Qiagen) for 1h at 37° C and 500µg/ml of proteinase K (Invitrogen) for 1h at 42° C. Finally, cells were incubated in the presence of Sytox Green (Molecular Probes) for 2h at 4° C. FACS profiles were analyzed using a BD Accuri C6 - Flow cytometer and CFlow® software.

Gross Chromosomal Rearrangements (GCR) assay

Rates of accumulating GCRs were determined by fluctuation analysis by taking the median rate of at least 15 cultures from at least two isolates (Lea and Coulson, 1949; Schmidt et al., 2006) and 95% confidence intervals were calculated according to (Nair, 1940). Cells with GCRs were identified by their resistance to canavanine and 5-fluoro-orotic acid (Canr 5-FOAr), which is indicative of simultaneous inactivation of the *CAN1* and *URA3* genes on the modified chromosome V. Selective media for the GCR assay was prepared as previously described (Schmidt et al., 2006).

Protein Extraction and Sample Preparation

"Light" and "heavy"-labeled cultures were combined, harvested by centrifugation in TE buffer pH 8.0 containing protease inhibitors and stored frozen at -80° C until cell lysis. Approximately 0.4 g of yeast cell pellet was lysed by bead beating at 4° C in 4 mL of lysis buffer containing 50 mM Tris-HCl, pH 7.5, 0.2% Tergitol, 150 mM NaCl, 5 mM

EDTA, complete EDTA-free protease inhibitor cocktail (Roche), 5 mM sodium fluoride and 10 mM β-glycerophosphate. Protein lysates were denatured in 1% SDS, reduced with DTT, alkylated with iodoacetamide and then precipitated with three volumes of a solution containing 50% acetone and 50% ethanol. Proteins were solubilized in a solution of 2 M urea, 50 mM Tris-HCl, pH 8.0, and 150 mM NaCl, and then TPCK-treated trypsin was added. Digestion was performed overnight at 37° C, and then trifluoroacetic acid and formic acid were added to a final concentration of 0.2%. Peptides were desalted with Sep-Pak C18 column (Waters). C18 column was conditioned with 5 column volumes of 80% acetonitrile and 0.1% acetic acid and washed with 5 column volumes of 0.1% trifluoroacetic acid. After samples were loaded, column was washed with 5 column volumes of 0.1% acetic acid followed by elution with 4 column volumes of 80% acetonitrile and 0.1% acetic acid. Elution was dried in a SpeedVac evaporator and resuspended in 1% acetic acid.

Phosphopeptide Enrichment

Phosphopeptide enrichment was performed as described in (Ohouo et al., 2013). After protein extraction and trypsin digestion, desalted peptides were resuspended in 1% acetic acid and loaded in a tip column containing 30µl of immobilized metal affinity chromatography (IMAC) resin prepared as previously described (Albuquerque et al., 2008). After loading, the IMAC resin was washed with 1 column volume of 25% acetonitrile, 100 mM NaCl, and 0.1% acetic acid solution followed by 2 column volumes of 1% acetic acid, 1 column volume of deionized water and finally, eluted with 3 column volumes of 12% ammonia and 10% acetonitrile solution.

HILIC Fractionation

After phosphopeptide enrichment, samples were dried in a SpeedVac, reconstituted in 80% acetonitrile and 1% formic acid and fractionated by hydrophilic interaction liquid chromatography (HILIC) with TSK gel Amide-80 column (2 mm x 150 mm, 5 µm; Tosoh Bioscience). One-minute fractions were collected between 10 and 22 min of the gradient. Three solvents were used for the gradient: buffer D (90% acetonitrile); buffer E (80% acetonitrile and 0.005% trifluoroacetic acid) and buffer F (0.025% trifluoroacetic acid). The gradient used consists of a 100% buffer D at time = 0 min; 98 % of buffer E and 2 % of buffer F at time = 5 min; 82 % of buffer E and 18 % of buffer F at time = 15 min; and 5 % of buffer E and 95 % of buffer F from time = 25 to 27 min in a flow of 150 µl/min.

MS Analysis

Phosphopeptides were subjected to LC-MS/MS analysis using a Q-Exactive Orbitrap or an Orbitrap XL mass spectrometer.

Mass Spectrometry Analysis and Data Acquisition

HILIC fractions were dried in a SpeedVac, reconstituted in 0.1% trifluoroacetic acid and subjected to LC-MS/MS analysis using a 20-cm-long 125-µm inner- diameter column packed in-house with 3 µm C18 reversed-phase particles (Magic C18 AQ beads, Bruker). Separated peptides were electrosprayed into a Q- Exactive Orbitrap

mass spectrometer (Thermo Fisher Scientific). Xcalibur 2.2 software (Thermo Fischer Scientific) was used for the data acquisition and the Q Exactive was operated in the data-dependent mode. Survey scans were acquired in the Orbitrap mass analyzer over the range of 380 to 2000 m/z with a mass resolution of 70.000 (at m/z 200). MS/MS spectra was performed selecting up to the 10 most abundant isotopes with a charge state ≥ than 2 within an isolation window of 2.0 m/z. Selected isotopes were fragmented by Higher-energy Collisional Dissociation (HCD) with normalized collision energies of 27 and the tandem mass spectra was acquired in the Orbitrap mass analyzer with a mass resolution of 17.500 (at m/z 200). Repeat sequencing of peptides was kept to a minimum by dynamic exclusion of the sequenced peptides for 30 seconds. Some analyses were performed in an Orbitrap XL mass spectrometer (Thermo Fisher Scientific) as previously described (Ohouo et al. 2013).

Peptide Identification and Quantitation

Raw MS/MS spectra were searched in a SORCERER (Sage N Research, Inc.) system using SEQUEST software and a composite yeast protein database, consisting of both the normal yeast protein sequences and their reversed protein sequences as a decoy to estimate the false discovery rate (FDR) in the search results. To increase the confidence of phosphopeptide identification, we performed a parallel search on Proteome Discoverer 1.4 software (Thermo Fisher Scientific) running SEQUEST and Percolator. Only phosphopeptides identified with high confidence in both SORCERER and Proteome discoverer/percolator searches were considered, which resulted in the complete elimination of any hits from the decoy database (FDR <

0.02%). Searching parameters included a semi-tryptic requirement, a mass accuracy of

15 ppm for the precursor ions, differential modification of 8.0142 daltons for lysine,

10.00827 daltons for arginine, 79.966331 daltons for phosphorylation of serine,

threonine and tyrosine and a static mass modification of 57.021465 daltons for alkylated

cysteine residues. XPRESS software, part of the Trans-Proteomic Pipeline (Seattle

Proteome Center), was used to quantify all the identified peptides. The phosphorylation

localization probabilities were determined using PhosphoRS within Proteome

Discoverer (version 1.4.1.14, Thermo Fisher Scientific). All checkpoint-dependent

phosphopeptides were manually inspected for phospho site assignment and

quantitation. The mass spectrometry data have been deposited to the Peptide Atlas.

Criteria for establishing kinase-dependency

As we were interested in defining phospho-events that are highly-dependent on

MEC1 and TEL1, we began by arbitrarily assigning a high cutoff value (> or = to 6-fold

WT/*mec1∆tel1∆*) to establish Mec1/Tel1-dependent events. This helped eliminate

phospho events whose regulation is partially affected by the lack of MEC1 and TEL1

and that are more likely to reflect indirect events. In addition, by establishing a high

cutoff for defining MEC1/TEL1-dependent events, we were able to employ a low cutoff

for defining Rad53-dependent events (which are already highly pre-filtered by the high

cutoff in MEC1/TEL1). Furthermore, as the high cutoff was previously used to

stringently assign Mec1/Tel1-dependent events, we were also able to apply a rather

lower cutoff of > or = to 2.5 fold to

establish which phosphopeptides were highly dependent on either Mec1 or Tel1. Briefly, the following criteria was used for assigning Mec1/Tel1-dependent phosphopeptides: (1) At least 6-fold increase in phosphopeptide abundance in WT relative to *mec1Δtel1Δ* cells. (2) For Mec1 or Tel1 we established a threshold of 2.5-fold increase in WT relative to *mec1Δ* or *tel1Δ* cells. (3) For Rad53- dependent phosphopeptides, we established a threshold of 2-fold increase in abundance in WT relative to *rad53Δ* cells. (4) Moreover, to be considered a Mec1/Tel1-dependent substrate, each phosphopeptide must be Mec1/Tel1- dependent but not Rad53-dependent and to be considered a Rad53-dependent substrate, each phosphopeptide has to be Mec1/Tel1-dependent and Rad53- dependent substrate. (4) Finally, we considered only phosphopeptides identified in at least 2 biological replicates.

Fold change calculation and QMAPS generation

Fold change calculation and QMAPS generation were done using custom-designed web tool. The web tool allowed upload of data files generated by the SORCERER software. Using this data, it calculated the normalized protein/peptide abundances and appropriate abundance ratios. These fold changes were used to generate QMAPS using Matlab (Mathworks). To generate the QMAPS, results of the phosphoproteome analysis were filtered using a list of kinase checkpoint-dependent phosphopeptides identified in this study. For each QMAPS, we considered phosphopeptides that were identified at least 3 times in 2 biological replicates. Phosphopeptides plotted on the QMAPS were manually inspected for phospho site assignment and quantitation.

Immunoprecipitation (IP) followed by IMAC

For immunoprecipitation (IP), cell cultures were collected at 25, 30, 35 and 45 minutes after release from alpha factor-arrested into S-phase. Cells collected at 25, 30 and 35 minutes were cultured in "light" media while cells collected at 45 minutes were cultured in "heavy" media. Cell pellet was lysed by bead beating at 4° C in lysis buffer containing 50 mM Tris-HCl, pH 7.5, 0.2% Tergitol, 150 mM NaCl, 5 mM EDTA, 1 mM PMSF, Complete, EDTA-free Protease Inhibitor Cocktail (Roche), 5 mM sodium fluoride and 10 mM β-glycerophosphate. After adjusting protein concentrations to about 5 mg/ml, lysates were incubated with either EZviewTM Red Anti-FLAG M2 agarose (Sigma) or acetyl lysine antibody agarose (Immunechem) for 2–3 h at 4° C. After three washes in lysis buffer, bound proteins were eluted with three resin volumes of elution buffer containing 100 mM Tris-HCl, pH 8.0, 1% SDS. Eluted proteins from "light" or "heavy" medium were combined accordingly, reduced, alkylated and precipitated with three volumes of a solution containing 50% acetone and 50% ethanol. Proteins were solubilized in a solution of 2 M urea and 12 mM Tris-HCl, pH 8.0 and then trypsinized O.N. at 37° C with 1μg of Trypsin Gold (Promega). For acetylation analysis of histone H3, samples were desalted with a Sep-Pak C18 column (Waters), dried in a SpeedVac evaporator and resuspended in 0.1% trifluoroacetic acid. For phosphorylation analysis of Mec1 and Rfa1, samples were loaded in a tip column containing 15μl of immobilized metal affinity chromatography (IMAC) resin. After loading, the IMAC resin was washed with 1 column volume of 25% acetonitrile, 100mM NaCl, and 0.1% acetic acid solution followed by 1 column volume of deionized water and finally, eluted with 3 column

volumes of 12% ammonia and 10% acetonitrile solution. Samples were dried in a

SpeedVac, and resuspended in 0.1% trifluoroacetic acid. Samples were subjected to

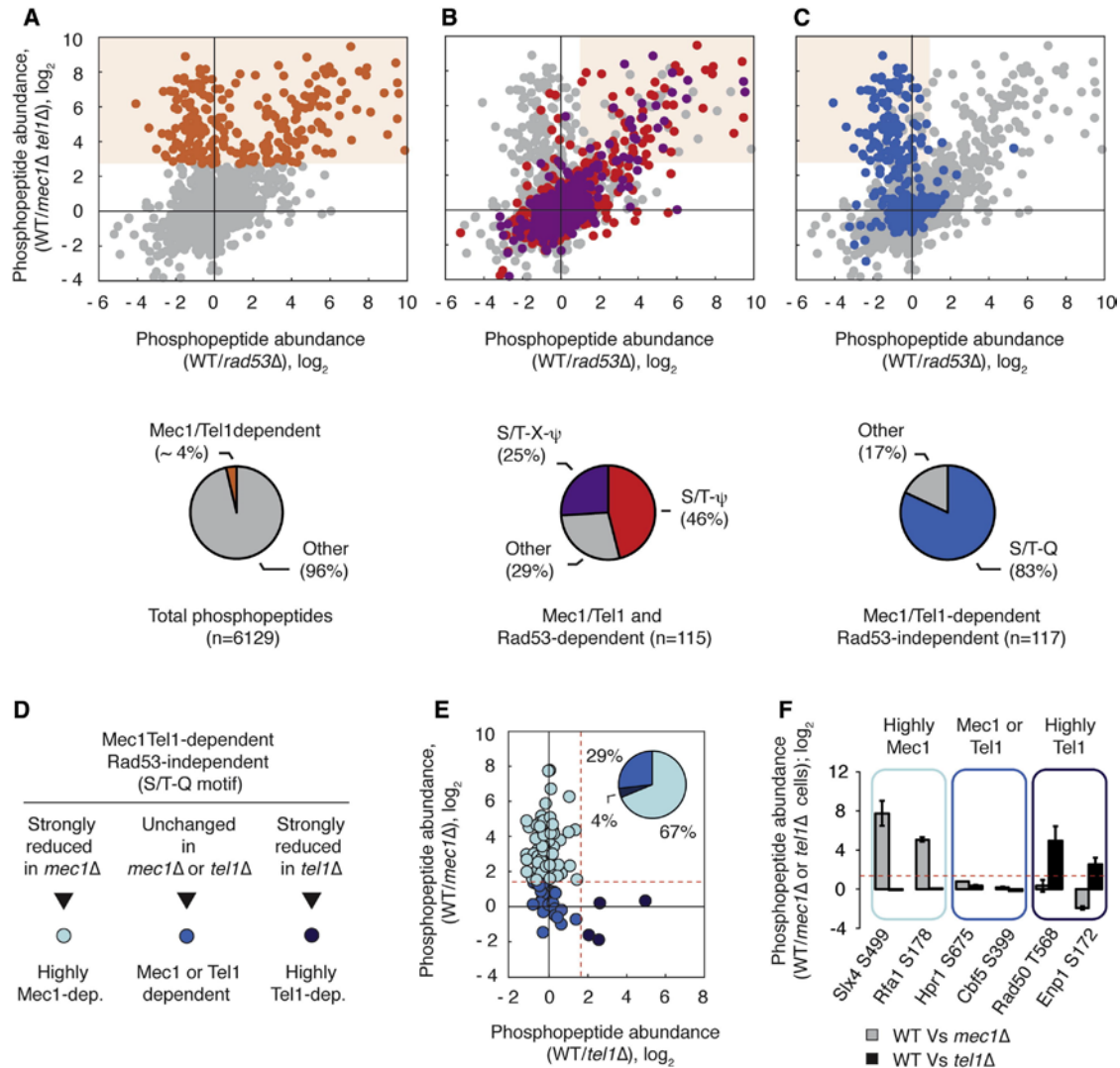LC-MS/MS quantitation analysis.

Figure A.1. Proteome-Wide Identification of Mec1/Tel1-Dependent Phosphorylation Events Using Quantitative MS (A) Identification of Mec1/Tel1-dependent phosphopeptides (cells treated with 0.2M HU or 0.04% MMS). Orange dots correspond to 238 Mec1/Tel1-dependent phosphopeptides. See text for details.(B) Mec1/Tel1- and Rad53-dependent phosphorylation events (light orange shade) are biased toward the S/T-c (red) and S/T-X-c (purple) motifs.(C) Mec1/Tel1 -dependent and Rad53-independent phosphorylation events (light orange shade) are biased toward the S/T-Q motif (blue). (D and E) The phosphoproteome of WT cells was compared to the phosphoproteome of *mec1Δ* or *tel1Δ* cells (all cells treated with 0.04% MMS) and phos- phopeptides carrying phosphorylation in the S/T-Q motif were categorized according to the observed change in abundance. Dotted red lines represent the established cutoff of 3-fold increase in WT relative to *mec1Δ* or *tel1Δ* cells.(F) Examples of phosphopeptides of each of the indicated groups. Data are represented as fold change in phosphopeptide abundance; log2 ± SEM (n R 2). See also Table S1.
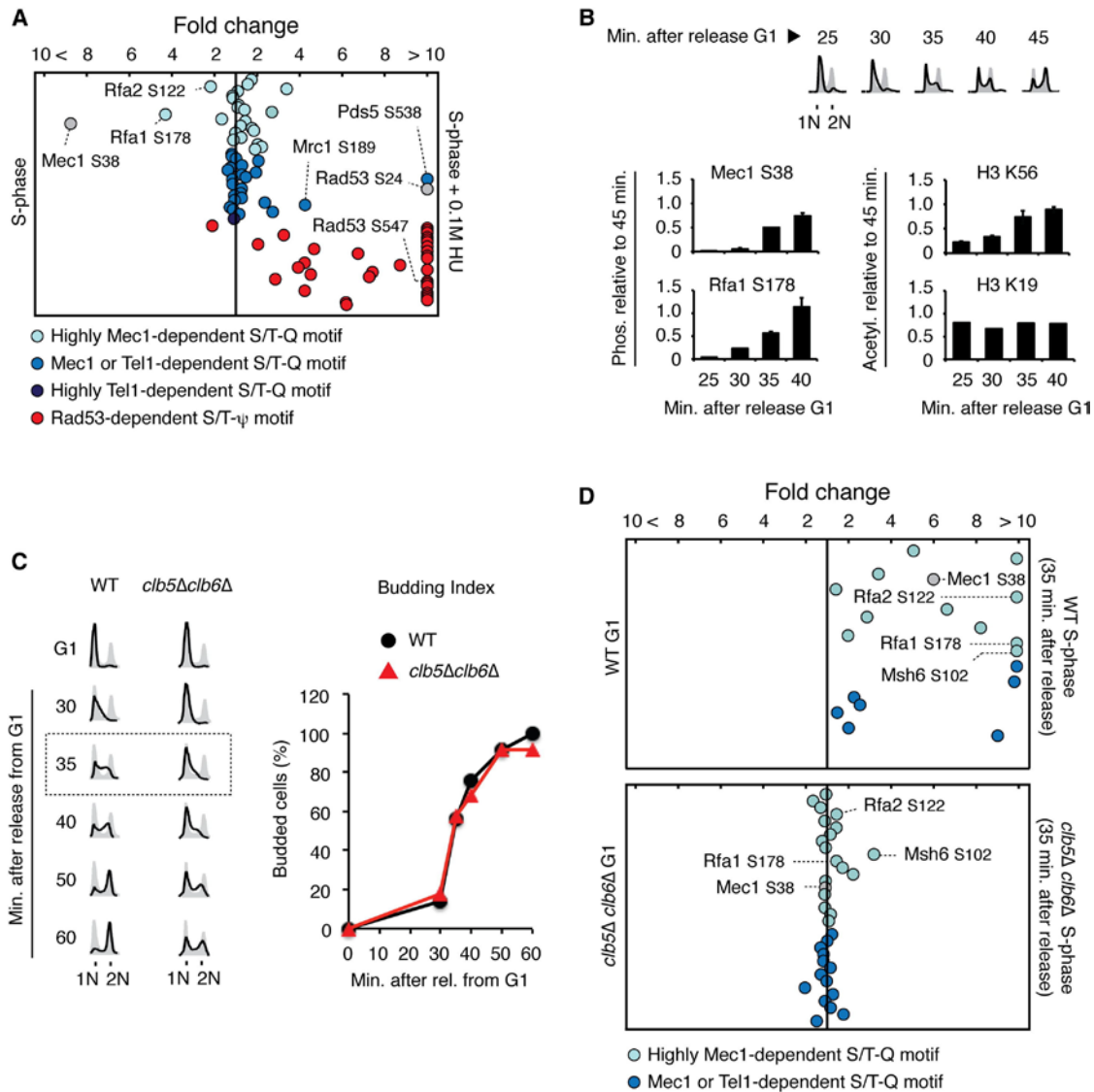
Figure A.2. Quantitative Analysis of Mec1/Tel1-Dependent Phosphorylation during Normal DNA Replication (A) QMAPS showing the relative abundance of phosphopeptides categorized according to results from Figure 1. Phosphopeptides carrying Mec1 autophosphorylation or Mec1-dependent Rad53 phosphorylation are indicated in gray. a-factor arrested cells were released from arrest in normal SILAC media or SILAC media containing 0.1 M HU for 45 min. Abscissa indicates fold change in phosphopeptide abundance (linear scale) between S-phase cells treated with 0.1 M HU and untreated. (B) Protein extracts were prepared from WT cells at indicated times after release from a-factor-arrest into fresh media. Mec1 (and Mec1-associated Rfa1) was pulled down, and phosphopeptides containing Mec1 autophosphorylation at S38 and Rfa1 phosphorylation at S178 were monitored by quantitative MS analysis. FACS analysis and H3K56 acetylation were used as positive controls for DNA replication progression while acetylation of H3K19 was used as a constitutive control. Data are represented as mean ± SEM (n R 2). (C) FACS analysis and budding index of WT and *clb5Δ clb6Δ* mutant cells following a-factor arrest and release in drug-free SILAC media.(D) QMAPS showing the relative abundance of phosphopeptides carrying

Mec1/Tel1-dependent S/T-Q motifs. Indicated cells were released from α-factor arrest in drug-free SILAC media for 35 min. For all the QMAPS in Figure 2, each dot corresponds to a different phosphopeptide identified at least three times in two independent biological replicates. See also Table S2.
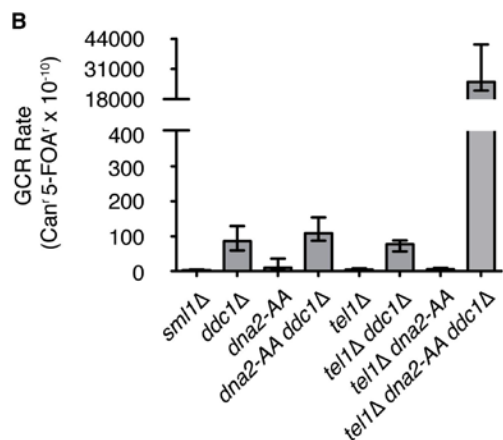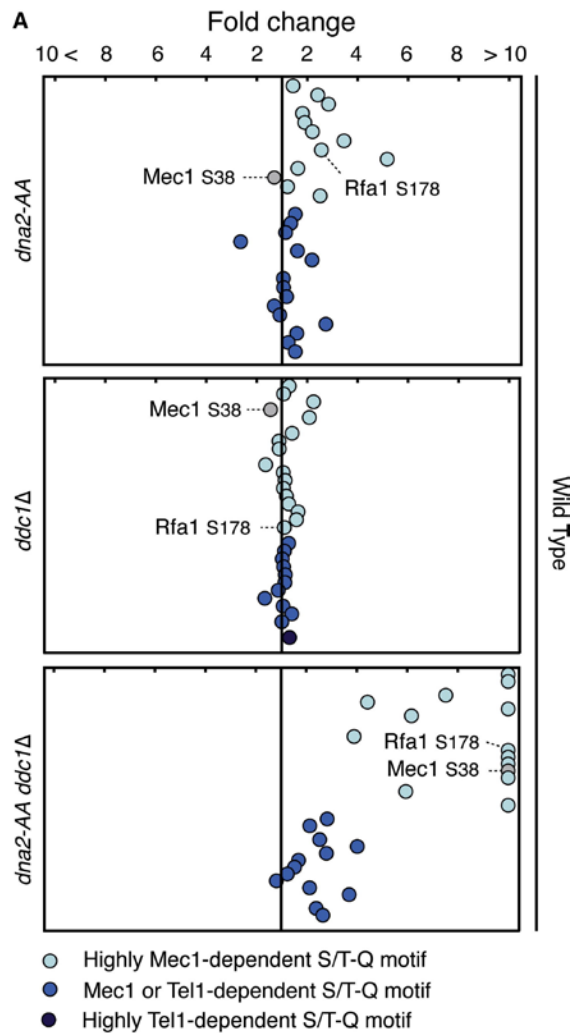
Figure A.3. Importance of Dna2 and Ddc1 for Replication-Correlated Mode of Mec1 Activation (A) QMAPS showing the relative abundance of phosphopeptides carrying Mec1/Tel1-dependent S/T Q motifs. WT, *dna2-AA*, *ddc1Δ*, and *dna2-AA ddc1Δ* cells were released from α-factor arrest in SILAC media for 45 min. See also Table S3.

(B) Effects of the *dna2-AA* mutation on accumulation of gross-chromosomal rearrangements in Ddc1 and Tel1 defective mutants. All strains are *sml1Δ*. Error bars indicate 95% confidence intervals (CI).
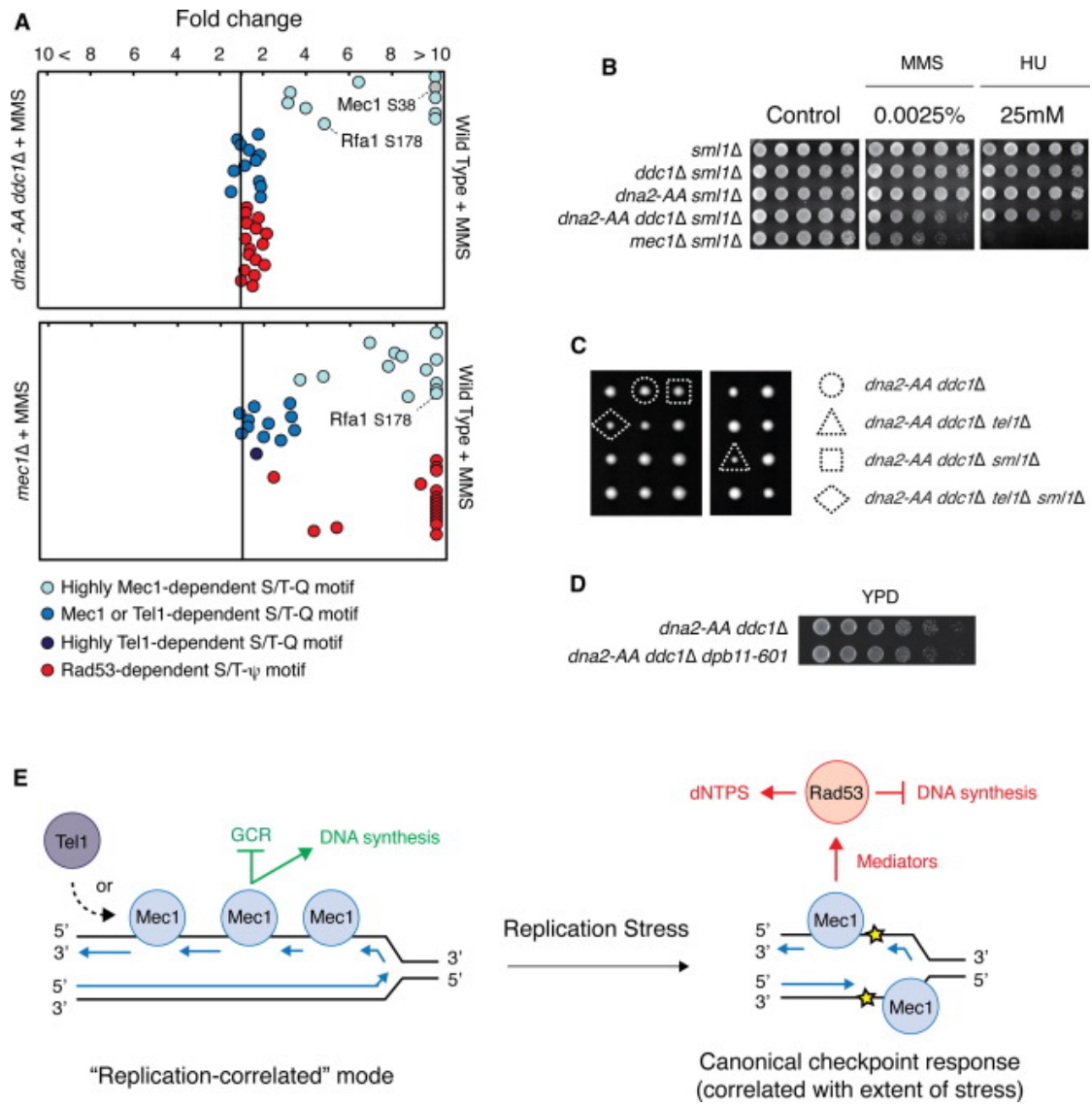
Figure A.4. Dna2 and Ddc1 Are Not Essential for Mec1 Activation during Replication Stress (A) QMAPS analysis comparing WT and indicated mutant cells. Cells were arrested with a-factor and released from arrest in SILAC media containing 0.04% MMS for 45 min. See also Table S4.(B) 5 -fold serial dilutions of indicated cells with *sml1Δ* background were plated on YPD plates containing indicated drugs and incubated at 30 C for 48 hr.(C) Meiotic tetrads from a *DNA2/dna-AA DDC1/ddc1Δ TEL1/tel1Δ SML1/sml1Δ* diploid strain were dissected on YPD plates and incubated at 30 C for 72 hr. (D) 4-fold serial dilutions of indicated cells were plated on YPD plates and incubated at 30 C for 36 hr. (E) Model depicting distinct modes of Mec1 action during DNA replication. See text in the discussion. Blue arrows correspond to newly synthesized DNA strands.
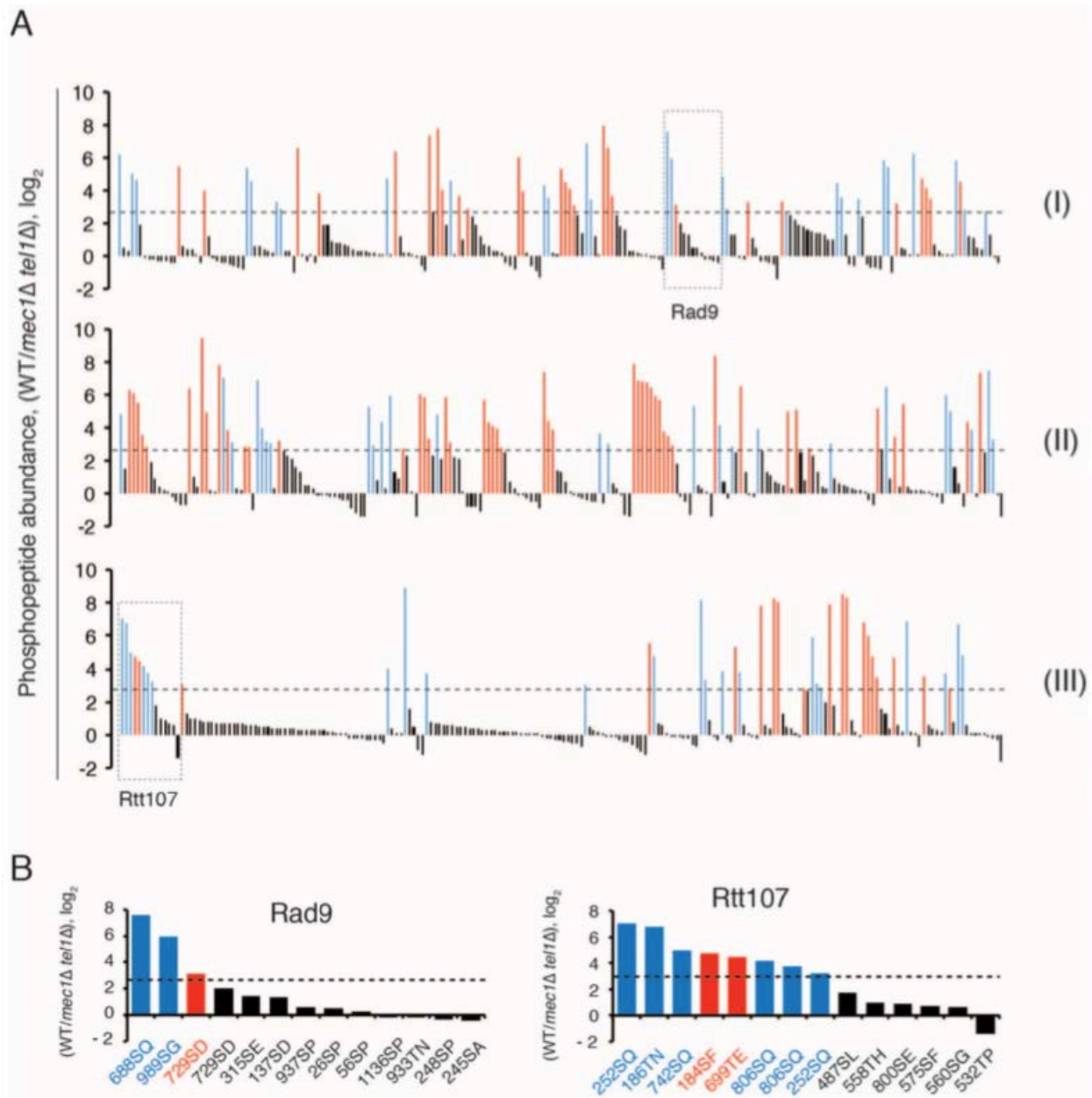
238

Figure A.S1, Related to Figure 1.
(A) Diagram comparing abundance changes between Mec1/Tel1-dependent and Mec1/Tel1-independent phosphopeptides. From 142 proteins found to have a Mec1/Tel1-dependent phosphorylation we found 92 representative Mec1/Tel1-independent phosphopeptides. Red and blue bars correspond to Mec1/Tel1-dependent phosphopeptides containing S/T-Q or S/T-ψ motifs, respectively. Black bars correspond to Mec1/Tel1-independent phosphopeptides. Dotted line represents the 6-fold threshold to establish Mec1/Tel1-dependent events. For detailed information see Supplemental Table S1. Dotted rectangles highlight Rad9 and Rtt107 phosphopeptides. (B) Representative examples for Rad9 and Rtt107 showing the abundance changes of theirs Mec1/Tel1-dependent and independent phosphopeptides.
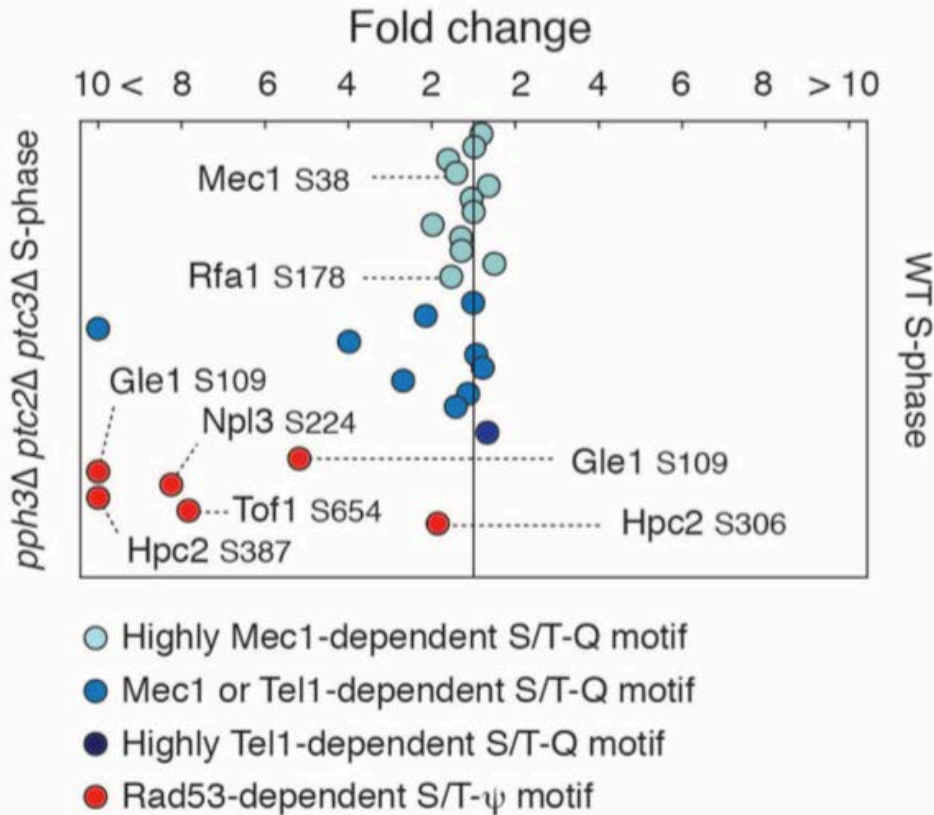
Figure A.S2, Related to Figure 2: QMAPS comparing wild-type vs *pph3Δptc2Δptc3Δ* mutant cells. Cells were released from α-factor arrest in SILAC media for 45 minutes. Abscissa shows relative fold change in phosphopeptide abundance (linear scale). Each dot corresponds to a different phosphopeptide identified at least 2 times out of 3 independent biological replicates.

Figure A.S3, Related to Figure 3: QMAPS comparing wild-type vs *dna2-AA ddc1∆* mutant cells. Cells were released from α-factor arrest in SILAC media for 45 minutes. Abscissa shows relative fold change in phosphopeptide abundance (linear scale). Each dot corresponds to a different phosphopeptide identified at least 2 times out of 3 independent biological replicates.
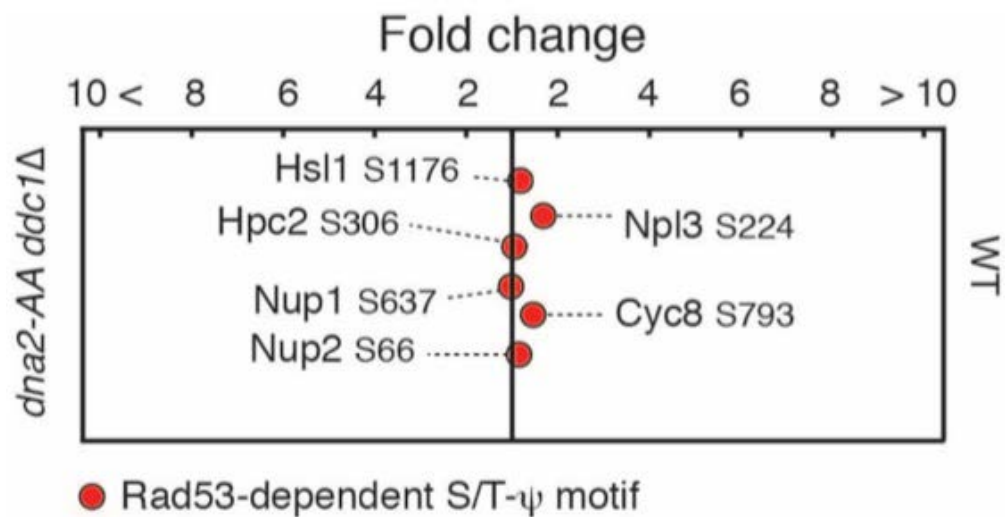
Table A.S1. All Quantified Phosphopeptides Related to Figure 1 Separate Excel file
http://dx.doi.org/10.1016/j.molcel.2015.01.043.

Table A.S2. QMAPS Related to Figure 2 Separate Excel file
http://dx.doi.org/10.1016/j.molcel.2015.01.043.

Table A.S3. QMAPS Related to Figure 3 Separate Excel file
http://dx.doi.org/10.1016/j.molcel.2015.01.043.

Table A.S4. QMAPS Related to Figure 4 Separate Excel file
http://dx.doi.org/10.1016/j.molcel.2015.01.043.

Table A.S5: Yeast strains used in this study

Strain ID	Genotype
KHSY4729	MATa, ura3-52, trp1Δ63, his3Δ200, leu2Δ1, lys2ΔBgl, hom3-10, ade2Δ1, ade8, hxt13::URA3, ddc1::HIS3, sml1::TRP1
KHSY4732	MATa, ura3-52, trp1Δ63, his3Δ200, leu2Δ1, lys2ΔBgl, hom3-10, ade2Δ1, ade8, hxt13::URA3, dna2-WY-AA::kanMX6 , sml1::TRP1
KHSY5024	MATa, ura3-52, trp1Δ63, his3Δ200, leu2Δ1, lys2ΔBgl, hom3-10, ade2Δ1, ade8, hxt13::URA3, ddc1::HIS3, sml1::TRP1, tel1::natMX
KHSY5025	MATa, ura3-52, trp1Δ63, his3Δ200, leu2Δ1, lys2ΔBgl, hom3-10, ade2Δ1, ade8, hxt13::URA3, ddc1::HIS3, dna2-WY-AA::kanMX6, sml1::TRP1
KHSY5027	MATa, ura3-52, trp1Δ63, his3Δ200, leu2Δ1, lys2ΔBgl, hom3-10, ade2Δ1, ade8, hxt13::URA3, sml1::TRP1, tel1::NatMX
KHSY5028	MATa, ura3-52, trp1Δ63, his3Δ200, leu2Δ1, lys2ΔBgl, hom3-10, ade2Δ1, ade8, hxt13::URA3, ddc1::HIS3, dna2-WY-AA::kanMX6, sml1::TRP1, tel1::natMX
KHSY5035	MATa, ura3-52, trp1Δ63, his3Δ200, leu2Δ1, lys2BΔgl, hom3-10, ade2Δ1, ade8, hxt13::URA3,dna2-WY-AA::kanMX6, sml1::TRP1,tel1::natMX
KHSY4726	MATa, ura3-52, leu2Δ1, trp1Δ63, his3Δ200, lys2ΔBgl, hom3-10, ade2Δ1, ade8, hxt13::URA3 sml1::TRP1
MBS164	MATa, ura3-52, leu2Δ1, trp1-63, his3-200, lys2ΔBgl, hom3-10, ade2Δ1, ade8, arg4Δ, sml1::TRP1 bar1::HIS3
MBS188	MATa, ura3-52, leu2Δ1, trp1-63, his3-200, lys2ΔBgl, hom3-10, ade2Δ1, ade8, arg4Δ, sml1::TRP1, bar1::HIS3, rad53::URA3
MBS189	MATa, ura3-52, leu2Δ1, trp1-63, his3-200, lys2ΔBgl, hom3-10, ade2Δ1, ade8, arg4Δ, sml1::TRP1, bar1::HIS3, mec1::URA3
MBS1964	MATa, ura3-52, leu2Δ1, trp1Δ63, his3Δ200, lys2ΔBgl, hom3-10, ade2Δ1, ade8, arg4Δ, sml1::TRIP1, bar1::HIS3, ddc1::kanMX6
MBS2035	MATa, ura3-52, leu2Δ1, trp1-63, his3-200, lys2ΔBgl, hom3-10, ade2Δ1, ade8, arg4Δ, sml1::TRP1, bar1::HIS3, tel1::URA3
MBS2042	ura3-52, leu2Δ1, trp1Δ63, his3Δ200, lys2ΔBgl, hom3-10, ade2Δ1, ade8, arg4Δ, sml1::TRIP1, bar1::HIS3, mec1::URA3, tel1::kanMX6
MBS2220	MATa, ura3-52, leu2Δ1, trp1Δ63, his3Δ200, lys2ΔBgl, hom3-10, ade2Δ1, ade8, arg4Δ, sml1::TRIP1, DNA2 WY-AA::kanMX6, ddc1::HIS3, bar1::URA3
MBS2223	MATa, ura3-52, leu2Δ1, trp1Δ63, his3Δ200, lys2ΔBgl, hom3-10, ade2Δ1, ade8, arg4Δ, sml1::TRIP1, DNA2 WY-AA::kanMX6, bar1::URA3
MBS2411	MATa, ura3-52, leu2Δ1, trp1-63, his3-200, lys2ΔBgl, hom3-10, ade2Δ1, ade8, arg4Δ, sml1::TRP1, bar1::HIS3, pph3::kanMX6, ptc2::URA3, ptc3::natMX
MBS2653	ura3-52, trp1-63, his3-200, lys2-Bgl, hom3-10, ade2Δ1, ade8,YEL069C::URA3, DNA2 WY-AA::kanMX6, ddc1::HIS3, DPB11(aa1-600)::TRP1
MBS2564	MATa, ura3-52, leu2Δ1, trp1-63, his3-200, lys2ΔBgl, hom3-10, ade2Δ1, ade8, arg4Δ, sml1::TRP1, bar1::HIS3, clb5::URA3, clb6::kanMX6

REFERENCES

1. Albuquerque, C.P., Smolka, M.B., Payne, S.H., Bafna, V., Eng, J., and Zhou, H. (2008). A multidimensional chromatography technology for in-depth phosphoproteome analysis. Mol Cell Proteomics *7*, 1389-1396.

2. Bandhu, A., Kang, J., Fukunaga, K., Goto, G., and Sugimoto, K. (2014). Ddc2 mediates Mec1 activation through a Ddc1- or Dpb11-independent mechanism. PLoS Genet. *10*, e1004136.

3. Branzei, D., and Foiani, M. (2010). Maintaining genome stability at the replica- tion fork. Nat. Rev. Mol. Cell Biol. *11*, 208–219.

4. Brown, E.J., and Baltimore, D. (2000). ATR disruption leads to chromosomal fragmentation and early embryonic lethality. Genes Dev. *14*, 397–402.

5. Chen, S.H., Albuquerque, C.P., Liang, J., Suhandynata, R.T., and Zhou, H. (2010). A proteome-wide analysis of kinase-substrate network in the DNA damage response. J. Biol. Chem. *285*, 12803–12812.

6. Donaldson, A.D., Raghuraman, M.K., Friedman, K.L., Cross, F.R., Brewer, B.J., and Fangman, W.L. (1998). CLB5-dependent activation of late replication origins in S. cerevisiae. Mol. Cell *2*, 173–182.

7. Heideker, J., Lis, E.T., and Romesberg, F.E. (2007). Phosphatases, DNA damage checkpoints and checkpoint deactivation. Cell Cycle *6*, 3058–3064.

8. Hustedt, N., Seeber, A., Sack, R., Tsai-Pflugfelder, M., Bhullar, B., Vlaming, H., van Leeuwen, F., Guenole, A., van Attikum, H., Srivas, R., et al. (2015). Yeast PP4

Interacts with ATR Homolog Ddc2-Mec1 and Regulates Checkpoint Signaling. Mol. Cell *57*, 273–289.

9. Kim, S.T., Lim, D.S., Canman, C.E., and Kastan, M.B. (1999). Substrate specificities and identification of putative substrates of ATM kinase family members. J. Biol. Chem. *274*, 37538–37543.

10. Kumar, S., and Burgers, P.M. (2013). Lagging strand maturation factor Dna2 is a component of the replication checkpoint initiation machinery. Genes Dev. *27*, 313–321.

11. Lea, D.E., and Coulson, C.A. (1949). The distribution of the number of mutants in bacterial populations. J. Genet. *49*, 264-285.

12. Lambert, S., and Carr, A.M. (2013). Replication stress and genome rearrangements: lessons from yeast models. Curr. Opin. Genet. Dev. *23*, 132–139.

13. MacDougall, C.A., Byun, T.S., Van, C., Yee, M.C., and Cimprich, K.A. (2007). The structural determinants of checkpoint activation. Genes Dev. *21*, 898–903.

14. Masumoto, H., Hawke, D., Kobayashi, R., and Verreault, A. (2005). A role for cell-cycle-regulated histone H3 lysine 56 acetylation in the DNA damage response. Nature *436*, 294–298.

15. Matsuoka, S., Ballif, B.A., Smogorzewska, A., McDonald, E.R., 3rd, Hurov, K.E., Luo, J., Bakalarski, C.E., Zhao, Z., Solimini, N., Lerenthal, Y., et al. (2007). ATM and ATR substrate analysis reveals extensive protein networks responsive to DNA damage. Science *316*, 1160–1166.

16. Meyn, M.S. (1993). High spontaneous intrachromosomal recombination rates in ataxia-telangiectasia. Science *260*, 1327–1330.

17. Morrow, D.M., Tagle, D.A., Shiloh, Y., Collins, F.S., and Hieter, P. (1995). TEL1, an S. cerevisiae homolog of the human gene mutated in ataxia telangiectasia, is functionally related to the yeast checkpoint gene MEC1. Cell *82*, 831–840.

18. Myung, K., Datta, A., and Kolodner, R.D. (2001). Suppression of sponta- neous chromosomal rearrangements by S phase checkpoint functions in Saccharomyces cerevisiae. Cell *104*, 397–408.

19. Nair, K.R. (1940). Table of confidence intervals for the median in samples from any continuous population. Sankhya *4*, 551-558.

20. Navadgi-Patil, V.M., and Burgers, P.M. (2008). Yeast DNA replication protein Dpb11 activates the Mec1/ATR checkpoint kinase. J. Biol. Chem. *283*, 35853–35859.

21. Navadgi-Patil, V.M., and Burgers, P.M. (2009). The unstructured C-terminal tail of the 9-1-1 clamp subunit Ddc1 activates Mec1/ATR via two distinct mecha- nisms. Mol. Cell *36*, 743–753.

22. Ohouo, P.Y., Bastos de Oliveira, F.M., Liu, Y., Ma, C.J., and Smolka, M.B. (2013). DNA-repair scaffolds dampen checkpoint signalling by counteracting the adaptor Rad9. Nature *493*, 120–124.

23. Puddu, F., Granata, M., Di Nola, L., Balestrini, A., Piergiovanni, G., Lazzaro, F., Giannattasio, M., Plevani, P., and Muzi-Falconi, M. (2008). Phosphorylation of the budding yeast 9-1-1 complex is required for Dpb11 function in the full acti- vation of the UV-induced DNA damage checkpoint. Mol. Cell. Biol. *28*, 4782– 4793.

24. Randell, J.C., Fan, A., Chan, C., Francis, L.I., Heller, R.C., Galani, K., and Bell, S.P. (2010). Mec1 is one of multiple kinases that prime the Mcm2-7 helicase for phosphorylation by Cdc7. Mol. Cell *40*, 353–363.

25. Rodriguez, J., and Tsukiyama, T. (2013). ATR-like kinase Mec1 facilitates both chromatin accessibility at DNA replication forks and replication fork progres- sion during replication stress. Genes Dev. *27*, 74–86.

26. Santocanale, C., and Diffley, J.F. (1998). A Mec1- and Rad53-dependent checkpoint controls late-firing origins of DNA replication. Nature *395*, 615–618.

27. Schmidt, K.H., Pennaneach, V., Putnam, C.D., and Kolodner, R.D. (2006). Analysis of gross-chromosomal rearrangements in Saccharomyces cerevisiae. Methods Enzymol *409*, 462-476.

28. Seeber, A., Dion, V., and Gasser, S.M. (2013). Checkpoint kinases and the INO80 nucleosome remodeling complex enhance global chromatin mobility in response to DNA damage. Genes Dev. *27*, 1999–2008.Shiloh, Y., and Ziv, Y. (2013). The ATM protein kinase: regulating the cellular response to genotoxic stress, and more. Nat. Rev. Mol. Cell Biol. *14*, 197–210. Smolka, M.B., Albuquerque, C.P., Chen, S.H., and Zhou, H. (2007). Proteome- wide identification of *in vivo* targets of DNA damage checkpoint kinases. Proc. Natl. Acad. Sci. USA *104*, 10364–10369.

29. Tercero, J.A., Longhese, M.P., and Diffley, J.F. (2003). A central role for DNA replication forks in checkpoint activation and response. Mol. Cell *11*, 1323–1336.Weinert, T.A., Kiser, G.L., and Hartwell, L.H. (1994). Mitotic checkpoint genes in budding yeast and the dependence of mitosis on DNA replication and repair. Genes Dev. *8*, 652–665.

30. Wright, J.A., Keegan, K.S., Herendeen, D.R., Bentley, N.J., Carr, A.M., Hoekstra, M.F., and Concannon, P. (1998). Protein kinase mutants of human ATR increase

sensitivity to UV and ionizing radiation and abrogate cell cycle checkpoint control.

Proc. Natl. Acad. Sci. USA *95*, 7445–7450.

31. Zhao, X., Muller, E.G., and Rothstein, R. (1998). A suppressor of two essential

checkpoint genes identifies a novel protein that negatively affects dNTP pools. Mol.

Cell *2*, 329–340.

Appendix B:

Permissions

In the following, we provide the licenses' summaries as they can be found on the Creative Commons website.

The Creative Commons Attribution License 4.0 provides the following summary (where 'you' equals 'the user'):

You are free to:

- Share — copy and redistribute the material in any medium or format.
- Adapt — remix, transform, and build upon the material for any purpose, even commercially.

The licensor cannot revoke these freedoms as long as you follow the license terms.

Under the following terms:

- Attribution— you must give *appropriate credit*, provide a link to the license, and *indicate if changes were made*. You may do so in any reasonable manner, but not in any way that suggests the licensor endorses you or your use.
- No additional restrictions—you may not apply legal terms or *technological measures* that legally restrict others from doing anything the license permits.

Notices

You do not have to comply with the license for elements of the material in the public domain or where your use is permitted by an applicable exception or limitation.

No warranties are given. The license may not give you all of the permissions necessary for your intended use. For example, other rights such as publicity, privacy, or moral rights may limit how you use the material.

Please note: For the terms set in italics in the summary above further details are provided on the Creative Commons web page from which the summary is taken (http://creativecommons.org/licenses/by/4.0/).

Figure B.1: Permissions for content in Appendix B provided by BioMedCentral.

This Agreement between Lillian Doerfler ("You") and Elsevier ("Elsevier") consists of your license details and the terms and conditions provided by Elsevier and Copyright Clearance Center.

License Number	4111910175467
License date	May 18, 2017
Licensed Content Publisher	Elsevier
Licensed Content Publication	DNA Repair
Licensed Content Title	Exo1 phosphorylation status controls the hydroxyurea sensitivity of cells lacking the Pol32 subunit of DNA polymerases delta and zeta
Licensed Content Author	Lillian Doerfler,Kristina H. Schmidt
Licensed Content Date	Dec 1, 2014
Licensed Content Volume	24
Licensed Content Issue	n/a
Licensed Content Pages	11
Start Page	26
End Page	36
Type of Use	reuse in a thesis/dissertation
Portion	full article
Format	both print and electronic
Are you the author of this Elsevier article?	Yes
Will you be translating?	No
Title of your thesis/dissertation	The Role of SGS1 and EXO1 in the Maintenance of Genome Stability

Figure B.2: Permissions for content in Appendix B provided by DNA Repair and Elsevier.

This Agreement between Lillian Doerfler ("You") and Elsevier ("Elsevier") consists of your license details and the terms and conditions provided by Elsevier and Copyright Clearance Center.

License Number	4127310129903
License date	Jun 13, 2017
Licensed Content Publisher	Elsevier
Licensed Content Publication	Molecular Cell
Licensed Content Title	Phosphoproteomics Reveals Distinct Modes of Mec1/ATR Signaling during DNA Replication
Licensed Content Author	Francisco Meirelles Bastos de Oliveira,Dongsung Kim,José Renato Cussiol,Jishnu Das,Min Cheol Jeong,Lillian Doerfler,Kristina Hildegard Schmidt,Haiyuan Yu,Marcus Bustamante Smolka
Licensed Content Date	Apr 2, 2015
Licensed Content Volume	58
Licensed Content Issue	1
Licensed Content Pages	1
Start Page	194
End Page	
Type of Use	reuse in a thesis/dissertation
Portion	full article
Format	both print and electronic
Are you the author of this Elsevier article?	Yes
Will you be translating?	No
Title of your thesis/dissertation	The Role of SGS1 and EXO1 in the Maintenance of Genome Stability

Figure B.3: Permissions for content in Appendix B provided Molecular Cell and Elsevier.